Final Report:

# Mississippi State University Cooling, Heating, and Power (Micro-CHP) and Bio-Fuel Center

Award Number: *DE-FC26-08NT01923*

Recipient: *Mississippi State University*

Technical Contact: *Pedro J. Mago*

Business Contact: *LeLe Newell*

DOE Project Officer: *Adrienne L. Riggi*

April 14, 2014

# Table of Contents

## Executive Summary

Between 2008 and 2014, the U.S. Department of Energy funded the MSU Micro-CHP and Bio-Fuel Center located at Mississippi State University. The overall objective of this project was to enable micro-CHP (micro-combined heat and power) utilization, to facilitate and promote the use of CHP systems and to educate architects, engineers, and agricultural producers and scientists on the benefits of CHP systems. Therefore, the work of the Center focused on the three areas: CHP system modeling and optimization, outreach, and research. In general, the results obtained from this project demonstrated that CHP systems are attractive because they can provide energy, environmental, and economic benefits. Some of these benefits include the potential to reduce operational cost, carbon dioxide emissions, primary energy consumption, and power reliability during electric grid disruptions. The knowledge disseminated in numerous journal and conference papers from the outcomes of this project is beneficial to engineers, architects, agricultural producers, scientists and the public in general who are interested in CHP technology and applications. In addition, more than 48 graduate students and 23 undergraduate students, benefited from the training and research performed in the MSU Micro-CHP and Bio-Fuel Center.

## Scope and Accomplishments

The project scope consisted of six separate, but related areas:

1. *Micro-CHP modeling* - Computational simulations and verification/validation studies of selected models for technical and economic viability.

2. *Fuel flexibility in micro-CHP applications* – Demonstrating and quantifying the operation of micro-CHP systems on alternative fuels.

3. *Outreach activities* – Providing provide educational materials for engineers and architects and conducting outreach seminars, workshops, and demonstrations for engineers and architects as well as for more general audiences.

4. *Biofuel and opportunity fuel processing and utilization* – Determining the processing requirements and feasibility to utilize biofuels and disaster debris for micro-CHP systems.

5. *CHP Systems Optimization* – Optimization of internal combustion and Stirling engines integrated with heat recovery systems for CHP operation.

6. *Distributed Generation and Grid Interconnection* – Developing requirements and control systems for interconnection of micro-CHP systems with the electrical grid.

All tasks proposed in the project have been completed. Table 1 shows all the specific tasks and the percent of completion of each task.

Table 1. Task description and percent of complete.

| Task | Description | Percent Complete |
|---|---|---|
| 1 | Micro-CHP modeling | 100% |
| 2 | Fuel flexibility in micro-CHP applications | 100% |
| 3 | Outreach activities | 100% |
| 4 | Biofuel and opportunity fuel processing and utilization | 100% |
| 5 | CHP Systems Optimization | 100% |
| 6 | Distributed Generation and Grid Interconnection | 100% |

In terms of accomplishments, the outcomes from this project were widely disseminated in journal papers, conference papers, posters, etc. An average of 14 journals papers and 12 conference papers per year were published with the results from this project. A summary of the publications is presented in Table 2. This table includes journal papers, conference papers, books, book chapters, posters, and thesis and dissertations.

Table 2. Summary of publications from the project outcomes.

| | Journal Papers | Conference Papers | Books | Book Chapters | Posters | Dissertations | Thesis |
|---|---|---|---|---|---|---|---|
| Task 1 | 41 | 9 | 1 | 3 | 2 | 12 | 5 |
| Task 2 | 8 | 5 | 0 | 0 | 4 | 3 | 3 |
| Task 4 | 15 | 37 | 0 | 0 | 30 | 4 | 7 |
| Task 5 | 4 | 3 | 0 | 0 | 3 | 0 | 2 |
| Task 6 | 2 | 9 | 0 | 0 | 3 | 4 | 2 |
| Total | 70 | 63 | 1 | 3 | 42 | 23 | 19 |

In addition to publication, this project has a strong participation of graduate and undergraduate students. A summary of the graduate students and undergraduate students involved in this project is presented in Table 3.

Table 3. Summary of the graduate students and undergraduate students involved in the project.

| | Ph.D. | M.S. | Undergraduate Students |
|---|---|---|---|
| Task 1 | 12 | 9 | 15 |
| Task 2 | 3 | 3 | 5 |
| Task 4 | 4 | 9 | 0 |
| Task 5 | 0 | 2 | 3 |
| Task 6 | 4 | 2 | 0 |
| Total | 23 | 25 | 23 |

In terms of outreach and education, the center participated in multiple workshops, seminars, and meetings to facilitate and promote the use of CHP systems and to educate architects, engineers, agricultural producers, and scientists on the benefits of CHP systems.

# Summary of Project Activities.

## Task 1. CHP Modeling

## Task 1.1. Develop a CHP systems energy consumption model

**Description:**
*The Recipient shall develop a transient model to simulate the energy consumption of CHP systems. The model will incorporate system component characteristics and building energy demand to predict CHP systems operation and performance.*

**Percentage of completion**: 100%

**Accomplishments:**

- A model to simulate the energy consumption of CHP system has been developed. This model incorporates system components characteristics as well as building energy demand to estimate the CHP system performance operation.

- A model to study the analysis of hybrid-cooling, heating, and power (hybrid-CCHP) systems that have an absorption chiller (CH) and a vapor compression system to handle the cooling load was developed.

- The effect of the size of both cooling mechanisms was analyzed in conjunction with the PGU size and efficiency.

- To account for the effect of climate conditions, hot and cold climates were considered by performing simulations for Tampa and Chicago weather conditions.

- The results from this task were published in the Journal of Power and Energy entitled: "Hybrid-cooling Combined Cooling, Heating, and Power Systems."

    An analysis of a CCHP system with dual cooling technology for cooling (hybrid-cooling CCHP), absorption CH, and VC, was performed for different sizes of absorption CH and VC system. The analysis included the use of different PGU sizes and two different PGU efficiencies. An increase of the PGU efficiency gives higher PEC reduction for both cities. For any particular PGU size, higher PEC reductions were achieved when using a hybrid-cooling system instead of a CH or VC alone. In general, a larger PGU size allows the use of a larger CH. However, the relationship between PGU size and CH size is defined by the CCHP characteristics and building energy profiles, which implies that every case needs a particular analysis. For a PGU efficiency of 0.25, the maximum PEC reduction found was 2.3 and 5.8 per cent for Tampa and Chicago, respectively. While for a PGU efficiency of 0.30, the maximum PEC reduction found was 6.4 and 10.8 per cent for Tampa and Chicago, respectively. Higher PEC reduction was found for Chicago than for Tampa because Tampa requires more cooling, which implies more energy consumption by the absorption CH because of its low efficiency. In

general, results proved that more primary energy reduction can be achieved for hybrid- cooling CCHP systems than for a CCHP system with only an absorption CH.

- A model to analyze CHP systems based on site energy consumption was developed and published in the Applied Energy Journal entitled: "Analysis of Cooling, Heating, and Power Systems Based on Site Energy Consumption."

  Feasibility of cooling, heating, and power systems frequently is based on economic considerations such as energy prices. However, a most adequate feasibility of CHP systems must be based on energy consumption followed by economic considerations. CHP systems designs must yield economical savings, but more importantly must yield real energy savings based on the best energy performance. For CHP systems, energy savings is related to primary energy and not to site energy. This paper presented a mathematical analysis demonstrating that CHP systems increase the site energy consumption (SEC). Increasing the SEC could yield misleading results in the economic feasibility of CHP systems. Three different operation modes are evaluated: (a) cooling, heating, and power; (b) heating and power; and (c) cooling and power, to represent the operation of the system throughout the year. Results show that CHP systems increase site energy consumption; therefore primary energy consumption (PEC) should be used instead of SEC when designing CHP systems.

**Publications / Presentations:**

*Journal Papers:*

1. Fumo, N., Mago, P. J., & Chamra, L. (Jul 2009). Hybrid-cooling Combined Cooling, Heating, and Power Systems. *IMechE Journal of Power and Energy*, 223(5), 761-770.

2. Fumo, N., Mago, P. J., & Chamra, L. (Jun 2009). Analysis of Cooling, Heating, and Power Systems Based on Site Energy Consumption. *Applied Energy*, *86*(6), 928-932.

*Posters:*

1. Fumo, N., Mago, P. J., and Chamra, L. M. (Apr 2009). Hybrid-Cooling, Combined Cooling, Heating, and Power Systems. *2nd Energy-Synergy Workshop,* Mississippi State University.

## Task 1.2. Determine the potential of energy saving strategies on the benefits of CHP systems.

**Description:**

*The Recipient shall utilize the CHP model developed under Task 1.1 and other tools, as needed, to simulate energy savings strategies from energy management practices. Simulations will be performed for building-CHP systems with various building energy use profiles based on the implementation of common energy saving strategies. Energy use (electricity and fuel) will be quantified for various energy management practices and CHP systems.*

**Percentage of completion**: 100%

**Accomplishments:**

- The CHP model developed in Task 1.1 was modified and improved to simulate energy savings strategies from energy management practices.

- The model was used to determine the potential of energy saving strategies based on primary energy savings on the benefits of CHP system. The outcomes from this research were published in Applied Energy Journal. The title of the paper is: "Energy and Economic Evaluation of Cooling, Heating, and Power Systems Based on Primary Energy."

  Feasibility of CHP systems is generally driven by economic savings. In addition, economic evaluation of CHP systems is based on site energy use and cost, which could lead to misleading conclusions about energy savings. Since energy savings from CHP systems only occurs in primary energy, the objective of this investigation is to demonstrate that feasibility of CHP systems should be performed based on primary energy savings fol- lowed by economic considerations. This paper also evaluates the effect of the power generation unit (PGU) efficiency over the primary energy reduction when a CHP system is utilized. The advantages of operating CHP systems under a primary energy operational strategy, such as the proposed Building Primary Energy Ratio (BPER) strategy, are also discussed. Results show that for some cases economic savings are attained without the corresponding primary energy savings. However, the use of the BPER operational strategy guarantees better energy performance regardless of economic savings. Regarding to the PGU efficiency, an increase of the efficiency reduces the primary energy use more than proportionally. For example, increasing the PGU efficiency from 0.25 to 0.35 (increase of 40%) can reduce the primary energy use from 5.4% to 16% (increase of 200%).

- Developed a model to determine the analysis and optimization of CCHP systems based on energy, economical, and environmental considerations

  Analysis of CCHP systems is frequently based on reduction of operating cost without measuring the actual energy use and emissions reduction. CCHP systems can be optimized based on different optimization criterion such as: energy savings, operation cost reduction or minimum environmental impact. In this study, CCHP systems operated following the electric load (FEL) and the thermal load (FTL) strategies are evaluated and optimized based on: primary energy consumption (PEC), operation cost, and carbon dioxide emissions (CDE). This study also includes the analysis and evaluation of an optimized operational strategy in which a CCHP system follows a hybrid electric–thermal load (HETS) during its operation. Results show that CCHP systems operating using any of the optimization criteria have better performance than CCHP systems operating without any optimization criteria. For the evaluated city, the optimum PEC and cost reduction are 7.5% and 4.4%, respectively, for CCHP-FTL, while the optimum CDE reduction is 14.8% for CCHP-FEL. Results also show that the HETS is a good alternative for CCHP systems operation since it gives good reduction of PEC, cost, and CDE. This optimized operation strategy provides a good balance among all the variables considered in this paper.

- A book chapter was written using the results obtained from this task. The book chapter focused on the evaluation of cooling, heating, and power systems based on primary energy operational strategy.
- A paper entitled: "Methodology to Perform a Combined Heating and Power System Feasibility Study for Industrial Manufacturing Facilities," was published based on the findings from this task.
- A paper was published based on some of the results from this task: "A Comparative Study of the Economic Feasibility of Employing CHP Systems in Different Industrial Manufacturing Applications."

**Publications / Presentations:**

*Book Chapter:*

1. Mago, P. J., Chamra, L., & Fumo, N. (2009). Evaluation of Cooling, Heating, and Power Systems Based on Primary Energy Operational Strategy. Lucas P. Gragg and Jan M. Cassell (Eds.), Progress in Management Engineering, New York: Nova Science Publishers, Inc., 199- 236. ISBN: 978-1-60741-310-3. (Invited).

*Journal Papers:*


1. Fumo, N., Mago, P. J., & Chamra, L. (Sep 2009). Energy and Economic Evaluation of Cooling, Heating, and Power Systems Based on Primary Energy. *Applied Thermal Engineering, 29(13),* 2665-2671.

2. Mago, P. J., & Chamra, L. (May 2009). Analysis and Optimization of CCHP Systems Based on Energy, Economical and Environmental Considerations. *Energy and Buildings, 41,* 1099-1106.

3. Wheeley, C., Mago, P. J., & Luck, R. (Jan 2012). Methodology to Perform a Combined Heating and Power System Feasibility Study for Industrial Manufacturing Facilities. *Distributed Generation and Alternative Energy Journal*, *27*(1), 8-32.

4. Wheeley, C., Mago, P. J., & Luck, R. (Dec 2011). A Comparative Study of the Economic Feasibility of Employing CHP Systems in Different Industrial Manufacturing Applications. *Energy and Power Engineering*, *3*, 630-640.

## Task 1.3. Develop a model that compares energy consumption from CHP operating under cost-oriented operational strategies and primary energy strategies using transient simulation.

**Description:**

*The Recipient shall account for the transient effects in the building due to changes in the weather or changes in the set points for the CHP equipment, i.e., the engine, fan, and A/C equipment. This work will adapt the controller based on short-term weather forecasting and linear programming to minimize the operational cost under the proposed strategies.*

**Percentage of completion**: 100%

**Accomplishments:**

- An analytic solution for optimal Power Generation Unit operation in CHP systems have been developed. This work has been published in the ASME Journal of Energy Resources Technology: "Analytic Solutions for Optimal Power Generation Unit Operation in Combined Heating and Power Systems."

  This work presents an analytic approach for defining optimal operation decisions for a power generation unit (PGU) in combined heating and power (CHP) systems. The system is optimized with respect to cost, and the independent variables are the thermal load and the electric load. Linear programming is a common tool used to find the optimal PGU operation for a given combination of thermal and electric loads, but these methods are more computationally intensive than the analytical approach proposed in this paper. The analytic process introduced in this paper shows that the optimal PGU operation for all possible thermal and electric loads can be decided by simple and explicit equations even when the efficiency of the PGU is allowed to vary with PGU loading. Moreover, the analysis reveals that for all possible load conditions, the optimal CHP system operation is based on either following the electric load (FEL) or following the thermal load (FTL) strategies. The cost ratio, i.e., the ratio of the electricity price to the fuel price, is introduced as the key parameter used for making optimal decisions. Cost ratios in Chicago, IL and Philadelphia, PA are used as case studies to show the effect that different cost ratios have on the optimal operation decisions for each possible input load.

- The evaluation of a turbine driven CCHP system for large office buildings under different operating strategies. This paper was published in the Power and Energy Journal.

  Combined cooling, heating, and power (CCHP) systems use waste heat from on-site electricity generation to meet the thermal demand of the facility. This paper models a CCHP system for a large office building and examines its primary

energy consumption (PEC), operational costs, and carbon dioxide emissions (CDE) with respect to a reference building using conventional technologies. The prime mover used in this investigation is a load share turbine, and the CCHP system is evaluated under three different operation strategies: following the electric demand of the facility, following the thermal demand of the facility, and following a seasonal strategy. For the various strategies, the percentages of total carbon dioxide emissions by source are presented. This paper explores the use of carbon credits to show how the reduction in carbon dioxide emissions that is possible from the CCHP system could translate into economic benefits. In addition, the capital costs available for the CCHP system are determined using the simple payback period. Results indicate that for the evaluated office building located in Chicago the CCHP operation reduces the operational cost, PEC, and CDE from the reference building by an average of 2.6%, 12.1%, and 40.6%, respectively, for all the different operational strategies.

- A real time CHP operational strategy using a hierarchical optimization algorithm has been developed and published in the Journal of Power and Energy: "Real Time Combined Heat and Power (CHP) Operational Strategy Using a Hierarchical Optimization Algorithm."

  An optimal, operational strategy based on transient simulation that do not require the use of linear programming has been developed and evaluated. A paper has been accepted in this topic. This paper considers the transient response of a building combined with a hierarchical CHP optimal control algorithm to obtain a real-time integrated system that uses the most recent weather and electric load information. This is accomplished by running concurrent simulations of two transient building models. The first transient building model uses current as well as forecast input information to obtain short term predictions of the thermal and electric building loads. The predictions are then used by an optimization algorithm, i.e., a hierarchical controller, that decides the amount of fuel and of electrical energy to be allocated at the current time step. The results indicate that the CHP engine operation dictated by the proposed hierarchical controller with uncertain weather conditions have the potential to yield significant savings when compared to conventional systems using current values of electricity and fuel prices.

- A paper was published on the Applied Thermal Engineering Journal based on some of the findings from this task: "Micro-combined Cooling, Heating and Power Systems Hybrid Electric-thermal Load Following Operation."

**Publications / Presentations:**

*Journal Papers:*

1. Yun, K., Luck, R., Mago, P. J., & Smith, A. (Jan 2012). Analytic Solutions for Optimal Power Generation Unit Operation in Combined Heating and Power Systems. *ASME Journal of Energy Resources Technology, 134(1),* 011301(8 pages).

2. Mago, P. J., & Hueffed, A. (Jun 2010). Evaluation of a Turbine Driven CCHP System for Large Office Buildings under Different Operating Strategies, Energy, and Buildings. *Journal of Power and Energy*, *42*(10), 1628-1636.

3. Yun, K., Cho, H., Luck, R., & Mago, P. J. (Jun 2011). Real Time Combined Heat and Power (CHP) Operational Strategy Using a Hierarchical Optimization Algorithm. *Journal of Power and Energy*, *225*, 403-412.

4. Mago, P. J., Chamra, L., & Ramsay, J. (Mar 2010). Micro-combined Cooling, Heating and Power Systems Hybrid Electric-thermal Load Following Operation. *Applied Thermal Engineering*, *30*(8-9), 800-806.

*Conference Papers:*

1. Cho, H., Luck, R., Eksioglu, S.D., Chamra, L. M., "Operation of a CCHP System using an Optimal Energy Dispatch Algorithm." *ASME Proceedings of Energy Sustainability* 2008, August 10-13, Jacksonville, FL.

*Posters:*

1. Cho, H., Luck, R., Chamra, L.M., "Supervisory Feed-Forward Control of Building CHP Systems Using Short-Term Weather Forecasting", Poster presentation in International Building Performance Simulation Association (IBPSA) – USA meeting, January 24, 2009, Chicago, IL, USA

## Task 1.4. Determine the potential of energy saving strategies on the benefits of CHP systems. (Duplicated in the SOPO)

## Task 1.5. Analysis of the timestep in CHP systems simulations.

**Description:**

*The Recipient shall utilize the model developed under Task 1.1 and other tools, as needed, to perform simulations for different building CHP systems. Simulations will be performed for hourly, monthly, annual, and other time steps, as needed, to develop a transient use profile. Results will be analyzed for the time steps to determine what appropriate time interval would best represent the actual electricity and thermal demand. A web-based tool will be developed to estimate the feasibility of CHP systems based on annual and monthly energy consumption.*

**Percentage of completion**: 100%

**Accomplishments:**

- The model developed in Task 1.1 and Task 1.2 was used to perform simulations for different building CHP systems. Simulations were performed for hourly, monthly, annual, and other time steps, as needed, to develop a transient use profile.

- An optimal power generation unit sizing and cost savings methodology using monthly vs. hourly time-steps applied to base-loaded combined heat and power systems was developed. A paper will be presented at the 2012 ASME International Mechanical Engineering Congress and Exposition (IMECE2012) to be held in Houston, TX.

  In many applications combined heat and power (CHP) systems provide both cost and environmental benefits when used in place of traditional grid utility systems. The benefits of CHP systems, however, are very sensitive to the proper selection of the system's components for given loading conditions. The most crucial component to size is the power generation unit (PGU). The PGU size should be selected based on the facility's electrical and thermal loading conditions to generate the maximum cost savings. Many researchers have presented methods for selecting the optimal PGU size using hourly load data. However, hourly load data is not always available for a facility. For this reason, this work provides a series of calculations for determining the optimal PGU size based on annual cost savings for a base-loaded CHP system using monthly load data, which is representative of a facility's utility bills and is always available. Unfortunately, in some cases monthly-based calculations do not provide enough information to properly size the PGU. A case study is performed to determine when a monthly-based strategy is valid. In this study, monthly-based calculations are compared to hourly-based calculations for sixteen benchmark buildings defined by the

Department of Energy to represent the commercial building stock in the United States using weather data from Chicago, IL. A statistical analysis of the results uncovers key parameters and thresholds for these parameters in cases where monthly-based calculations can be used. Results indicate that the proposed monthly-based calculations can determine the optimal PGU size, and calculate annual cost savings for half of the facilities in Chicago. Further studies must be performed to determine a broader range of locations where a monthly-based strategy is valid.

- A web-based tool has been developed to estimate the feasibility of CHP systems based on annual and monthly energy consumption. This tool was presented at the 2010 ASME Energy Sustainability conference in Phoenix, AZ.

  Building energy consumption analysis is a difficult task because it depends on the characteristics and interaction among the building, the heating/cooling system, and the surroundings (weather). Since building energy profiles are usually required on an hourly basis, which often is not available for existing buildings, the hourly energy consumption must be estimated or predicted. The dynamic behavior of the weather conditions and building operation makes computer simulations a good practice for reliable solutions. However, energy building computer simulations require considerable amount of detailed input data and user time, which is a drawback for a cost-effective solution. Therefore, simplified models based on statistics or a combination of statistics and simulations may be a better solution with reasonable uncertainty.

  This paper presents the tool Small Office Hourly Energy Consumption Estimator (SOHECE). The tool estimates hourly building energy consumption for small office buildings. The proposed tool has been developed in Microsoft Excel and it uses simulation data from EnergyPlus benchmark models to convert monthly energy consumption from utility bills into hourly energy consumption. Since benchmark models were developed by the U.S. government to provide a consistent baseline of comparison, energy consumption data from simulations of the benchmark models are considered reasonable representations of energy consumption profiles. Results account for baseline and variable energy consumption for electricity and fuel. The site weather conditions, for which the energy consumption is estimated, are considered using the sixteen climate zones of the U.S. benchmark models. The tool has been applied to a hypothetical building placed in Meridian, MS, and errors obtained for the estimated hourly energy consumption are mainly lower than ten percent.

**Publications / Presentations:**

*Conference Papers:*

1. Robert Thomas, Rogelio Luck, and Pedro J. Mago, "Optimal Power Generation Unit Sizing and Cost Savings Methodology Using Monthly vs. Hourly Time-steps Applied to Base-Loaded Combined Heat and Power Systems", *ASME International Mechanical Engineering Congress and Exposition (IMECE2012)*, Houston, TX.

2. Fumo, N., & Mago, P. J. (May 2010). Tools for Small Office Buildings Energy Consumption Estimation. *ASME Energy Sustainability 2010 - Paper No. ES2010-90135*, Phoenix, Arizona.

## Task 1.6. Develop a model that compares energy consumption from CHP operating under cost-oriented operational strategies and primary energy strategies.

**Description:**

*The Recipient shall develop a model to estimate energy consumption of CHP systems operating under cost-oriented and primary energy operational strategies. Energy savings and cost of the strategies will be compared. The model will allow simulating both cost-oriented and primary energy operational strategies as well as performing a cost comparison of both strategies. The model will also allow evaluating the performance of CHP systems by varying the energy cost (electricity and fuel). Since, generally, the economic analysis prevails in the feasibility of CHP systems, the energy cost will be also considered to show that the economic decisions could yield misleading results.*

**Percentage of completion**: 100%

**Accomplishments:**

- A model to estimate energy consumption of CHP systems operating under cost-oriented and primary energy operational strategies has been developed. A paper that addresses the energy, economical, and environmental benefits of the use of CHP systems for small commercial buildings for the north American climate has been published from some of the results of this task. The paper was published in the International Journal of Energy Research.

  This paper analyzed a natural gas engine CHP system together with a vapor compression system for different American climate zones. Performance was measured in terms of operational costs, PEC, and carbon dioxide emissions as a percent of a reference building. The objective of this paper is to compare the performance of a CHP system operating 24h a day with a system that only operates during typical office hours. Furthermore, the system was optimized based on reducing PEC, minimizing costs, and reducing emissions. In addition, the benefits of CHP systems based on the Energy Star program and the Leadership in Energy and Environmental Design (LEED) program are presented. Results show that, in general, it is more beneficial to operate the CHP system during typical office hours than to operate the system 24 h a day. Also, the CHP system performance strongly depends on the location where it is installed. In addition to reductions in cost, primary energy, and emissions, CHP systems can help achieve the Energy Star label for commercial office buildings and help obtain LEED points that go toward achieving LEED certification status. [J1]

- A book chapter that focused on the energy, economic, and environmental analysis of CHP and CCHP systems was published.

This chapter first reviews the economical, energetic, and environmental benefits of CHP systems and presents some non-traditional benefits of this technology. For example, the use of an optimized CHP system increased the building's energy star rating above 75, which makes it eligible to receive the Energy Star label. Furthermore, a rating above 71 allows the building to obtain LEED-EB points to achieve LEED-EB certification. In addition, this chapter investigates the critical role of the prime mover on the performance of CHP and CCHP systems under different pricing structures. Three different size natural gas engines are simulated for a small office under different operational strategies such as: follow the facility's electric demand, follow the facility's thermal demand, and follow a constant load. Then, simple optimizations are carried out and improve the system's performance. In general, the smallest engine simulated yielded the lowest costs and lowest PEC, and the best operating strategy depended on the location, engine size, and the building's priority.

- A model that asses CHP system performance operation in commercial building benchmark models in different u.s. climate zones was presented at the 2009 ASME Energy Sustainability Conference in San Francisco, CA.

**Publications / Presentations:**

*Book Chapter:*

1. Mago, P. J., & Hueffed, A. (May 2011). Energy, Economic, And Environmental Analysis of CHP and CCHP Systems. Morena J. Acosta (Eds.), *Advances in Energy Research - Volume 7*, New York: Nova Science Publishers, Inc., 229-271. ISBN: 978-1-61122-956-1. (Invited).

*Journal Papers:*

1. Mago, P. J., Chamra, L., & Hueffed, A. (May 2009). A Review on Energy, Economical, and Environmental Benefits of the Use of CHP Systems for Small Commercial Buildings for the North American Climate. *International Journal of Energy Research*, *33*, 1252-1265.

*Conference Papers:*

1. Cho, H., Luck, R., Mago, P. J., & Chamra, L. (Jul 2009). Assessment of CHP System Performance with Commercial Building Benchmark Models in Different U.S. Climate Zones. *ASME Proceedings of Energy Sustainability 2009*, San Francisco, CA.

## Task 1.7. Optimize CHP systems operation based on emissions reduction and compare and combine the results with the optimization of CHP systems based on primary energy and cost.

**Description:**

*The Recipient shall develop a model to estimate energy consumption of CHP systems operating under cost-oriented and primary energy operational strategies. Energy savings and cost of the strategies will be compared. The model will allow simulating both cost-oriented and primary energy operational strategies as well as performing a cost comparison of both strategies. The model will also allow evaluating the performance of CHP systems by varying the energy cost (electricity and fuel). Since, generally, the economic analysis prevails in the feasibility of CHP systems, the energy cost will be also considered to show that the economic decisions could yield misleading results.*

**Percentage of completion**: 100%

**Accomplishments:**

- A model to simulate CHP system based on an emission operational strategy has been developed. The outcomes from this task have been published in the Applied Energy Journal: "Emission Operational Strategy for Combined, Cooling, and Power Systems."
    - Integrated Energy Systems (IES), as technology that use thermal activated components to recover waste heat, are energy systems that offer key solution to global warming and energy security through high overall energy efficiency and better fuel use. Combined cooling, heating, and power (CCHP) systems are IES that use recovered thermal energy from the prime mover to produce heating and cooling for the building. The CCHP operational strategy is critical and it has to be considered in a well designed system since it defines the ultimate goal for the benefits expected from the system. One of the most common operational strategies is the cost-oriented strategy, which allows the system to operate at the lowest cost. A primary energy strategy (PES) optimizes energy consumption instead of cost. However, as a result of the worldwide concern about global warming, projects that target reduction of greenhouse gas (GHG) emissions have gained a lot of interest. Therefore, for a CCHP system, an emission strategy (ES) would be an operational strategy oriented to minimize emission of pollutants. In this study, the use of an ES is proposed for CCHP systems targeted to reduce emission of pollutants. The primary energy consumption (PEC) reduction and carbon dioxide (CO2) emission reduction obtained using the proposed ES are compared with results obtained from the use of a PES. Results show that lower emission of CO2 is achieved with the ES when compared with the PES, which prove the advantage of the ES for the design of CCHP systems targeted to emissions reduction.

- A model was developed to evaluate the environmental benefits of base-loaded CHP systems for different climate conditions in the US. The results were presented in the International Journal of Ambient Energy: "Environmental Evaluation of Base-Loaded CHP Systems for Different Climate Conditions in the US."

  This paper examines a methodology to illustrate the emissions reduction potential by a base-loaded combined heating and power (CHP) system in a given building across different US regions. In addition, the size of the prime mover that may potentially reduce the carbon dioxide emissions is determined. The potential carbon dioxide emission savings from a CHP system considers the ratio of emissions conversion factors applied to imported electricity to emissions conversion factors applied to fuel consumed $R_{CDE}$: Results indicate that to be able to achieve savings in carbon dioxide emissions, $R_{CDE}$ must be larger than a unique constant $R_{Min}$ that only depends on the CHP components efficiencies. A hospital benchmark building developed by the Department of Energy in different climate conditions was used as an example to apply the methodology presented in this article. The effects of the CHP power generation unit (PGU) size and the CHP system efficiency on carbon dioxide emissions are also considered and a range of possible values for PGU size and emissions reductions are presented. Results indicate that one of the main variables that affect the potential of a CHP system to reduce carbon dioxide emission is the efficiency of PGU.

- A model to evaluate the potential emissions reductions from the use of CHP systems in different commercial buildings was developed. This model was published in the Building and Environment Journal: "Evaluation of the Potential Emissions Reductions from the Use of CHP Systems in Different Commercial Buildings."

  Under the right conditions, a CHP system can reduce the harmful emissions resulting from power production, causing less greenhouse gases to be released than a reference system where power is purchased from the electricity grid. Different building types may be more or less likely to save emissions with CHP systems based on the electrical and thermal needs of the building. This investigation evaluated seven different types of buildings located in Chicago, Illinois for their potential to reduce CO2, NOx, and CH4 emissions using a CHP system. The CHP system modeled is sized to provide 30% of the average hourly electricity needs of each building. The total carbon equivalent emissions, primary energy consumption (PEC), and operational cost of a CHP system are presented along with those of a reference system. In addition, the CHP system efficiency is analyzed with respect to the fraction of the thermal load that is satisfied by the CHP system (Rh). Results show that a CHP system would reduce emissions for all buildings studied, with more than 21% of carbon equivalent emissions reduced for an outpatient health care building. PEC and operational cost would be reduced with the use of a CHP system for some of the buildings. In general it is

beneficial to have high Rh values to provide better emissions, cost and PEC reduction from the CHP system operation.

**Publications / Presentations:**

*Journal Papers:*

1. Fumo, N., Mago, P. J., & Chamra, L. (Nov 2009). Emission Operational Strategy for Combined, Cooling, and Power Systems. *Applied Energy Journal, 86(11),* 2344-2350.

2. Mago, P. J., Luck, R., & Smith, A. (Nov 2011). Environmental Evaluation of Base-Loaded CHP Systems for Different Climate Conditions in the US. *International Journal of Ambient Energy*, *32*(4), 203-214.

3. Mago, P. J., & Smith, A. (Jul 2012). Evaluation of the Potential Emissions Reductions from the Use of CHP Systems in Different Commercial Buildings. *Building and Environment, 53, 74–82*

## Task 1.8. Perform a detailed verification and validation of simulation results.

**Description:**

*The Recipient shall utilize process measurements from a micro-CHP system at MSU to verify and validate the technical and economical results from a previously-developed micro-CHP dynamic model. The micro-CHP system model will be calibrated and simulation results will be compared with the actual measurements, including building heating and cooling load. Fuel consumption from the engine and electricity imported from the grid will be recorded to verify the economic results from the simulation. Detailed uncertainty analysis of the micro-CHP facility will be performed to validate the technical and economic results from the simulation, including transient operation of the micro-CHP facility.*

**Percentage of completion**: 100%

**Accomplishments:**

- A paper entitled "Integrated Parameter Estimation of Multicomponent Thermal Systems with Demonstration on a Combined Heat and Power System" has been submitted to the International Society of Automation: "Integrated Parameter Estimation of Multicomponent Thermal Systems with Demonstration on a Combined Heat and Power System." This paper describes a novel methodology for calibrating interconnected equipment such as heat exchangers, boilers, engines, etc., and applied to microCHP research facility.

  In experimental models of multi-component thermal systems, small errors in each sub-model can propagate detrimentally through the overall model resulting in large prediction errors as the prediction time increases. These errors can be difficult to overcome when using open loop or feed-forward control schemes. This paper demonstrates the advantages of a whole-system or integrated parameter estimation approach as opposed to component-by-component estimation approach that is widespread in the literature. The approach is demonstrated on a combined heat and power system at a laboratory facility and the resulting model is used to predict the system temperatures up to 20 minutes in advance. Results show that, when compared to conventional component-by-component parameter estimation, the integrated parameter estimation approach improves the model prediction accuracy significantly.

- A solar radiation sensor has been designed, constructed, and installed.

- A detailed calibration of the computational models of the CHP equipment in the microCHP has been performed and the comprehensive simulation model based on the individual calibrated models has been verified and validated.

- An analysis of a CCHP system model under different operating strategies with input and model data uncertainty have been performed and the results have been published in Energy and Buildings: "Analysis of a CCHP System Model under Different Operating Strategies with Input and Model Data Uncertainty."

  Combined Cooling, Heating, and Power (CCHP) system models have been used by many researchers to compare their performance with conventional systems. However, decisions based on the results of computer simulations need to take into account the uncertainty of these results to get insight into the level of confidence in the predictions. This paper presents an analysis of a CCHP system model under different operating strategies with input and model data uncertainty. However, the uncertainties that underlie the variation in input parameters such as the thermal load, natural gas prices and electricity prices are not readily available. Additionally, engine performance uncertainty can be difficult to characterize because of the nonlinearity of engine efficiency curves. This paper presents practical and novel approaches to estimating the uncertainty in these and other input parameters. A case study using a small office building located in Atlanta, GA is described to illustrate the importance of the use of uncertainty and sensitivity analysis in CCHP system performance predictions, and how the primary energy consumption, operational cost, and carbon dioxide emissions are affected by the uncertainty associated with the model input parameters.

- A modular approach to uncertainty analysis was developed and the results have been published in ISA Transactions: "A Modular Approach to Uncertainty Analysis." The modular approach was in used during the validation and verification process of the model for the microCHP building.

  A methodology to simplify the uncertainty analysis of large-scale problems where many outputs and/or inputs are of interest was developed. The modular approach provides the same results as the traditional propagation of errors methodology with significantly fewer conceptual steps, allowing for a fast implementation of a comprehensive uncertainty analysis effort. The modular technique allows easy integration into most experimental/modeling programs or data acquisition systems. The methodology also accounts for correlation information between all outputs, thus providing information not easily obtained using the traditional uncertainty process based on analyzing one data reduction equation (DRE)/model at a time. Finally, a simple and structured approach was developed to obtain the covariance matrix for the input variables using uncorrelated elemental sources of systematic uncertainties along with uncorrelated sources corresponding to random uncertainties.

- A comparison between Univariate statistics and Monte-Carlo based multivariate statistics was performed and the results were published in the journal of Reliability

Engineering and System Safety: "An Exercise in Model Validation: Comparing Univariate Statistics and Monte-Carlo based Multivariate Statistics."

The complexity of mathematical models (for instance, a mathematical model of a CHP system) used by practicing engineers is increasing due to the growing availability of sophisticated mathematical modeling tools and ever-improving computational power. For this reason, the need to define a well-structured process for validating these models against experimental results has become a pressing issue in the engineering community. This validation process is partially characterized by the uncertainties associated with the modeling effort as well as the experimental results. The net impact of the uncertainties on the validation effort is assessed through the 'noise level of the validation procedure', which can be defined as an estimate of the 95% confidence uncertainty bounds for the comparison error between actual experimental results and model-based predictions of the same quantities of interest. Although general descriptions associated with the construction of the noise level using multivariate statistics exists in the literature, a detailed procedure outlining how to account for the systematic and random uncertainties is not available. In this paper, the methodology used to derive the covariance matrix associated with the multivariate normal probability density function based on random and systematic uncertainties is examined, and a procedure used to estimate this covariance matrix using Monte-Carlo analysis is presented. The covariance matrices are then used to construct approximate 95% confidence constant probability contours associated with comparison error results for a practical example. In addition, the example is used to show the drawbacks of using a first-order sensitivity analysis when nonlinear local sensitivity coefficients exist. Finally, the example is used to show the connection between the noise levels of the validation exercise calculated using multivariate and Univariate statistics.

- As part of the verification and validation process of CHP models, a comprehensive uncertainty analysis of a Wiebe function-based combustion model for pilot-ignited natural gas engines has been performed and the results were published in J. Automobile Engineering: "Comprehensive uncertainty analysis of a Wiebe function-based combustion model for pilot-ignited natural gas engines."

  This work considered a comprehensive uncertainty analysis of a Wiebe function-based combustion model for advanced low-pilot-ignited natural gas (ALPING) combustion in a single cylinder research engine. The sensitivities, uncertainty magnification factors (UMFs), and uncertainty percentage contributions (UPCs) of different experimental input variables and model parameters were investigated. First, the Wiebe function model was validated against experimental heat release/mass burned fraction profiles and cylinder pressure histories for three pilot injection timings (start of injection (SOI)): 220u, 240u, and 260u after top

dead center (ATDC). Second, the sensitivities and UMFs of predicted cylinder pressure histories were determined. Finally, crank angle-resolved uncertainties were quantified and mapped as 'uncertainty bounds' in predicted pressures, which were compared with measured pressure curves with error bars for cyclic variations. The Wiebe function-based combustion model with a quadratic interpolation equation for the specific heat ratio (c) provided reasonable cylinder pressure and heat release/mass burned fraction predictions for all SOIs (better for220u and260u ATDC SOIs compared with 240u ATDC). Uncertainty analysis results indicated that c (parameters in the quadratic interpolation equation), compression ratio, mass and lower heating value of natural gas trapped in the cylinder, overall trapped mass, and ignition delay were important contributors to the overall uncertainty in predicted cylinder pressures. For all SOIs, c exhibited the highest UPC values (80–90 per cent) and therefore, c must be determined with the minimum possible uncertainty to ensure satisfactory predictions of cylinder pressure histories. While the importance of c in single-zone combustion models is well recognized, the specific contribution of the present analysis is quantification of the crank angle-resolved UPCs of c and other model parameters to the overall model uncertainty. In this paper, it is shown that uncertainty analysis provides a unique methodology for quantitative validation of crank angle-resolved predictions for many type of engine combustion model with the corresponding experimental results. It is also shown that uncertainties in both predicted and measured cylinder pressures and heat release rates must be considered while validating any engine combustion model.

**Publications / Presentations:**

*Journal Papers:*

1. Smith, A., Luck, R., & Mago, P.J. (2012). Integrated Parameter Estimation of Multicomponent Thermal Systems with Demonstration on a Combined Heat and Power System. *ISA Transactions,* 51(4):507-13.

2. Smith, A., Luck, R., & Mago, P. J. (Sep 2010). Analysis of a CCHP System Model under Different Operating Strategies with Input and Model Data Uncertainty. *Energy and Buildings*, *42*, 2231-2240.

3. Weathers, J.B., Luck, R., Weathers, J.W. "A Modular Approach to Uncertainty Analysis", *ISA Transactions*, Vol. 49, pp. 19-26, 2010

4. Weathers, J.B., Luck, R., Weathers, J.W., "An Exercise in Model Validation: Comparing Univariate Statistics and Monte-Carlo based Multivariate Statistics",

*Reliability Engineering and System Safety*, Volume 94, Issue 11, November 2009, Pages 1695-1702.

*5.* Cho, H., Krishnan, S.R., Luck, R. and Srinivasan, K.K. Comprehensive uncertainty analysis of a Wiebe function-based combustion model for pilot-ignited natural gas engines. *Proc. IMechE, Part D: J. Automobile Engineering,* Vol. 223, No. 11, 2009

## Task 1.9. Optimal Control Strategy for Minimizing the Operational Costs of the Micro-CHP System.

**Description:**

*The Recipient shall develop an energy dispatch algorithm for the micro-CHP system at MSU to increase operational efficiency and optimize operational cost. The optimization scheme will be completed, and a deterministic network model of the micro-CHP at MSU will be developed as part of the algorithm. The algorithm will include the cost of the electricity and fuel as inputs, with operational signals to the cogeneration system as output. The algorithm will be used to investigate various scenarios, including varying heating and cooling loads, various scenarios will also be presented to demonstrate the feasibility of the algorithm.*

**Percentage of completion**: 100%

**Accomplishments:**

- Evaluation of CCHP systems performance based on operational cost, primary energy consumption, and carbon dioxide emission by utilizing an optimal operation scheme was performed. The results from this research were published in the Applied Energy Journal: "Evaluation of CCHP Systems Performance Based on Operational Cost, Primary Energy Consumption, and Carbon Dioxide Emission by Utilizing an Optimal Operation Scheme."

  Optimization of combined cooling, heating, and power (CCHP) systems operation commonly focuses only on energy cost. Different algorithms have been developed to attain optimal utilization of CCHP units by minimizing the energy cost in CCHP systems operation. However, other outcomes resulting from CCHP operation such as primary energy consumption and emission of pollutants should also be considered during CCHP systems evaluation as one would expect these outcomes can be subject to regulation. This paper presents an optimization of the operation of CCHP systems for different climate conditions based on operational cost, primary energy consumption (PEC), and carbon dioxide emissions (CDE) using an optimal energy dispatch algorithm. The results for the selected cities demonstrate that in general there is not a common trend among the three optimization modes presented in this paper since optimizing one parameter may reduce or increase the other two parameters. The only cities that show reduction of PEC while also reducing the CDE are Columbus, MS; Minneapolis, MN; and Miami, FL. For these cities the operational cost always increases when compared to the reference case consisting of using a vapor/compression cycle for cooling and natural gas for heating. On the other hand, for San Francisco and Boston, CCHP systems increase the CDE. In general, if CCHP systems increase the cost of

operation, as long as energy savings and reduction of emissions are guaranteed, the implementation of these systems should be considered.

- A model to study the cost-optimized real -time operation of CHP systems was developed and published in the Energy and Buildings Journal: "Cost-optimized real -time operation of CHP systems."

  The total energy cost of CHP systems can be highly dependent on the operation of individual components. This paper presented an energy dispatch algorithm that minimizes the cost of energy (e.g., cost of electricity from the grid and cost of natural gas into the engine and boiler) based on energy efficiency constrains for each component. A deterministic network flow model of a typical CHP system was developed as part of the algorithm. The advantage of using a network flow model was that the electric and thermal energy flows through the CHP equipment was easily visualized allowing for easier interpretation of the results. This algorithm was used in simulations of a case study on the operation of an existing micro-CHP system. The results from the simulation demonstrated the economical advantages resulting from optimal operation.

**Publications / Presentations:**

*Journal Papers:*


1. Cho, H., Mago, P. J., Luck, R., & Chamra, L. (Oct 2009). Evaluation of CCHP Systems Performance Based on Operational Cost, Primary Energy Consumption, and Carbon Dioxide Emission by Utilizing an Optimal Operation Scheme. *Applied Energy, 86,* 2540-2549.

2. Cho, H., Luck, R., S.D. Eksiouglu, Chamra, L. M., "Cost-optimized real -time operation of CHP systems," Energy and Buildings, Vol. 41, No. 4, April, pp. 445-451, 2009.

## Task 1.10. Optimization on Size of the Micro-CHP Components

**Description:**

*The Recipient shall perform analyses on the MSU micro-CHP system components to match them relative to other system components for optimal efficiency. In order to resize the components, analytical calculations are required to determine the characteristics of each component, including efficiency, flow rates, and temperatures. Simulations of the system will be performed with the existing dynamic model utilizing TRNSYS or other computational tools.*

**Percentage of completion**: 100%

**Accomplishments:**

- The effect of the power generation unit (PGU) size on the energy performance of CHP Systems was evaluated and presented at the 2008 ASME Power Conference.

  The objective of this investigation was to determine the effect of the power generation unit (PGU) size on the energy performance of CHP systems. Since CHP systems energy performance varies with the building energy profiles, in this study the same building was evaluated for three different cities with different climate conditions. This paper includes simulation results for the cases when a CHP system operates with and without a primary energy strategy. Results show that for any PGU size energy savings are guaranteed only when the primary energy strategy is applied. Since CHP system energy performance depends on the building energy use profiles, which depend on climate conditions and other factors such as building characteristic and operation, each case requires a particular analysis in order to define the optimum size of the power generation unit.

- The influence of prime mover size and operational strategy on the performance of CCHP systems under different cost structures was studied. The model developed for this task and the results were published in the Journal of Power and Energy: "Influence of Prime Mover Size and Operational Strategy on the Performance of CCHP Systems under Different Cost Structures."

  The objective of this investigation was to study the effect of the prime mover size and operational strategy on the energy, economical, and environmental performance of CCHP systems under different pricing structures. Three different sizes for the prime mover, a natural gas engine, were simulated under different operational strategies such as: following the electric demand of the facility, following the thermal demand of the facility, and following a constant load. The results obtained for the CCHP system will be compared with a reference building operating under conventional technologies to determine the advantages or disadvantages of the CCHP system's operation. In addition, a simple

optimization of the system's operation determines the best engine load for each hour during the simulation that minimizes cost, primary energy consumption (PEC), or carbon dioxide emissions (CDEs). For this study, three locations in different climate zones that have different electricity rate structures were chosen: one with a constant flat rate; one that uses seasonal rates; and one that incorporates block charges. Historical monthly natural gas rates were also used. Since most authors perform cost analyses using a fixed constant rate for both electricity and natural gas, a comparison is made between the cost results from using the actual cost data to those that use an average fixed rate. In general, among the three engine sizes that were simulated, the smallest engine yielded the lowest costs and lowest PEC; but, no such trend was found with regard to the CDE. The results also showed that the performance of the evaluated CCHP system can be improved by optimizing the system based on cost or primary energy.

**Publications / Presentations:**

*Journal Papers:*

1. Hueffed, A., & Mago, P. J. (Jun 2010). Influence of Prime Mover Size and Operational Strategy on the Performance of CCHP Systems under Different Cost Structures. *IMechE Journal of Power and Energy*, *224*(5), 591-605.

*Conference Papers:*

1. Fumo, N., Mago, P. J., & Chamra, L.M., (July 2008). Effect of the Power Generation Unit Size on the Energy Performance of Cooling, Heating, and Power Systems. *ASME Power Conference, Paper No. PWR2008-60057*, Orlando, FL, 635-640.

## Task 1.11. Investigate the Effects of using a Variety of Fuels

**Description:**
The Recipient shall investigate alternative fuels in an internal combustion (IC) engine model utilizing TRNSYS or other computational tools. Formulation and combustion characteristics of each fuel will be incorporated into the model. Comparison of the performance and efficiency of the engine using a variety of fuels will be made.

**Percentage of completion**: 100%

**Accomplishments:**

- A reciprocating internal combustion engine model with the ability to account for the effect of different kinds of fuels have been developed. The purpose of the model is to predict the amount of useful mechanical energy as well as the amount of heat loss through the exhaust manifold of the engine. Results of the model have been shown to be consistent with experimental and engine manufacturers data.

- A power generation and heat recovery model of reciprocating internal combustion engines for CHP applications was developed. This model can be used to determine the performance and efficiency of the engine using a variety of fuels. The results obtained from this model have been submitted for publication in the Applied Energy Journal: "Power Generation and Heat Recovery Model of Reciprocating Internal Combustion Engines for CHP Applications."

  This paper presents a power generation and heat recovery model for reciprocating internal combustion engines (ICEs). The purpose of the proposed model is to provide realistic estimates of performance/efficiency maps for both electrical power output and useful thermal output for various capacities of engines for use in a preliminary CHP design/simulation process. The proposed model will serve as an alternative to constant engine efficiencies or empirical efficiency curves commonly used in the current literature for simulations of CHP systems. The engine performance/efficiency calculation algorithm have been coded to a publicly distributed FORTRAN Dynamic Link Library (DLL), and a user friendly tool have been developed using Visual Basic programming. Simulation results using the proposed model are validated against manufacturer's technical data.

**Publications / Presentations:**

*Journal Papers:*

1. Yun, K, Cho, H, Luck, R., & Mago, P.J., Power Generation and Heat Recovery Model of Reciprocating Internal Combustion Engines for CHP Applications. *Applied Energy, Under Review.*

## Task 1.12. Model Alternative Cogeneration Systems and Investigating their Performance using TRNSYS

**Description:**

*The Recipient shall investigate alternative cogeneration systems for optimal efficiency of the MSU micro-CHP facility. A Stirling engine will be investigated for high efficiency and favorable heat rejection for cogeneration. A Stirling engine model will be implemented and integrated into the existing dynamic model in TRNSYS. The performance of the Stirling engine along with the rest of the components will be evaluated and compared to the current cogeneration system. Several other cogeneration systems will be modeled in the TRNSYS and the simulation results can be evaluated.*

**Percentage of completion**: 100%

**Accomplishments:**

Stirling engines were incorporated into the existing dynamic model in TRNSYS. The inclusion of the Stirling engine model was rather straight-forward as it only required changing the efficiency curve for the engine module. Although, the Stirling engine provided better economics, the analysis done was not novel enough to justify a publication at this point in time

## Task 1.13. Investigate the Effects of using a Variety of Fuels. (Duplicated Task)

## Task 1.14. Investigate a detailed implementation of energy storage devices (electric and thermal) for the micro-CHP facility at MSU

**Description:**

*The Recipient shall determine the effect of energy storage devices the transient performance and operational cost of CHP facilities. Specific details on the hardware, software, operation procedures, installation, and cost of the energy storage devices such as thermal storage tanks, batteries, super-capacitors, inverters, etc. This includes all hardware and software considerations required to export electrical energy to the grid as well as synchronizing the local electric generation with the electricity imported from the grid for local consumption.*

**Percentage of completion**: 100%

**Accomplishments:**

- The effect of energy storage devices on the transient performance and operational cost of CHP facilities has been investigated. Some of the results from this task have been published in the International Journal of Energy Research: "Evaluation of a Base-Loaded Combined Heating and Power System with Thermal Storage for Different Small Buildings Applications."

  The objective of this paper was to demonstrate the advantages of using a combined heating and power (CHP) system operating at full load to satisfy a fraction of the facility electric load, that is, a base load. In addition, the effect of using thermal storage during the CHP system operation (CHP-TS) is evaluated. A small office building and a restaurant with the same floor area, in Chicago, IL, and Hartford, CT, were used to evaluate the base-loaded CHP and CHP-TS operation based on operational cost, primary energy consumption (PEC), and carbon dioxide emissions (CDEs). Results indicate that, in general, the use of thermal storage is beneficial for the CHP system operation because it reduces cost, PEC, and CDEs compared with a CHP with no thermal storage. The CHP and CHP-TS operation is more beneficial for a restaurant than for a small office building for the evaluated cities, which clearly indicates the effect of the thermal load on the CHP system performance.

- The impact of thermal storage option for CHP systems on the optimal prime mover size and the need for additional heat production has been also investigated. Results will be

presented at the ASME 2012 6th International Conference on Energy Sustainability & 10th Fuel Cell Science, Engineering and Technology Conference.

In the model presented in this paper, the CHP system is base-loaded, providing a constant power-to-heat ratio. The power-to-heat ratio demanded by the building depends on the location and the needs of the building, which vary throughout the day and throughout the year. At times when the CHP system does not provide the electricity needed by the building, electricity is purchased from the grid, and when the CHP system does not provide the heat needed by the building, heat is generated with a supplemental boiler. Thermal storage is an option to address the building's load variation by storing excess heat when the building needs less heat than the heat produced by the CHP system, which can then be used later when the building needs more heat than the heat produced by the CHP system. The potential for a CHP system with thermal storage to reduce cost, PEC, and emissions is investigated, and compared with both a CHP system without thermal storage and with the standard reference case. This proposed model is evaluated for three different commercial building types in three different U.S. climate zones. The size of the power generation unit (PGU) is varied and the effect of the correspondingly smaller or larger base load on the cost, PEC, and emissions savings is analyzed. The most beneficial PGU size for a CHP system with the thermal storage option is compared with the most beneficial PGU size without the thermal storage option. The need for a supplemental boiler to provide additional heat is also examined in each case with the thermal storage option.

**Publications / Presentations:**

*Journal Papers:*

1. Mago, P. J., & Luck, R. (2013). Evaluation of a Base-Loaded Combined Heating and Power System with Thermal Storage for Different Small Buildings Applications. International Jour- nal of Energy Research, 37(2), 179-188.

*Conference Papers:*

1. Smith, A. & Mago, P. J. (July 2012). Impact of Thermal Storage Option for CHP Systems on the Optimal Prime Mover Size and the Need for Additional Heat Production. *ASME 2012 6th International Conference on Energy Sustainability & 10th Fuel Cell Science, Engineering and Technology Conference*, San Diego, CA.

## Task 1.15. Characterize office buildings energy consumption to define CHP baseline design based on the objective functions: primary energy consumption, CO2 emission reduction, and minimum net present value for the life-cycle of the CHP project

**Description:**

*The Recipient shall characterize the energy consumption of office buildings with respect to primary energy consumption, CO2 emission reduction, and minimum net present value for the life-cycle of the CHP system. Characterization of buildings energy consumption for CHP design will provide the baseline for the design of CCHP systems.*

**Percentage of completion**: 100%

**Accomplishments:**

- A screening tool for the evaluation of CHP systems in existing office buildings has been developed. This screening tool will be presented at the ASME 2012 6th International Conference on Energy Sustainability & 10th Fuel Cell Science, Engineering and Technology Conference to be held in San Diego, CA.

  Combined Cooling, Heating, and Power (CCHP) systems have been widely recognized as a key alternative for heat and electricity generation because of their ability to consume fuel more efficiently, which translates into a reduction in carbon dioxide emission, considered the main factor contributing to global warming. However, economic analyses do not always favor the implementation of this technology. Even though CCHP systems offer other benefits such as power reliability, power quality, and fuel source flexibility, they are often negated as a feasible alternative because of these poor economic indicators. Therefore, a more comprehensive evaluation of the system should be considered. This is particularly true in an environment where economic, environmental, political, and logistical problems associated with increasing centralized electrical power production are becoming more difficult to overcome. In addition, as consumers continue to be more involved and to develop a better understanding of energy choices, the demand for technology that better meets their energy needs is increasing. To promote the development of CCHP projects, it is important to facilitate, without any cost, a first order analysis of this technology to determine if a more cost intensive, in-depth analysis should be performed. This analysis can be done by using screening tools such as the CCHP Screening Tool for Existing Office Buildings (CCHP-ST-EOB) proposed in this study. Screening tools should be as accurate as possible while maintaining the simplicity of their data input in order to make it easy to use by a broad audience that may include building owners and managers without engineering background. In this sense, the CCHP-ST-EOB

uses a methodology that translates energy consumption from utility bills as input into hourly energy consumption for a more accurate analysis of the matching between the demand and supply sides. This tool takes into consideration partial load efficiencies for the power generation unit and absorption chiller for a more realistic simulation of the system performance. Results are presented in terms of cost, primary energy consumption, and CO2 emission. The tool is available to be downloaded free of charge at http://microchp.msstate.edu/thankyou.html.

**Publications / Presentations:**

*Journal Papers:*

1. Smith, J. A., Fumo, N., Luck, R., & Mago, P. J. (Jun 2011). Robustness of a Methodology for Estimating Hourly Energy Consumption of Buildings Using Monthly Electrical Bills. *Energy and Buildings*, *43*, 779-786.

*Conference Papers:*

1. Fumo, N., Mago, P. J., & Spence, J. D. (July 2012). Screening Tool for the Evaluation of Combined, Heating, and Power Systems in existing Office Buildings. *ASME 2012 6th International Conference on Energy Sustainability & 10th Fuel Cell Science, Engineering and Technology Conference*, San Diego, CA.

## Task 1.16. Determine the effect of the power generation unit (PGU) operation on the energy, economic, and environmental performance of CHP systems

**Description:**

*The Recipient shall develop a model to study the effect of the PGU operation on the energy, economic, and environmental performance of CHP systems. The PGU will be simulated under different operational strategies such as: following the electric demand of the facility, following the thermal demand of the facility, and operating at constant load. In this investigation an internal combustion engine will be used as the PGU in the CHP system to meet hourly cooling, heating, and electric loads of a typical office building for a year. Annual operational cost, primary energy consumption, and carbon dioxide emissions will be determined for the different engine operational strategies. The results obtained for the CHP system will be compared to a reference building operating under conventional technologies to determine the advantages or disadvantages of the CHP system's operation. The system operation will be optimized to determine the best engine load for each hour during the simulation.*

**Percentage of completion**: 100%

**Accomplishments:**

- A model to study the effect of the PGU operation on the energy, economic, and environmental performance of CHP systems has been developed.

- The model developed allows simulating the CHP system under different operational strategies such as: following the electric demand of the facility, following the thermal demand of the facility, and operating at constant load.

- Some of the outcomes from this Task have been presented in a paper published in the International Journal of Energy Research: "Performance Analysis of CCHP and CHP Systems Operating Following the Thermal and Electric Load."

  The results presented in this paper include a comparison of CCHP and CHP systems based on primary energy consumption (PEC), operation cost, and carbon dioxide reduction (CDE). In addition, two different operation modes were evaluated: operating the systems FEL and operating the system FTL. CCHP-FTL reduces the PEC for all the evaluated cities. For CCHP-FTL, the highest PEC reduction is obtained for Boston while the lowest is obtained for Miami. Therefore, the results suggest that more PEC reduction is achieved for cities that required more heating during the year. Similarly, CHP-FTL reduces the PEC consumption for all the evaluated cities. For all the cities, CHP-FEL increases the PEC. The results for CHP-FEL show that the highest PEC increase is obtained for Miami while the lowest is obtained for Boston. Therefore, it seems

that more primary energy is consumed for the cities that required more cooling during the year.

For the reference case, it can be concluded that the higher the amount of coal in the fuel mix of the region the higher the CDE. For the different operation modes the reduction on emissions strongly depends on the site energy consumption and the emission conversion factors for electricity and natural gas. Depending on the emission conversion factor for electricity, substituting electricity to natural gas is not always beneficial for all locations. CHP-FTL is the only operation mode that reduces PEC, cost, and CDE for all the evaluated cities, except for Miami that it was not Subscripts considered since it has no heating load. CHP-FEL is the worst case since it always increases the PEC and emissions. CCHP-FEL is beneficial for the city of Columbus, since even though the cost of operation increases, this mode of operation decreases the PEC as well as the emissions of carbon dioxide. On the other hand, CCHP-FTL is good for the cities of Miami, Columbus, and Boston, since this mode of operation reduces the PEC and CDE regardless of the operation cost.

- Some of the outcomes from this Task have been presented in a paper published in the Journal of Power and Energy: "Analysis of Combined Cooling, Heating, and Power Systems Operating Following the Electric Load and Following the Thermal Load Strategies with No Electricity Exporting." This paper presented an analysis of the governing energy equation to define the best CCHP operational strategy between FEL and FTL, when excess electricity is not allowed.

  The analysis took into consideration partial-load operation of the PGU through the ratio of the electric load and the PGU nominal capacity. In addition, the absorption chiller energy consumption at partial load was considered as part of the thermal energy demand. The equation derived for PEC (PECn) allows defining which operational strategy (FEL or FTL) has the lowest PEC. Results obtained using the PECn equation indicate that in general, for CCHP systems, the FTL strategy will offer a better system performance than the FEL strategy.

  For low power-to-heat demand ratio (PHRd), both REFERENCES operational strategies gave the same results, but FTL was better as PHRd increases. For PHRd where FTL was better than FEL, the advantage of FTL was more noticeable for low electric load (CE) and it was negligible for higher values of CE. The variation of PECn for different PGU size illustrated that there is an optimum PGU size that offers the lowest PEC for each operational strategy. The PEC is more sensitive to changes in PGU size for FTL with low PHRd, while it is more sensitive for FEL with high PHRd. The relevance of the derived PECn equation is that it can be used to generate a set of figures for different values of

PHRd that can be used to define which operational strategy is better based on the electric load (CE). However, since PECn is related to a specific electric load and PHRd, which are dynamic parameters if the system is not designed to operate at full load, the analysis of a particular system requires the use of the equation (PECn) in each incremental time of the analysis. Therefore, the value of PECn pro- posed in this study will be optimum when an equivalent PHRd (ePHRd) is available to represent all the step-by-step (hour-by-hour) energy loads. Since operating costs and emissions are functions of energy consumption, substitution of the site-to- source energy conversion factors with energy rates and emission factors, allows the analysis of FEL and FTL for operation cost and emissions, making the presented analysis useful for full analysis of a CCHP project.

- In addition, a conference that presented the Effect of the Power Generation Unit Operation on the Energy, Economical, and Environmental Performance of CCHP Systems for Small Commercial Building was presented ASME International Mechanical Engineering Congress and Exposition (IMECE2009), Orlando, FL.

  This research modeled the performance of a CCHP system designed for a small office building. A natural gas, reciprocating engines produced electricity for the building, while the waste heat was used to provide cooling, heating, and hot water. Three different size engines were used in the model while considering the following different operation methods: running the engine to follow the electric load, running the engine to follow the thermal load, or running the engine at a constant load. Performance of the CCHP system, measured in terms of annual operational cost, primary energy consumption, and carbon dioxide emission, was compared to a reference building operating with a vapor compresion air conditioner and a boiler. Finally, the CCHP system was optimized to minimize one of the following: cost, primary energy, or emissions. Two locations were evaluated, and, when considering operational costs, real electric utility rates and monthly gas rates were used. One location, Dulluth, MN, involved seasonal rates, while the other, Chicago, incorporated block charges. According to typical electricity billing schedules the average cost of electricity decreases as consumption increase, so using a non-CCHP average electricity rate can results in erroneous estimates of the true cost of electricity to the CCHP building. Also, using real monthly gas rates accounts for price fluctuations that occur month-to-month and variations among different regions.

  In general, optimizing the system provided vast improvements over the CCHP system without optimization. This in large part is due to turning off the system when it is beneficial to do so, which, for most cases, occurs a large portion of the time. For the city of Dulluth, an optimized CCHP system was able to lower the

annual operational costs, primary energy consumption, and carbon dioxide emissions when compared to the reference case. In Chicago, however, an optimized system was capable of lowering the carbon dioxide emissions and barely lower the primary energy consumption; but, the annual operation costs increased by over 20% when compared to the reference building. In both locations operating the system to minimize costs and primary energy resulted in a high CCHP system efficiency, ranging from about 70% to 80%, but optimizing the CDE only resulted in CCHP efficiencies between 40% and 60%. It was also observed that the overall efficiency of the building using an optimized CCHP system was comparable to the reference building, in all cases hovering around 42%.

- A model to size the prime mover for Based-Loaded CHP Systems has been developed. The model was published in the Journal of Power and Energy: "Prime Mover Sizing for Based-Loaded Combined Heating and Power Systems."

  This article considers the problem of sizing prime movers for combined heating and power (CHP) systems operating at full load to satisfy a fraction of a facility's electric load, i.e. a base load. Prime mover sizing is examined using three criteria: operational cost, carbon dioxide emissions (CDE), and primary energy consumption (PEC). The sizing process leads to consider ratios of conversion factors applied to imported electricity to conversion factors applied to fuel consumed. These ratios are labeled Rcost, RCDE, RPEC depending on whether the conversion factors are associated with operational cost, CDE, or PEC, respectively. Analytical results show that in order to achieve savings in operational cost, CDE, or PEC, the ratios must be larger than a unique constant RMin that only depends on the CHP components efficiencies. Savings in operational cost, CDE, or PEC due to CHP operation are explicitly formulated using simple equations. This facilitates the process of comparing the tradeoffs of optimizing the savings of one criterion over the other two – a task that has traditionally been accomplished through computer simula- tions. A hospital building, located in Atlanta, Georgia, was used as an example to apply the methodology presented in this article.

**Publications / Presentations:**

*Journal Papers:*

1. Mago, P. J., Fumo, N., & Chamra, L. (Jun 2009). Performance Analysis of CCHP and CHP Systems Operating Following the Thermal and Electric Load. *International Journal of Energy Research, 33,* 852-864.

2. Fumo, N., Mago, P. J., & Smith, A. (Dec 2011). Analysis of Combined Cooling, Heating, and Power Systems Operating Following the Electric Load and Following the Thermal Load Strategies with No Electricity Exporting. *Journal of Power and Energy, 225(8),* 1016-1025.

3. Mago, P. J., and Luck, R. (Jan 2012). Prime Mover Sizing for Based-Loaded Combined Heating and Power Systems. *IMechE Journal of Power and Energy*, *226*(1), 17-27.

*Conference Papers:*

1. Hueffed, A., Mago, P. J., & Chamra, L. (Nov 2009). Effect of the Power Generation Unit Operation on the Energy, Economical, and Environmental Performance of CCHP Systems for Small Commercial Building. *ASME International Mechanical Engineering Congress and Exposition (IMECE2009),* Orlando, FL.

## Task 1.17. Model multiple power generating units (PGU) and perform strategy simulations

**Description:**

*The Recipient shall develop a model for micro CHP operating with multiple power generating units (PGU) and evaluate cost-oriented operational strategies, primary energy strategies, and emission strategies using transient simulation. Multiple smaller PGUs will be considered instead of a single larger PGU. The approach is to increase the efficiency of the overall system by running a subset of smaller PGUs at their top efficiency. The PGU being base-loaded will be selected as needed in order to diminish maintenance costs. This work will adapt the controller based on short-term weather forecasting and linear programming to minimize the operational cost under the proposed strategies.*

**Percentage of completion**: 100%

**Accomplishments:**

- A model to evaluate the CHP systems performance with dual power generation units was developed. Results from the model has been presented at the ASME 2012 6th International Conference on Energy Sustainability & 10th Fuel Cell Science, Engineering and Technology Conference.

  This paper evaluates the economic, energetic, and environmental feasibility of using two power generation units (PGUs) to operate a combined heat and power (CHP) system. A benchmark building developed by the Department of Energy for a full-service restaurant in Chicago, IL is used to analyze the proposed configuration. This location is selected since it usually provides favorable CHP system conditions in terms of cost and emissions reduction. In this investigation, one PGU is operated at base load to satisfy part of the electricity building requirements (PGU1), while the other is used to satisfy the remaining electricity requirement operating following the electric load (PGU2). The dual-PGU configuration (D-CHP) is modeled for several different scenarios in order to determine the optimum operating range for the selected benchmark building. The dual-PGU scenario is compared with the reference building using conventional technology to determine the economical, energetic, and environmental benefits of this proposed system. This condition is also compared to a CHP system operating following the electric load (FEL) and base-loaded CHP system, and it provides greater savings in operating cost, primary energy consumption, and carbon dioxide emissions than the optimized conditions for base-loading and FEL.

- A Journal article entitle: "Combined Heat and Power (CHP) Systems with Dual Power Generation Units and Thermal Storage," has been submitted to the International Journal of Energy Research. The objective of this paper is to study the performance of a combined heat and power (CHP) system that uses two power generation units (PGU). In addition, the effect of thermal energy storage is evaluated for the proposed dual-PGU CHP configuration (D-CHP). Two scenarios are evaluated in this paper. In the first scenario, one PGU operates at base loading condition while the second PGU operates following the electric load. In the second scenario, one PGU operates at base loading condition while the second PGU operates following the thermal load. The D-CHP system is modeled for the same building in four deferent locations to account for variation of the electric and thermal loads due to weather data. The D-CHP system results are compared with the reference building using conventional technology to determine the benefits of this proposed system in terms of operational cost and carbon dioxide emissions. The D-CHP system results, with and without thermal storage, are also compared with that of single-PGU CHP systems operating following the electric load (FEL), following the thermal load (FTL), and base-loaded(BL). Results indicate that the D-CHP system operating either FEL or FTL in general provides better results than a single-PGU CHP system operating FEL, FTL, or BL. The addition of thermal storage enhances the potential benefits from D-CHP system operation in terms of operational cost savings and emissions savings.

- A Journal article entitle: "Evaluation of the Performance of Combined Cooling, Heating, and Power Systems with Dual Power Generation Units," was published in the Energy Policy Journal. In this paper, the benefits of using a combined cooling, heating, and power system with dual power generation units (D-CCHP) is examined in nine different climate conditions in several U.S. locations. In the D-CCHP system, one power generation unit (PGU) is operated at base load to satisfy part of the electricity building requirements, while the other is used to satisfy the remaining electricity requirement operating following the electric load. The waste heat from both PGUs is used toward meeting the heating demand and toward meeting the cooling demand via an absorption chiller. The D-CCHP configuration is studied for a full-service restaurant benchmark building, and its performance is quantified in terms of operational cost savings, primary energy consumption (PEC), and carbon dioxide emissions (CDE). Cost spark spread, PEC spark spread, and CDE spark spread are examined as performance indicators for the D-CCHP system. The performance of the D-CCHP system, in terms of operational cost, PEC, and CDE savings over the separate heat and power (SHP) reference case, correlates well to the respective spark spreads, with higher spark spreads signifying greater savings with the implementation of a D-CCHP system. The performance of the proposed D-CCHP configuration is also compared to the performance of a dual power generation unit combined heat and power system (D- CHP). A new parameter, the thermal difference, is introduced and used to investigate the relative performance of a D-

CCHP system compared to a D-CHP system. It is shown that the thermal difference, together with spark spread, can be used to explain the variation in savings of a D-CCHP system over a D-CHP system for each location. Finally, the effect of carbon credits on operational cost savings with respect to the reference case is shown for selected locations.

**Publications / Presentations:**

*Journal Papers:*

1. Mago, P. J., Luck, R. and Knizley, A. (2013), Combined heat and power systems with dual power generation units and thermal storage. *International Journal of Energy Research*. doi: 10.1002/er.3089.

2. Knizley, A., Mago, P.J., Smith, A.D. (2014). Evaluation of the performance of combined cooling, heating, and power systems with dual power generation units, Energy Policy, Volume 66, pages 654-665.

*Conference Papers:*

1. Knizley, A. & Mago, P. J. (July 2012). Evaluation of Combined Heat and Power (CHP) Systems Performacne with Dual Power Generation Units. *ASME 2012 6th International Conference on Energy Sustainability & 10th Fuel Cell Science, Engineering and Technology Conference*, San Diego, CA.

## Task 1.18. Develop and validate a methodology/tool to estimate building hourly energy consumption from energy information from utility bills

**Description:**
*The Recipient shall develop and validate a methodology/tool to estimate building hourly energy consumption from energy information from utility bills.*

**Percentage of completion**: 100%

**Accomplishments:**

- A methodology/tool to estimate building hourly energy consumption from energy information from utility bills was developed and validated.
- A paper was published in the Energy and Building Journal with the results from this task: "Methodology to Estimate Building Energy Consumption Using EnergyPlus Benchmark Models."

  The evaluation of building energy consumption usually requires building energy profiles on an hourly basis. Computer simulations can be used to obtain this information but generating simulations requires a significant amount of experience, time, and effort to enter detailed building parameters. This paper presents a simple methodology to estimate hourly electrical and fuel energy consumption of a building by applying a series of predetermined coefficients to the monthly energy consumption data from electrical and fuel utility bills. The advantage of having predetermined coefficients is that it relieves the user from the burden of performing a detailed dynamic simulation of the building. The coefficients provided to the user are obtained by running EnergyPlus Benchmark Models simulations; thus, the simulation process is transparent to the user. The methodology has been applied to a hypothetical building placed both in Atlanta, GA, and in Meridian, MS, and in both cases, errors obtained for the estimated hourly energy consumption are mainly within 10%.

- The robustness of a methodology for estimating hourly energy consumption of buildings using monthly electrical bills has been evaluated and determined. This has been published in the Energy and Buildings Journal: "Robustness of a Methodology for Estimating Hourly Energy Consumption of Buildings Using Monthly Electrical Bills."

  The evaluation of building energy consumption under typical meteorological conditions requires building energy profiles on an hourly basis. Computer simulations can be used to obtain this information, but generating simulations requires a significant amount of experience, time, and effort to enter detailed building parameters. This paper considers a simple methodology for using existing EnergyPlus bench- mark building energy profiles to estimate the energy profiles of buildings with similar characteristics to a given benchmark model. The

method utilizes the building monthly energy bills to scale a given benchmark building energy profile to approximate the real building energy profile. In particular, this study examines the robustness of the methodology considered with respect to the parameter discrepancies between a given building and the corresponding EnergyPlus benchmark model used to estimate its profile. Test buildings are defined by perturbing several combinations of the parameters defined in the benchmark building model. The test buildings examined are similar to the EnergyPlus, medium sized office, benchmark building in Baltimore, MD, and a total of 72 distinct test building configurations are examined. The analysis reveals that the methodology can significantly reduce the errors introduced by discrepancies from the EnergyPlus benchmark model.

- A paper was published in the Energy and Building Journal with the results from this task: "Building Hourly Thermal Load Prediction using an Indexed ARX model."

  This paper introduced an easily implementable and computationally efficient, ARX (autoregressive with exogenous, i.e., external, inputs) time and temperature indexed model for 1 h ahead building thermal load prediction. Time and temperature indexing implies that different sets of coefficients are used in the predictive equation depending on the time of the day or the ambient temperature. The indexing and proposed structure of the model follows physically motivated interpretations of the loading conditions and thermal response of the building. One of the main contributions of the proposed model is that it allows determining the dominant factors that affect the thermal load at a given time. A free and widely adopted building energy and thermal load simulation program from the U.S. Department of Energy is used to determine the prediction accuracy of the proposed model on several different benchmark-building types: a small office building, a medium office building, a midrise apartment, and a high-rise apartment.

**Publications / Presentations:**

*Journal Papers:*


1. Yun, K.4, Luck, R., Mago, P. J., & Cho, H. (2012). Building Hourly Thermal Load Prediction using an Indexed ARX model. *Energy and Buildings*, 54, 225-233.

2. Fumo, N., Mago, P. J., & Luck, R. (Oct 2010). Methodology to Estimate Building Energy Consumption Using EnergyPlus Benchmark Models. *Energy and Buildings*, *42*, 2331-2337.

3. Smith, J. A., Fumo, N., Luck, R., & Mago, P. J. (Jun 2011). Robustness of a Methodology for Estimating Hourly Energy Consumption of Buildings Using Monthly Electrical Bills. *Energy and Buildings*, *43*, 779-786.

## Task 1.19. Investigate the influence of altitude on the energy performance of combined cooling, heating, and power systems

**Description:**
*The Recipient shall determine the effect of altitude on the performance of CCHP systems as a consequence of the de-rated capacity of the components. Generally, specifications of equipment that comprise combined cooling, heating, and power systems are given by manufacturer for operation at sea level. If the system is designed without taking into consideration the effect of altitude due to change in air psychrometric (density and humidity ratio), the system performance will not be optimal.*

**Percentage of completion**: 100%

**Accomplishments:**

- The effect of altitude on the performance of CHP systems as a consequence of the de-rated capacity of the components has been determined.

- The outcomes from this task have been published in the Journal of Energy Conversion and Management.

  Generally, for CCHP systems' components, manufacturers include specifications on the performance of the equipment. However, these specifications are normally given for sea level operation. Changes in altitude affect the performance of any of the CCHP systems' components that are open to the atmosphere due to changes in the properties of the air, such as atmospheric pressure and humidity. This study focuses on considerations for CCHP systems design at altitude. The analysis covers the processes affected by altitude and their specific application on how to assess the performance of the individual components of CCHP systems when operating at altitude. This paper also summarizes the analysis by presenting equations that can be used in the design stage of CCHP systems in order to account for equipment capacity variation, or in simplified simulations such as those for screening tools, without having a detailed simulation that some times are not cost-effective due to the time and human effort to accomplish it.

  Equipment in CCHP systems that are affected by altitude include the power generation unit, the boiler, heat exchangers, the absorption chiller/ cooling tower, and any pump with the suction side open to the atmosphere. Due to reduction of air mass with altitude, components having a combustion process associated to them, such as the power generation unit and the boiler, will be negatively

affected. Effect of altitude on heat exchanger processes, such as the found in the exhaust heat exchanger and the air-blown cooler, are evaluated by computing the effectiveness at altitude. The cooling tower will experience a positive change in performance as the air will increase its ability to hold heat as altitude increases. This increase in cooling tower performance has a positive effect on the absorption chiller since the absorption chiller relies directly upon the cooling water inlet temperature. Pumps in the system which have suction-side reservoirs open to the atmosphere will not necessarily be affected negative or positively, but must be considered in the design of the system due to vaporization. If water starts to evaporate due to a decrease of pressure as consequence of altitude, a decrease of pump efficiency and damage to the impeller blades will be the consequences. The equations proposed to estimate performance of CCHP systems' equipment at altitude are presented as function of altitude. At the design stage, these equations can be used to estimate performance reduction in order to select equipment with higher capacity. For simulations, the equations can be incorporated in the code to assess the performance of CCHP systems at altitude.

**Publications / Presentations:**

*Journal Papers:*

1. Fumo, N., Mago, P. J., & Jacobs, K. (Jan 2011). Design Considerations for Combined Cooling, Heating, and Power Systems at Altitude. *Energy Conversion and Management, 52(2),* 1459-1469.

## Task 1.20. Develop and model a strategy for CHP operation for multiple facilities with several buildings

**Description:**

*The Recipient shall model multiple facilities sharing their CHP operation. A variety of strategies for sharing the electrical and thermal energy from PGUs distributed through the facilities will be researched or developed. The economical and environmental effects of sharing distributed CHP resources will be considered. In particular, the use of absorption refrigeration can be more effective when implementing larger units that can serve several smaller buildings.*

**Percentage of completion**: 100%

**Accomplishments:**

- A model to investigate the operation of a CHP system in a facility with several buildings is being investigated. A paper entitle: "Screening Tool for the Evaluation of Combined, Heating, and Power Systems in existing Office Buildings," was presented at the ASME 2012 6th International Conference on Energy Sustainability & 10th Fuel Cell Science, Engineering and Technology Conference, San Diego, CA. To promote the development of CCHP projects, it is important to facilitate, without any cost, a first order analysis of this technology to determine if a more cost intensive, in-depth analysis should be performed. This analysis can be done by using screening tools such as the CCHP Screening Tool for Existing Office Buildings (CCHP-ST-EOB) proposed in this study. Screening tools should be as accurate as possible while maintaining the simplicity of their data input in order to make it easy to use by a broad audience that may include building owners and managers without engineering background. In this sense, the CCHP-ST-EOB uses a methodology that translates energy consumption from utility bills as input into hourly energy consumption for a more accurate analysis of the matching between the demand and supply sides. This tool takes into consideration partial load efficiencies for the power generation unit and absorption chiller for a more realistic simulation of the system performance. Results are presented in terms of cost, primary energy consumption, and CO2 emission.

**Publications / Presentations:**

*Conference Papers:*

1. Fumo, N., Mago, P. J., & Spence, J. D. (July 2012). Screening Tool for the Evaluation of Combined, Heating, and Power Systems in existing Office Buildings. *ASME 2012 6th International Conference on Energy Sustainability & 10th Fuel Cell Science, Engineering and Technology Conference*, San Diego, CA.

## Task 1.21. Integrating CHP with technologies including passive and adaptive methods for load managing of buildings

**Description:**
*The Recipient shall investigate integration of CHP technology with a variety of passive and adaptive thermal and electric load managing methods for improved climate control of buildings. The goal is to demonstrate how integrating other energy saving technologies with CHP can obtain maximum benefit regarding energy consumption, cost, reliability, and reduced emissions. This research effort will consist in implementing strategies available for building climate and load managing methods in dynamic simulation models that incorporate CHP equipment.*

**Percentage of completion**: 100%

**Accomplishments:**

- A literature survey on the use of passive and adaptive technologies for improved climate control of buildings has been done. Most of the reviewed literature focused on control of blinds (radiation), windows (fresh air), and artificial intelligence techniques for control for lighting (based on occupation) and temperature control of individual rooms. It was concluded that one of the most effective approaches for thermal load management was that of load leveling through energy storage devices as performed in Task 1.14 which consisted on investigating the detailed implementation of energy storage devices.

- A finite difference simulation of a building wall with PCM was created and validated with experimental data from the literature. This model was used in a single room simulation with active control of the thermal load. While the PCM reduced the energy used in the evening, extra energy was required in the morning to reheat the PCM layer. Therefore, the building thermal load was not significantly reduced. These results led to the conclusion that it would be beneficial to decouple the PCM from the building.

- A TRNSYS model based on an Energy Plus model building was created and verified against the Energy Plus model in order to be modified for passive and adaptive load managing of buildings. The walls, ceilings, and floor of the TRNSYS building model are being modified to incorporate copper tubes. Fluid moving through the tubes will move heat between walls, ceilings, and floors and an energy storage tank with PCM material.

- A TRNSYS building model was developed to study the potential of using passive energy management through increased thermal capacitance (ITC) on the building cooling load by circulating water through a piping system located in the building walls or ceiling and then through a water storage tank. The cooling load obtained from the application of the

ITC on the building walls and the ceiling has been compared with the cooling load of a reference building without ITC. The reference building, which was located in Atlanta GA, as well as the building with the ITC were simulated in TRNSYS for the month of July. Several parameters that affect the performance of the proposed ITC were also analyzed, including the tank size, the mass flow rate of the working fluid, and initial working fluid temperature. In addition, the effect of the window-to-wall-ratio was analyzed for the ITC case in the walls and it was found that as the window-to-wall-ratio increases the amount of potential of the ITC to reduce the cooling load decreases.


Figure 1. Reference building model in TRNSYS

In order to establish the benefits of using ITC, a reference building model was used as a baseline for comparisons. Both, the reference building and the building with ITC were modeled in TRNSYS, which is a simulation program primarily used in the fields of renewable energy engineering and building simulation. Figure 1 shows the dynamic model generated in TRNSYS for the reference building. This model along with the input weather data was used to estimate the cooling and heating loads of the reference building. The building icon is called Type 56 Multizone building that can model thermal behavior of a building. Within the TNRSYS simulation environment, DOE's typical meteorological weather data (TMY2) is provided to the building model. TRNBuild, a building visual interface in TRNSYS, is used to characterize the reference-building model. During the simulation, TRNSYS calculates the heating and cooling loads for the building model.

The effect of ITC was determined by modifying the reference building to include proposed ITC in either the walls or the ceiling. Figure 2 illustrates the dynamic model of a building with the ITC added in either the walls or the ceiling. For this case, a piping system was inserted into the walls or into the ceiling to increase the thermal capacitance of these surfaces. The working fluid can either add or remove energy to the zone depending on its temperature. By adding or removing energy from the zone through increased thermal capacitance due to the liquid in the pipes and in the storage tank, the amount of heating or cooling required can be reduced, respectively. In order to establish the merit of this idea, a system presented in Figure 2 has been implemented in the model. This system consists of a single speed pump and a vertical tank connected to the building with the purpose of circulating water through the walls or the ceiling. The pump component in the TRNSYS simulation is used to control the working fluid flow rate for the entire system and as well as to transmit information such as water

temperature and flow rate to the building component. The building component calculates the water temperature change through the pipes in the walls and then conveys this data to the tank. A thermally insulated vertical tank with a single inlet and a single outlet was selected as the water storage tank. The insulated tank was assumed to be placed outside of the building and exposed to ambient weather conditions.

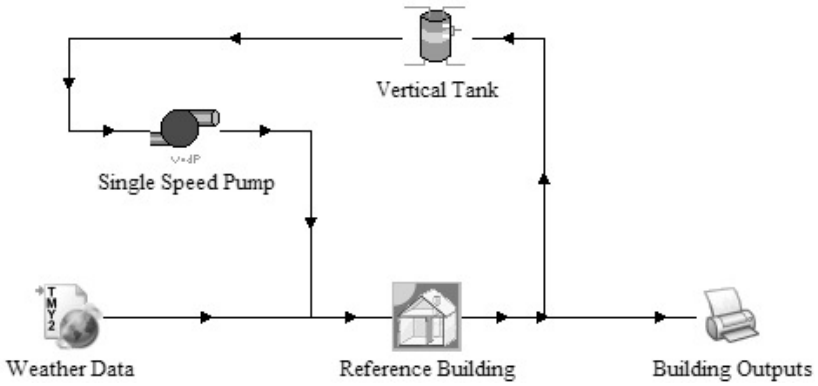


Figure 2. Schematic of the TRNSYS model with ITC on the walls or ceiling.

- A paper entitle: "Effect of different parameters on the performance of the passive energy management through increased thermal capacitance (ITC)," was published in the Energy and Buildings Journal.

- A paper entitle: "Parametric Analysis of Passive Energy Management Through Increased Thermal Capacitance," was submitted for publication in the Energy and Buildings Journal [J2]. This paper evaluates the influence of several parameters on the potential of using increased thermal capacitance (ITC) as a passive energy management system to decrease the building cooling load by circulating water from a storage tank through a piping system located in the building's ceiling. The cooling load of the ITC enhanced building is compared to the cooling load of a reference building that is without any form of ITC. The transient system simulation software TRNSYS is used to simulate both the ITC enhanced building and the reference building. Then several parameters that affect the performance of the ITC are analyzed, including the pipe material, pipe wall thickness, location of pipe in the ceiling, and the specific heat of the working fluid. As a whole, the results reveal that the application of ITC reduces the cooling load, with the best scenario being a piping system located near the interior of the building.

**Publications / Presentations:**

*Journal Papers:*

1. Carpenter, J., Mago, P.J., Luck, R., and Cho, H. (2014). Passive Energy Management Through Increased Thermal Capacitance, *Energy and Buildings*, 75, 465-471.

2. Carpenter, J, Mago, P.J., Luck, R., & Cho, H. Parametric Analysis of Passive Energy Management Through Increased Thermal Capacitance, *Energy and Buildings. Under Review.*

## Task 1.22. Analysis of the use of organic Rankine cycle (ORC) as waste heat recovery technique to be used in CHP system applications

**Description:**

*The Recipient shall study the energetic, economical, and environmental performance of a combined CHP-ORC system and compare its performance to a stand-alone CHP system and a reference building for different climate zones. When the recovered exhaust heat is more than the heat required, the excess is usually discarded to the atmosphere. An ORC can be used to recover the surplus exhaust heat to generate extra electricity. Therefore, combining the ORC system with the CHP system reduces the electricity that has to be produced by the CHP system, thereby reducing the total primary energy, cost, and overall emissions.*

**Percentage of completion**: 100%

**Accomplishments:**

- A model to determined the energy, economic, and environmental performance of CHP-organic Rankine cycle (ORC) and CCHP-ORC systems has been developed. The systems were modeled under the operational strategies of FEL and FEL/OFF and the economic, energetic, and environmental performance was determined for the city of Boulder, Colorado. These results were published in the IMechE Journal of Power and Energy.
    - It was found that under the FEL operation, the addition of an ORC to either the CHP or CCHP system lowered the operational costs, PEC, and CDE by about 12 per cent, 13 per cent, and 17 per cent, respectively, from the stand-alone system. Also, the addition of an ORC is more beneficial to a CHP system when it is operated FEL. However, the performances of the CHP-ORC and CCHP-ORC systems under FEL do not outperform the reference building. The costs and PEC are about 15 per cent and 10 per cent higher, respectively, while reductions in CDE of about 20 per cent are possible for both systems.
    - Under the FEL/OFF operation, the addition of an ORC lowers the cost, PEC, and CDE from the respective stand-alone system operating under the same strategy. The FEL/OFF provides reductions in cost and PEC compared to the FEL strategy. The FEL/OFF operation yields approximately 15 per cent lower costs and 11 per cent lower PEC. The addition of an ORC is more beneficial to a CCHP system while minimizing cost or PEC; while the addition of an ORC is more beneficial to a CHP system while minimizing CDE. Only the FEL/OFF-minimize cost and FEL/OFF-minimize PEC strategies could reduce cost and PEC below the levels of the reference building.

- The exhaust waste heat recovery potential of a microturbine (MT) using an organic Rankine cycle (ORC) has been examined. These results were published in a paper

entitled: “Energetic And Exergetic Analysis Of Waste Heat Recovery From A Micro-Turbine Using Organic Rankine Cycles.”

- 
    - It was determined that possible improvements in electric and exergy efficiencies as well as specific emissions by recovering waste heat from the MT exhaust gases. Different dry organic working fluids have been considered during the evaluation (R113, R123, R245fa, and R236fa). In general, it has been found that the use of an ORC to recover waste heat from MTs improves the combined electric and exergy efficiencies for all the evaluated fluids, obtaining increases of an average of 27% when the ORC was operated using R113 as the working fluid. It has also been found that higher ORC evaporator effectiveness values correspond to lower pinch point temperature differences and higher exergy efficiencies. Three different MT sizes were evaluated, and the results indicate that the energetic and exergetic performance as well as the reduction of specific emissions of a combined MT-ORC is better for small MT power outputs than for larger MTs.

- A model to evaluation of the potential use of a combined micro-turbine organic Rankine cycle for different geographic locations has been developed and a paper has been submitted for review in the Applied Energy Journal : “Evaluation of the Potential Use of a Combined Micro-Turbine Organic Rankine Cycle for Different Geographic Locations.”

    This paper presents an analysis to determine the economic, energetic, and environmental potential benefits that can be obtained from the implementation of a combined micro-turbine organic Rankine cycle (MT-ORC) versus a simple micro-turbine or a topping-cycle combined heat and power (CHP) system. The analysis was performed for sixteen different geographic locations using micro-turbines of sizes 30, 65, and 200 kW. It is found that for some cities where the use of a micro-turbine is not cost effective, the combination of MT-ORC is a viable alternative to grid power. Results also show that, for the micro-turbines considered, in terms of the total electric power, the ones with smaller power levels benefit the most (percentagewise) when combining them with an ORC. Finally, a minimum bound for the power-to-heat ratio of a building that results in MT-ORC operation being superior to that of CHP operation, is obtained.

- A model was developed to analyze and optimize the Use of CHP-ORC systems for small commercial buildings. The results from this model were published in the Energy and Buildings Journal: “Analysis and Optimization of the Use of CHP-ORC Systems for Small Commercial Buildings.”

    The use of combined heating and power (CHP) systems is increasing rapidly due to their high potential of reducing primary energy consumption (PEC), cost, and carbon dioxide emissions (CDE). These reductions are mainly due to capturing the exhaust heat to satisfy the thermal demand of a building. However, when the

CHP system is operated following the electric load, the recovered exhaust heat may or may not be sufficient to satisfy the thermal demand of the facility. When the recovered exhaust heat is more than the heat required, the excess is usually discarded to the atmosphere. An organic Rankine cycle (ORC) can be used to recover the surplus exhaust heat to generate extra electricity. Therefore, combining the ORC system with the CHP system (CHP–ORC) reduces the electricity that has to be produced by the CHP sys- tem, thereby reducing the total PEC, cost, and CDE. The objective of this paper is to study the energetic, economical, and environmental performance of a combined CHP–ORC system and compare its perfor- mance to a standalone CHP system and a reference building for different climate zones. A comparison of a CHP–ORC system operating 24 h with a system operating during typical office hours is also performed.

**Publications / Presentations:**

*Journal Papers:*

1. Hueffed, A., & Mago, P. J. (Feb 2011). Energy, Economic, and Environmental Analysis of Combined Heating and Power-organic Rankine Cycle and Combined Cooling, Heating, and Power-organic Rankine Cycle Systems. *IMechE Journal of Power and Energy, 225(1),* 24-32.

2. Mago, P. J., & Luck, R. (2013). Energetic And Exergetic Analysis Of Waste Heat Recovery From A Micro-Turbine Using Organic Rankine Cycles. International Journal of Energy Research, 37(8), 888-898.

3. Mago, P. J., & Luck, R. Evaluation of the Potential Use of a Combined Micro-Turbine Organic Rankine Cycle for Different Geographic Locations. *Applied Energy, Under Review*

4. Mago, P. J., Hueffed, A., & Chamra, L. (Sep 2010). Analysis and Optimization of the Use of CHP-ORC Systems for Small Commercial Buildings. *Energy & Buildings*, *42*(9), 1491-1498.

## Students Involved in Task 1.0

*Ph.D. Students*

1. Fumo, N. (Summer 2008). "Cooling, Heating, and Power Systems Energy Performance and Non-Conventional Evaluation Based On Energy Use."
2. Weathers, J. (2008). "Verification and Validation of Micro-CHP Simulation at multiple levels."
3. Cho, H. (2009). "Dynamic Simulation and Optimal Real-Time Operation of CHP Systems for Buildings."
4. Hueffed, A. (Spring 2010). "Analysis and Optimization of CHP, CCHP, CHP-ORC, and CCHP-ORC Systems."
5. Giffin, P. (Spring 2010). "Energy Analysis of a Micro-CHP Demonstration Facility."
6. Wheeley, C. (Fall 2011). "Experimental Study and Feasibility of an Stirling Engine-CHP System."
7. Smith, A. (Fall 2012). "Combined Heat and Power Systems for Commercial Buildings: Investigating Cost, Emissions, and Primary Energy Reduction Based on System Components."
8. Yun, K. (Spring 2012). "Optimal PGU Operation Strategy in CHP Systems."
9. Smith, A. (Fall 2012). "Methodologies for Addressing Errors and Uncertainty in CHP System Modeling."
10. Knizley, A. (Summer 2013). "Evaluation of Dual Power CHP System Operation in Different Types of Commercial Buildings."
11. Long, W. (Fall 2015). "Using Modular Uncertainty Analysis to Evaluate the Performance of Energy Systems."
12. Ledbury, E. (Fall 2015). "Evaluation of a Solar Powered Organic Rankine Cycle."

*Masters Students*

1. Giffin, P. (2008). "Instrumentation of a Micro-CCHP Demonstration Facility."
2. Ramsay, J. (Fall 2008). "Evaluation of Propane Fueled Combined Heating and Power Systems for Small Commercial Applications."
3. Crespo, R. (Spring 2009). "Evaluation of Energy Usage in the Chemical Industry and Effective Measures to Reduce Energy Losses."
4. Withmire, B. (Spring 2009). "Optimization of Combined Cooling, Heating, and Power Systems (CCHP) Operational Strategies for Different Climate Conditions."
5. Wrigth, B. (Summer 2010). "Case Studies in Industrial Energy Efficiency Measure"
6. Welsh, J. (Spring 2012). "Town Branch Waste Water Treatment Plant: CHP Feasibility Assessment."
7. Thomas, R. (Fall 2013). "Simulation of CHP and CCHP System under Different Operation Strategies."

8. Rhodes, C. (Spring 2013). “CHP Feasibility for Tronox Hamilton Operations.”
9. Carpenter, J. (Spring 2014). “Passive Energy Management Through Increase Thermal Capacitance.”

## Publications - Task 1.0

*Journal Papers:*


1. Knizley, A., Mago, P.J., Smith, A.D. (2014). Evaluation of the performance of combined cooling, heating, and power systems with dual power generation units, Energy Policy, Volume 66, pages 654-665.

2. Carpenter, J., Mago, P.J., Luck, R., and Cho, H. (2014). Passive Energy Management Through Increased Thermal Capacitance, *Energy and Buildings*, 75, 465-471.

*3.* Carpenter, J, Mago, P.J., Luck, R., & Cho, H. Parametric Analysis of Passive Energy Management Through Increased Thermal Capacitance, *Energy and Buildings. Under Review.*

4. Mago, P. J., & Luck, R. (2013). Energetic And Exergetic Analysis Of Waste Heat Recovery From A Micro-Turbine Using Organic Rankine Cycles. *International Journal of Energy Research*, 37 (8), 888–898.

5. Mago, P. J., & Luck, R. (2013). Evaluation of the Potential Use of a Combined Micro-Turbine Organic Rankine Cycle for Different Geographic Locations. *Applied Energy,* 102, 1324-1333

6. Mago, P. J., Luck, R. and Knizley, A. (2013), Combined heat and power systems with dual power generation units and thermal storage. *International Journal of Energy Research*. doi: 10.1002/er.3089.

7. Mago, P. J., and Luck, R. (Jan 2012). Prime Mover Sizing for Based-Loaded Combined Heating and Power Systems. *IMechE Journal of Power and Energy*, *226*(1), 17-27.

8. Mago, P. J., & Smith, A. (Jul 2012). Evaluation of the Potential Emissions Reductions from the Use of CHP Systems in Different Commercial Buildings. *Building and Environment, 53, 74–82*

9. Yun, K., Luck, R., Mago, P. J., & Smith, A. (Jan 2012). Analytic Solutions for Optimal Power Generation Unit Operation in Combined Heating and Power Systems. *ASME Journal of Energy Resources Technology*, *134*(1), 011301(8 pages).

10. Wheeley, C., Mago, P. J., & Luck, R. (Jan 2012). Methodology to Perform a Combined Heating and Power System Feasibility Study for Industrial Manufacturing Facilities. *Distributed Generation and Alternative Energy Journal*, *27*(1), 8-32.

11. Mago, P. J., Luck, R., & Smith, A. (Nov 2011). Environmental Evaluation of Base-Loaded CHP Systems for Different Climate Conditions in the US. *International Journal of Ambient Energy*, *32*(4), 203-214.

12. Yun, K.4, Luck, R., Mago, P. J., & Cho, H. (2012). Building Hourly Thermal Load Prediction using an Indexed ARX model. Energy and Buildings, 54, 225-233.

13. Fumo, N., Mago, P. J., & Smith, A. (Dec 2011). Analysis of Combined Cooling, Heating, and Power Systems Operating Following the Electric Load and Following the Thermal Load Strategies with No Electricity Exporting. *Journal of Power and Energy*, *225*(8), 1016-1025.

14. Mago, P. J., & Luck, R. (2013). Evaluation of a Base-Loaded Combined Heating and Power System with Thermal Storage for Different Small Buildings Applications. *International Journal of Energy Research*, 37(2), 179-188.

*15.* Smith, A., Luck, R., & Mago, P.J. (2012). Integrated Parameter Estimation of Multicomponent Thermal Systems with Demonstration on a Combined Heat and Power System. *ISA Transactions,* 51(4):507-13.

16. Yun, K.4, Cho, H., Luck, R., & Mago, P. J. (2011). Real Time Combined Heat and Power (CHP) Operational Strategy Using a Hierarchical Optimization Algorithm. *Journal of Power and Energy*, 225, 403-412.

17. Wheeley, C., Mago, P. J., & Luck, R. (Dec 2011). A Comparative Study of the Economic Feasibility of Employing CHP Systems in Different Industrial Manufacturing Applications. *Energy and Power Engineering*, *3*, 630-640.

18. Hueffed, A., & Mago, P. J. (Feb 2011). Energy, Economic, and Environmental Analysis of Combined Heating and Power-organic Rankine Cycle and Combined Cooling, Heating, and Power-organic Rankine Cycle Systems. *IMechE Journal of Power and Energy*, *225*(1), 24-32

19. Yun, K., Cho, H., Luck, R., & Mago, P. J. (Jun 2011). Real Time Combined Heat and Power (CHP) Operational Strategy Using a Hierarchical Optimization Algorithm. *Journal of Power and Energy*, *225*, 403-412.

20. Fumo, N., Mago, P. J., & Jacobs, K. (Jan 2011). Design Considerations for Combined Cooling, Heating, and Power Systems at Altitude. *Energy Conversion and Management*, *52*(2), 1459-1469.

21. Smith, A., Fumo, N., & Mago, P. J. (Feb 2011). Spark Spread - A Screening Parameter for Combined Heating and Power Systems. *Applied Energy*, *88*, 1494-1499.

22. Smith, J. A., Fumo, N., Luck, R., & Mago, P. J. (Jun 2011). Robustness of a Methodology for Estimating Hourly Energy Consumption of Buildings Using Monthly Electrical Bills. *Energy and Buildings*, *43*, 779-786.

23. Mago, P. J., & Hueffed, A. (Jun 2010). Evaluation of a Turbine Driven CCHP System for Large Office Buildings under Different Operating Strategies, Energy, and Buildings. *Journal of Power and Energy*, *42*(10), 1628-1636.

24. Mago, P. J., Chamra, L., & Ramsay, J. (Mar 2010). Micro-combined Cooling, Heating and Power Systems Hybrid Electric-thermal Load Following Operation. *Applied Thermal Engineering*, *30*(8-9), 800-806.

*25.* Weathers, J.B., Luck, R., Weathers, J.W. "A Modular Approach to Uncertainty Analysis", *ISA Transactions*, 49, pp. 19-26, 2010

26. Mago, P. J., Hueffed, A., & Chamra, L. (Sep 2010). Analysis and Optimization of the Use of CHP-ORC Systems for Small Commercial Buildings. *Energy & Buildings*, *42*(9), 1491-1498.

27. Fumo, N., Mago, P. J., & Luck, R. (Oct 2010). Methodology to Estimate Building Energy Consumption Using EnergyPlus Benchmark Models. *Energy and Buildings*, *42*, 2331-2337.

28. Hueffed, A., & Mago, P. J. (Jun 2010). Influence of Prime Mover Size and Operational Strategy on the Performance of CCHP Systems under Different Cost Structures. *IMechE Journal of Power and Energy*, *224*(5), 591-605.

29. Smith, A., Luck, R., & Mago, P. J. (Sep 2010). Analysis of a CCHP System Model Under Different Operating Strategies with Input and Model Data Uncertainty. *Energy and Buildings*, *42*, 2231-2240.

30. Mago, P. J., & Chamra, L. (May 2009). Analysis and Optimization of CCHP Systems Based on Energy, Economical and Environmental Considerations. *Energy and Buildings*, *41*, 1099-1106.

31. Mago, P. J., Chamra, L., & Hueffed, A. (May 2009). A Review on Energy, Economical, and Environmental Benefits of the Use of CHP Systems for Small Commercial Buildings

for the North American Climate. *International Journal of Energy Research*, *33*, 1252-1265.

32. Cho, H., Luck, R., S.D. Eksiouglu, Chamra, L. M., "Cost-optimized real -time operation of CHP systems," Energy and Buildings, Vol. 41, No. 4, April, pp. 445-451, 2009.

33. Fumo, N., Mago, P. J., & Chamra, L. (Jun 2009). Analysis of Cooling, Heating, and Power Systems Based on Site Energy Consumption. *Applied Energy*, *86*(6), 928-932.

34. Mago, P. J., Fumo, N., & Chamra, L. (Jun 2009). Performance Analysis of CCHP and CHP Systems Operating Following the Thermal and Electric Load. *International Journal of Energy Research*, *33*, 852-864.

35. Fumo, N., Mago, P. J., & Chamra, L. (Sep 2009). Energy and Economic Evaluation of Cooling, Heating, and Power Systems Based on Primary Energy. *Applied Thermal Engineering*, *29*(13), 2665-2671.

*36.* Weathers, J.B., Luck, R., Weathers, J.W., "An Exercise in Model Validation: Comparing Univariate Statistics and Monte-Carlo based Multivariate Statistics", *Reliability Engineering and System Safety*, Volume 94, Issue 11, November 2009, Pages 1695-1702.

37. Cho, H., Mago, P. J., Luck, R., & Chamra, L. (Oct 2009). Evaluation of CCHP Systems Performance Based on Operational Cost, Primary Energy Consumption, and Carbon Dioxide Emission by Utilizing an Optimal Operation Scheme. *Applied Energy*, *86*, 2540-2549.

*38.* Cho, H., Krishnan, S.R., Luck, R. and Srinivasan, K.K. Comprehensive uncertainty analysis of a Wiebe function-based combustion model for pilot-ignited natural gas engines. *Proc. IMechE, Part D: J. Automobile Engineering,* Vol. 223, No. 11, 2009

39. Fumo, N., Mago, P. J., & Chamra, L. (Nov 2009). Emission Operational Strategy for Combined, Cooling, and Power Systems. *Applied Energy Journal*, *86*(11), 2344-2350.

40. Hueffed, A., Chamra, L., & Mago, P. J. (May 2009). A Simplified Model of Heat and Mass Transfer Between Air and Falling-Film Desiccant in Parallel-Plate Humidifier. *ASME Journal of Heat Transfer*, *131*, 0520011-0520017.

41. Fumo, N., Mago, P. J., & Chamra, L. (Jul 2009). Hybrid-cooling Combined Cooling, Heating, and Power Systems. *IMechE Journal of Power and Energy*, *223*(5), 761-770.

*Book Chapters:*

1. Fumo, N., Mago, P. J., & Chamra, L. (Sep 2009). Energy and Economic Evaluation of Cooling, Heating, and Power Systems Based on Primary Energy. *Applied Thermal Engineering, 29(13),* 2665-2671.

2. Mago, P. J., & Hueffed, A. (May 2011). Energy, Economic, And Environmental Analysis of CHP and CCHP Systems. Morena J. Acosta (Eds.), *Advances in Energy Research - Volume 7*, New York: Nova Science Publishers, Inc., 229-271. ISBN: 978-1-61122-956-1. (Invited).

3. Mago, P. J., Luck, R., & Smith. (2013). Evaluation of the Potential Carbon Dioxide Emissions Reductions from the Use of CHP Systems in Commercial Buildings. Mitchell Carpenter and Everett J. Shelton (Eds.), Carbon Dioxide Emissions: New Research, New York: Nova Science Publishers, Inc. 61-76. ISBN: 978-1-62257-436-0. (Invited).

*Conference Papers:*

1. Cho, H., Luck, R., Eksioglu, S.D., Chamra, L. M., "Operation of a CCHP System using an Optimal Energy Dispatch Algorithm." *ASME Proceedings of Energy Sustainability* 2008, August 10-13, Jacksonville, FL.

2. Robert Thomas, Rogelio Luck, and Pedro J. Mago, "Optimal Power Generation Unit Sizing and Cost Savings Methodology Using Monthly vs. Hourly Time-steps Applied to Base-Loaded Combined Heat and Power Systems", *ASME International Mechanical Engineering Congress and Exposition (IMECE2012)*, Houston, TX

3. Fumo, N., & Mago, P. J. (May 2010). Tools for Small Office Buildings Energy Consumption Estimation. *ASME Energy Sustainability 2010 - Paper No. ES2010-90135*, Phoenix, Arizona.

4. Cho, H., Luck, R., Mago, P. J., & Chamra, L. (Jul 2009). Assessment of CHP System Performance with Commercial Building Benchmark Models in Different U.S. Climate Zones. *ASME Proceedings of Energy Sustainability 2009*, San Francisco, CA.

5. Fumo, N., Mago, P. J., & Chamra, L.M., (July 2008). Effect of the Power Generation Unit Size on the Energy Performance of Cooling, Heating, and Power Systems. *ASME Power Conference, Paper No. PWR2008-60057*, Orlando, FL, 635-640.

6. Smith, A. & Mago, P. J. (July 2012). Impact of Thermal Storage Option for CHP Systems on the Optimal Prime Mover Size and the Need for Additional Heat

Production. *ASME 2012 6th International Conference on Energy Sustainability & 10th Fuel Cell Science, Engineering and Technology Conference*, San Diego, CA.

7. Fumo, N., Mago, P. J., & Spence, J. D. (July 2012). Screening Tool for the Evaluation of Combined, Heating, and Power Systems in existing Office Buildings. *ASME 2012 6th International Conference on Energy Sustainability & 10th Fuel Cell Science, Engineering and Technology Conference*, San Diego, CA.

8. Hueffed, A., Mago, P. J., & Chamra, L. (Nov 2009). Effect of the Power Generation Unit Operation on the Energy, Economical, and Environmental Performance of CCHP Systems for Small Commercial Building. *ASME International Mechanical Engineering Congress and Exposition (IMECE2009),* Orlando, FL.

9. Knizley, A. & Mago, P. J. (July 2012). Evaluation of Combined Heat and Power (CHP) Systems Performacne with Dual Power Generation Units. *ASME 2012 6th International Conference on Energy Sustainability & 10th Fuel Cell Science, Engineering and Technology Conference*, San Diego, CA.

*Dissertations*

1. Fumo, N. (2008). "Cooling, Heating, and Power Systems Energy Performance and Non-Conventional Evaluation Based On Energy Use." Mississippi State University.

2. Weathers, J. (2008). "Verification and Validation of Micro-CHP Simulation at multiple levels." Mississippi State University.

3. Cho, H. (2009). "Dynamic Simulation and Optimal Real-Time Operation of CHP Systems for Buildings." Mississippi State University.

4. Hueffed, A. (2010). "Analysis and Optimization of CHP, CCHP, CHP-ORC, and CCHP-ORC Systems." Mississippi State University.

5. Giffin, P. (2010). "Energy Analysis of a Micro-CHP Demonstration Facility." Mississippi State University.

6. Harrod, J. (2010). "The Stirling Engine: Thermodynamics and Applications in Combined Cooling, Heating, and Power Systems." Mississippi State University.

7. Wheeley, C. (2011). "Experimental Study and Feasibility of an Stirling Engine-CHP System." Mississippi State University.

8. Smith, A. (2012). "Combined Heat and Power Systems for Commercial Buildings: Investigating Cost, Emissions, and Primary Energy Reduction Based on System Components." Mississippi State University.

9. Yun, K. (2012). "Optimal PGU Operation Strategy in CHP Systems." Mississippi State University.

10. Smith, A. (2012). "Methodologies for Addressing Errors and Uncertainty in CHP System Modeling." Mississippi State University.

11. Knizley, A. (2013). "Evaluation of Dual Power CHP System Operation in Different Types of Commercial Buildings." Mississippi State University.

*Posters:*

1. Fumo, N., Mago, P. J., and Chamra, L. M. (Apr 2009). Hybrid-Cooling, Combined Cooling, Heating, and Power Systems. *2nd Energy-Synergy Workshop,* Mississippi State University.

2. Cho, H., Luck, R., Chamra, L.M., "Supervisory Feed-Forward Control of Building CHP Systems Using Short-Term Weather Forecasting", Poster presentation in International Building Performance Simulation Association (IBPSA) – USA meeting, January 24, 2009, Chicago, IL, USA

# Summary of Project Activities

## Task 2. Fuel Flexibility In Micro-CHP Applications

## Task 2.1 - Optimize efficiency of the MSU micro-CHP natural gas fired IC engine genset

**Description:** *The Recipient shall identify optimum strategies, including adopting novel ignition systems and modified compression ratios to achieve optimum performance and to improve the fuel conversion efficiency of the MSU micro-CHP natural gas engine for optimal performance at full load operation. Independent dynamometer tests will be performed on a single cylinder research engine to provide experimental data for optimal operation. The optimal strategies will be identified and implemented in the MSU micro-CHP IC engine, and the performance documented.*

**Percentage of completion**: 100%

**Accomplishments:**

Recognized that many IC engines used for CHP applications are not optimized for best efficiency-emissions tradeoffs

- For natural gas fired CHP gensets, it is concluded that spark ignition is not the most conducive ignition strategy for high efficiencies.

- Dual fuel combustion with small (pilot) diesel sprays acting as the ignition source was identified as a viable alternative to spark ignition. The paper titled, "C.M. Gibson1, A. Polk1, N. Shoemaker1, K.K. Srinivasan, and S.R. Krishnan (2011). Comparison of propane and methane performance and emissions in a turbocharged direct injection dual fuel engine. Trans. ASME: Journal of Engineering for Gas Turbines and Power, 133(9), Article GTP-092806, (DOI: 10.1115/1.4002895)," discusses the efficiency-emissions benefits from dual fuelling.

- An existing multi-cylinder engine setup has been modified for dual fuel operation with alternative fuels such as natural gas and propane. Most of the required instrumentation such as temperature and pressure sensors, flow meters, and data acquisition hardware has been installed and calibrated. An integrated emissions bench has been ordered for simultaneous measurement of exhaust emissions including CO, CO2, O2, NOx, and HC during dynamometer testing of engines. Dual fuel experiments are planned on single/multi-cylinder engines with diesel pilot ignition of natural gas and/or propane. The knowledge gained in these experiments will be translated to the MSU micro-CHP natural gas fired IC engine.

- A Volkswagen 1.9 L TDI engine was instrumented with flow, temperature and pressure sensors. The fuel injector corresponding to cylinder number three looking from the

flywheel side was also instrumented with a needle-lift sensor. This enables the identification of start of injection event when using different fuels such as biodiesel, hydrodeoxygenated biooil etc.

- A diesel engine generator was commissioned and installed at the CHP demonstration center. This installation enables the implementation of multiple fuels including diesel, biodiesel, propane and natural gas. Experiments to optimize fuel (natural gas and diesel) delivery were investigated on a similar engine coupled to a dynamometer test stand. Dynamometer experiments were conducted to identify the optimal diesel-natural gas ratio fuelling strategies to allow for increased thermal efficiency of the engine and optimized heat recovery from the exhaust.

- The diesel engine generator installed and commissioned at the CHP demonstration center was operated during the period of inclement weather at Mississippi and useful data regarding the effect of external conditions on fuel consumption and exhaust and coolant waste heat recovery were obtained

- The optimal strategies has been identified and implemented in the MSU micro-CHP IC engine.

**Publications / Presentations:**

*Journal Papers:*


1. M.M. Tripathi, S.R. Krishnan, K.K. Srinivasan, F.-Y. Yueh, J.P. Singh (2011). "Chemiluminescence-based multivariate sensing of local equivalence ratios in premixed atmospheric methane-air flames," Fuel, doi:10.1016/j.fuel.2011.08.038

2. C.M. Gibson[1], A. Polk[1], N. Shoemaker[1], K.K. Srinivasan, and S.R. Krishnan (2011). Comparison of propane and methane performance and emissions in a turbocharged direct injection dual fuel engine. Trans. ASME: Journal of Engineering for Gas Turbines and Power, 133(9), Article GTP-092806, (DOI: 10.1115/1.4002895)

3. S. R. Krishnan and K. K. Srinivasan (2010). Multi-Zone Modeling of Partially Premixed Low Temperature Combustion in Pilot-Ignited Natural Gas Engines. Proc. Instn. Mech. Engrs.: Part D: Journal of Automobile Engineering, 224, pp. 1597-1622 (DOI 10.1243/09544070JAUTO1472) (This paper won the 2010 SAGE Best Paper Award by the Editor and Editorial Board of Proceedings of the Institution of Mechanical Engineers, Part D: Journal of Automobile Engineering)

4. K. K. Srinivasan, P. J. Mago, S. R. Krishnan (2010) "Analysis of Exhaust Waste

Heat Recovery from a Dual Fuel Low Temperature Combustion Engine using an Organic Rankine Cycle," Energy, Vol. 35, pp. 2387-2399, doi:10.1016/j.energy.2010.02.018

*Conference Papers:*

1. N. Shoemaker[1], C.M. Gibson[1], A. Polk[1], K.K. Srinivasan, and S.R. Krishnan, 2011, "Performance and Emissions Characteristics of Bio-Diesel Ignited Methane and Propane Combustion in a Four Cylinder Turbocharged Compression Ignition Engine," Paper No. ICEF2011-60081, (accepted) Proceedings of the ASME IC Engines Division 2011 Fall Technical Conference (ICEF2011), October 2-5, Morgantown, West Virginia, USA, *Presenter – C. M. Gibson*

2. A. Polk[1], C.M. Gibson[1], N. Shoemaker[1], S.R. Krishnan, and K.K. Srinivasan, 2011, "Analysis of Ignition Delay Behavior in a Dual Fuel Turbocharged Direct Injection Engine Using Propane and Methane as Primary Fuels," Paper No. ICEF2011-60080, (accepted) Proceedings of the ASME IC Engines Division 2011 Fall Technical Conference (ICEF2011), October 2-5, Morgantown, West Virginia, USA, *Presenter – A C Polk*

3. C.M. Gibson[1], A. Polk[1], N. Shoemaker[1], K.K. Srinivasan, and S.R. Krishnan, 2010, "Comparison of Propane and Natural Gas Performance and Emissions in a Turbocharged Direct Injection Dual Fuel Engine," Paper No. ICEF2010-35128, Proceedings of the ASME IC Engines Division 2010 Fall Technical Conference (ICEF2010), September 12-15, San Antonio, TX; *Presenter – C. M. Gibson*

*Posters:*

1. Wang, Z., Srinivasan, K. K., Krishnan, S. R., Som, S. "A computational investigation of diesel and biodiesel combustion and NOx formation in a light-duty compression ignition engine," To be presented at the Central States Meeting of the Combustion Institute, Hosted by the University of Dayton, Dayton, OH, April 22-24, 2012.

2. M.M. Tripathi, S.R. Krishnan, K.K. Srinivasan, F.-Y. Yueh, J.P. Singh, "Development of a Robust Sensor for Monitoring Equivalence Ratio in Premixed Flames Using Chemiluminescence and Multivariate Data Analysis," presented at the 7th US National Technical Meeting of the Combustion Institute, Hosted by the Georgia Institute of Technology, Atlanta, GA, March 20-23, 2011.

3. A.A. Knizley, K.K. Srinivasan, S.R. Krishnan, "Fuel and Diluent Effects on Entropy Generation in a Constant Internal Energy-Volume (UV) Combustion Process,"

presented at the 7th US National Technical Meeting of the Combustion Institute, Hosted by the Georgia Institute of Technology, Atlanta, GA, March 20-23, 2011.

## Task 2.2- Demonstrate and optimize a multi-fuel compression ignition engine for micro CHP applications

### *Task 2.2.1 Demonstrate operation of a multi-fuel engine powered micro CHP system*

**Description:** *The Recipient shall acquire, commission, and demonstrate a multi-fuel engine for use in the MSU micro-CHP facility. Subtask 2.2.1.1. Dual fuel experiments on the multi-fuel compression ignition engine genset in the CHP facility at MSU: The Recipient shall modify the engine genset setup to facilitate the performance of dual fuel experiments. New flow meter and allied instrumentation to measure gaseous fuel flow rates will be installed. In addition, dual fuel combustion experiments with diesel as the pilot fuel and a gaseous fuel (e.g., natural gas, propane, etc.) as the main fuel will be performed. This will allow quantifying CHP performance and overall efficiencies with dual fuel combustion*

### *Task 2.2.2 Optimize the efficiency and reduce exhaust emissions from multi-fuel engine*

**Description:**
*The Recipient shall optimize geometric and combustion parameters for a single-cylinder research engine operating on multiple fuels, which may include conventional petroleum-based fuels, natural gas, propane, and bio-based fuels. The best operating point in terms of fuel conversion efficiency and exhaust emissions, including carbon dioxide, will be determined for each fuel. Baseline conditions will be established for each fuel in the multi-fuel engine. A matrix of fuel injection strategies will be investigated to achieve optimal fuel conversion efficiencies with minimal exhaust emissions. Results from the single-cylinder engine will be transferred to the multi fuel engine in the CHP demonstration facility to assess the real time performance of the entire multi fuel micro CHP system*

**Percentage of completion**: 100%

**Accomplishments:**

- A Volkswagen 1.9L TDI industrial diesel engine was modified for dual fuel operation with diesel-ignited propane and diesel-ignited natural gas. The required instrumentation was procured and calibrated.

- Preliminary dual fuel experiments were performed on an existing Volkswagen TDI multi-cylinder industrial engine to set the baseline for further optimization studies. In these experiments, diesel was used to ignite premixed propane-air mixtures over a range

of engine operating conditions. It was found that the maximum amount of propane that could be substituted was at best about 57% at very low loads (75 N-m torque) with higher NOx emissions compared to straight diesel fueling at these conditions (about 20% increase). At higher torques (100 N-m), the maximum amount of propane substituted was about 20%; however NOx emissions were reduced at these conditions (about 15% compared to straight diesel). Propane substitutions beyond this limit were impossible at these loads owing to instability in engine operation indicated by high torque fluctuations.

- A turbocharged 4 cylinder Yanmar compression ignition engine was purchased. An extra cylinder head has been purchased to enable fixing a pressure transducer in communication with the combustion chamber to acquire cylinder pressure data. This data was used to estimate heat release rates while combusting different fuels and optimize injection timing and other initial conditions to achieve optimal performance and reduced emissions. In addition, another multifuel engine has been purchased and set up for demonstration in the CHP demonstration site. It is currently being operated on diesel fuel. But, it can operated to run on dual fuel mode to burn syngas, propane or natural gas, with very little modifications. The VW TDI engine was instrumented with flow, temperature and pressure sensors. In addition, the engine was instrumented with a cylinder pressure transducer to acquire instantaneous combustion pressure. The five gas emissions bench was installed and commissioned and is coupled to the VW TDI to acquire steady state emissions of nitrogen oxides, carbon dioxide, carbon monoxide, unburned hydrocarbons etc.

- The four-cylinder Volkswagen diesel engine was installed on a dynamometer. Data of engine performance and emissions have been acquired from this engine for diesel and diesel-propane dual fuel operation. These results show the potential of diesel-propane dual fuel operation to reduce NOx, smoke, and $CO_2$ emissions with some efficiency penalty. Some of the main findings included:

    - Maximum Propane Substitution: The maximum propane substitution for dual fuel propane operation was 91% at 3/4 load (100 Nm), on an energy basis, i.e., of the total fuel chemical energy supplied to the engine, 91% was obtained from propane and 9% was obtained from diesel.
    - Full Load Operation: The maximum 4/4 load (134 Nm) brake thermal efficiency obtained from 90% propane substitution was 31.3% compared to 36.7% for straight diesel operation. The reason for the lower efficiency with propane operation is likely due to the reduction of volumetric efficiency with increasing propane substitution and the fact that the diesel injection timing in the VW engine is not variable. Higher propane substitutions led to the engine knock.

- Low Load Operation: The maximum 1/4 load brake thermal efficiency from propane dual fuel operation was 13.2% compared to the corresponding straight diesel value of 30.5%. The maximum percent energy substitution from propane at 1/4 load was only 84%.
- Emissions Reduction: At all engine loads, dual fuel operation yielded significantly lower brake-specific NOx (BSNOx), exhaust smoke (measured as Filter Smoke Number or FSN), and $CO_2$ emissions compared to straight diesel operation. Compared to full load straight diesel emissions of BSNOx (4.8 g/kWh), smoke (4.6 FSN), and $CO_2$ (11.9%), dual fuel operation yielded 0.84 g/kWh of BSNOx, very low smoke (<0.5 FSN), and 7.6% $CO_2$. Controlling BSNOx and exhaust smoke is inherently difficult with diesel combustion and therefore, this advantage of dual fuel operation is very attractive. Since $CO_2$ emissions are also lower, dual fueling is also attractive from a greenhouse gas reduction perspective. The only disadvantages for dual fueling are higher brake-specific unburned hydrocarbon (BSHC) and carbon monoxide (BSCO) emissions at all engine loads, but especially at low loads. However, it is possible (in principle) to reduce these emissions using an oxidation catalyst in the exhaust, if necessary.
- Waste Heat Recovery Potential: The maximum waste heat recovery potential from the engine coolant is significantly lower than from the exhaust gases. Measured post-turbo exhaust temperatures are somewhat similar for straight diesel and dual fuel operation at intermediate loads. Diesel operation shows higher exhaust waste heat potential at 4/4 load, while dual fuel operation shows higher potential at 1/4 load.
- Operating Cost Comparison: Assuming fuel costs of 258 cents/gal for diesel and 204 cents/gal for propane, a simple cost analysis shows that straight diesel operation is more economical, especially at low engine loads. Dual fuel propane operation has some credibility only at full load operation where the cost of operation in the dual fuel and straight diesel mode are comparable (26 cents/hr and 18 cents/hr, respectively). However, diesel-propane dual fuel operation is more attractive from an emissions perspective.

- The data matrix for diesel ignited propane dual fuel combustion was completed. Optimal propane substitutions subject to $CO_2$ emissions and exhaust temperatures were identified. These results show the potential of diesel-propane dual fuel operation to reduce NOx, smoke, and $CO_2$ emissions with some efficiency penalty.

*Task 2.2.3 Perform a comprehensive analysis of the Spark Spread for CHP systems.*

**Description:** *The Recipient shall perform a comprehensive analysis of the Spark Spread for CHP systems. Spark Spread is an accepted index used by the industry when considering combined heating and power (CHP) systems. This index is used as a rough assessment of the feasibility of CHP systems. The analysis to be performed is intended to determine or develop a variation of the spark spread index for combined cooling, heating, and power (CCHP) systems operating at partial load.*

**Percentage of completion**: 100%

**Accomplishments:**

- A detailed model, based on the spark spread, that compares the electrical energy and heat energy produced by a CHP system against the same amounts of energy produced by a traditional, or separate heating and power (SHP) system has been developed. This work has been published in the Applied Energy Journal [J1]

  An expression for the spark spread based on the cost of the fuel and some of the CHP system efficiencies as well as an expression for the pay- back period for a given capital cost and spark spread is also presented in this paper. The developed expressions can be used to determine the required spark spread for a CHP system to produce a net operational savings over the SHP in terms of the performance of system components.

  Although a spark spread of \$0.0409/kW h is typically used to indicate the potential for favorable payback of a CHP system, the analysis presented in this paper showed that the spark spread de- pends on the performance of system components, the desired pay- back period or capital cost, and the price of fuel itself. The equations developed and presented in this paper consider all these effects, which may result in savings, during the spark spread calcu- lations. A CHP system may be economically viable with a spark spread much less than \$0.0409/kW h in some cases, and in others a spark spread even greater than \$0.0409/kW h may not result in a favorable payback. The required SS (No Savings Case) strongly de- pends on the efficiency of the SHP heating system, the efficiency of the CHP system, and the relationship between electricity output and heat output (or, PGU efficiency relative to CHP thermal effi- ciency). Larger spark spreads are necessary in order to guarantee: shorter payback periods, lower CHP efficiencies, higher SHP heat- ing system efficiencies, and higher fuel prices.

  The introduced PBPCHP is a simple indicator of the economic viability of a CHP system which takes into account the CHP and SHP thermal efficiencies, power-to-heat ratio of the CHP system, capital cost of the CHP system, and the

cost of fuel and its relationship to the cost of electricity. Rather than specifying a spark spread which may or may not be met in order to indicate economic viability of a CHP system, the PBPCHP indicates if net savings over an SHP system could be achieved.

- An emissions spark spread and primary energy spark spread as screening parameters for indicating whether a CHP system shows potential to reduce harmful emissions and PEC have been developed. This work has been published in the Applied Energy Journal [J2]. The minimum ESS and minimum PESS were determined as a performance basis to show where a CHP system and SHP system would have similar results for emissions and primary energy consumption, respectively. When ESS and PESS are found to be greater than ESS and PESS , the CHP system shows a potential benefit and the magnitude of this benefit may be gauged with the ratios ESS/ESSmin and PESS/PESSmin.

  Low ESS/ESSmin ratios (Table 5) correspond to low EEFs (Table 1). For example, Helena does not show very favorable emissions po- tential for CHP system applications in the way that the other colder climate cities do, resulting from Helena's much lower EEF of 409 kg/MWh. Helena receives almost half of its electricity from hydropower sources and uses less coal, oil, and natural gas than the national average. Therefore, since the electricity purchased by an SHP system causes less CO2 emissions in Helena than it does in Boulder, the energy generated by a CHP system cannot reduce emissions as much.

  Low PESS/PESSmin ratios (Table 6) correspond to low ECFs (Ta- ble 2). The state of Washington has a very low ECF of 1.5, meaning that a certain amount of electricity purchased from the grid in Seattle would not require as much primary energy as the same amount purchased in any of the other cities investigated. A CHP system in Seattle would use more primary energy than an SHP sys- tem, if both systems have the characteristics used above. If the emissions factors for electricity and fuels as well as the site-to-source conversion factors are known, the ratios ESS/ESSmin and PESS/PESSmin can be can be applied to any location to evaluate the potential of CHP systems in order to determine if a more thor- ough analysis is of interest. The screening tool provided in this paper indicates CHP systems' potential to reduce CDE or to reduce PEC, which can then be used to establish better energy policies and incentives for CHP systems installations.

- In addition a conference paper that impact of CHP system component efficiencies on the economic benefits of CHP systems using spark spread analysis was presented at the *ASME International Mechanical Engineering Congress and Exposition (IMECE2011),* Denver, CO [C1]. In general it was determined that the sizing of the PGU with respect

to the building demand has no effect on overall CHP efficiency or on the *CR* or *SS* required under these conditions. Increasing $\eta_{pgu}$ or increasing $\eta_{chr}$ in this case results in a linear increase in $\eta_{CHP}$ and a linear decrease in required *CR.*

**Publications / Presentations:**

*Journal Papers:*

1. Smith, A., Fumo, N., & Mago, P. J. (Feb 2011). Spark Spread - A Screening Parameter for Combined Heating and Power Systems. *Applied Energy, 88,* 1494-1499.

2. Smith, A., Mago, P. J., & Fumo, N. (May 2011). Emissions Spark Spread and Primary Energy Spark Spread - Environmental and Energy Screening Parameters for Combined

*Conference Papers:*

1. Smith, A., Mago, P. J., & Fumo, N. (Nov 2011). Impact of CHP System Component Efficiencies on The Economic Benefits of CHP Systems Using Spark Spread Analysis. *ASME International Mechanical Engineering Congress and Exposition (IMECE2011),* Denver, CO.

## Task 2.3 – Demonstrate and optimize a Stirling external combustion engine capable of burning a wide range of unprocessed fuels such as bio-oils and biomass for micro CHP applications

### *Task 2.3.1 Demonstrate a Stirling engine-powered micro CHP system*

**Description:** The Recipient shall demonstrate an existing Stirling engine on natural gas to achieve grid-independent operation of the micro CHP system.

**Percentage of completion**: 100%

**Accomplishments:**

- A Stirling engine rated at 25 kW and manufactured by STM Power Inc was procured through the Mississippi Technology Alliance. The engine was shipped to us in a "non-working condition." Different components of the Stirling engine were identified. However, upon further investigation, it was found that the Stirling engine had many obsolete parts, a damaged combustion chamber, and a dysfunctional hydrogen generator. All attempts to replace these items were unsuccessful as this engine was a Beta prototype and the company that manufactured this engine no longer supported this engine model.

- This task could not be completed to the extent expected due to difficulties in obtaining spare parts to start the Stirling engine that was donated by TVA. The purchase of a new 43 kW Stirling engine was initiated. Since the CHP demonstration center utilized only about 10 kW (maximum), therefore, the remaining power generated has to be sold back to the central grid. A detailed investigation with the local power company indicated that this idea of selling power back to the grid was infeasible due to excessive operational costs. A detailed report in this regard is being prepared.

- A phenomenological model of the Stirling engine was developed to provide a foundation for better design of future Stirling power plants. A journal article was published from the computational effort. The paper was published in the the Journal of Mechanical Engineering Science.
    - This articled discusses the thermodynamic performance of an ideal Stirling cycle engine. This investigation uses the first law of thermodynamics to obtain trends of total heat addition, net work output, and thermal efficiency with varying dead volume percentage

and regenerator effectiveness. Second law analysis is used to obtain trends for the total entropy generation of the cycle. In addition, the entropy generation of each component contributing to the Stirling cycle processes is considered. In particular, parametric studies of dead volume effects and regenerator effectiveness on Stirling engine performance are investigated. Finally, the thermodynamic availability of the system is assessed to determine theoretical second law efficiencies based on the useful exergy output of the cycle. Results indicate that a Stirling engine has high net work output and thermal efficiency for low dead volume percentages and high regenerator effectiveness. For example, compared to an engine with zero dead volume and perfect regeneration, an engine with 40 per cent dead volume and a regenerator effectiveness of 0.8 is shown to have ~60 per cent less net work output and a 70 per cent smaller thermal efficiency. Additionally, this engine results in approximately nine times greater overall entropy generation and 55 per cent smaller second law efficiency.

*Task 2.3.2 Optimize the combustion chamber design of the Stirling engine to accommodate bio-oils and biomass*

**Description:** The Recipient shall modify the combustion chamber of the Stirling cycle engine to accommodate unprocessed fuels such as bio-oils and other bio-based fuels. The engine will be used to demonstrate grid-independent operation of the micro CHP building on those fuels.

**Percentage of completion**: 100%

**Accomplishments:**

- In March 2010, a Stirling engine generator (~43 kW) capable of operating on alternative fuels was ordered. The Stirling engine was originally scheduled to be delivered in January 2011. Toward the end of December, MSU received ane-mail from the Stirling engine manufacturer (Stirling Biopower) indicating that the delivery would be delayed. On January 18, 2011, in a conference call with Stirling Biopower, MSU researchers were informed that the Stirling engine delivery would be delayed to an unknown future date due to internal issues within Stirling Biopower. Clearly, this new information implied that the performance of this task would be delayed to an unacceptable extent. Therefore, the purchase order for the Stirling engine from Stirling Biopower was cancelled. Immediately, MSU researchers contacted several other potential Stirling engine suppliers to investigate the feasibility of procuring a Stirling engine. Unfortunately, despite the best efforts of MSU researchers, it has become clear that no other supplier can provide a suitable Stirling engine in an appropriate timeframe to enable the successful completion of this task. The initial idea when this task was proposed was to also evaluate the feasibility of re-routing excess power not consumed by the micro-CHP facility back to the utility grid and receive a purchase back rate through the Tennessee Valley Authority's Green Power Switch Generation Partners Program. MSU project members met with representatives from TVA and Starkville Electric Department to evaluate this issue. After extensive investigations (involving MSU team, TVA, and Starkville Electric) and due to the high cost of interconnection equipment and monthly fees as well as the fact that the cost to produce electricity by the system exceeded the proposed electricity purchase back rate under TVA's incentive, it was determined that grid-interconnected net metering was not an economically feasible option for the Stirling engine at the Micro-CHP facility.

- A detailed model Performance analysis of a combined cooling, heating, and power system driven by a waste biomass fired Stirling engine was developed and a paper was published in the Journal of Mechanical Engineering Science: "Performance Analysis of a CCHP System Driven by a Waste Biomass Fired Stirling Engine."
    - The objective of this study was to analyse the performance of a CCHP system driven by a biomass fired Stirling engine. The study was carried out by considering an hour-by-hour CCHP simulation for a small office building located in Atlanta, Georgia. The hourly thermal and electrical demands for the building were obtained using the EnergyPlus software. Results for burning waste wood chip biomass are compared to results obtained burning natural gas to illustrate the effects of fuel choice and prime mover power output on the overall CCHP system performance. Based on the specified utility rates and including excess production buyback, the results suggest that fuel prices of less than $23/MWh must be maintained for savings in cost compared to the conventional case. In addition, the performance of the CCHP system using the Stirling engine is compared with the conventional system performance. This comparison was based on operational cost and primary energy consumption. When electricity can be sold back to the grid, results indicate that a wood chip fired system yields a potential cost savings of up to 50 per cent and a 20 per cent increase in primary energy consumption as compared with the conventional system. On the other hand, a natural gas fired system is shown to be ineffective for cost and primary energy consumption savings with increases of up to 85 per cent and 24 per cent compared to the conventional case, respectively. The variations in the operational cost and primary energy consumption were also shown to be sensitive to the electricity excess production and buyback rate.

- A methodology that allows sizing combined cooling, heating, and power system using a wood waste biomass-fired Stirling engine was developed. The outcomes from this research were presented in a paper published in the International Journal of Energy research: "Sizing Analysis of a Combined Cooling, Heating, and Power System for a Smal Office Building Using a Wood Waste Biomass-Fired Stirling Engine."
    - When wood chips are available and used to fuel a combined cooling, heating, and power (CCHP) waste heat recovery system, they can represent an economically viable source of biomass energy that can meet a facility's electric and thermal demands. Using a Stirling engine as the CCHP prime mover provides several important advantages over conventional internal combustion engines including no additional processing of the waste wood chips, a potentially higher thermal efficiency, flexibility of fuel sources, and low maintenance. This study showed how the operational characteristics of a constant output, biomass-fired, Stirling engine-based CCHP system are affected by the performance of the individual

components, including the prime mover, heat recovery system, auxiliary boiler, absorption chiller, and heating coil unit The results wereassessed by examining the primary energy consumption and operational cost compared with a reference case. The analysis provided insight on the prime mover sizing and selection of each component to properly implement the system. In addition to examining the effects of each component, the effect of excess electricity production and buyback are considered.

- A sensitivity analysis of CHP Stirling Engine Systems was carried out and the results were presented at the 2010 *ASME International Mechanical Engineering Congress and Exposition* help in Vancouver.

- A poster on the First and Second Law Analysis of a Stirling Engine with Imperfect Regeneration and Dead Volume and its Application in CHP Systems was presented at the *2nd Energy-Synergy Workshop* help in Mississippi State University.

**Publications / Presentations:**

*Journal Papers*

1. Harrod, J., & Mago, P. J. (Jan 2011). Performance Analysis of a CCHP System Driven by a Waste Biomass Fired Stirling Engine. *Journal of Mechanical Engineering Science*, 225(2), 420-428.

2. Harrod, J., Mago, P. J., & Luck, R. (Jan 2012). Sizing Analysis of a Combined Cooling, Heating, and Power System for a Small Office Building Using a Wood Waste Biomass-Fired Stirling Engine. *International Journal of Energy Research*, *36*(1), 64-74.

*Conference Papers:*

1. Harrod, J., & Mago, P. J. (Nov 2010). Sensitivity Analysis of CHP Stirling Engine Systems. In Paper No. IMECE2010-37316 (Eds.), *ASME International Mechanical Engineering Congress and Exposition (IMECE2010)*, Vancouver.

*Posters:*

1. Harrod, J., Mago, P. J., Srinivasan, K. K., & Chamra, L. M. (Apr 2009). First and Second Law Analysis of a Stirling Engine with Imperfect Regeneration and Dead Volume and its Application in CHP Systems. *2nd Energy-Synergy Workshop*, Mississippi State University.

## Students Involved in Task 2

*Ph.D. Students:*

1. Harrod, J. (Fall 2010). "The Stirling Engine: Thermodynamics and Applications in Combined Cooling, Heating, and Power Systems."

2. Jha, S. K. (Spring 2012) " A phenomenological investigation of ignition and combustion in alternative-fueled engines,"

3. Tripathi, M. M. "Optical and Laser Spectroscopic Diagnostics for Energy Applications,", Ph.D. dissertation, May 2012.

*M.S. Students:*

1. "Development of sub-models for a phenomenological investigation of diesel engine combustion," Qiu, L., M.S. Thesis, August 2011.

2. "Entropy generation in a constant internal energy-volume combustion process," Knizley, A. A., M.S. Thesis, August 2011

3. "Dual-fuelling concepts: A comparison of methane and propane as primary fuels with biodiesel and ultra-low sulfur diesel as separate pilot fuels," Shoemaker, N. T., M.S. Thesis, December 2011

## Publications – Task 2

*Journal Papers:*

1. Harrod, J., & Mago, P. J. (Jan 2011). Performance Analysis of a CCHP System Driven by a Waste Biomass Fired Stirling Engine. *Journal of Mechanical Engineering Science*, 225(2), 420-428

2. Harrod, J., Mago, P. J., & Luck, R. (Jan 2012). Sizing Analysis of a Combined Cooling, Heating, and Power System for a Smal Office Building Using a Wood Waste Biomass-Fired Stirling Engine. *International Journal of Energy Research*, *36*(1), 64-74.

3. Smith, A., Fumo, N., & Mago, P. J. (Feb 2011). Spark Spread - A Screening Parameter for Combined Heating and Power Systems. *Applied Energy, 88,* 1494-1499.

4. Smith, A., Mago, P. J., & Fumo, N. (May 2011). Emissions Spark Spread and Primary Energy Spark Spread - Environmental and Energy Screening Parameters for Combined.

5. M.M. Tripathi, S.R. Krishnan, K.K. Srinivasan, F.-Y. Yueh, J.P. Singh (2011). "Chemiluminescence-based multivariate sensing of local equivalence ratios in premixed atmospheric methane-air flames," Fuel, doi:10.1016/j.fuel.2011.08.038

6. C.M. Gibson[1], A. Polk[1], N. Shoemaker[1], K.K. Srinivasan, and S.R. Krishnan (2011). Comparison of propane and methane performance and emissions in a turbocharged direct injection dual fuel engine. Trans. ASME: Journal of Engineering for Gas Turbines and Power, 133(9), Article GTP-092806, (DOI: 10.1115/1.4002895)

7. S. R. Krishnan and K. K. Srinivasan (2010). Multi-Zone Modeling of Partially Premixed Low Temperature Combustion in Pilot-Ignited Natural Gas Engines. Proc. Instn. Mech. Engrs.: Part D: Journal of Automobile Engineering, 224, pp. 1597-1622 (DOI 10.1243/09544070JAUTO1472) (This paper won the 2010 SAGE Best Paper Award by the Editor and Editorial Board of Proceedings of the Institution of Mechanical Engineers, Part D: Journal of Automobile Engineering)

8. K. K. Srinivasan, P. J. Mago, S. R. Krishnan (2010) "Analysis of Exhaust Waste Heat Recovery from a Dual Fuel Low Temperature Combustion Engine using an Organic Rankine Cycle," Energy, Vol. 35, pp. 2387-2399, doi:10.1016/j.energy.2010.02.018

*Conference Papers:*

1. Harrod, J., & Mago, P. J. (Nov 2010). Sensitivity Analysis of CHP Stirling Engine Systems. In Paper No. IMECE2010-37316 (Eds.), *ASME International Mechanical Engineering Congress and Exposition (IMECE2010)*, Vancouver.

2. Smith, A., Mago, P. J., & Fumo, N. (Nov 2011). Impact of CHP System Component Efficiencies on The Economic Benefits of CHP Systems Using Spark Spread Analysis. *ASME International Mechanical Engineering Congress and Exposition (IMECE2011),* Denver, CO.

3. N. Shoemaker[1], C.M. Gibson[1], A. Polk[1], K.K. Srinivasan, and S.R. Krishnan, 2011, "Performance and Emissions Characteristics of Bio-Diesel Ignited Methane and Propane Combustion in a Four Cylinder Turbocharged Compression Ignition Engine," Paper No. ICEF2011-60081, (accepted) Proceedings of the ASME IC Engines Division 2011 Fall Technical Conference (ICEF2011), October 2-5, Morgantown, West Virginia, USA, *Presenter – C. M. Gibson*

4. A. Polk[1], C.M. Gibson[1], N. Shoemaker[1], S.R. Krishnan, and K.K. Srinivasan, 2011, "Analysis of Ignition Delay Behavior in a Dual Fuel Turbocharged Direct Injection Engine Using Propane and Methane as Primary Fuels," Paper No. ICEF2011-60080, (accepted) Proceedings of the ASME IC Engines Division 2011 Fall Technical Conference (ICEF2011), October 2-5, Morgantown, West Virginia, USA, *Presenter – A C Polk*

5. C.M. Gibson[1], A. Polk[1], N. Shoemaker[1], K.K. Srinivasan, and S.R. Krishnan, 2010, "Comparison of Propane and Natural Gas Performance and Emissions in a Turbocharged Direct Injection Dual Fuel Engine," Paper No. ICEF2010-35128, Proceedings of the ASME IC Engines Division 2010 Fall Technical Conference (ICEF2010), September 12-15, San Antonio, TX; *Presenter – C. M. Gibson.*

*Dissertations:*

1. Harrod, J. (2010). "The Stirling Engine: Thermodynamics and Applications in Combined Cooling, Heating, and Power Systems." Mississippi State University.

2. Jha, S. K. (2012) " A phenomenological investigation of ignition and combustion in alternative-fueled engines." Mississippi State University.

3. Tripathi, M. M. (2012) "Optical and Laser Spectroscopic Diagnostics for Energy Applications," Mississippi State University.

*Posters:*

1. Harrod, J., Mago, P. J., Srinivasan, K. K., & Chamra, L. M. (Apr 2009). First and Second Law Analysis of a Stirling Engine with Imperfect Regeneration and Dead Volume and its Application in CHP Systems. *2nd Energy-Synergy Workshop*, Mississippi State University.

2. Wang, Z., Srinivasan, K. K., Krishnan, S. R., Som, S. "A computational investigation of diesel and biodiesel combustion and NOx formation in a light-duty compression ignition engine," To be presented at the Central States Meeting of the Combustion Institute, Hosted by the University of Dayton, Dayton, OH, April 22-24, 2012.

3. M.M. Tripathi, S.R. Krishnan, K.K. Srinivasan, F.-Y. Yueh, J.P. Singh, "Development of a Robust Sensor for Monitoring Equivalence Ratio in Premixed Flames Using Chemiluminescence and Multivariate Data Analysis," presented at the 7th US National Technical Meeting of the Combustion Institute, Hosted by the Georgia Institute of Technology, Atlanta, GA, March 20-23, 2011.

4. A.A. Knizley, K.K. Srinivasan, S.R. Krishnan, "Fuel and Diluent Effects on Entropy Generation in a Constant Internal Energy-Volume (UV) Combustion Process," presented at the 7th US National Technical Meeting of the Combustion Institute, Hosted by the Georgia Institute of Technology, Atlanta, GA, March 20-23, 2011.

# Summary of Project Activities

## Task 3. Outreach Activities

## Task 3. Outreach Activities

**Description:**

The Recipient shall promote and disseminate the use of CHP systems as a viable technology to reduce the energy consumption in the US. In addition, the center will educate engineers, architects, homeowners, building owners, and building operators about the energy, economical, and environmental benefits of this technology. The Micro-CHP Center will provide educational material and conduct outreach seminars and demonstrations for engineers, architects, and students as well as for more general audiences. The outreach efforts of the Micro-CHP Center will be built around the following: the micro CHP optimization site, the alternative fuels research and optimization projects, and the CHP models being developed. In addition, personnel from the Micro-CHP Center will participate in conferences to promote the work developed in the Center and the feasibility of CHP systems operation.

**Percentage of completion**: 100%

**Accomplishments:**

- A presentation was made on October 28, 2013 at the 2013 Mid-South Area Engineering and Sciences Conference. The title of the presentation was: "Wide- cut diesel production from an integrated gasification, syngas cleaning, and catalytic conversion process."

- Presentation "CHP 101" to the ASHRAE Student Chapter in MSU, April 2012.

- Presented a poster at the MSU the 2011 AHFA Manufacturers' Summit at the MSU Franklin Center, March 2011.

- Make a presentation regarding the findings of this project to the Energy Institute and the MSU Energy Working Group at Mississippi State University, November 2011.

- Presented several posters at the Mississippi Biofuels conference, October 5-7, 2012. Mississippi State University.

- Make a presentation followed by a tour of the micro-CHP lab to the ASHRAE student members at MSU. This was coordinate by the MSU ASHRAE student Chapter and the Micro-CHP laboratory. More than 20 students participated in this activity.

- Participate and Co-Organize a Webinar: "CHP for Agricultural Applications"

- Presented a Webinar on "Biomass Combined Heat and Power" June 30, 2011

- Presented at the Biomass Combined Heat and Power Technical Course, Biloxi, MS, May 10, 2011.

- Presented a Seminar on "Introduction to CHP systems and its implication in energy conservation." Engineering Week, University of Louisiana at Lafayette, March, 2011.

- Presented a seminar at the Save Energy Now Southeast Partners Roadmap Workshop, February 2011.

- Presented a poster at the MSU the 2011 AHFA Manufacturers' Summit at the MSU Franklin Center, March 2011.

- Attended the USCHPA annual conference and participated as a resource provider.

- Attended and presented a poster at the Biomass South 2010 conference.

- Presentation at the 2010 Mississippi Energy Coordinators Association (MECA) Convention and Expo, Philadelphia, MS. September 29 – October 1, 2010. The title of the presentation was "Screening Your Building for the Most Efficient Technology for Energy Reduction."

- Presented a webinar on the MSU IAC/SE CEAC Collaboration, June 2010.

- Presented a poster at the MSU Biofuels Conference in Jackson, MS on August 12.

- A presentation was made for the AHSRAE Students at the Micro-CHP facility.

- Collaborate with the organization of a DOE Steam System Assessment Tool (SSAT) Qualified Specialist training held in Atlanta on May 24-26.

- Collaborate in a webinar on June 21, 2010– Clean Energy 101.

- "District Energy and CHP in the Southeast". It was presented at the IDEA's 23 Campus Energy Conference in Reno, NV on February 9-12, 2010.

- A presentation was made for the ASME and AHSRAE Students at the Micro-CHP facility. Around 25 students attended the presentation.

- A tour of the Micro-CHP facility was held for the Jackson Chapter of AHSRAE, where more than 16 people attended.

- A tour of the Micro-CHP facility was held for students of the College of Architecture.

- A workshop on "Energy Savings Practice for the the Chemical Industry," was organized and held in Hattiesburg, MS in July 2009.

- The 2nd *Energy-Synergy Workshop* was organized and held at Mississippi State University in April 15, 2009.

# Summary of Project Activities

## Task 4. Biofuel and Opportunity Fuel Processing and Utilization

## Task 4.1 – Utilize biofuels to generate electricity though micro-CHP system

*Task 4.1.1. Modify, test, and optimize commercially available portable gasoline and diesel electric generation units to use biofuels*

**Description:**
The Recipient shall investigate pertinent operational parameters: biofuel quality, carburetion methodology, control and regulation, and fuel mixture that influence the performance of electrical energy generation units in terms of power generation, operational stability and continuity, and pollution potential (exhaust constituents). Economic analysis of electrical energy generation using the syngas-diesel engine arrangement in will be performed.

**Percentage of completion**: 100%

**Accomplishments:**
A 15 KVA asynchronous diesel engine driven power generator was successfully instrumented and operated with diesel-syngas fuel mixture using syngas produced from biomass gasification. The machine was connected to the power grid via a temporary metering system. The achievable syngas-diesel composition was determined by measuring the reduction of diesel fuel consumption from pure diesel to syngas-diesel mixture without causing the engine to stall. The reduction of diesel fuel consumption achievable was 60% and the average power output was 7.3 KWh. The fuel consumption at this output level was computed to be approximately 3.75 $m^3$/kwh of syngas and 0.35 L/kwh diesel. The efficiency of power production decreases with the increase in syngas proportion and the efficiency was around 11% at 58% syngas level in relation to 18% efficiency at 100% diesel. The instrumentation was implemented using a National Instrument embedded system and the software associated with was developed. Control of the machine operation implemented included remote engine start/stop. Data collected include: Engine shaft speed (RPM), coolant temperature, voltage, current, frequency output of the generator, oil pressure, syn-gas flow rate, diesel fuel flow rate, air intake flow rate, operating time. Exhaust gas was measure with an external instrument. Mechanical improvements: Problems associated with using syn-gas as fuel include moisture accumulation in the fuel mixer system. Solution used was a modified mixer chamber enclosure modification to enable rapid cleanup. A spreadsheet cost model was developed for quantifying the costs of producing electricity using syngas from biomass gasification.

A 5 hp Briggs-Stratton generator was successfully operated on syngas produced from biomass gasification. Maximum power output for gasoline operation was 2451 W and maximum power output for syngas operation was 1392 W. Overall efficiencies of the generator were same at maximum electrical power outputs for operation with both the fuels. At four different electrical power output categories, the exhaust concentrations of carbon monoxide and oxides of nitrogen were significantly lower while the carbon dioxide emissions were significantly higher for the syngas operation. The unit cost of electricity generation was $6.38/kWh for syngas operation and $0.56/kWh for gasoline operation. Manuscript from our CHP work titled "Performance and Emissions of a Spark-Ignited Engine Driven Generator on Biomass Based Syngas" has been published in Bioresource Technology.

**Publications / Presentations:**

*Journal Papers:*

1. Shah, A., Srinivasan, R., To, F.D., and Columbus, E.P. 2010. Performance and emissions of a spark-ignited engine driven generator on biomass based syngas. Bioresource Technol. 101:4656-4661.

*Task 4.1.2. Develop and evaluate storage systems for syngas for rural micro-CHP applications*

**Description:**
The Recipient shall continue exploring pressurization as a means of syngas storage, optimize the system, and develop guidelines/recommendations regarding syngas storage procedures especially related to pressurization levels and length of storage.

**Percentage of completion**: 100%

**Accomplishments:**
Syngas storage characteristics in terms of variation in composition of $H_2$, CO, $CH_4$, $CO_2$, and $N_2$ under two pressures (2758 and 8274 kPa) and three temperatures (-288K, 288K, and 318K) were studied. We also evaluated tar, particulate, and moisture content of the stored syngas. Syngas generated from a down-drift gasifier using 95% hardwood chips as the feedstock contained an average of 17.0% $H_2$, 23.9% CO, 1.4% $CH_4$, 11.0% $CO_2$, and 46.7% $N_2$. The compositional elements of the stored syngas under different pressures and temperatures were periodically determined for a three-week period of storage. This study showed that syngas could be stored with no major adverse affects caused by temperatures of -15°C to 45°C. Also, pressures up to 8274 kPa had no effect on syngas composition at the tested temperatures. The syngas generation costs for a syngas-based generator system, operating for emergencies for 8 h per day and for 30 days per year, would be $13,886/yr. This system would require 30 commercial 0.1 $m^3$ (25 gal) stainless steel LPG tanks storing syngas at 200 psi. Compression and storage costs would be $3,570/yr.

**Publications / Presentations:**

*Journal Papers:*


1. Yang, P., E.P. Columbus, J. Wooten, W.D. Batchelor, P. R. Buchireddy, X. Ye and L. Wei. 2009. Evaluation of syngas storage under different pressures and temperatures. *Applied Engineering in Agriculture* 25(1):121-128.

2. L. Wei, L. O. Pordesimo, S. D. Filip To, C. W. Herndon, W. D. Batchelor. Evaluation of Micro-Scale SYNGAS Production Costs Through Modeling. *Trans ASAE* Vol. 52(5): 1649-1659.

*Task 4.1.3. Develop optimal process to provide conditioned syngas fuel to electrical generator sets*

**Description:**
The Recipient shall design and install a simplified filtration system and gas cleanup train that will permit extended operation of a downdraft gasifier producing syngas for electric generation. The Recipient shall develop a computer model describing the relationship of various degrees of conditioning of syngas to the generator engine exhaust gas composition and will use the model to determine the optimal process.

**Percentage of completion**: 100%

**Accomplishments:**
Physicochemical properties of biomass feedstocks, such as composition, shape, size, moisture content, etc., have profound effects on the gasification process. The properties affect feedstock selection, sizing, transportation, and storage; gasification and syngas recovery, and residue or co-product processing. The extent of the effects of feedstock properties depend on gasifier type, operating conditions, and syngas quality product requirements. Fixed-bed downdraft gasifiers are widely used in small-scale biomass gasification facilities because of their simple and robust construction, easy and reliable operation, suitability with various feedstocks, high conversion rate, and production of relatively clean syngas containing low tar and particulate concentrations. A series of gasification tests using different biomass feedstocks, including hardwood chips, softwood chips, softwood sawdust, corn cubes, crude glycerol (a byproduct of biodiesel production), and switchgrass, were conducted under similar operating conditions using a pilot scale fixed-bed downdraft gasifier. The results show that downdraft gasifier is suitable for gasifying diverse feedstocks to produce good quality syngas with good low heating value and low tar and particle concentrations. There are no significant differences in gas composition, low-heating value, tar and particle concentrations among the different feedstocks used in the experiments. The syngas produced by the gasification process can be directly be used as fuel in internal combustion engines (ICE), however the physicochemical properties of feedstock such as shape, size, porosity, and the chemical contents, was found to affect the performance of the fixed-bed downdraft gasifier. Feedstocks with small sizes, low porosity, or containing highly compounds that can caramelize in high temperature could cause problems with bridging, lumping, collapsing, or clogging inside the reaction chamber and could cause the gasifier to fail. Hardwood chips mixed with 20% of liquid crude glycerol can be gasified well in the downdraft gasifier and produced syngas with significant higher CH4 content, good low-heating value and lower tar concentration than those of regular hardwood chips. Feasibility of biomass gasification is very much dependent on the cost of the gasification facility and its operation.

A cost analysis model was accordingly developed to analyze the unit cost of syngas production from micro-scale biomass gasification facilities. Costs considered included all capital and operating costs. The model was applied to evaluate a scenario for Mississippi in 2008. Results of the modeling indicated that operating cost was the major part of the syngas production cost, and the single-shift operating cost could be up to 83.64% of the total annual cost of syngas production at the 60 Nm3 h-1 capacity level. Labor cost was the largest part of the operating cost and the total annual cost. The labor cost could be up to 73.60% of the total of annual operating cost and 61.56% of the total annual cost of syngas production. The unit cost and energy cost of syngas production of the 60 Nm3 h-1 facility were $0.55 Nm-3 and $0.095 MJ-1, respectively, which were higher than the $0.357 Nm-3 and $0.009 MJ-1 natural gas average retail prices in the U.S. in the fourth quarter of 2008. When the production capacity increased, the total syngas production annual cost continually increased, but the syngas unit cost markedly decreased. Therefore, the effective way to reduce costs is to plan for a higher-capacity micro-scale facility.

Sensitivity analysis showed that, from the lower bound to the upper bound of the production capacity range tested (60 to 1800_Nm3 h-1), there was a shift from labor cost to equipment cost as the factor of greatest influence on syngas unit cost. Such information provided by the model identifies considerations for planning and/or operating micro-scale gasification facilities. The model can be a tool for analyzing the economics of syngas production and, in that regard, it can generate useful information for the design of smaller gasification plants. With increasing production of biodiesel, a glut of glycerol (C3H8O3) is expected in the world market. The market will likely to be saturated because of limited utilization of glycerol in the world. As a result, the price of glycerol decreases dramatically. Therefore, it is essential to find other useful applications for glycerol to improve the economic viability of biodiesel production. One possibility is using glycerol as an additive in the gasification of biomass. Essentially the co-gasification of crude glycerol with hardwood chips was undertaken in this study involving a pilot-scale downdraft gasifier. The effect of glycerol addition to the wood chips (0 to 20%) on the gasification performance was evaluated. The results revealed that addition of crude glycerol up to 10% (wt/wt) was technically possible with the benefit of simple substitution of glycerol for wood chips on a mass basis.

**Publications / Presentations:**

*Conference Papers:*

1. Effects of Feedstock Properties on the Performance of A Downdraft Gasifier. Lin Wei, Lester O. Pordesimo, S. D. Filip To, James R. Wooten, Agus Haryanto, and Eugene P. Columbus. Paper no. 096873, presented at the

2009 ASABE Annual International Meeting ASABE, Reno, Nevada, June 21 – June 24, 2009.

2. Crude Glycerol Co-gasification with Hardwood Chips in a Pilot-Scale Downdraft gasifier. Agus Haryanto, Lester R. Pordesimo, Sandun D. Fernando, James R. Wooten, Eugene P. Colombus, and Lin Wei. Paper no. 09742, presented at the 2009 ASABE Annual International Meeting ASABE, Reno, Nevada, June 21 – June 24, 2009.

3. Production of Syngas from Downdraft Fixed-bed Biomass Gasification Systems, Lin Wei, Filip To, Eugene Columbus, Fei Yu, James Wooten, William D. Batchelor, Presentation, International Conference on Bioenergy Technology (ICBT), Beijing China, August 22, 2010.

4. Biomass-based Syngas from Downdraft Fixed-bed Gasifier, Lin Wei, Filip To, Eugene Columbus, Fei Yu, James Wooten, William D. Batchelor, Poster, International Sustainable Energy Technology (ISET), Shanghai, China, August 25, 2010.

## Task 4.2. Demonstrate and test application of bio-fuel driven micro-CHP system in an agricultural application.

**Description:**
The Recipient shall design parameters for a two-stage evaporative cooling system in a tunnel-ventilated commercial broiler facility, install the design involving CHP system driven by syngas, and test and evaluate the system. Data from this effort will be used in the development of an economic analysis model for a two-stage evaporative cooling system utilizing CHP technologies in a tunnel-ventilated commercial broiler facility.

**Percentage of completion**: 100%

**Accomplishments:**
A study was conducted to evaluate the effectiveness of growing commercial broiler birds in an environment achievable by a two-stage evaporative cooling system. The objectives were a) to estimate conditions in a commercial broiler house using a two-stage evaporative cooling system and b) determine if the thermal conditions achieved by the two-stage system affect production characteristics of heavy broilers. A live production experiment was conducted in eight environmental chambers to compare typical evaporative conditions against two-stage evaporative conditions. Four treatments with two replications consisted of a) single stage evaporative, b) single stage evaporative, c)two-stage evaporative, and d) two-stage evaporative. The two conditions represented extremes in environmental conditions (Meridian, MS and Salisbury, MD) seen were large populations of birds are grown (figure 1). Outdoor temperature cycles (figure 2) were estimated from ASHRAE design data (dry-bulb). Constant dew-point over a 24 h cycle was assumed. Evaporative cooling was assumed to be used from 0900 to 1900, after which outdoor conditions were used (figure 3).

A total of 400 Ross x Ross 708 broilers were used. Fifty birds were placed in each chamber at age 35 d. Typical water and feeding programs were used. With two replications, live production characteristics of heavy broilers are not different for two-stage systems. However, processing data shows a significant increase in fillet meat (10.2%) and tender (11.5%) yields (figure 4). At current market price for white meat ($3.31/kg), this would increase fillet, tender and total meat production by $215,000, $36,000 and $250,000 per broiler complex respectively. This is assuming a one million bird per week production level. While differences in foot pad scores exist, occurrence of non-saleable feet (FPS = 3) were rare (2.5%). No major deviations from stated goals and objectives.

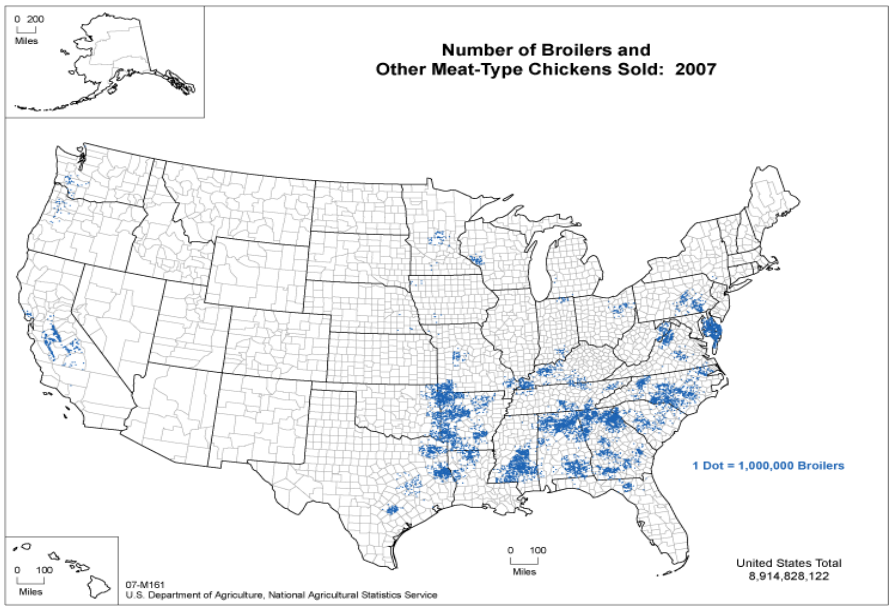


Figure 1: Broiler production numbers by location in the US.

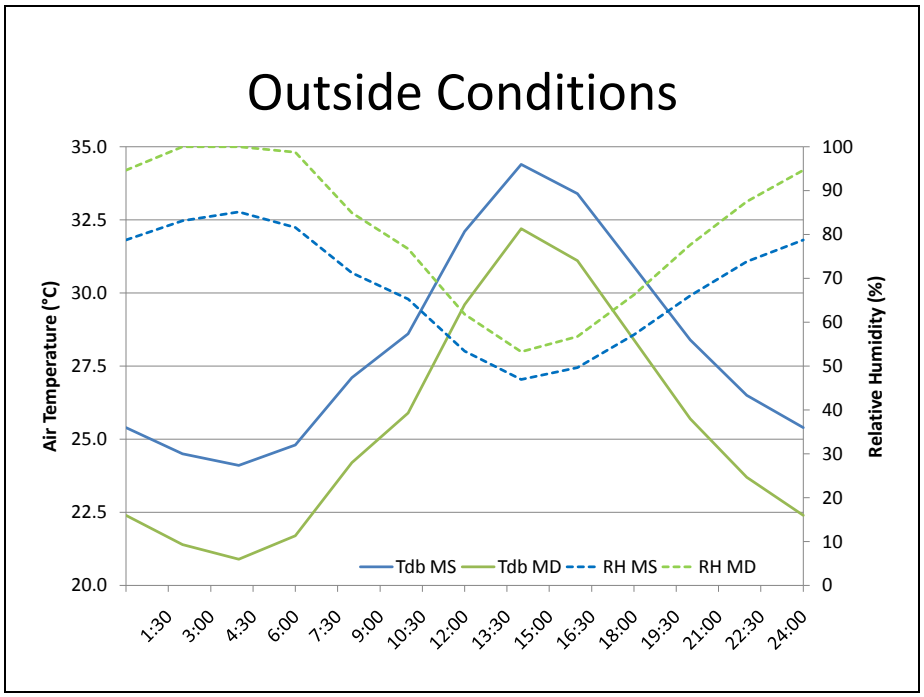


Figure 2: Outside conditions used in the environmental chambers.

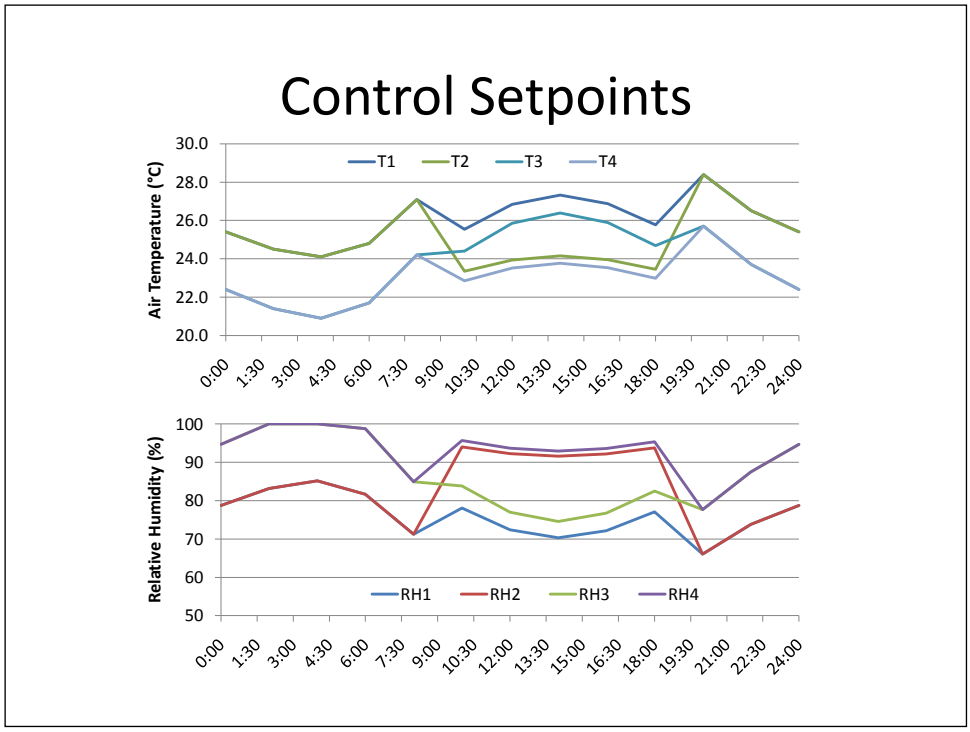


Figure 3: Single and two-stage evaporative cooling treatments.

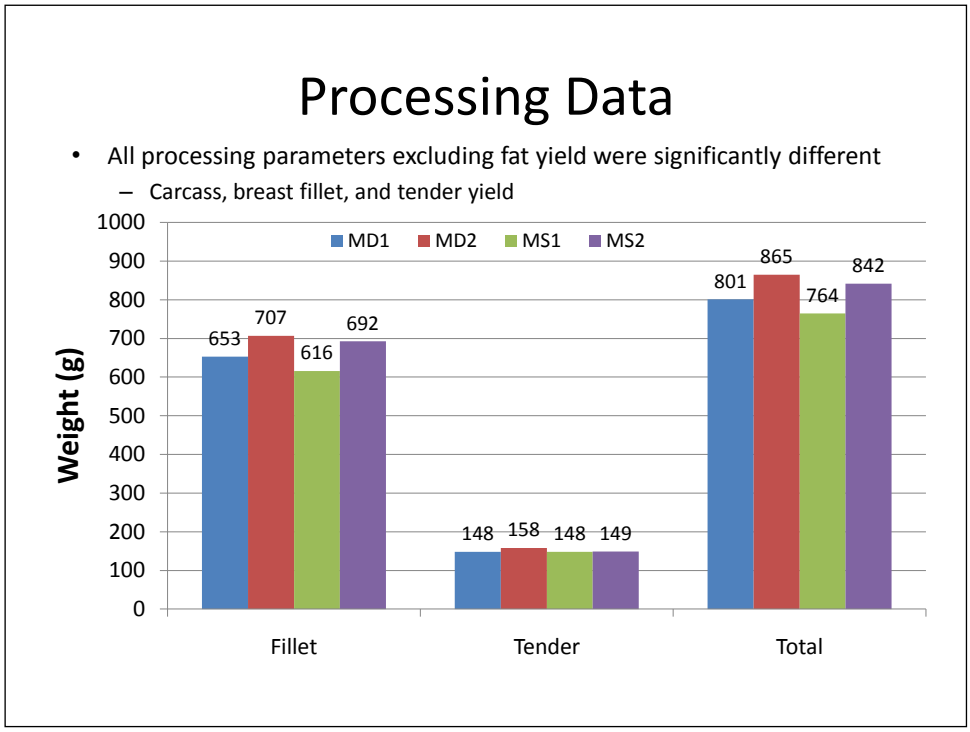


Figure 4: Meat yields for each treatment.

*Task 4.2.1 Develop a commercial poultry broiler house model that includes parameters for CHP technologies.*

**Description:**

The Recipient shall develop a commercial poultry broiler house model that will be integrated with CHP technology. A complete literature review for existing poultry house models will be performed. In addition, a testing poultry broiler house will be developed in this subtask. Model validation and verification will be performed.

**Percentage of completion**: 100%

**Accomplishments:**

The use of solar heated attic air is an area of increasing interest in commercial poultry production. Attic inlets satisfy the demand for alternative heating of broiler chicks while being simple to implement in an existing poultry house. However little attention has been given to the configuration of the attic space and its influence on thermal energy extraction. This issue was approached in three steps; 1) measure thermal parameters in a commercial house field study, 2) develop a two-dimensional computational fluid dynamics (CFD) Attic Inlet Ventilation Model (AIVM) using the test house information, and 3) Use the AIVM model to run simulations that investigate the efficiency of attic inlet system improvements. A field study was conducted in northern Alabama to collect environmental conditions in a typical commercial broiler chicken house (13.1 x 155.4 m oriented east-west). Air enters into the attic space through a ridge cap and eave openings (fig. 1). The attic space had 16 total attic inlets (AC3010, Double L Group, Dyersville, IA). Eight were located 61 cm south of the ceiling peak on the west half while eight were located 61 cm north of the ceiling peak on the east half. Each attic vent opening was 57.2 x 57.2 cm and was actuated by a cable.

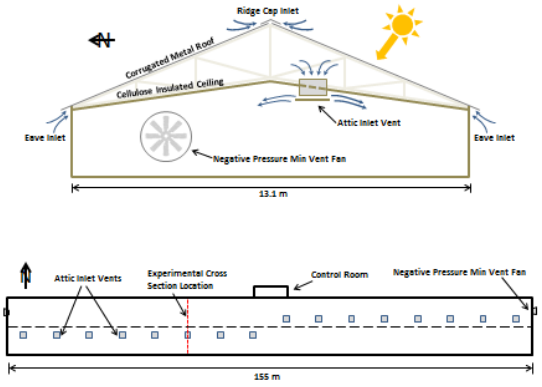


Figure 1: (above) cross-section of the attic inlet heated broiler house showing physical arrangements and air flow directions, (below) plan view of the broiler house illustrating attic inlet placement and the experimental cross-section.

An initial site visit was performed to understand the broiler house attic environment and aid in data acquisition system development. Flow visualization was performed to qualitatively characterize air flow patterns in the attic (Fig. 2). Neutrally buoyant smoke was emitted separately at the south eave and ridge cap after opening the attic inlet vent and actuating the minimum ventilation fans. The difference in flow patterns observed during flow visualization illustrated the effect of buoyant forces on air flow within the attic space. When the attic thermal state was fully charged (i.e. immediately after opening the attic inlet vent), the flow patterns were driven by buoyant forces. The ridge cap inlet jet was forced to the north side of the attic by the hot air rising up the underside of the south side of the roof. Operating the minimum ventilation fans continuously either depleted the attic space of its energy content or mixed the air until stratification is minimized. When the attic temperature profile was more homogeneous, the ridge cap jet was affected less by buoyant forces.

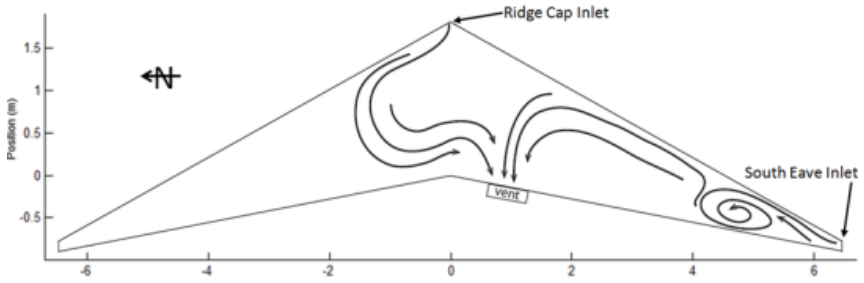

Figure 2: Schematic of observed smoke patterns during smoke tracing.

The attic space was simulated as a 2D flow field because of the continuous extent of all attic features and predominantly transverse flow patterns. A cross-sectional array constructed of 56 thermocouples, 10 hot-wire anemometers, and 6 relative humidity sensors were suspended along a 2D cross-section of the attic space centered over one attic vent (fig. 3). Temperature and velocity sensors were also placed in the attic vent to quantify the airflow characteristics entering the house. Four thermocouples were attached directly to roof metal to determine surface temperatures. Data was collected with a datalogger and multiplexer via a telemetry system. A weather station was located outside to collect ambient conditions (solar radiation, temperature, relative humidity, and wind speed). For the purpose of developing a simulation model, a single fan cycle on a sunny wind free early winter day was chosen. The fans were run for 60 s during a 5 min cycle during the test case.

Figure 4 shows the temperature field immediately before a fan cycle. The low sun angle perpendicular to the axis of the building caused asymmetric heating of the attic space. For the single fan cycle, the average roof surface temperatures (two north and two south sensors) were 20.6°C (SD=0.71 K) and 51.4°C (SD=0.83 K) for the north and south side of the roof, respectively. This difference in roof surface temperature caused the air space on the south side of the attic to have a higher average temperature. Ambient air

(11.4°C) entered the attic through the eaves while thermally stratified hot air (approximately 32°C) was buoyantly vented out through the ridge cap when fans were not operating. When the fans were operating, ambient air entered the attic through the eave and ridge cap openings and exhausted from the attic space through the attic inlet vent. The average temperature of the air passing through the vent into the house was 25.1°C (SD=1.63 K). A summary of parameters for the measured test house are listed in Table 1.

**Figure 3: Graduate students installing thermocouples on the cross-sectional array made with dowels.**

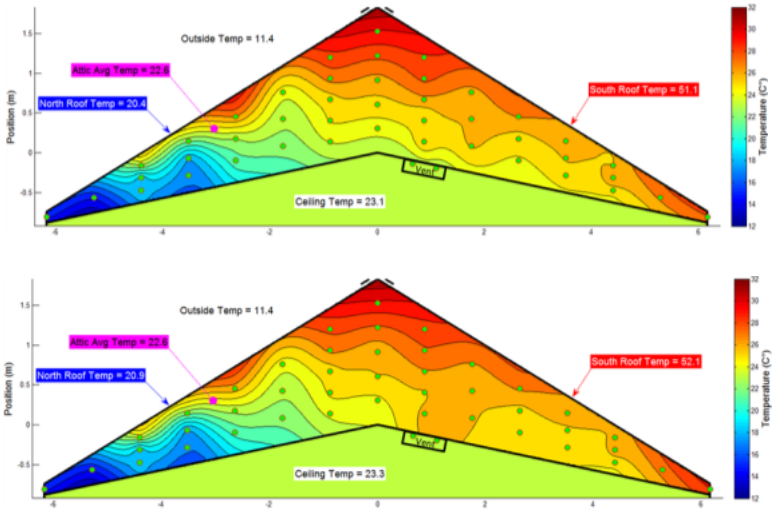


Figure 4: Attic temperature distribution contour plot (above) four minutes after the attic inlets are closed, and (below) after the attic inlets have been opened for one minute.

Table 1: Test case parameters necessary for the development of the Attic Inlet Ventilation Model (AIVM)

| Parameter | Value |
|---|---|
| Wind Velocity | 0 m/s |
| Vent Velocity | 1.41 m/s |
| Ambient Temperature | 11.4°C |
| Atmospheric Pressure | 97940 Pa |
| Ambient Relative Humidity | 61.7% |
| Ambient Density | 1.19 $kg/m^3$ |
| | |
| Flat Plate Solar Radiation | 451 $W/m^2$ |
| Zenith Angle | 58.7° |
| North Roof Incident Angle | 36.9° |
| South Roof Incident Angle | 80.8° |
| | |
| South Roof Temperature | 51.4° |
| North Roof Temperature | 20.6° |
| Attic Differential Pressure | 12 Pa |
| Attic Humidity Ratio | 0.0084 $g_{H20}/g_{dry\ air}$ |
| | |
| Cycle Date | Dec. 31st, 2011 |
| Cycle Start Time | 10:53:30 |
| Fan Start Time | 10:57:30 |
| Fan Stop Time | 10:58:30 |

The Attic Inlet Ventilation Model was developed in a commercial CFD package (COMSOL Multiphysics) and validated with experimental data collected in test house (Table 1). Fluid flow and heat transfer physics were solved using the finite element method. The complete details of the governing physics, model inputs, model geometry, boundary and initial conditions were included in Olsen, 2012. Within the model simulation, the attic temperature and flow fields were allowed to develop for 240 s before the attic inlets were opened. The simulation quickly transitioned from attic inlets closed to opened for a 60 s period. Figure 5 shows the simulated temperature distribution of the measured attic configuration.

Figure 5 shows similar thermal stratification as was seen in the experimental data (fig. 4). The low sun angle caused the south side of the attic to be hotter than the north side of the attic. The average temperature of the air passing through the attic inlet during operation was 25.0°C which is only 0.1°C lower than the experimental data. Average temperature was 48.9° C for the north roof and 19.9° C for the south roof. These temperatures compare well to the measured roof temperatures of 51.4° and 20.6° C.

On average, the simulation over predicted the experimental data by 2.0 K at the beginning of the fan cycle and 1.2 K at the end of the fan cycle. The over prediction of the temperature could have been due to several factors. The emissivities of the attic construction materials were estimates. The general over prediction in the high thermal gradient region between the hot roof and the floor suggests that radiative heat transfer was higher than expected. Accurate emissivities could reduce the over prediction in this region. However, the simulation was sufficient to predict the behavior of the attic thermal and airflow environment. The AIVM was then used to develop attic design changes tailored to increase the thermal energy extraction from the attic space for supplemental heating of the broiler chicks.

The AIVM simulation showed three initial areas for improvement. First, typical attic inlets pull cooler air from the attic floor. Constructing a riser on top of the attic inlet would allow the house to pull much hotter stratified air near the peak of the attic. Second, when the attic inlets were closed, hot air buoyantly vented out through the ridge cap. If this air could be slowed down or partially retained then thermal extraction potential of the attic space could be increased. When the fans were on, cool air entered through the ridge cap and flowed through the hot air region, absorbing some of the hot air's thermal energy along the way. Diverting this cool air stream away from the valuable hot air could improve thermal storage. Constructing a ridge diverter along the rafters could keep both the hot air retained and the cooler incoming air from directly diluting the heated air near the peak. The third area for improvement was the horizontal placement of the vent along the attic floor.

The AIVM was used to simulate changes in energy extraction from 24 combinations of ridge diverter location, ridge diverter length, vent riser location, and vent riser length (fig. 6). The comparison criteria was based on the quantity of heat that passed through the vent while the fans were operational. The quantity of energy passing through the vent was calculated relative to outside temperature. Thus, extracting attic air that was warmer than outside air produced positive heat gains (J $m^{-1}$ for a single 5-min fan cycle). A comparative value was also calculated as percent gain for each case compared to the base case (Case 1).

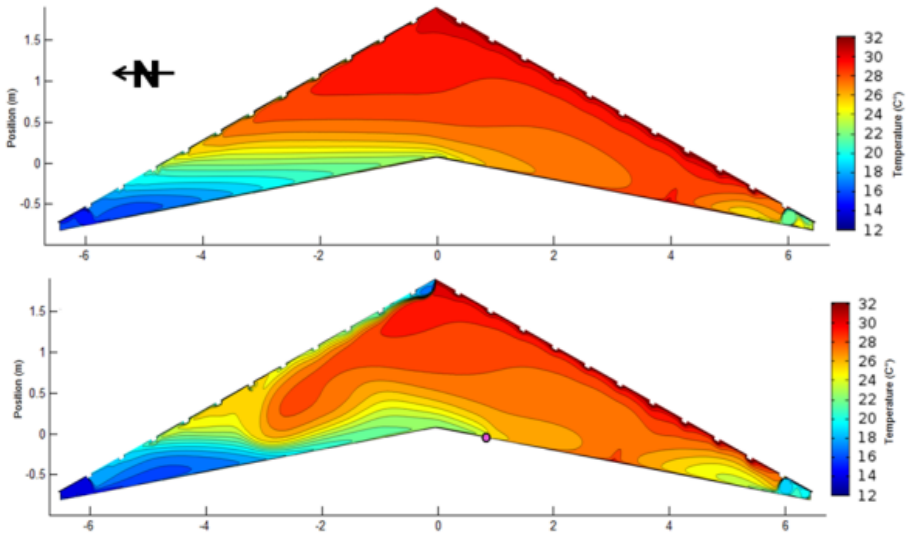


Figure 5: Simulated attic temperature distribution for (above) closed attic and (below) attic inlet open. Note: magenta dot (o) represents vent opening location.

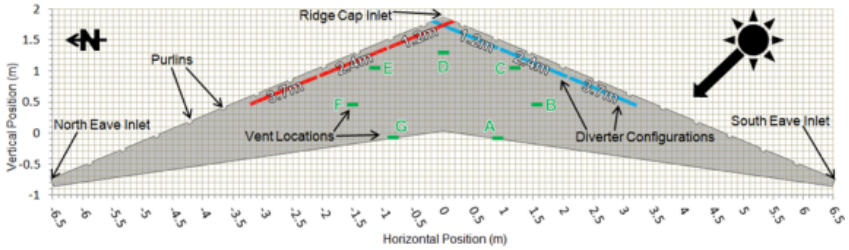


Figure 6: Schematic of potential diverter locations, diverter lengths, attic inlet riser location, and riser lengths that were simulated.

Twenty-four different combinations of diverters and vent locations were simulated using a simplified version of AIVM (Table 2). The simplifications included the following: neglect radiation within the attic space, roof temperature fixed at measured temperatures from experimental data, and no conduction across the diverter. In addition to these simplifications the vent velocity was set to a value of 2 m $s^{-1}$, pressure was set to one standard atmosphere, and density was calculated based on dry air at ambient temperature. All other model inputs were the same as the test case parameters. These simulations were intended to examine energy output for the possible attic space design changes relative to other configurations.

Table 2: Relative thermal energy output combinations of diverters and vent riser locations.

| Case | Vent Location | Diverter Length | Diverter Location | $q_{60}$ | Gain |
|---|---|---|---|---|---|
| | | m | | kJ/m | % |
| 1 | A | 0 | N/A | 61.6 | 0 |
| 2 | B | 0 | N/A | 73.4 | 19 |
| 3 | C | 0 | N/A | 78.8 | 28 |
| 4 | E | 0 | N/A | 78.8 | 28 |
| 5 | F | 0 | N/A | 73.1 | 19 |
| 6 | G | 0 | N/A | 51.1 | -17 |
| 7 | D | 1.22 | South | 74.9 | 22 |
| 8 | A | 2.44 | South | 61.6 | 0 |
| 9 | B | 2.44 | South | 70.6 | 15 |
| 10 | C | 2.44 | South | 72.0 | 17 |
| 11 | D | 2.44 | South | 70.9 | 15 |
| 12 | A | 3.66 | South | 55.4 | -10 |
| 13 | B | 3.66 | South | 65.2 | 6 |
| 14 | C | 3.66 | South | 65.9 | 7 |
| 15 | D | 3.66 | South | 65.9 | 7 |
| 16 | B | 1.22 | North | 74.5 | 21 |
| 17 | D | 1.22 | North | 93.6 | 52 |
| 18 | B | 2.44 | North | 78.1 | 27 |
| 19 | C | 2.44 | North | 89.3 | 45 |
| 20 | D | 2.44 | North | 100.8 | 64 |
| 21 | E | 2.44 | North | 93.6 | 52 |
| 22 | B | 3.66 | North | 80.6 | 31 |
| 23 | C | 3.66 | North | 94.3 | 53 |
| 24 | D | 3.66 | North | 103.3 | 68 |

Cases 1-6 were variations of attic inlet location without the addition of ridge-cap diverters. Increases in thermal energy extraction can be seen in all vent configurations which were not flush with the attic floor. Placing the vent riser intake higher in the attic space allowed warmer air to be extracted from the stratified air. Cases 7 - 15 examined diverter placement on the south side of the roof. While these configurations did increase contact time between the ridge cap inlet stream and the hot metal roof, the diverter also caused most of the heat from the south roof to be vented out of the ridge cap when the fans were off. Thus, south roof diverters were not beneficial. Cases 16 through 24 examined diverter placement on the north side of the roof. These configurations diverted cooler inlet air away from the hot buoyant air mass at the top of the attic. The diverters also trap and store hot air underneath them. Vent configuration D took advantage of this hot stored air most efficiently. Case 24 has the highest thermal energy extraction overall; however, a diverter this large could cause moisture problems with the attic trusses. Any hot moist air that flows back through the open vent would be trapped under this long diverter. Unwanted heat buildup under the

diverter in the summer could also be a problem when cooling the house. A smaller diverter (Case 17 or 20) still improves thermal energy extraction, but would trap less moisture under the diverter. Case 20 was presented as the best configuration (2.44 m diverter on north roof with a vent placed high in the center of the attic space) from the first round of simulations. The second round of simulations was intended to realistically simulate the thermal output of the attic design improvements. Six cases were chosen from the first round of simulations to investigate further using the full AIVM (Table 3). All simplifications made on the full model in the previous simulations were omitted. Boundary conditions were derived only from data that could be collected with a standard weather station and the velocity sensors located within the attic inlet vent. The 30 to 120 s time periods represent fan runtimes. These runtimes correlate to duty cycles of 10, 20, 30, and 40%. The different configurations of Cases 1-6 deplete the attic of thermal energy at different rates; thus energy output varied according to the fan duty cycle. All energy outputs were again compared against the test case attic configuration (Case 1).

Table 3: Thermal energy output through the attic inlet for select simulation cases.

| | | | | Energy output for fan runtime specified (s) and relative gains over Case 1 | | | | | | | |
|---|---|---|---|---|---|---|---|---|---|---|---|
| Case | Vent Location | Diverter Length | Diverter Location | $q_{30}$ | Gain | $q_{60}$ | Gain | $q_{90}$ | Gain | $q_{120}$ | Gain |
| | | m | | kJ/m | % | kJ/m | % | kJ/m | % | kJ/m | % |
| 1 | A | 0 | N/A | 26.3 | 0 | 51.3 | 0 | 76.3 | 0 | 101.8 | 0 |
| 2 | C | 0 | N/A | 31.2 | 19 | 61.7 | 20 | 90.7 | 19 | 118.1 | 16 |
| 3 | G | 0 | N/A | 23.4 | -11 | 45.3 | -12 | 68.4 | -10 | 92.5 | -9 |
| 4 | D | 2.44 | South | 29.4 | 12 | 59.2 | 15 | 88.1 | 16 | 116.1 | 14 |
| 5 | C | 2.44 | North | 33.3 | 27 | 67.1 | 31 | 99.7 | 31 | 130.4 | 28 |
| 6 | D | 2.44 | North | 36.3 | 38 | 72.3 | 41 | 106.3 | 39 | 138.3 | 36 |

The prior lack of knowledge on the thermal environment of the poultry house attic led to the practice of installing attic inlet vents in an alternating pattern (half of the vents on the north side of the ceiling and half on the south side of the ceiling). This was done under the assumption that alternating the location of the vents would improve ventilation distribution. While air distribution may be improved, placing vents on the north side of an east-west oriented building will decrease the thermal energy extraction potential of the system by approximately 11% (Case 3 compared to Case 1). Case 1 and 3 demonstrated that attic inlets installed flush with the floor should be installed on the south side of the attic in an east-west oriented building. Placing the inlets on the south side of the attic takes advantage of the uneven heating of the attic space.

A comparison of Cases 4 and 6 confirms the earlier finding that a diverter mounted parallel to the underside of the roof on the south side of the attic is not as effective as a similar diverter on the north side of the attic. The north side diverter (Case 6) shields the thermally stratified air at the top of the attic space from incoming ambient air from the ridge cap. The south side diverter (Case 4) acts as a solar chimney and radiation shield whenever the fan is off; buoyantly venting air through the ridge cap which absorbed the solar heat trapped between the diverter and the roof. This behavior was

not desirable. With the north side diverter in place, an attic configuration with the vent at location D has a 10% energy extraction advantage over the vent at location C for a 60 s fan runtime. Thermal stratification permitted a vent mounted higher in the attic space to extract more thermal energy. However, this advantage is about half of that seen in the first round of simulations. It's likely the addition of interior radiation to the model reduced the thermal stratification of the attic space by introducing an additional heat flux away from the roof to the attic floor. The attic configuration consisting of a 2.44 m diverter on the north side of the attic and a vent mounted high in the center of the attic (1.3 m from the insulation surface) under the diverter is once again presented as the best case attic configuration. Case 6 had a 38% and 41% (30 s and 60 s fan runtime, respectively) improvement in thermal energy capture over the test case configuration (Case 1). The temperature and flow fields of Case 6 with a 60 s fan runtime can be seen in Figure 7. The velocity distribution plots (fig. 8) show how this attic configuration acts as a thermal siphon. Cool ambient air is redirected to the floor area of the attic while pushing warmer buoyant air up into the peak of the roof under the diverter. The vent then taps into this stratified region to extract the most thermally valuable air.

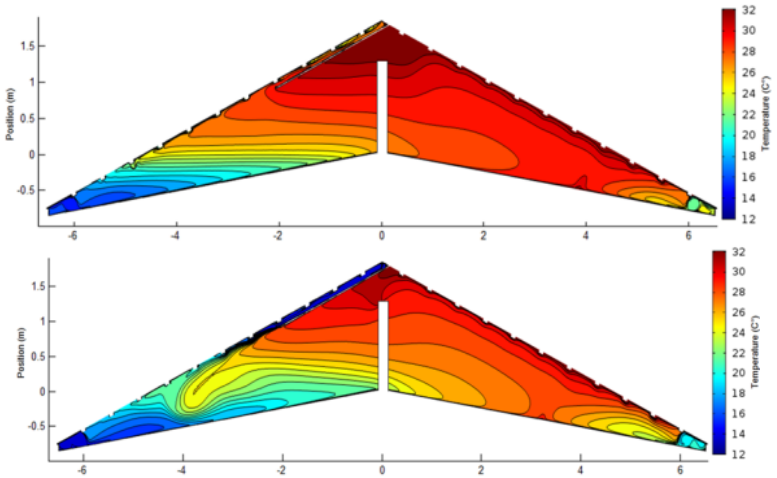


Figure 7: Simulated attic temperature distribution for the full simulation of Case 6 with the (above) attic inlet closed and (below) attic inlet open (60 s).

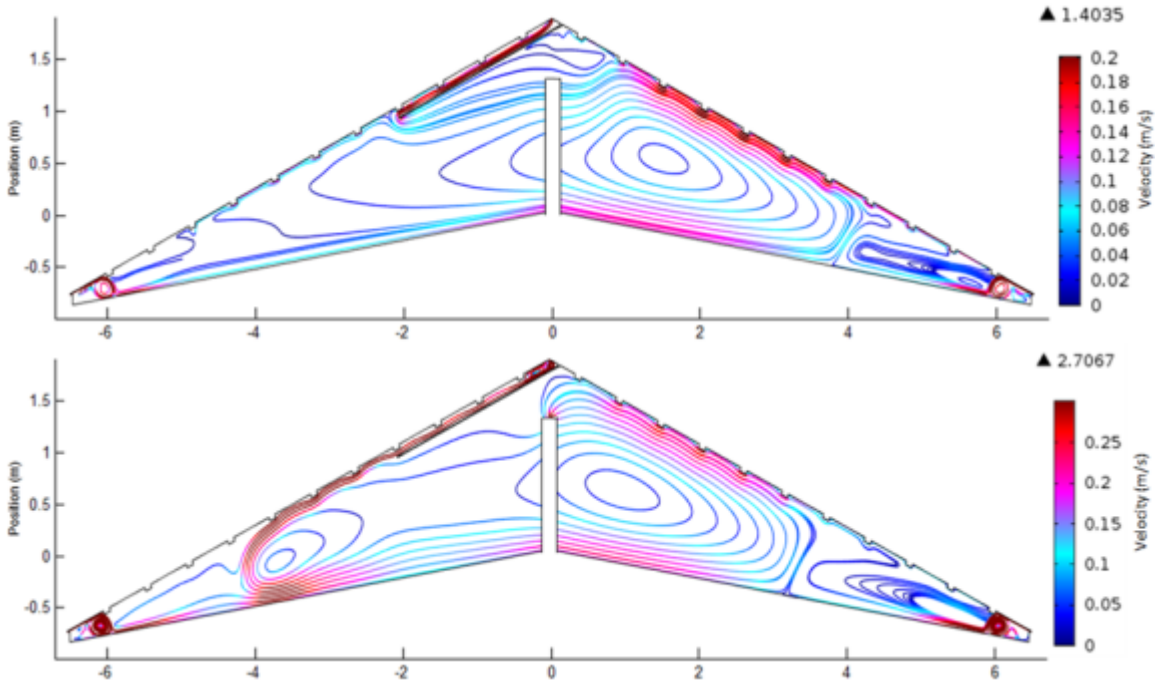


Figure 8: Simulated attic velocity distribution for the full simulation of Case 6 with the (above) attic inlet closed and (below) attic inlet open (60 s).

The simulation of Case 2 demonstrates that a thermal energy gain of approximately 19% can be obtained by placing the vent near the hot side of the roof even without a diverter in place (fig. 9). Vent C was located 1.2 m to the south of the attic center and 1.3 m higher than the attic floor. Buoyantly rising air on the underside of the south roof shielded the attic inlet from cool ridge cap air short circuiting the attic space (fig. 10). However, efficiency was less than Case 6 because a hot air mass was not generated and stored under a diverter while the attic inlets were closed. An estimation of fuel savings by the implementation of the proposed attic inlet design modifications was important to illustrate their economic viability. The fuel savings gained by standard attic inlet ventilation systems (Case 1; vent flush with attic floor) has been estimated by the National Poultry Technology Center for broiler facilities located in Alabama. A grower using Case 1 can save 794 and 1,019 gallons of propane over 5 flocks and 7 flocks, respectively. Assuming propane is $2 per gallon, the savings would be $1,588 and $2,038 per house per year, respectively. A grower using Case 2 should save $1,890 and $2,425 per house per year, respectively. A grower using Case 6 should save $2,207 and $2,833 per house per year, respectively. These cost savings represent weather conditions and solar angles observed in the test case. However, the improvement percentages will likely vary throughout the year. The seasonal and weather effects have yet to be determined.

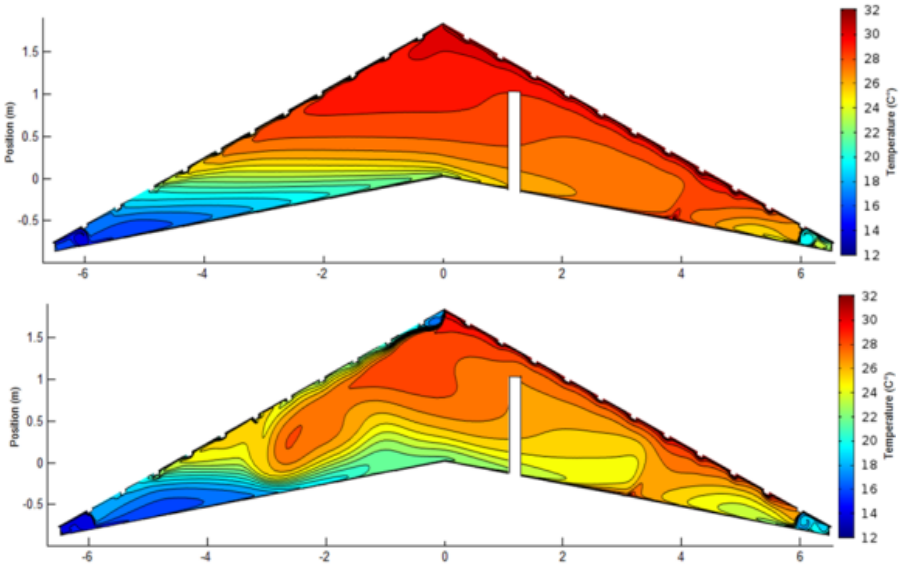


Figure 9:Simulated attic temperature distribution for the full simulation of Case 2 with the (above) attic inlet closed and (below) attic inlet open (60 s).

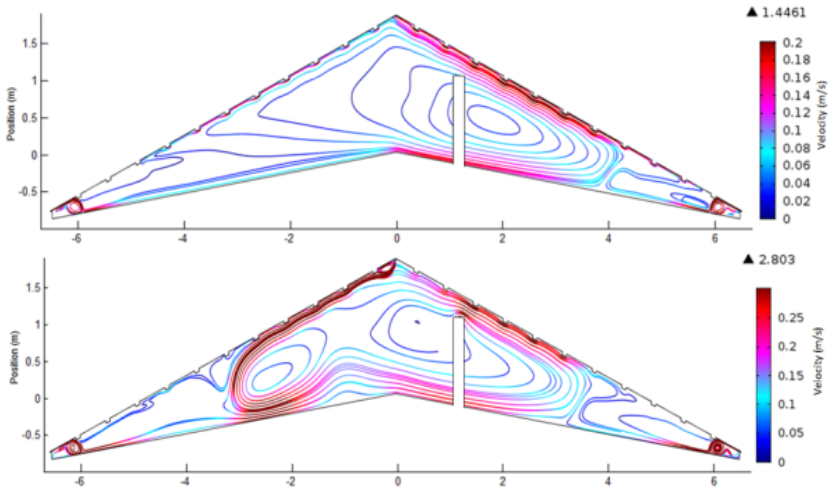

Figure 10: Simulated attic velocity distribution for the full simulation of Case 2 with the (above) attic inlet closed and (below) attic inlet open (60 s).

**Publications / Presentations:**

*Conference Papers:*

1. Olsen, J.W.W., J.D. Davis, J.L. Purswell, and B.D. Luck. 2013. Improving attic inlet ventilation through CFD simulation. Poult. Sci. 92(E-suppl. 1): 199. (Abstract)

2. Olsen, J.W.W., J.L. Purswell, J.D. Davis, B.D. Luck and E.J. Koury. 2012. Improving commercial broiler attic inlet ventilation through CFD analysis. Procs. Of the 9th International Symposium: Livestock Env. IX. Jul 8-12. Valencia, Spain.

3. Olsen, J.W.W., J.D. Davis, J.L. Purswell. 2011. 2D simulation of air flow in commercial broiler house attics. Presentation for the 2011 ASABE International Meeting, Aug 7-10. Louisville, KY.

*Thesis and Dissertations*

1. Olsen, J.W.W. 2012. Improving commercial broiler attic inlet ventilation through data acquisition coupled with CFD analysis. M.S. Thesis, Agricultural & Biological Engineering Department, Mississippi State University, Mississippi State, MS.

## Task 4.3. Assess utilization of disaster debris to produce emergency power in a micro-CHP system.

**Description:**
The Recipient shall survey the quantity and composition of debris produced for a given location and intensity of weather related disaster and then test the feedstock potential of debris considering type and level of deterioration.

**Percentage of completion**: 100%

**Accomplishments:**
Part 1 of the Debris Emergency Power Production Simulation (DEPPS) model was developed to characterize the volume of woody debris (forest residues) for a given hurricane event (fig 1). Wind speed, associated with hurricane category, was correlated to composition of debris (stem volume and branch volume, fig 2). Hurricane Katrina data were used in the area of the 10 Mississippi Gulf Coast counties. Predominate tree type present in the disaster area was Pinus (species included slash pine and loblolly pine). Figure 3 shows the observed damage versus predicted damage for the area. The point data represent Mississippi Forest Inventory (MIFI) damage plots that had observable wind damage after Hurricane Katrina. The orange shaded area represents considerable forest damage (Stem Damage > 43%, Branch Damage > 68%) and the yellow represents moderate foliage damage (Stem Damage: 42% to 20%, Branch Damage: 67% to 52%) predicted by DEPPS Part 1. Fifty-eight percent of the MIFI points with wind damage were within the Orange damage area. This estimate is more conservative than that of the US Forest Service in late 2005. DEPPS Part 1 ultimately produces a point feature along road networks associated with volumetric woody debris after a hurricane. Figure 4 shows a screen shot of debris supply points for Wiggins, MS. The simulation created 207,147 supply points over the ten county study area. The mean woody debris volume for each supply point was 13.08 cubic meters. These staging points will be used for debris retrieval, transportation and chipping. Task 4.3 is finished with the completion of DEPPS Part 1. DEPPS Part 2 will be conducted as part of Task 4.7.


Figure 1: GUI for DEPPS Part 1.

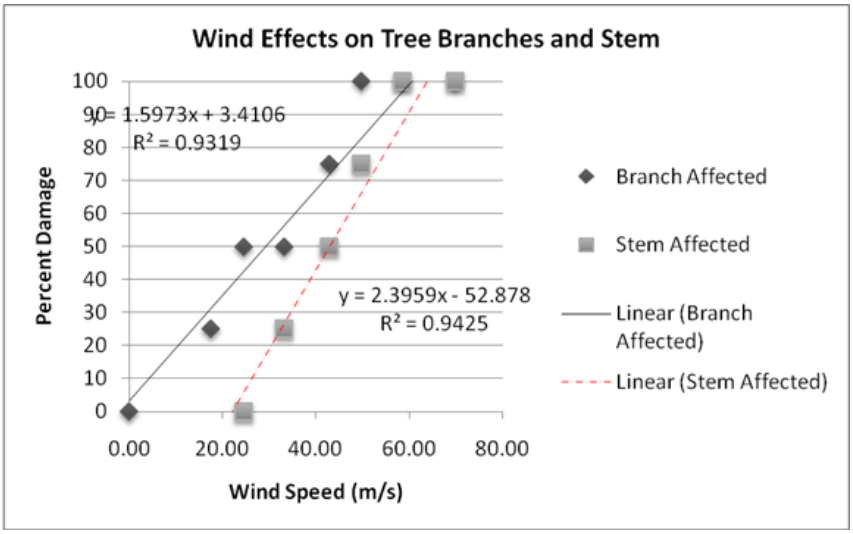


Figure 2: Branch and stem damage associated with wind speed.

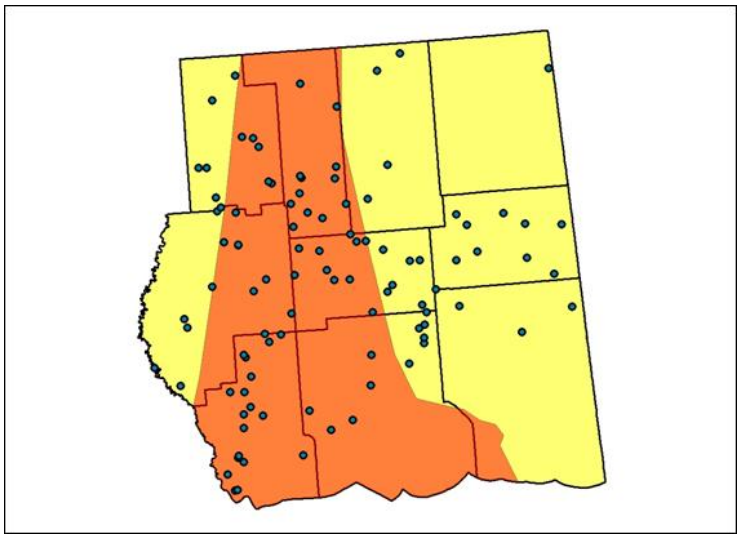

Figure 3: Observed woody damage (point data) vs. Predicted woody damage. Orange is extreme damage, Yellow is moderate damage.

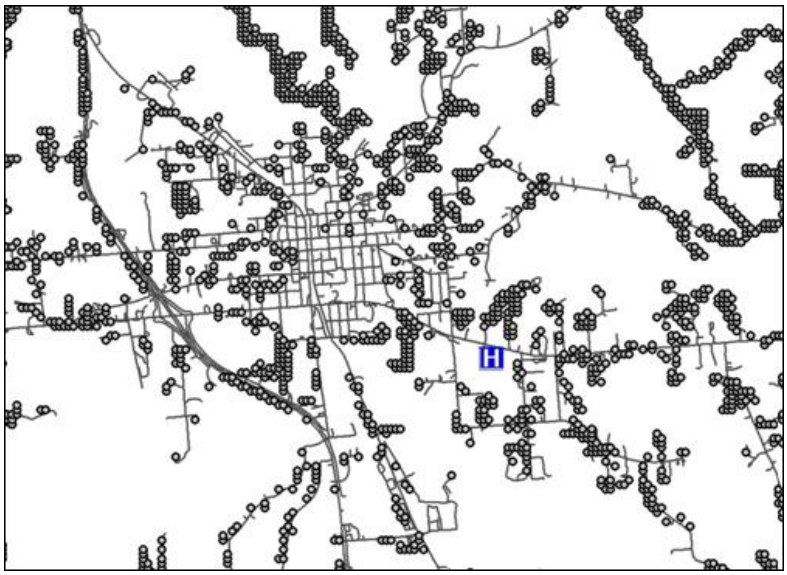


Figure 4: Estimated debris supply in Wiggins, MS.

**Publications / Presentations:**

*Conference Papers:*

Ryals, C.S., J.D. Davis, and E. Columbus. 2009. The energy potential of disaster debris to produce emergency power in a micro-cooling, heating, and power (m-CHP) system. Presentation for the 2009 ASABE International Meeting, June 21- 24. Reno, NV.

## Task 4.4. - Biomass feedstock handling for CHP Systems

**Description:**
The Recipient shall design unit operations for the biomass handling in an integrated syngas production facility with CHP technologies. The test cases will involve locally available biomass feedstocks collected and processed by the Recipient. The date will be utilized to develop an economic profile for an integrated syngas production facility involving CHP technologies.

**Percentage of completion**: 100%

**Accomplishments:**
Giant miscanthus, switchgrass, and wheat straw have been harvested and hammer milled and pellets will be made. Ash content of the three biomass crops ranged from 4.3 to 8.7% while wheat straw was 5.0% Heat value of the feedstocks ranged from nearly 7700 to 8100 BTU/lb Switchgrass pellets had about the same ash content and heat value as the raw switchgrass. Some of the chemical analysis were somewhat different for switchgrass and the switchgrass pellets. Biomass feedstocks all contain a range of elements that include heavy metals. High quality and high density pellets can be made from switchgrass and the pellets had uniform density and strength. Pellet mill operational parameters observed to affect pellet properties were die types and steam conditioning whereas feedstock parameters were material, moisture, and grind size.

An initial study using an in-field hay cuber to densify Bermuda grass into cubes was completed. The grass materials would produce cubes in the 8-25% moisture content range. An overall higher percentage of cubed material was produced between the 9% and 16% MC. The largest percentage of cubes (78%) were produced at 15% MC. No cubed material was produced at the 25% MC. The John Deere 425 Hay cuber showed promise of providing densified cubes in the field, however, efforts were directed towards the use of a binding agent to increase the percentage of cubes developed. A larger study was conducted to densify Bermuda grass using a binding agent. The study compared the efficacy of no binding agent and a binding agent (lignin sulfonate @ 50lb/ton) on the densification into cubes. Eight rows of grass were divided into three 100 ft sections each. Within each 100 ft section the cuber material discharge was collected for cube production. Cubes were separated from fines through sifting. Mean cube production was 80% and 85% with the no binder and binder treatments, respectively. The use of a binder increased cubing production efficiency. Further work needs to be conducted in the application rate of the binder as well as comparison to other economical binders.

Measurement of surface area, volume, and density is an essential for quantifying, evaluating, and designing the biomass densification, storage, and transport operations.

Acquiring accurate and repeated measurements of these parameters for hygroscopic densified biomass are not straightforward and only a few methods are available. A 3D laser scanner was used as a measurement device and the 3D images were analyzed using image processing software. The validity of the method was verified using reference objects of known geometry and the accuracy obtained was in excess of 98%. Cotton gin trash briquettes, switchgrass pellets, switchgrass cubes, hardwood pellets, and softwood chips were the test materials. Most accurate results of the surface area and volume required the highest possible resolution of the scanner, which increased the total scan-process times, and image file size. Physical property determination using the 3D scanning and image analysis physical property determination methodology is an alternative, non-invasive, accurate, and is highly repeatable (coefficient of variation $<$ 0.3%). The various limitations and merits of the developed method were also enumerated.

All the goals were not met due to the departure of a faculty member; however, it has been decided to shift the focus of this research to one that will model a biomass handling system for CHP. That focus is represented in Task 4.6 where the research will be continued.

**Publications / Presentations:**

*Journal Papers:*

1. Igathinathane, C., J.D. Davis, J.L. Purswell, and E.P. Columbus. 2010. Application of 3D scanned imaging methodology for volume, surface area, and envelope density evaluation of densified biomass. *Bioresource Technology*. 101(11): 4220-4227.

*Conference Papers:*

1. Columbus, Eugene P., Steven H. Elder, Brian S. Baldwin, William D. Batchelor, James R. Wooten, G. Daniel Chesser, and David L. Trammell. Physical Properties of Pelletized Biomass. 2006 ASABE Annual International Meeting, Portland, OR, 9 – 12 July 2006.

2. Massey, W.A., C. Igathinathane, J.D. Davis, J.L. Purswell, and E.P. Columbus. 2009. Densified biomass mass properties determination using 3D laser scanning and image analysis. Abstract for the MSU Biofuels Conference. August 6-7. Jackson, MS.

3. Massey, W.A., C. Igathinathane, J.D. Davis, J.L. Purswell, and E.P. Columbus. 2009. Densified biomass mass properties determination using 3D laser scanning and image analysis. Abstract for the MSU 8th Annual Graduate Research Symposium. Nov. 6th. Starkville, MS.

## Task 4.5. - Determine Feasibility and Limitations of Low Quality Syngas for CHP Application

**Description:**

- Quantify and compare pertinent parameters between syngas generated by downdraft gasifier, updraft, and from O'neal Stove
- Develop method of pre-treatment of grass and other woody feedstock by reshaping into aggregates that are not chips or pellets.

**Percentage of completion**: 100%

**Accomplishments:**

- Perform wood chips and grass cubes gasification and investigate the process problems.
- Develop method of pre-treatment of grass and other woody feedstock by reshaping into aggregates that are not chips or pellets.

Description of BioMax 25 gasification system: The gasifier, BioMax 25, was manufactured by Community Power Corporation. It is a downdraft gasifier with a host computer to control the gasification process. This gasification system is highly automatic. Scheme 1 displays its components. Main components include the feeding system, the gasifier, the heat exchanger and the filters. All the components are connected to and controlled by the computer. There are thermocouples and pressure transducers installed to monitor the running of the gasification system and provide input to the computer.

An auger feed system is installed with the gasifier. When the fuel level in the gasifier falls below the setting point, the motor of the feeder will be turned on and input new fuels. The gasifier is the place where the gasification reactions occur and complete. It is designed with 5 levels of air injection loops and each loop has 5 injection points, which ensured the air was distributed into the gasifier evenly at the same level. The amount and rate of air injection were controlled by the computer according the temperatures inside the gasifier.

The heat exchanger cools down the producer gas from 500-700 $^{o}$C to about 110 $^{o}$C. This system uses room-temperature air to cool the producer gases. The producer gas then goes through parallel bag filters to remove the fine particles. After filtration, the producer gases then go through an activated carbon filter to remove the tars. The outlet syngas contains about 48% $N_2$, 21% CO, 18% $H_2$, 10% $CO_2$, 1.5% $CH_4$, some water vapor and trace amount of other gases. The cool syngas is then compressed to a storage tank or sent to a burner.

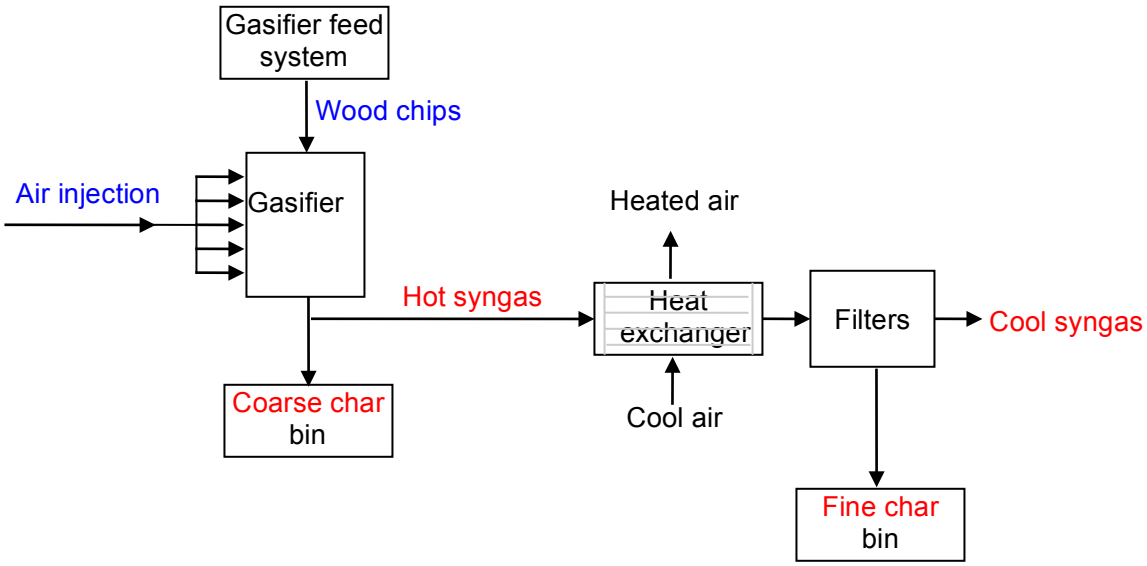


Scheme 1. BioMax 25 gasification system.

*Description of process profile:*

A downdraft gasification process was applied. The wood chips inside the gasifier would experience drying, pyrolysis, oxidation and reduction reactions (Figure 1, 2). The boundaries of these zones in Figure 1 were not strict. It depended on where the flame front was in each run. The energy for reduction reactions and gasifier heating was provided by the combustion of wood chips. No external energy was provided. The processing temperatures and pressures were monitored and controlled by the program (BioMax 25 version 1.28) in the host computer, which acquired the data form installed thermocouples and pressure transducers.

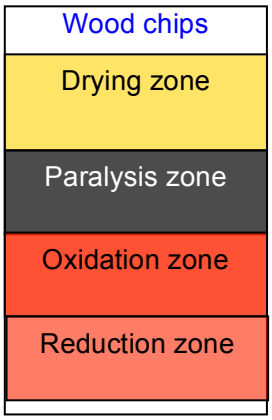


Figure 1. Processes happening inside the gasifier.

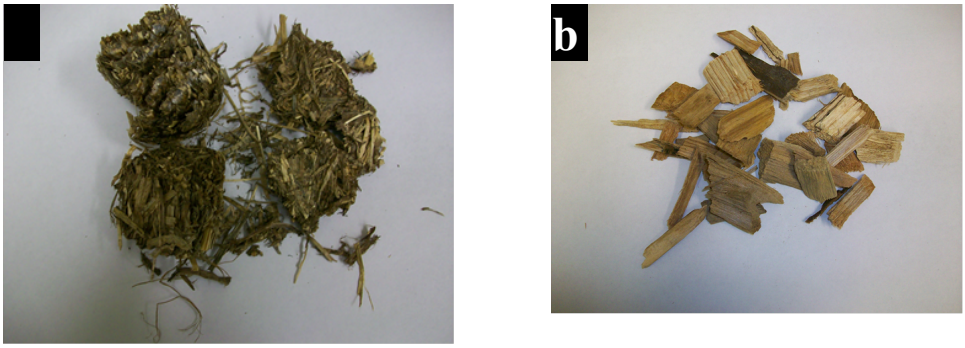


Figure 2. (a) picture of grass cubes; (b) picture of wood chips.

*Temperature profile:*

The gasifier temperatures were automatically controlled by the computer according to the settings in the program. The air was injected and temperatures were monitored at 5 levels as displayed in Figure 3. The temperatures in the combustion and reduction zones (Level 3-5) were maintained between 600-900 oC. The temperatures at Levels 1 and 2 fluctuated when new fuel was added to the gasifier. The temperature profile at Levels 1 and 2 may change greatly when wood species and moisture content changed. The temperatures were much lower for gasification with oak tree wood chips with 10-11% moisture content than that with 9.5% moisture content, but the temperatures at Levels 4 and 5 changed little. In this research, only wood chips with 9.5% moisture content was investigated for material balance and energy balance calculation.

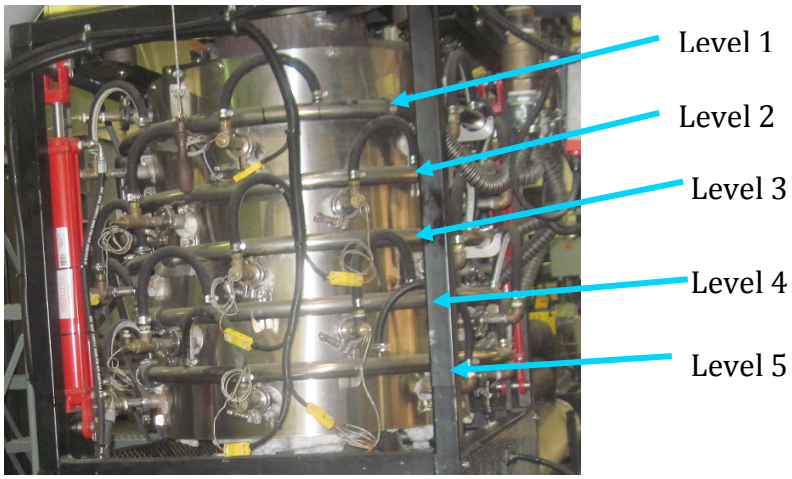


Figure 3. The air injection levels and temperature monitoring positions of the gasifier.

Gas flow rate:

The gas flow rate was pretty stable and fluctuated very gently around the setting value, 65 $Nm^3/h$, once the gasifier started running (see Figure 4).

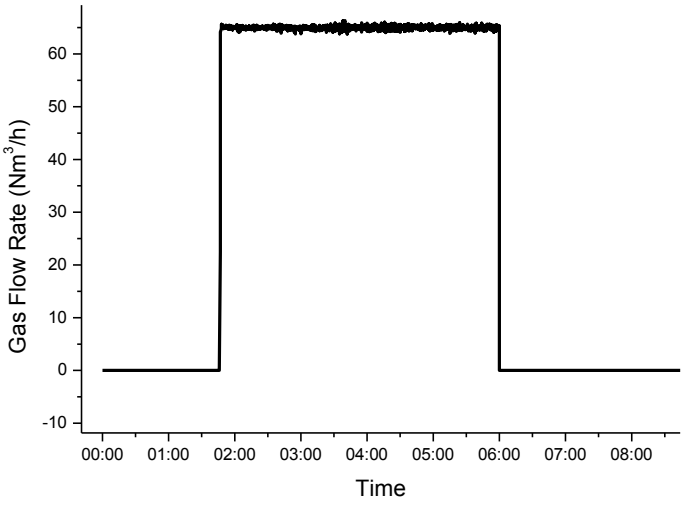


Figure 4. The producer gas flow rate during a gasification run.

**Publications / Presentations:**

*Conference Papers:*

1. Yu, F., Q. Yan, J. Hu, Y. Lu, L. Wei, J. Wooten, E. Columbus and W. Batchelor. 2010. Mixed Hydrocarbons from Biomass Gasification Syngas over Mo/HZSM-5 Catalyst. 9th International Conference on Sustainable Energy Technologies (SET). Shanghai, China. August 24-27.

2. Yu, F., Q. Yan, J. Hu, L. Wei, E. Columbus and J. Wooten. 2010. Mixed Hydrocarbon Production from Biomass-derived Syngas over A Bi-functional Catalyst. International Symposium on Renewable Feedstock for Biofuel and Bio-based Products. Austin, TX, August 11-13.

3. Hu, J., Yu, F., Wei, L., Columbus, E., and Batchelor, W. Preliminary Study of the Conversion of Biomass Gasification Syngas to Gasoline-range Hydrocarbons over Mo/HZSM-5. Paper 1008573, ASABE 2010 Annual International Meeting, Pittsburgh, Pennsylvania, June 20-23, 2010.

*Posters:*

1. Street, J., Columbus, E., Warnock, J., Wooten, J., White, M. Scale-Up of Gasoline-range Hydrocarbons over Mo/H-Y and Mo/HZSM-5 Catalysts. An IBE Poster Presentation presented for IBE 2010 Conference. Cambridge, MA, March 4-6, 2010.

2. Street, J., Columbus, E., Warnock, J., Wooten, J., White, M., Yu, F. Scale-Up of Gasoline-Range Hydrocarbon Production over Mo/HZSM-5 using Synthesis Gas. A Poster Presentation presented for the Mississippi State 2010 Biofuels Conference. Jackson, MS, August 12-13, 2010.

## Task 4.6. - Biomass Handling for CHP Systems

**Description:**

- Design unit operations particularly biomass handling for an integrated syngas production facility involving CHP technologies.
- Develop an economic profile for an integrated syngas production facility involving CHP technologies through modeling.

**Percentage of completion**: 100%

**Accomplishments:**

*Design unit operations particularly biomass handling for an integrated syngas production facility involving CHP technologies.*

We have completed the analysis of potential increase in energy capacity of two existing CHP plants, based on available corn stover and forest logging residue feedstock. Corn stover (CS) residue values were determined by averaging the county-level corn yields and converted corn yield to stover using a 1:1 ratio, that is, for every ton of corn grain harvested, one ton of corn stover is produced. Forest logging residue (FLR) data from 1995, 1999, and 2002 were obtained from Mississippi Institute for Forestry Inventory (MIFI). Different percentages of CS and FLR availability for CHP use were evaluated. The maximum utilization rates of CS and FLR were 33% and 30%, respectively. The energy produced using CS and FLR was calculated for each county.

We identified five counties, namely: Wilkinson, Wayne, Clarke, Copiah, and Amite, that have forest logging residue feedstock to sustain a CHP facility with a range of capacity between 8,257kW to 9,766kW. Using corn stover alone, Washington, Yazoo, Sunflower, Leflore, and Sharkey counties can produce 8,021kW and 13,497kW of energy, respectively. Considering both feedstocks and based on a conservative amount of 30% available forest logging residue and 33% corn stover, we found that 20 counties have adequate supply for a CHP facility with a capacity of 8,257 kW to 19,564kW. Forest logging residue accounted for the highest percentage of biomass to the total available feedstock in these counties. Higher utilization rates of CS (33%) and FLR (30%) can potentially support higher CHP capacity.

Data on 22 existing CHP facilities in Mississippi and their capacities were obtained from the U.S. Department of Energy (DOE) database. Two CHP facilities – one in Washington and one in Scott county – were selected based on the primary type of available biomass feedstock in the surrounding counties. The minimum corn stover utilization level to supply a 5,000 kW CHP facility in Washington county was 13%, while a 1,000 kW facility in Scott county required 7%. Corn production in the Mississippi Delta Region provides high levels of corn stover to support an increase in

CHP capacity in Washington county. Combining both types of feedstock sources (CS and FLR) can potentially increase the CHP capacity to 14,922 and 5,193kW in Washington and Scott, respectively. The availability of CS and FLR within a 10-mile radius of the CHP plants in Scott and Washington counties provides the potential for increased CHP capacity. Extending the buffer area to 30 miles can provide enough CS and FLR feedstock to support 24,500 kW and 27,500 kW CHP plants in Scott and Washington counties, respectively.

*Develop an economic profile for an integrated syngas production facility involving CHP technologies through modeling.*

An economic model was developed using a parametric cost approach and C++ computer programming language. Preliminary results of model development, and economic analysis were presented in several national and local meetings (e.g. IBE, ASABE, MSU Biofuel). Economic modeling and analysis of pilot-scale bio-gasification system using woodchips feedstock source data from Mississippi State University's bio-gasifier has been performed. The economic costs with production capacities ranging from 60 to 1800 $Nm^3h^{-1}$ in three operating modes were analyzed with sensitivity analysis. Preliminary sensitivity analysis of the economic model input parameters with production capacities ranging from 60 to 2,400 $Nm\text{-}^3h^{-1}$ showed that larger bio-gasification capacity and higher operating modes will have lower syngas production unit cost. When the production capacity with a higher operating mode increased from 60 to 2,400 $Nm^{-3}$ $h^{-1}$, the total annual production cost increased, while the syngas unit cost decreased. Sensitivity analysis of the model results indicated that equipment purchase cost ranked the top as followed by pay rate of employees, feedstock price, loan life, interest rate, electricity price, and waste treatment price. We are also analyzing economics of potential feedstock source yields from the Mississippi watershed using a regional scale model.

**Publications / Presentations:**

*Conference Papers:*

1. Yangyang Deng, and Parajuli P. B. 2011. Economic Evaluation of Electricity Generation from a Small-Scale Bio-Gasification Facility using an Optimization Model. IBE Annual Conference, Loews Atlanta, March 3-5, 2011, Atlanta, GA.

2. HakKwan Kim, Parajuli P. B., Fei Yu, Joel O. Paz, and Eugene Columbus. 2011. Economic Model for Evaluating Syngas Production Cost of Bio-gasification Facility. IBE Annual Conference, Loews Atlanta, March 3-5, 2011, Atlanta, GA.

3. Hakkwan Kim, Parajuli P. B., Yu F., and Columbus E. P. 2011. Economic Analysis and Assessment of Syngas Production using a Modeling Approach. ASABE Publication No. 1110814, ASABE, St. Joseph, MI. Available at: http://asae.frymulti.com/azdez.asp?search=1&JID=5&AID=37322&CID=lou i2011&v=&i=&T=2.

4. Yangyang Deng, and Parajuli P. B. 2011. Evaluation of Syngas Production Unit Cost of Bio-Gasification Facility using Regression Analysis Techniques. ASABE Publication No. 1110711, ASABE, St. Joseph, MI. Available at: http://asae.frymulti.com/azdez.asp?search=1&JID=5&AID=37284&CID=lou i2011&v=&i=&T=2.

5. Parajuli P. B. 2011. Bio-energy Feedstock Yields and their Water Quality Benefits in Mississippi. ASABE Publication No. 1111416, ASABE, St. Joseph, MI. Available at: http://asae.frymulti.com/azdez.asp?search=1&JID=5&AID=38511&CID=lou i2011&v=&i=&T=2.

6. Hakkwan Kim, and Parajuli P. B. 2011. Assessment of the Potential Crop Yield for Bio-Energy Production Using the SWAT Model. ASA/CSSA/SSSA, International annual meeting, October 16-19, San Antonio, TX.

## Task 4.7. - Utilizing disaster debris to produce emergency power in a CHP system

**Description:**

- Determine the quantity and composition of debris produced for a given size, location and type of disaster.
- Determine the feedstock potential for different types of debris materials and states of deterioration.
- Develop an economic analysis model for the production of emergency power using disaster debris as a feedstock in a CHP system.

**Percentage of completion**: 100%

**Accomplishments:**

*Determine the quantity and composition of debris produced for a given size, location and type of disaster.*

A feasibility analysis was conducted using DEPPS Part 2. The simulation showed the operational feasibility for a set of CHP systems strategically placed across the Southern ten counties in Mississippi (fig. 1). Meeting the demand of the CHP unit with available debris created a supply and demand problem. The cost attribute was based on time of retrieval. If the CHP demand could be met within the time constraints, then the CHP unit would be feasible. Time attributes were based on debris chipping and loading, transportation, and machine preparation times. Each CHP depot was allocated three trucks; one for chip delivery and two for debris retrieval. Speed was based on road type (primary roads, secondary and rural and city streets were 55, 45 and 35 mph, respectively. Each truck could only operate between 7 am and 7 pm (fig 2). This constraint forced simulation to retrieve from major highways first because of the higher speed limit. DEPPS Part 2 determined that 5 of the 6 CHP depots were capable of retrieving enough fuel to power the CHP units in that area (table 1). Each successful depot could operate its units for multiple days with one day of debris retrieval.

One of the CHP locations (Greene County Hospital) failed to supply enough debris for emergency operation for a single day after Hurricane Katrina (Table 1). All other locations were operational within a 5 km buffer. Interestingly, the simulation tended to clear highways first because of the higher travel speeds and then clear rural gravel roads. This will prove important when clearing for emergency transportation traffic.

Table 1: Number of CHP units, total energy demand, and retrieval volume for each of six locations in Southern Mississippi.

| Depot Location | # of CHP Units | CHP Demand | Retrieval (m3/12hr) |
|---|---|---|---|
| Forrest County Hospital | 6 | 78 | 169.12045 |
| Greene County Hospital | 3 | 39 | 2.57327 |
| George County Hospital | 2 | 26 | 130.45646 |
| Hancock General Hospital | 5 | 65 | 270.67128 |
| Pearl River County Hospital | 4 | 52 | 109.86533 |
| Singing River Hospital | 7 | 91 | 146.38436 |

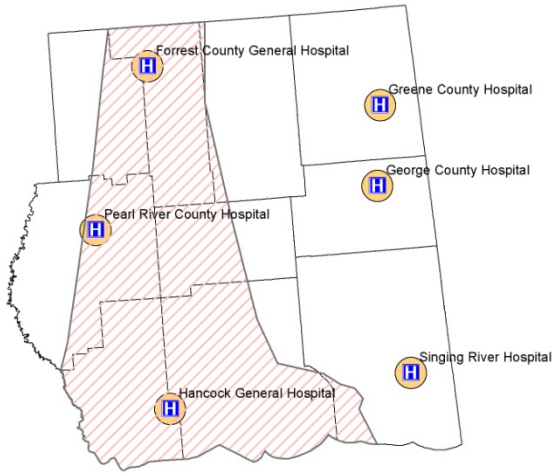


Figure 1: Location of six CHP depots associated with county hospitals in Southern Mississippi. The shaded area is the impact of Hurricane Katrina.

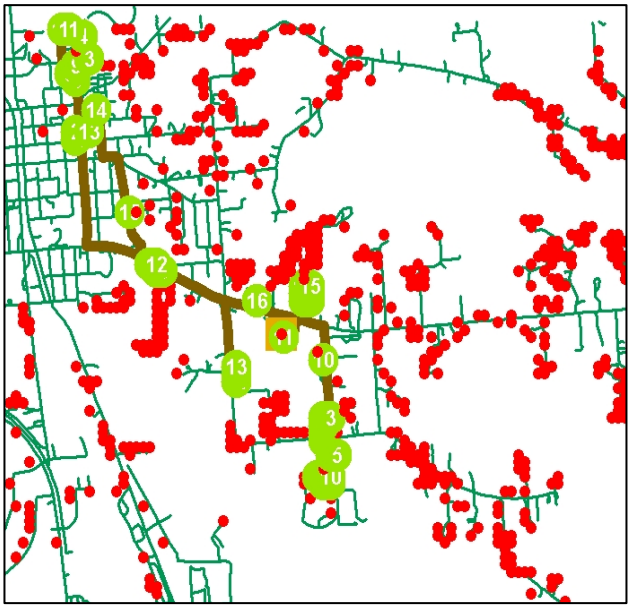


Figure 2: GIS illustration of roads and debris points (red). Numbered points illustrate the pickup locations for a single truck route over a 12 hour period.

*Determine the feedstock potential for different types of debris materials and states of deterioration.*

A study was conducted to assess energy availability from wood chips under different degradation scenarios. Bulk mixed wood chips were purchased from a local commercial pulp mill. The wood chips were randomly collected into 0.5 kg samples and placed into mesh nylon bags. There were four treatments: air, water, soil, and paved with five replications (fig. 3). These treatments were inspired by conditions that disaster debris or stored chips could be exposed to before being utilized in a CHP device. A tree could be lodged in the air before being brought to the ground for chipping, or it could land in standing surface water. A felled tree could also lay on soil or on a paved surface. There were five time periods being considered: week 0, week 3, week 6, week 9, and week 12. Week zero was considered an initial condition prior to degradation under treatment conditions. Gross energy content was measured for all samples with a bomb calorimeter using standardized methods. Ash contents were determined using standard furnace methods. Hemicellulose, cellulose, and lignin carbon fractions were determined using standard chemical digestion methods. Data were analyzed as a mixed model with repeated measures at a 0.05 significance level. Means were grouped into letter classifications at a 0.05 significance level.


Figure 3. Wood chip samples exposed to their assigned treatments: (a) air, (b) paved, (c) soil, and (d) water.

Complete analysis of results and development of publication grade figures are on-going. Differences among replications were insignificant for all analyses. Repeated measures ANOVA of the gross calorific value indicated that the treatment (degradation scenario)

was significant. The water treatment had lower energy content that the other treatments (table 2). Differences among other treatments were insignificant.

Table 2. Gross Calorific Value Means Differences by Treatment

| Treatment | Ho (J/g) | Std Error | Group |
|---|---|---|---|
| Air | 19789 | 78.4026 | A |
| Paved | 19860 | 79.9528 | A |
| Soil | 19691 | 92.2982 | A |
| Water | 19343 | 79.2685 | B |

Ash content treatments differed significantly in the study period. There were no interactions between replication and treatment Effect slicing revealed that the air and paved treatments had the lowest ash content, followed by soil and then water (table 3). Figure 4 indicates ash content could more than double for disaster debris on soil or in water. This would mean that debris stored under these conditions would have less carbonaceous material available for combustion and would create more ash on a mass basis than debris stored under paved conditions.

Table 3. Ash Content Means Differences by Treatment

| Treatment | Ash (%) | Std Error | Group |
|---|---|---|---|
| Air | 0.6213 | 0.0680 | C |
| Paved | 0.5481 | 0.0686 | C |
| Soil | 0.8468 | 0.0782 | B |
| Water | 1.1524 | 0.0717 | A |

Analysis of hemicellulose, cellulose, and lignin fraction data are continuing. Initial results indicate significant differences among treatments for all carbon types. These results should provide significant insight into precisely how the wood chips degrade over time.

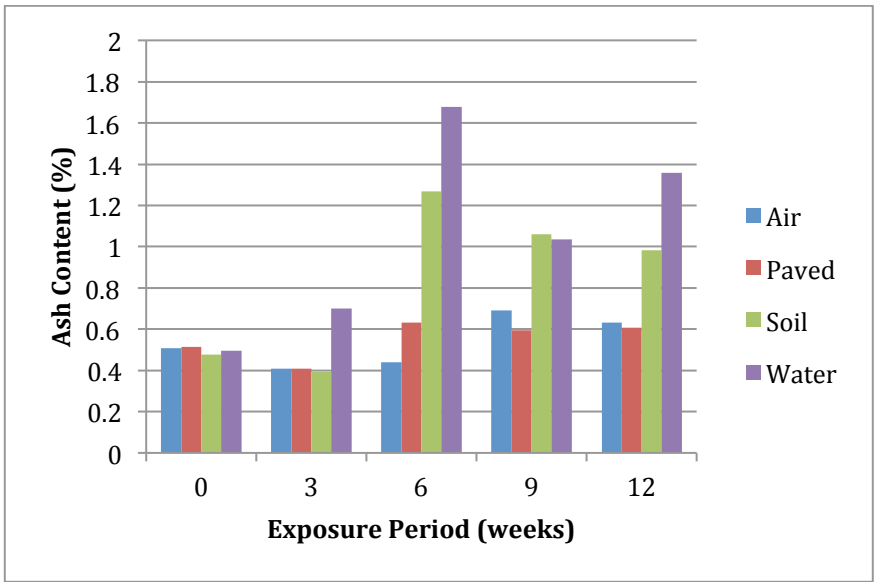

Figure 4. Ash content for all treatments along study exposure periods.

*Develop an economic analysis model for the production of emergency power using disaster debris as a feedstock in a CHP system.*

An analysis looked at a 21-day (3 wk) retrieval period for the Pearl River County Hospital location (fig. 1). A comparison of debris volume (cubic meters) and miles travelled are illustrated in Figure 5. On Day 1 through Day 9, the simulation routed trucks throughout the city for debris. Daily debris retrieval averaged 110 $m^3$ with travel distances totaling around 30 miles per day. Within the urban areas, the trucks are picking up small debris volumes per unit travel distance. On the other hand, the simulation starts to send trucks into rural areas on Day 10. The simulation showed that the trucks were gathering larger debris volumes for distance travelled. From Day 15 to Day 21, the simulation calculated debris volumes of 270 m3 for distances totalling 20 miles per day. If the simulation were allowed to retrieve and deliver debris for 12 hours per day over the 21-day period, the resulting debris could power the Pearl River County Hospital Depot CHP units for 74 days. Fuel consumed by transportation over the 21-day period was 2% (15,512 MJ) as compared to energy potential for the retrieved debris 98% (814,928 MJ).

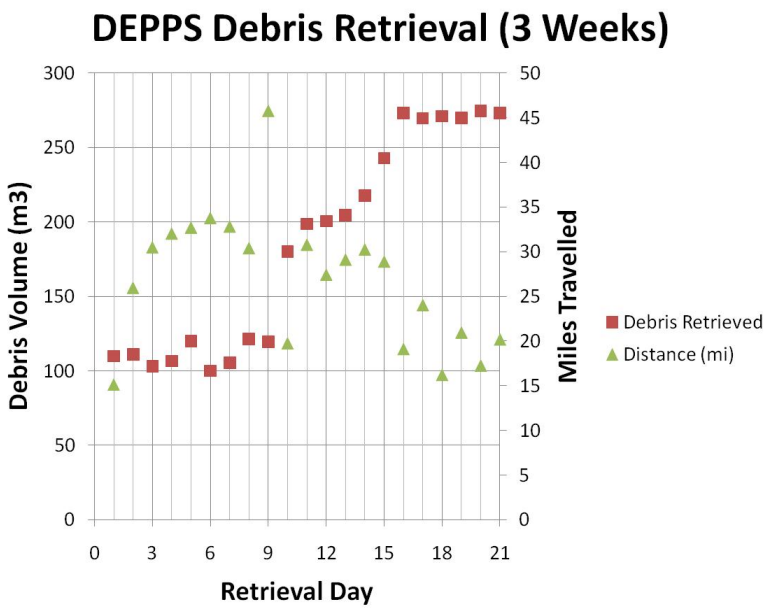


Figure 5: Illustration of debris volume and daily transport distance for each day over a 21-day period.

**Publications / Presentations:**

*Conference Papers:*

1. Ryals, C.S., J.D. Davis, S. Samson, and D. Evans. 2011 Prediction of woody debris from a hurricane event using geographic information systems. Presentation for the 2011 ASABE International Meeting, Aug 7-10. Louisville, KY.

*Thesis and Dissertations:*

1. Ryals, C.S. 2011. Geographic information system (GIS) simulation of energy potential of disaster debris to produce emergency power in a combined heat and power (CHP) unit.

## Task 4.8. - Integration of biofuels

**Description:** The Recipient shall include the design of unit operations for an integrated syngas and bio-oil production facility involving CHP technologies and the development of an economic profile for such systems. Using the conversion of wood chips into synthesis gas as the test case, alternative integrated processes/systems covering unit operations from field collection to bio-fuel production will be designed and developed and the suitability, cost, reliability, and efficiencies of operation of systems in rural applications will be assessed through statistical analysis and modeling.

**Percentage of completion**: 100%

**Accomplishments:**

The existing downdraft gasifier (BioMax 25 gasifier, Denver, CO) at Mississippi State University is producing syngas from biomass. Currently, the syngas from the gasifier contains about 20 % hydrogen, 19 % CO, 12 % CO2, 2% CH4 and 49% N2. The N2 and CO2 contents are too high for the hydrocarbon synthesis if we use existing technologies including catalysts. Developing high activity and high stability catalysts is the key for a better overall performance when using the bio-syngas from the gasifier. Existing syngas to gasoline technologies are mostly based on using pure syngas or low level nitrogen syngas, while the biomass derived syngas from the gasifier contains N2 up to 50% to 60% (vol). Most of the catalysts for the syngas to gasoline process have low performance under such high nitrogen content. Moreover, the operation cost of the syngas compression press is a large portion of the overall invests. A series proprietary catalysts with high activity and high stability are developed at Mississippi State University for a single stage hydrocarbon mixture production process from biomass-derived nitrogen rich syngas when using the bio-syngas from the gasifier. The complete process design for a commercial plant to make liquid hydrocarbons from synthesis gas derived from biomass-synthesis gas was performed. For the pilot reactor design we would like to determine if the size and amount of catalyst used in a scaled up reactor (2 inches in diameter and 80 inches long) could feasibly be used due to the exothermic nature of the reaction. The effect of cooling coils on the temperature profile within a reactor system was investigated.

A simple, two-dimensional (2-D) model was used to approximate the energy transport within the system along with a three-dimensional (3-D) model. One major objective was to determine the effectiveness of using an internal fin with inter-cooling to control the extreme exothermic reactions within the reactor. Comsol was used to computationally determine the temperature profile due to its ability to easily change the variables that contribute to the ability to effectively control the temperature.

Two different reactor models were used which both contained fins made out of inert material with levels of catalyst. One model made use of cooling coils with water to cool the exothermic reaction and one did not. A calculated heat generation based on a literature rate equation was used in each of the models, and an obtained heat generation from literature was also used in each model to determine the accuracy of the models. A model for strictly gasoline creation was modeled along with a model for strictly CO2 creation (worst case scenario). Another model was used from a group doing similar research with a $H_2$ mole ratio of 40% and a CO mole ratio of 20% contained in their syngas. The syngas from the gasifier was first compressed to approximately 50 psig and then scrubbed and dried through a water scrubber and gas drying apparatus assembled after the gasifier. Two 25-gallon 304 stainless steel (SS) wide mouth tanks were connected for the water scrubber. The first tank was outfitted with 13 SS exhaust mufflers with a filtration rating of 50 microns. These mufflers were used to create the maximum amount of syngas bubbles so that the utmost possible surface area of syngas could come in contact with the water and contaminates (i.e. ammonia) could be scrubbed by dissolving into the water. After the water scrubbing process, the syngas was flowed through another 25-gallon tank which contained 80 lbs. of silica gel desiccant to remove moisture. Finally, the syngas was compressed to approximately 2000 psig using a 2-stage pneumatic air pump obtained from Hydraulics International (Chatsworth, CA). A lab-scale syngas purification process (Figure 1) was designed after identifying the possible poisonous or negative components in the syngas for the FTS process, e.g., moisture, $CO_2$, oxygen, sulfur, ammonia, and tar. The catalysts and adsorbents were selected from alumina-supported metal catalysts, 13 X molecular sieves, active carbon, silica gels, and other high surface area materials. These catalysts/adsorbents were loaded into purification reactors in series. The reactor system was built with controlling parameters, such as temperature, pressure, and flow rate. The pilot-plant scale cleaning unit was built in Pace Seed Laboratory of Mississippi State University. The cleaned syngas should meet the basic requirements for the following catalytic conversion of syngas to liquid fuels and chemicals, i.e., total sulfurs ($H_2S$ + COS) $<$ 10 ppb, $NH_3<$ 1 ppm, oxygen$<$ 1 ppm.

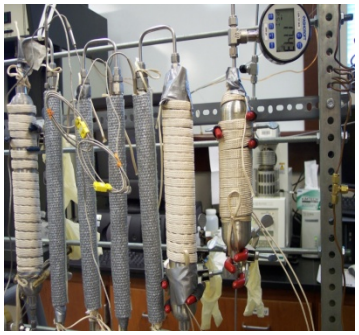

Figure 1. Syngas cleaning lab-scale unit.

Carbon-encapsulated and iron-core nanoparticle catalysts with high activity and stability were synthesized through the solid state carbothermal reduction from iron-impregnated carbon black. The core-shell nanoparticles were characterized by scanning electron microscopy (SEM), transmission electron microscopy (TEM), high resolution transmission electron microscopy (HRTEM), and X-ray diffraction (XRD). TEM results indicated that high purity spherical carbon-encapsulated iron nanoparticles were formed after thermal treatment at 1000 $^{o}$C for one hour, with core diameters of 10-30 nm, and shell thickness of 2-5 nm. The XRD results showed the core consisting of α-iron and cementite ($Fe_3C$). These hybrid core-shell nanoparticle catalysts were used to convert wood-derived syngas to liquid fuels and demonstrated high activity and stability. The CO conversion was as high as 90% with liquid hydrocarbon selectivity up to 60%, and no significant performance loss was observed after 200 hours of life testing. Quantitative results of liquid fuels showed that they were composed of about 51% olefins with distribution between $C_5$ and $C_{13}$, 11.4% iso-paraffins, 8.2% aromatics, 7% napthenes, and 3.6% paraffins.

*Catalyst characterization*

*X-ray diffraction (XRD)*

Figure 2 shows the XRD patterns of the carbon black doped with iron nitrate but no calcination, the calcined iron-promoted carbon black, and the thermal treated iron-promoted carbon black after being used in the catalytic conversion process. Diffraction peaks are hardly observed for the dried sample (Sample a). Since iron most likely existed as amorphous FeOOH or $Fe_2O_3$, there was no carbon black peaks from the XRD patterns of the dried carbon black doped with iron nitrate. Carbon black is generally a non-graphite carbon and consists of amorphous carbon fragments and small amounts of polycyclic aromatic hydrocarbons. The crystallites inside the particles of carbon black are randomly arranged with intrusions of amorphous carbon, which makes difficult detecting the XRD peaks of the untreated carbon black.

The XRD pattern of the calcined sample (Sample b in Figure 2) shows several peaks at values of 2ϑ equal to 30.10, 35.42, 37.05, 43.05, 53.40, 56.95, 62.51, and 73.95, are assigned to mixed iron oxide, $FeO{\bullet}Fe_2O_3$ ($Fe_3O_4$), corresponding to the following crystallographic planes: (220), (311), (222) , (422), (400), (511), (440) and (533), respectively (PDF#00-019-0629). Fig. 2 shows that $Fe_2O_3$ was partially reduced to FeO since iron existed significantly as $Fe_3O_4$ after being calcinated at 300 $^{o}$C under a nitrogen flow. The peak at 2ϑ=24.9° can be ascribed to the reflection (002) of graphite.

For the patterns of used iron-impregnated carbon black (Sample c in Fig. 2), two peaks at 44.68° and 65.03° that correspond to the α-iron (110) and (200) planes, respectively (PDF#97-005-3802), confirmed the participation of iron in the catalytic conversion of the wood-derived syngas. The peak at 26.55° may correspond to carbon (002) plane,

which indicated that the iron-doped carbon black was partially graphited after the thermal treatment. The peaks at 37.75°, 40.7°, 42.6°, 43.75°, 44.56°, 44.94°, 45.86°, 49.12°, 57.8°, 70.9°, 77.9°, and 78.6° are assigned to cementite, $Fe_3C$ with correspondence planes of (121), (210), (201), (211), (102), (220), (031), (112), (221), (301), (123), (401), and (133), respectively (PDF#00-035-0772). The diffraction peaks of Fe and Fe3C proved that iron oxides were all reduced after thermal annealing at 1000 ºC for 1 hour.

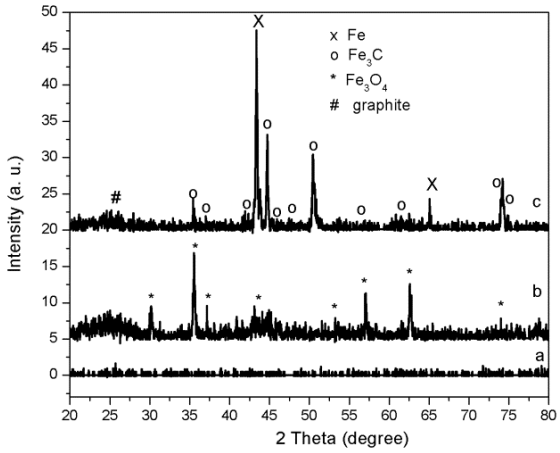


Figure 2 XRD patterns of carbon black samples: Sample a, carbon black doped with iron nitrate, dried at 150 ºC overnight in an oven; Sample b, carbon black doped with iron ion and calcined at 300 ºC; and Sample c, used iron-impregnated carbon black after thermal annealing at 1000 ºC for 1 hour.

*Morphology of the samples by SEM*

A SEM image of dried iron doped carbon black is shown in Fig. 3a. Spherically shaped carbon black particles, almost with a uniform particle size of 20-50 nm, were observed. The morphology of the used carbon black obtained at 1000ºC (Fig. 3b) is similar to the freshly reduced carbon black sample (Fig. 3a).

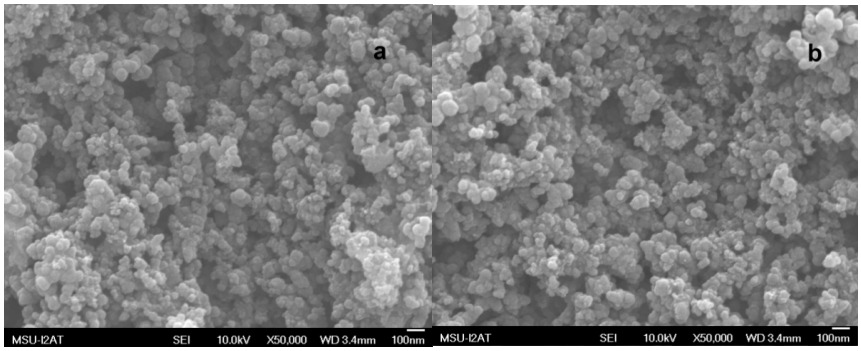


Figure 3 SEM images of iron doped nano carbon black samples: freshly reduced (a) and used (b).

*TEM and HRTEM analyses*

Fig. 4a shows a low-magnification TEM image of the fresh iron-impregnated carbon black. Since iron most likely exists as amorphous FeOOH, or $Fe_2O_3$, the fresh iron-impregnated carbon black possesses the significant characteristic feature of the XC72 particle which shows spherical morphology with an average diameter of 20-30 nm, combined in chains and aggregates.

Fig. 4b also shows a low-magnification TEM image of the iron-doped carbon black after carbonization. It can be observed that most products were spherical particles with diameters in the range 10-50 nm after carbonization. Fig.4c illustrates TEM image of the carbonization sample after FT testing. This sample is similar to the fresh carbonization one in the morphology and particle size.

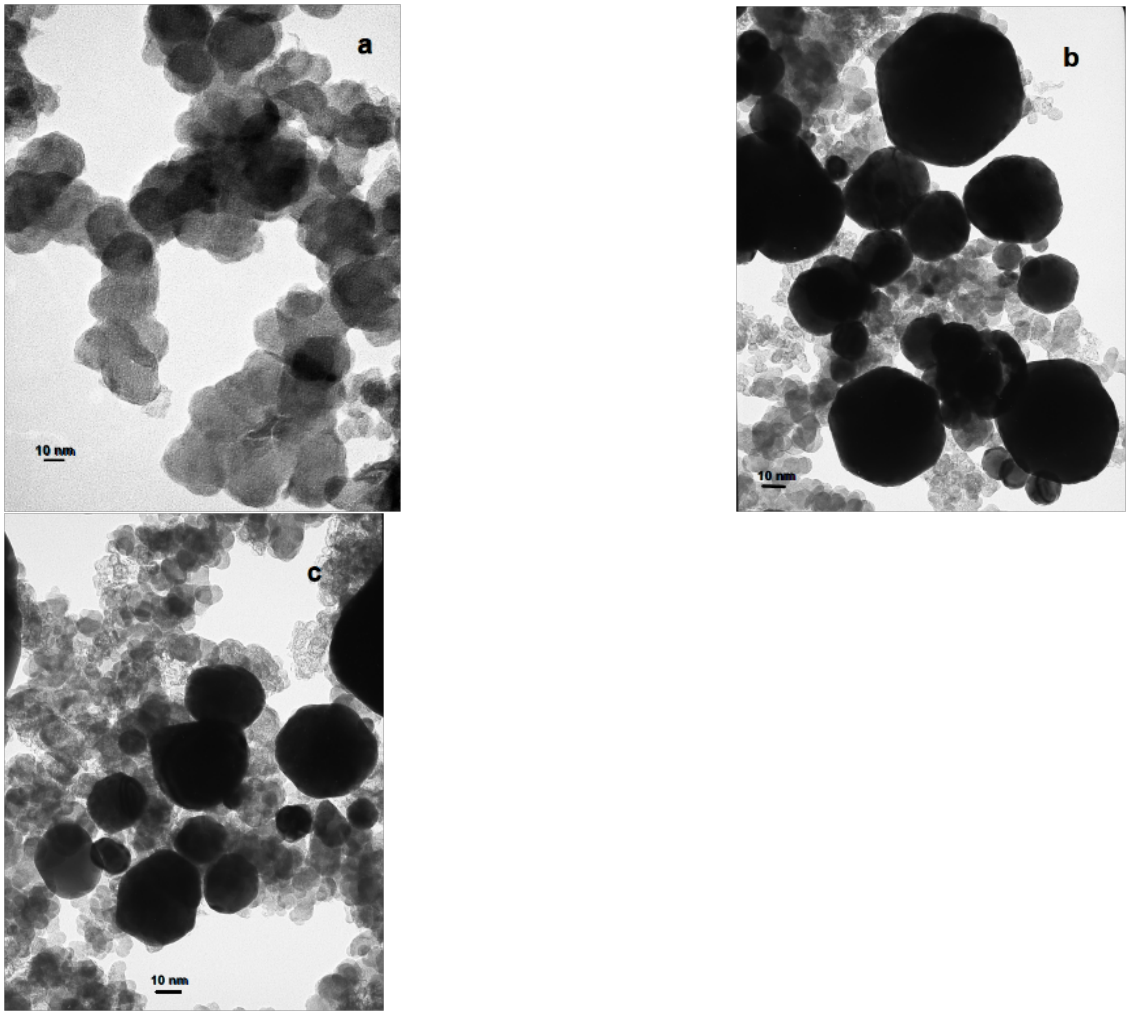


Figure 4 TEM images of carbon black samples: (a) dried iron-doped carbon black, (b) carbothermal reduced iron-doped carbon black at 1000 ºC for 1 hour, and (c) used carbon encapsulated iron nanoparticles.

As low-magnification TEM image (Fig. 4) cannot provide more structure details of the samples, the HRTEM technique was used to further investigate the structure of the carbon black-derived samples.

Fig. 5a is the HRTEM image of the fresh iron-impregnated carbon black sample. High resolution examination of the sample reveals that carbon black is amorphous and in a disorderly structure; however, there is also part of the carbon black consisting of concentrically parallel graphite layer plane, which is similar to the pattern of a fingerprint.

Fig. 5b shows the HRTEM image of the iron-doped carbon black after carbonization. The carbonized sample is mainly composed of carbon-encapsulated metallic particles with a diameter of 10-30 nm. Carbon encapsulation over the metallic particles is with a thickness of approximately 2-5 nm. EDX analysis makes it clear that the particle is composed of Fe and that the coating is carbon.

The HRTEM images (Fig. 5c) show that these nanoparticles had spherical shape and dark cores enclosed by light shells. Most of these carbon encapsulated nanoparticles had core diameters about 10-20 nm and shell thickness ranging from 2 to 5 nm. The outer shell of these nanostructures is in an amorphous state, which is different from previous work that reported a high ordered graphite layers. This may be due to the carbonization annealing temperature in this work that was 1000 ºC and lower than the working temperature in previous work.This may emphasize that the temperature is the main variable to drive the formation of core-shell structure and graphitization of the shell.

The electron diffraction pattern consists of three sets of patterns: one of arcs originated from the carbon, and the other two of rings of spots from the crystalline core. Most of the outer carbon shells of these nanostructures are in an amorphous state. The selected area electron diffraction pattern did not show any spots but an internal dim diffusion ring originating from the graphitic carbon shell (002G). Fourier Transformed electron diffraction pattern (Fig. 5d) shows that the encapsulated iron core nanoparticle (Fig. 5b) has a body centered cubic (bcc) crystalline structure with a lattice constant close to a value of 0.354 nm for bulk α-Fe [PDF#97-005-3802]. The diffraction rings belong to the (110), (200) and (211) planes of bcc iron.

In addition to the α-iron, the diffraction spot rings which originate from the crystalline core coinciding with those expected for orthorhombic $Fe_3C$ were also observed. In the current work, the iron carbide was generated by reduced nano iron particles that reacted with surrounding carbon to form the molten iron–carbon alloy at high temperature (up to 1000 ºC), and then transferred into the carbides during cooling.

Probably, carbon atoms dissolved in the molten iron–carbon alloy that precipitated in the form of graphite layers on the surface of the carbide nanoparticles.

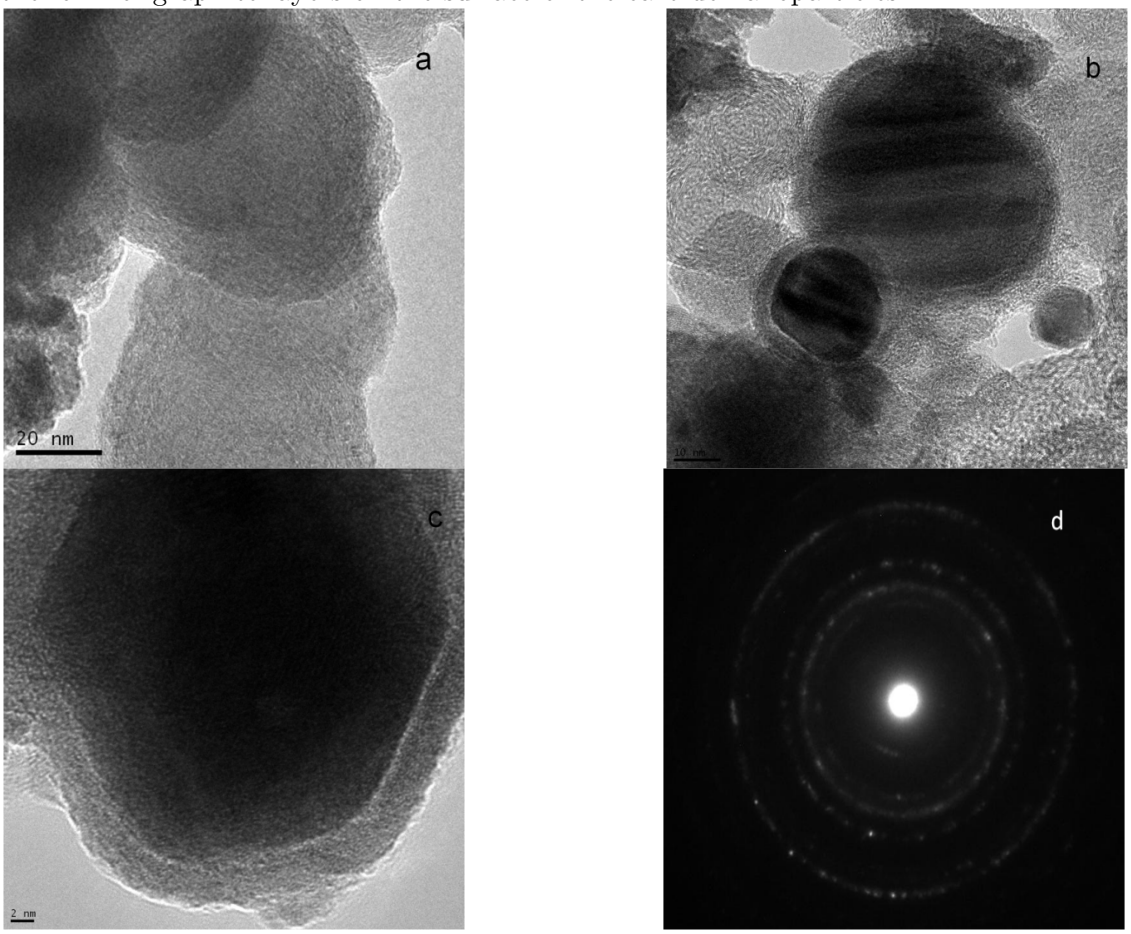


Figure 5 HRTEM images of multilayer graphene shell-encapsulated iron-core nanoparticles produced at 1000 ºC with a heating rate of 10 ºC /min under nitrogen flow.

*Raman spectra*

The Raman spectra can identify the presence of the graphite and disordered amorphous carbon in the samples. The Raman spectrum obtained for the fresh char, Fig. 6a, exhibits two strong peaks at the D- and G-bands. The D-band is the Raman band at a shift of 1368 $cm^{-1}$, while the G-band is the Raman band at a shift of 1600 $cm^{-1}$, which is attributed to a stretching vibration mode of graphite C=C bonds. The peak area ratio ($A_D/A_G$) of D band to G band was estimated to be 2/1. The Raman spectrum of the calcined carbon black sample was also obtained (Fig. 6b). The sample was thermally treated at 1000 ºC with a heating rate of 10 ºC /min in a nitrogen atmosphere and kept for 1 h. There are two peaks around 1605 and 1354 $cm^{-1}$, which can be attributed to the G band and D band in the carbonaceous solid, having a peak area ratio of 3/2. This value of $A_D/A_G$ decreased after the thermal treatment, suggesting that the uniformity of carbonaceous structure increased as the degree of graphite increased. Upon addition of the iron ion to the carbon black but without any

heat treatment, Fig. 6c, the Raman spectrum shows two peaks with a ratio ($A_D/A_G$) of approximate 2/1 similar to the fresh carbon black (Fig. 6a). Raman spectrum of thermally treated iron-doped carbon black at 1000 ºC (Fig. 6d) shows general trends that the $A_D/A_G$ value decreased to 3/2. The differences in the spectra may be interpreted to show that the thermal treatment and the iron-promotion followed by carbonization/ graphitization of the char matrix: 1) a more uniform, carbonaceous structure in the iron-impregnated char after thermal treatment, and 2) greater amounts of graphite structure generated in these samples. These results agree with the XRD and HRTEM data (Figs. 2 and 5).

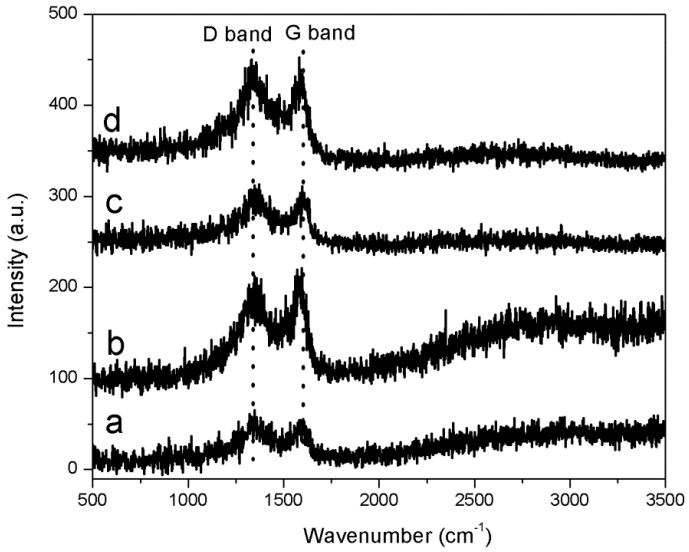


Figure 6 Raman spectra of (a) fresh XC-72carbon black; (b) thermal-treated char at 1000°C for 1 hour; (c) iron nitrate doped carbon black but no heat treatment; and (d) iron nitrate doped carbon black thermal-treated at 1000°C for 1 hour.

*Temperature-programmed desorption (TPD)*

The reactivity of the carbon materials is related to the surface functional groups present on the surface. Temperature-programmed desorption (TPD) and spectroscopic methods such as x-ray photoelectron spectroscopy (XPS) and diffuse reflectance infrared spectroscopy (DRIFT) have been used to characterize carbonaceous functional groups. XPS results demonstrated that the functional groups, C=C C-C C-O C-OH C=O and COOH, were presented on the surface of the pristine *carbon black* XC72 with relative rations of 35.3, 26.9, 7.3, 4.3, 2.0, and 6.3 %, respectively. In current work, carbon black XC72 was characterized using a TPD technique. Five (5) grams of carbon black sample were loaded into the quartz reactor. A high purity nitrogen flow of 20 mL/min was purged through the sample while the sample temperature was ramped from room temperature to 1000 ºC with a heating rate of 2 ºC /min. The desorbing gases during TPD experiments were monitored using an on-line gas chromatography (GC), hydrogen, carbon monoxide and carbon dioxide were detected.

The corresponding peak temperature of $CO_2$ desorption was 400-700 ºC for the anhydride group. The corresponding peak temperatures of CO desorption were 300-750 ºC for the anhydride group, 800-1000 ºC for the carbonyls and/or quinines groups. Hydrogen was present on a carbon surface as chemisorbed water, as surface functionalities (e.g., carboxylic acids, phenolic groups, amines), or was bonded directly to carbon atoms as a part of aromatic or aliphatic structures.

The TPD results of the carbon black are shown in Fig. 7a. It is observed with ne weak, broad peak between 100 and 260 ºC, and two sharp $CO_2$ peaks between 260 and 850 ºC with the concentration level of 0.3-0.85 % in the purging gas. The low-temperature peak (100-260 ºC) is assigned to the decomposition of carboxylic acids (COOH → $CO_2$), and the high-temperature $CO_2$ evolution peaks are attributed to carboxylic anhydrides (260-430 ºC) and lactones (430-850 ºC). There are two distinct CO desorption peaks at 680 ºC and 850 ºC, respectively. The CO-yielding peaks are represented by two distinct groups of peaks, corresponding to ether structures 680°C), and phenols and quinine (600-1000 ºC). The peak concentrations of CO in the carrier gas are 0.75% (˜680 ºC) and 0.8 %( ˜850 ºC) from Fig. 7a. Fig. 8 demonstrates that most of oxygen-containing functional groups are eliminated after heat treatment at 1000 ºC. Trace amounts of hydrogen in carbon black are chemically bonded to carbon through C-H bonds. The carbon-hydrogen bond is very stable but breaks down on high temperature heating. Nevertheless, the complete desorption of hydrogen does not occur at temperatures below 1200 ºC. Heat treatment in an inert atmosphere eliminates part of the hydrogen via surface reduction. Fig. 6a shows hydrogen desorption begun at 800 ºC and increased gradually to 0.3 % at 1000 ºC. Since there are not much surface functional groups existing on the carbon black, solid phase carbon atoms should play the key roles when the reactions occur during carbothermal reduction process.

Fig. 7b shows the trends of purging gas species during the temperature-programmed carbothermal reduction process of the iron promoted carbon black sample. TPD curves were significantly different from those of the carbon black. There is an expansive $CO_2$ peak between 100 to 800 ºC which can be deconvoluted to four peaks corresponding to the steps of carbothermal process of iron-doped carbon black sample. As a catalyst precursor, iron nitrate-doped carbon black sample first decomposed into ferric oxide between 100-150 ºC (Eq. (1)). Simultaneously, oxygen generated from decomposition of iron nitrate reacts with amorphous carbon, $CO_2$ was released out (Eq. (2)) which is corresponding to $CO_2$ peak of 100˜250 ºC. With the increasing temperature, ferric oxide ($Fe_2O_3$) was gradually reduced to $Fe_3O_4$, FeO, and $Fe^0$ (Eqs. 3-5). Each reaction would correspond to one $CO_2$ peak in Fig. 7b, i.e., eq.3 to the peak between 250 and 350 ºC, eq. 4 to the peak at 420 ºC, eq. 5 to the peak of 750 ºC. While the $CO_2$ peak at 620 ºC should be assigned to the decomposition functional groups of lactones.

$$4\ Fe\ (NO_3)_3{\cdot}9H_2O = 2Fe_2O_3 + 12NO_2 + 3O_2 + 36H_2O \quad (1)$$

$$O_2 + C = CO_2 \quad (2)$$

$$6Fe_2O_3 + C = 4Fe_3O_4 + CO_2 \quad (3)$$

$$2Fe_3O_4 + C = 6FeO + CO_2 \quad (4)$$

$$3FeO + 2C = 3Fe + CO + CO_2 \quad (5)$$

Fig. 7b illustrated three CO desorption peaks which located at 620, 750, and > 800 ºC. The peak of 620 ºC should be attributed to the decomposition functional groups of lactones; the peak centered at 750 ºC is corresponding to eq. 5, and the peak (> 800 ºC) is due to the decomposition of phenols and quinine. Hydrogen evolution was observed when the temperature was above 800 ºC, which was assigned to decompose of C-H bonds.

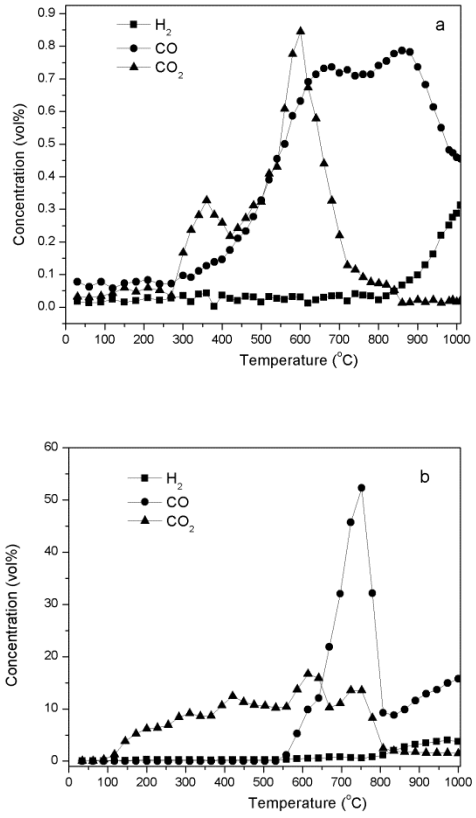


Figure 7 Hydrogen, carbon monoxide, and carbon dioxide evolution for the temperature-programmed thermal treatment of iron-doped carbon black heated to 1000 ºC at a heating rate of 2 ºC /min and with a nitrogen purging gas rate of 20 mL/min.

*Thermogravimetric analysis (TGA)*

TGA experiments were performed in order to examine a reaction process of iron-doped carbon black (Fig. 8). Fig. 8a shows the TG and DTG curves of the carbon black heated at a rate of 2 ºC /min in $N_2$ atmosphere. Fig. 7a indicates that there are two

possible steps of weight loss for the carbon black sample. The initial weight loss corresponds to the loss of physically adsorbed water and occurs between ambient temperature and 120 ºC, which proves there is about 1wt% moisture in the carbon black sample. It is followed by a plateau region for the rate of weight loss from 120 to 730 ºC. The second significant mass loss happened at 730 to 1000 ºC. In this zone, mass loss is mainly attributed to the decomposition of surface functional groups of phenols, quinine, and C-H, which gives out CO and $H_2$ as the main products (Fig. 7a).The mass loss is about 3% in this step.

Fig. 8b indicates that the TGA results of the iron-doped carbon black are significantly different from these of the carbon black. The first mass loss of the Fe/carbon black occurred in the temperature range from room temperature to 110 ºC, which was due to the escape of physical adsorbed water from the sample, there was about 2wt% moisture in the sample. The second mass loss occurred in the range 110–370 ºC with the mass loss of 12wt%. Three reactions involved in this step (eqs. 1-3): ferric oxide ($Fe_2O_3$) was slowly reduced to $Fe_3O_4$, and part of amorphous carbon was consumed, and finally discharged as $CO_2$. The TPD results (Fig. 7) also demonstrates the reduction reaction in the iron-doped carbon black sample with the detection of $CO_2$ peak. The rest of $Fe_2O_3$ and $Fe_3O_4$ could be reduced to FeO in the zone of 370-650 ºC (eq.4) with the mass loss of about 4%. The most mass loss of the sample occurred in the temperature range of 680-790 ºC with a peak temperature of 756 ºC. CO was the main product in the gas phase, which suggested that C reduced FeO to $Fe^0$ (eq.5) during which the mass loss is about 10 %. $Fe^{2+}$ was reduced to $Fe^0$ in this zone. After 800 ºC until 1000 ºC, the mass of the sample decreased gradually, due to the decomposition of phenols, quinine and C-H bonds, and then discharged CO and $H_2$ as the main products.

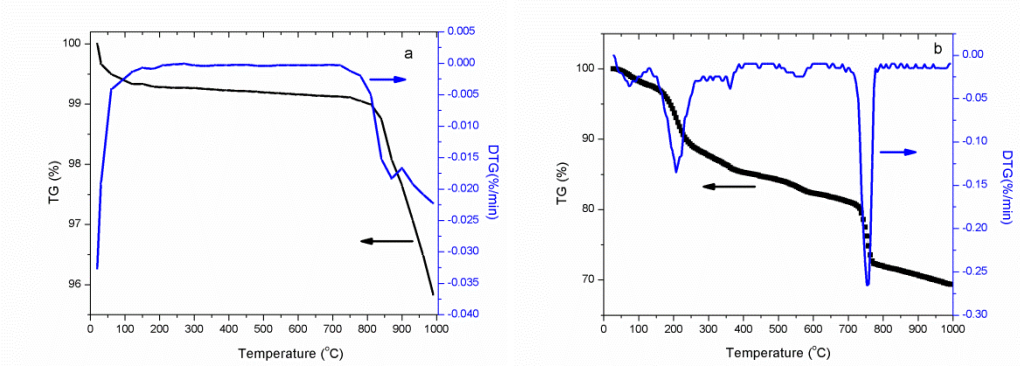


Figure 8 TGA and DTG curves of the XC 72 carbon black (a) and the iron-doped carbon black (b) heated at a rate of 2 ºC /min in $N_2$ atmosphere.

*Catalytic conversion wood-derived syngas to liquid hydrocarbons*

*Influence of process conditions on the activity*

In this study, the carbon encapsulated iron nanoparticles synthesized from thermal treatment of iron-doped carbon black were used as a FTS catalyst to catalytic convert wood-derived syngas to liquid fuels. The CO conversion and hydrocarbon distribution

were measured in a fixed bed flow reactor operated at six temperature levels of 250, 270, 290, 310, 330 and 350°C, respectively. Gas hourly space velocity (GHSV) and pressure were maintained at 1000 to 3000 $h^{-1}$ and 3.45-8.62 MPa, respectively for each of the six temperature runs. Results of typical runs are illustrated in Figs. 9 and 10. Figure 9a shows the variation of CO conversion, $C_1$ ~ $C_5^+$ selectivity for six temperature levels evaluated. CO conversion increases from 85.2% at 250 °C to 96% at 350°C. Figure 9b clearly shows the hydrocarbon selectivity changes with temperature, and the light hydrocarbons are favored at higher process temperatures. Higher hydrocarbons are more sensitive to temperature change, undergoing cracking and de-alkylation reactions that become increasingly important with increasing temperature. Fig. 9c shows the liquid fuel distribution of paraffins, iso-paraffins, aromatics, naphthenes (cycloalkanes), olefins, and oxygenates. Results indicate that as the temperature evaluated from 250 to 350 ºC, paraffins decreased from 15.0% to 6.0%, iso-paraffins decreased from 25% to 17.3%, olefins increased from 38% to 50%, aromatics increased from 8.5% to 13.6%, and oxygenates decreased from 6.3% to 2.2%. Fig. 9d shows the liquid olefin distribution between $C_4$ and $C_{13}$ with $C_7$, $C_6$, $C_5$, $C_9$ and $C_4$ as the main components. It is found the effect of temperature on olefin distribution was complex. The amounts of $C_4$ and $C_5$ olefins increased with the increasing temperature, while the amounts of $C_6$ and $C_7$ olefins decrease with increasing temperature.

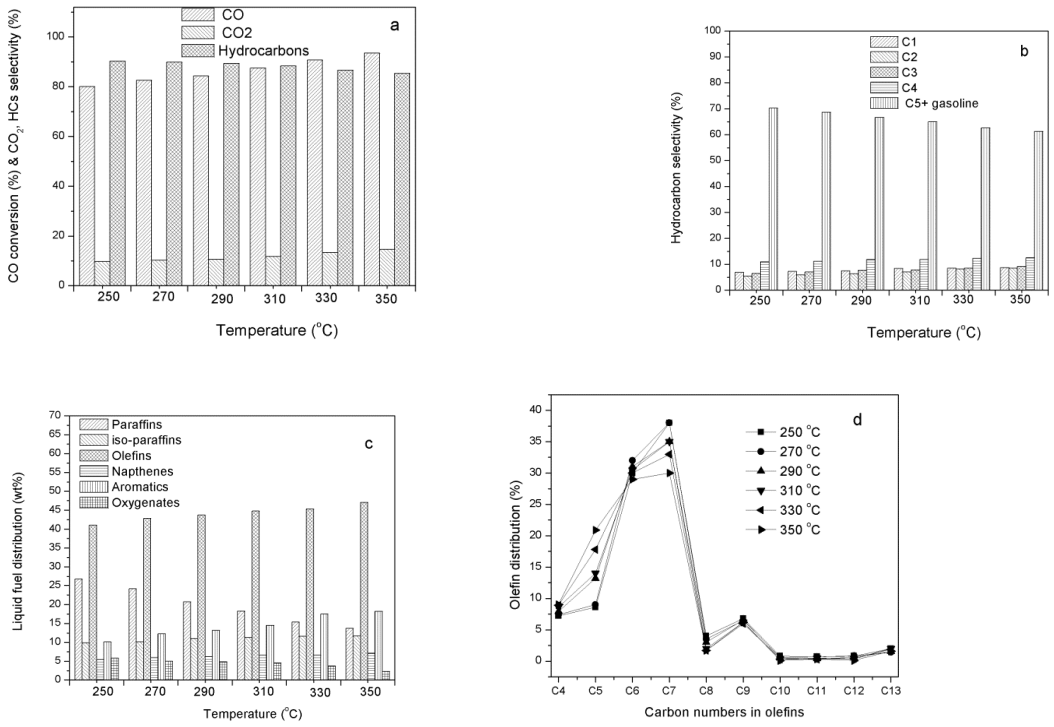


Figure 9 Effect of temperature on (a) CO conversion, CO2 and hydrocarbon selectivity, (b) hydrocarbon distribution, and (c) liquid hydrocarbon distribution.

Effect of temperature on (a) CO conversion, $CO_2$ and hydrocarbon selectivity, (b) hydrocarbon selectivity, and (c) liquid hydrocarbon distribution, at 6.89 MPa, with wood-derived syngas, GHSV of 3000 $h^{-1}$; 3 g of catalyst was used in the reaction. Time on stream was 48-100 h.

***Properties and detailed liquid hydrocarbon distributions***

After reaction, liquid samples (both the oil phase and the aqueous phase) were collected from the condenser during the FTS run. The typical GC-MS spectrum of the oil phase is given in Fig. 10a. GC-MS product distribution can be separated to three zones, The first zone is the retention time between 1.5 to 3.8 minutes, including C4-C7 products, olefins, iso-parafins, paraffins, and naphthenes as the main species; oxygenates also come out in this zone. In the second zone of 3.9˜7.9 minutes, C7-C8 hydrocarbons are located in this period of time, and the main products are aromatics, olefins, isoparaffins, and naphthenes. In the third zone of 8.0- 21.7 minutes, products of C8+ are detected, mainly C9 and C10 aromatics, naphthenes and long chain paraffins and isoparaffins. There was about 10% oxygenates in the aqueous phase. The typical GC-MS spectrum of the oxygenates is given in Fig. 10b, showing that the oxygenates are mainly composed of $C_1$–$C_5$ alcohols, acetone, butanone, and pentanone.

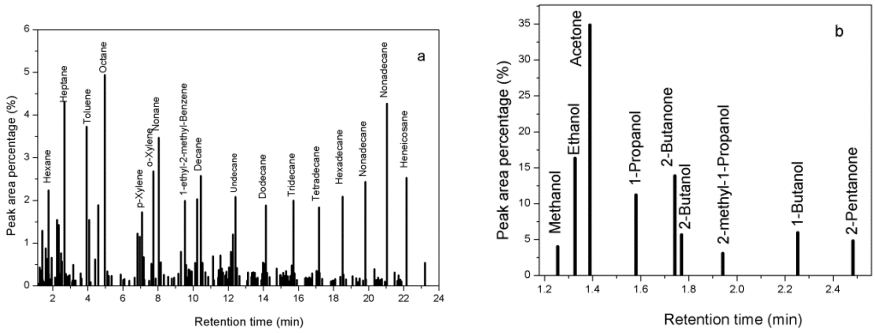


Figure 10 GC-MS spectra of liquid products from wood-derived syngas: oil phase (a), and aqueous phase (b).

The liquid products from wood-derived syngas were analyzed by a gas chromatography using the PIANO method. Liquid oil products were quantitatively reported in the volatile range up to molecules with 13 carbons of five families of hydrocarbon groups, i.e., paraffins, isoparaffins, aromatics, naphthenes (cycloalkanes), and olefins. Table 1 shows typical liquid product fuels obtained using the carbon-encapsulated iron nanoparticles (we need to use the same terminology such as multi-carbon-layers encapsulated or shell iron-core nanoparticles) as the catalyst. In general, it was observed that the main reaction products were olefins (totally about 51%mol) with predominance of C5 (10.6%), C6 (14.7%), C7 (14.8%), and C9 (4.8%) components. The second most prosperous group was iso-paraffins, contributing to 11.7% (mol) of the liquid product with main components of C7 (0.9), C8 (1.0%), C9 (3.7%), C10 (3.2%), and C11 (2.2%). Aromatics contributed to 8.2% of the liquid product, from C10˜C12

components. Napthenes, and paraffins contributed to 7.0% and 3.3% of the liquid product, respectively. There were also 12.7% unidentified components in the liquid product due to the limitation of the data base. If the liquid hydrocarbons were reported based on carbon numbers, C7s contributed to the most, about 19% overall, followed by C6s (15.5%), C9s (13.1%), C5s (10.9%), C10s (10.2%), C8s (8.2%), C11s (4.4%), C12s (3.5%), and C13s (2.8%). Besides hydrocarbons, there were also 3.0% oxygenates found in the liquid oil phase.

Table 1. Typical product distribution of the $C_5$+ liquid fraction for the Fe@C nanoparticle catalyst by the group type and carbon number (in mol percent).

| | Paraffins (%) | I-Paraffins (%) | Olefins (%) | Napthenes (%) | Aromatics (%) | Unknowns (%) | Total (%) |
|---|---|---|---|---|---|---|---|
| C5 | 0.01 | 0.01 | 10.63 | 0.22 | 0 | 0 | 10.87 |
| C6 | 0.6 | 0.15 | 14.72 | 0.01 | 0 | 0.5 | 15.98 |
| C7 | 1.37 | 0.86 | 14.83 | 1.3 | 0.01 | 1.89 | 20.26 |
| C8 | 0.51 | 1.03 | 3.89 | 1.76 | 0.19 | 4.32 | 11.7 |
| C9 | 0.21 | 3.68 | 4.83 | 3.02 | 0.34 | 3.22 | 15.3 |
| C10 | 0.75 | 3.23 | 1.04 | 0.46 | 5.03 | 2.67 | 13.18 |
| C11 | 0.09 | 2.14 | 0.19 | 0.2 | 1.36 | 2.44 | 6.42 |
| C12 | 0.01 | 0.3 | 0.04 | 0.01 | 1.27 | 1.83 | 3.46 |
| C13 | 0.01 | 0.01 | 0.81 | 0.01 | 0.01 | 1.98 | 2.83 |
| Total | 3.56 | 11.41 | 50.98 | 6.99 | 8.21 | 18.85 | 81.15 |

Catalytic tests for oxygen removal from wood syngas: Three oxidative catalysts (i.e., 1wt % $Pt/CeO_2/Al_2O_3$, 1wt %$Pd/CeO_2/Al_2O_3$, 8wt %$Cu/CeO_2/Al_2O_3$) were examined for selective $O_2$ removal from wood syngas. The wood syngas used in this study contained about 46% $N_2$, 21% CO, 18% $H_2$, 12% $CO_2$, 2% $CH_4$, and 0.82% $O_2$. The wood syngas was free of other potential toxic component, such as moisture, ammonia, sulfur compounds ($H_2S$, and COS) and tar, by passing through a pre-cleaning system. The reaction pressure and gas hourly space velocity (GHSV) were 206.8 kPa and 4000 $h^{-1}$ GHSV, respectively, unless stated otherwise.

*Syngas cleaning*

*Effect of temperature on oxygen removal:*

Figure 11 compares the temperature dependence of $O_2$, CO and $H_2$ conversion during $O_2$ removal from wood syngas over different catalysts. $O_2$ was completely removed over the Pt catalyst at the reaction temperature of 75 °C or above (Figure 11a). CO conversion first increased with temperature and reached a maximum value of 5.4% at 100°C, then decreased (Figure 11b), while $H_2$ conversion increased with the temperature (Figure 11c). The results suggested that $O_2$ was mainly consumed by CO oxidation reaction below 100 °C over the Pt catalyst. However, the amount of $O_2$ consumed by CO decreased when the temperature was above 100°C (Figure 11b). This may be due to the fact that increasing temperature limited the CO oxidation reaction

as this reaction was an exothermic process. In contrast, the amount of oxygen used by $H_2$ increased with the increasing temperature. $H_2$ oxidation reaction proceeded in competition with CO oxidation since all reactive gases were adsorbed over active metal Pt surface during the catalytic oxidation process. As the reaction temperature increased, $H_2$ oxidation became faster than CO oxidation reaction, leading to a higher selectivity towards $H_2$ oxidation. The Cu catalyst was not very active at the temperature below 100 °C for selective oxygen removal. Oxygen conversion of 100% was achieved above 150 °C (Figure 11a). Similar to the Pt catalyst, $O_2$ mainly reacted with CO at low temperature (below 150 °C for the copper catalyst). The oxygen conversion decreased with increasing reaction temperature because of predominant $H_2$ oxidation at high temperatures. The catalyst Pd demonstrated the best oxygen removal performance at low temperature (Figure 11a). The oxygen conversion was very high at low temperatures, i.e., 98% at 50 °C. A complete oxygen conversion was observed at temperatures higher than 75 °C. It should be noted that the Pd catalyst showed very higher selectivity for the $O_2$ reduction reaction with $H_2$ than the Pt and Cu catalysts. However, this catalyst showed much lower selectivity towards CO oxidation, especially at low temperatures (Figure 11b).

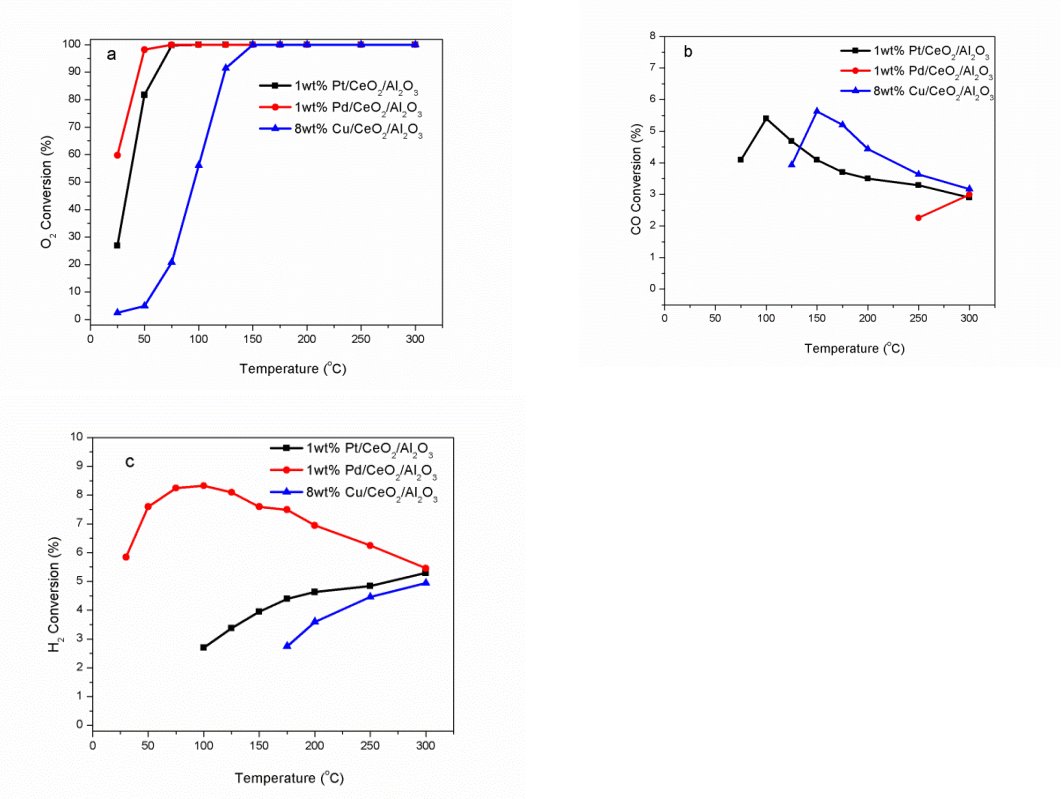


Figure 11 Effect of temperature on the performance of the catalysts: $O_2$ conversion (a), CO conversion (b), and $H_2$ (c) conversion.

*Effect of GHSV on oxygen removal:*

The effects of hourly space velocities (GHSV) on oxygen removal from wood syngas were evaluated at varying temperatures. For the Pt catalyst (Figure 12a), complete oxygen conversion was obtained at GHSV below 4000 $h^{-1}$ when the reactor was run at 100 °C. Further increasing of GHSV led to an increased $O_2$ level in the exit gas (Figure 12a), regardless of reaction temperatures. For the Pd catalyst $O_2$ conversion reached 100% at GHSV below 6,000 $h^{-1}$ when the reaction temperatures were 125 and 150 °C (Figure 12b). The residual oxygen in the exit gas increased with the increasing of GHSV above 8000 $h^{-1}$. For the Cu catalyst, when it was tested at 150 °C, the lowest exit oxygen was 1.5 ppm at GHSV of 2000 $h^{-1}$, while the highest oxygen level of 0.12% was detected at GHSV of 12000 $h^{-1}$ (Figure 12c). $O_2$ conversion reached 100% at GHSV below 4,000 $h^{-1}$ at 175 and 200 °C. Significant decrease in oxygen conversion at the higher GHSV can be due to the short residence time of the reactants. The contact time decreased from 1.8 s to 0.3 s when GHSV increased from 2000 to 12,000 $h^{-1}$.

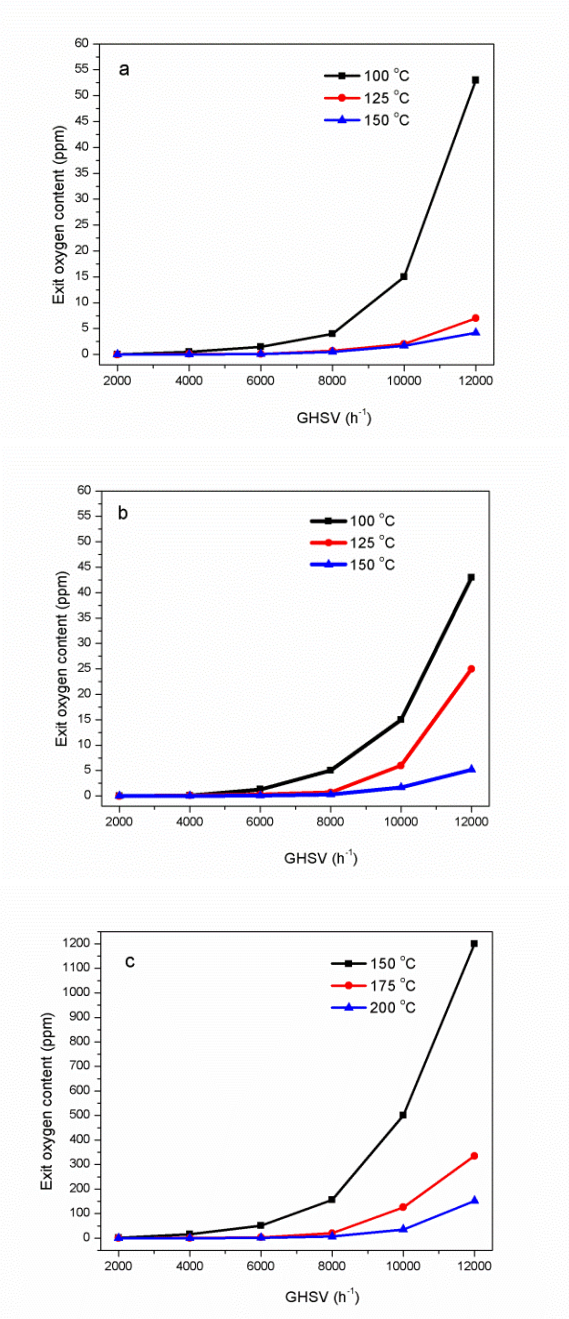


Figure 12 Effect of GHSV on oxygen removal by Pt (a), Pd (b), and Cu (c) catalysts.

*Effect of $CO_2$ pre-capture on oxygen removal:*

$CO_2$ may have a negative effect on oxygen removal since there was up to 12% $CO_2$ in the pre-cleaned wood syngas. To investigate the effect of $CO_2$ on the oxygen removal performance, wood syngas passed through a $CO_2$ capture system packed with absorbents of active carbon, zeolites, and CaO. After $CO_2$ capture, the syngas contained 23.8 % CO, 20.5% $H_2$, 2.2% $CH_4$ and 1.0% $O_2$, and 52% $N_2$. The results showed that the presence of $CO_2$ resulted in slight decrease in oxygen conversion at the

low temperature (<50 °C) by both Pt and Pd catalysts. For the Cu catalyst, $O_2$ conversion increased by 9% after $CO_2$ pre-capture. Moreover, the absence of $CO_2$ resulted in a shift of the maximum CO conversion temperature to a lower temperature. The reasons for the difference in catalytic behavior with the presence of $CO_2$ are unclear so far. However, the negative effect of $CO_2$ on catalyst activity can be due to formation of carbonate or carboxylate species during oxidative reaction which in turn block the active sites of the catalysts and prevent adsorption and reaction of the reactants on the catalyst surfaces. On the other hand, the reverse water gas shift reaction (RWGS, $CO_2 + H_2 \leftrightarrow CO + H_2O$) between $CO_2$ and $H_2$ could lead to the CO formation and CO conversion thus decreased in the presence of $CO_2$ in the feed gas. As mentioned above, $CO_2$ had an unfavorable effect on the catalytic activity. In other words, $CO_2$-free wood syngas allowed the catalyst to have a good performance.

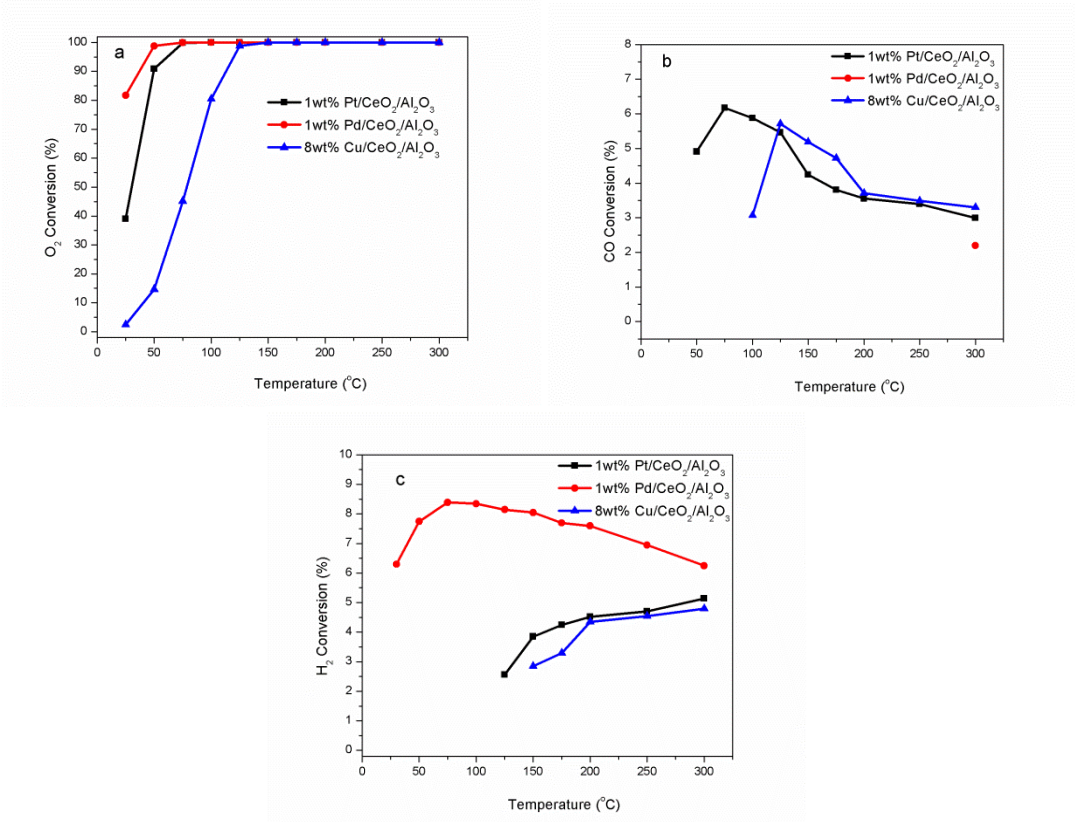


Figure 13 Effect of pre-captured $CO_2$ on performance of the catalysts: (a) $O_2$ conversion, (b) CO conversion and (c) $H_2$ conversion.

*Effect of moisture on oxygen removal:*

The catalytic activity of a catalyst can be significantly depressed with the presence of water in the feed stream. The wood syngas that exits the gasifier usually contains 5-10% water. Therefore, it is important to investigate the effect of moisture on catalytic removal of oxygen. In the current work, pre-cleaned wood syngas was adjusted with 5% moisture and then used for oxidative reaction. The results showed that for the Pd catalyst moisture negatively affected both $O_2$ and $H_2$ conversion while positively

affecting CO conversion at the low temperatures (<100°C) (Figure 14a and 14c). Similar performance was also observed with the Pd catalyst (Figure 14a and 14c). In contrast, a significant decrease in $O_2$ conversion was observed with the Cu catalyst at the temperature below 150 °C (Figure 14a and 14c). The CO conversion also increased a little bit but with conversion peak temperature shifting to 175 °C. $H_2$ conversion declined slightly. However, the oxidative activities of all three catalysts were not significantly influenced by the moisture at higher temperatures (Figure 14a-c).

The negative effect of the moisture in the feed gas on the catalytic performance may be due to water molecular competing with adsorption of $O_2$, CO and $H_2$ on the metal surface and water molecular blocking parts of the active sites. The increasing of CO conversion and decreasing of $H_2$ conversion over the entire temperature range might be due to the water-gas shift reaction (WGSR, $CO + H_2O \leftrightarrow CO_2 + H_2$), through which part of CO was converted while $H_2$ and $CO_2$ were formed in the presence of water. Loss of catalyst activity caused by water vapor could diminish at higher temperatures.

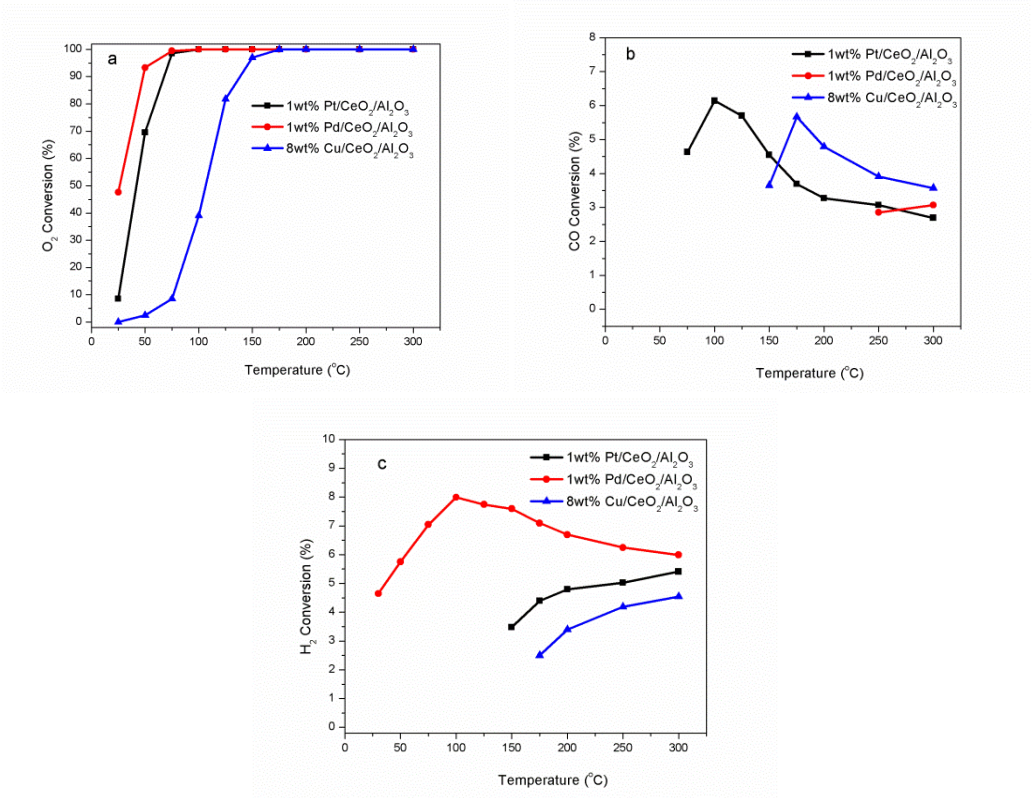


Figure 14 Effect of moisture on the performance of the catalysts: $O_2$ conversion (a), CO conversion (b), and $H_2$ conversion (c).

*Stability test:*

The long-term activity and stability of the catalysts were examined for up to 300 hours. The reaction temperature was100 °C for both Pt and Pd while 150 °C for the Cu catalyst. GHSV of 4000 $h^{-1}$ was for all three catalysts. As shown in Figure 15, both

Pt and Pd catalysts exhibited high stability with the exit oxygen concentration kept below 0.5 ppm over 300 hours testing period. For the Cu catalyst, the exit oxygen level was below 1.0 ppm at first 40 hours and then kept increasing, reaching 5.0 ppm after 90 hours. It drastically increased to 205 ppm after 220 hours, indicating catalyst deactivation. Attempt was made to recover the activity of the Cu catalyst by increasing reaction temperature to 200°C. It was found that the catalyst activity was gradually recovered after 20 hours and the exit oxygen level was kept below 0.5 ppm throughout the rest of the reaction period (Figure 15). Deactivation of the catalyst at 150°C may be due to accumulation of carbonates on active sites of copper. When the reaction temperature increased to 200 °C, carbonates accumulated could be decomposed and the Cu oxide species could be reduced.

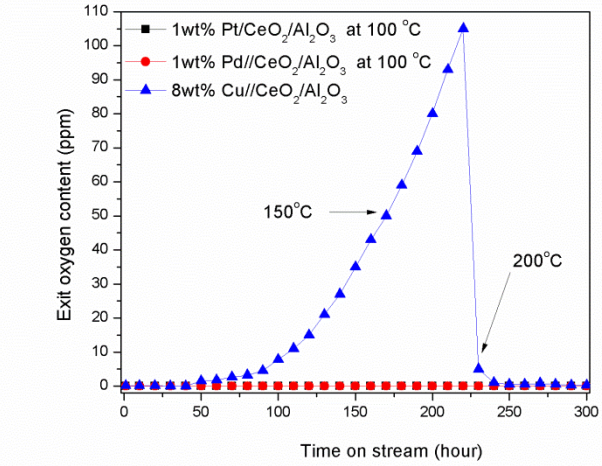


Figure 15 Stability test of the catalysts for oxygen removal.

***Catalyst characterization***

As compared to γ-$Al_2O_3$, ceria modified support and all catalyst samples had decreased BET surface area and pore sizes (Table 2). Both Pt and Pd catalysts had similar properties while the Cu catalyst had the smallest surface area and pore size. The catalyst preparation process, especially with steps involving drying and calcination, mainly contributed to changes in physical properties of the catalysts.

Table 2 Physical property of the catalysts

| Catalyst | BET Surface Area ($m^2/g$) | Pore Volume ($cm^3/g$) | Average Pore diameter (nm) |
|---|---|---|---|
| γ–Aλ₂O₃ | 252 | 0.95 | 10.5 |
| $CeO_2$/g-$Al_2O_3$ | 193 | 0.73 | 8.2 |
| Pt/$CeO_2$/$Al_2O_3$ | 185 | 0.5 | 7.5 |

| | | | |
|---|---|---|---|
| $Pd/CeO_2/Al_2O_3$ | 187 | 0.49 | 7.2 |
| $Cu/CeO_2/Al_2O_3$ | 129 | 0.31 | 4.7 |

TPR was carried out to elucidate the state of metal oxides and metallic platinum, palladium, and copper. The reduction peak at 89 ºC was observed with the Pt catalyst (Fig.16a), which related to reduction of $PtO_2$. In contrast, the Pd catalyst was more easily reduced than the Pt catalyst, exhibiting one positive peak at 65 ºC and one negative peak at 118 ºC (Fig.16b). The positive peak was attributed to the reduction of PdO, and the negative peak most likely attributed to the decomposition of palladium hydride. The TPR profile of the Cu catalyst shows a distinct profile from which a single large peak was observed at 207 ºC (Fig.16c), elucidating the reduction of CuO at that temperature.

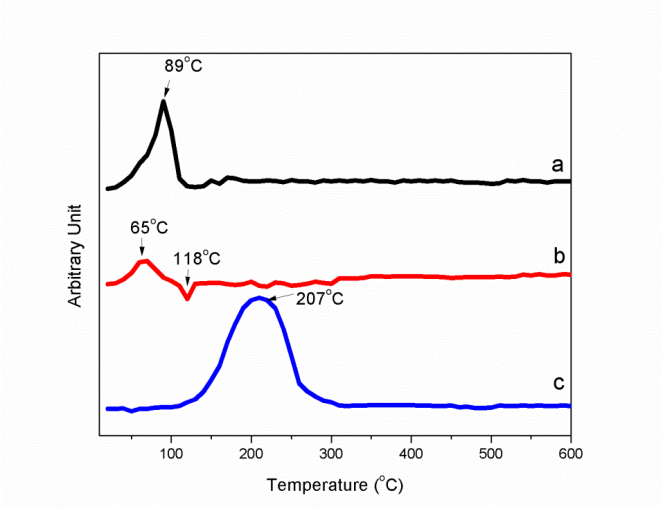


Fig.16 TPR profiles of the Pd (a), Pd (b), and Cu (c) catalysts

***$O_2$ content of producer gas during the gasification process***

The gas composition of producer gas was monitored by an on-line GC at 20 minute intervals during the gasification process. The gasifier was first purged with air for 20 min and then ignited for wood gasification. As shown in Figure 17, $O_2$ decreased quickly from 21% to 3.8% after the gasifier was ignited for 20 min, and then to 1.7% for another 20 min. After this point, the $O_2$ levels dropped to about 0.4~0.5% for the remaining period of gasification. Incomplete conversion of $O_2$ during gasification was most likely due to a high flow rate ($65m^3/h$) of the gas through the fixed downdraft gasifier bed. In this scenario, air was forced to pass through "short cut channels" of the gasifier bed before it can be exposed to the wood chips or char. Other gaseous products formed during gasification included $CO_2$, CO, $H_2$ and $CH_4$, which increased with prolonged gasification time and reached steady levels after the gasifier was fully started up at around 90 min. The producer gas collected during the steady gasification run was

composed of 21% CO, 18% $H_2$, 12% $CO_2$, 2.5% $CH_4$ and 0.5% $O_2$. $N_2$ was the balance gas in the producer gas.

***Influence of $O_2$ in syngas conversion***

The producer gas was pre-cleaned and tested for the effects of $O_2$ on the FTS process. As shown in Fig.18, $O_2$ content as low as 0.5% was highly toxic to the FT catalyst which deactivated the catalyst within several hours. As a result, conversion efficiency of raw syngas drastically decreased. In contrast, a stable conversion was obtained with $O_2$-free syngas (cleaned). Since frequent regeneration of the FTS catalyst generally leads to increased operation costs and reduced catalyst lifetime, it is necessary to remove $O_2$ from bio-syngas before it can be used as a feedstock gas for FTS.

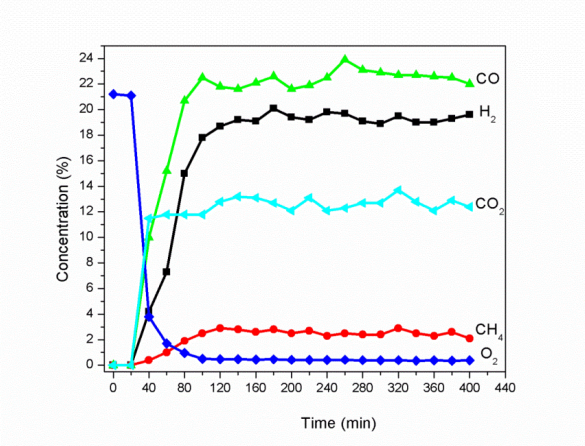


Fig 17 Syngas composition monitored throughout the gasification process

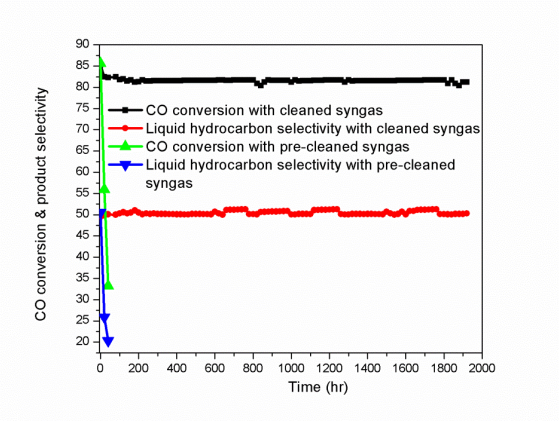


Fig.18 Influence of $O_2$ on syngas conversion.

**Publications / Presentations:**

*Journals:*

1. Wan, C., F. Yu, Y. Zhang, Q. Li, and J. Wooten. *2013.* Material Balance and Energy Balance Analysis for Syngas Generation by a Pilot-plant Scale Downdraft Gasifier. *Journal of Biobased Materials and Bioenergy.* 7: 690-695.

2. Yan, Q., C. Wan, J. Street, D. Yan, J. Han, and F. Yu. *2013.* Catalytic Removal of Oxygen from Biomass-derived Syngas. *Bioresource Technology.* 147:117–123.

3. Zhang, Y., C., Wan, Q. Li, P.H. Steele, and F. Yu. *2013.* Studies of Biochars Generated from Pilot-scale Downdraft Gasification. *Transactions of the ASABE. 56(3): 995-1001.*

4. Yan, Q., C. Wan, J. Liu, J. Gao, F. Yu, J. Zhang, and Z. Cai. *2013.* Iron Nanoparticles in situ Encapsulated in Biochar-based Carbon as an Effective Catalyst for Conversion of Biomass-derived Syngas to Liquid Hydrocarbons * *Green Chemistry.* 15:1631-1640.

5. Yan, Q., F. Yu, Z. Cai, and J. Zhang. 2012. Catalytic upgrading nitrogen-riched wood syngas to liquid hydrocarbon mixture over a Fe–Pd/ZSM-5 catalyst. Biomass and Bioenergy. 47: 469-473.

6. Yan, Q., F. Yu, J. Liu, J. Street, J. Gao, Z. Cai, and J. Zhang. 2012. Catalytic Conversion Wood Syngas to Synthetic Aviation Turbine Fuels over A Multifunctional Catalyst. Bioresource Technology.127:281-290.

7. Wang, H., D. Livingston, R. Srinivasan, Q. Li, P. Steele, and F. Yu. 2012. Detoxification and fermentation of pyrolytic sugar for ethanol production. Applied Biochemistry and Biotechnology. 168:1568–1583.

*Conferences:*

1. Yu, F. 2013. Wide-cut diesel production from an integrated gasification, syngas cleaning, and catalytic conversion process. 2013 Mid-South Area Engineering and Sciences Conference. October 28-29. Oral presentation.

2. Lu, Y., F. Yu, J. Hu, and P. Zhou. 2013. CO hydrogenation to higher alcohols over three-dimensionally ordered macroporous Cu-Fe catalysts. 246$^{th}$

American Chemical Society National Meeting. Indianapolis, IN. September 8-12. Oral presentation.

3. Lu, Y., F. Yu, J. Hu, and P. Zhou. 2013. Higher alcohols synthesis from syngas over three-dimensionally ordered macroporous Cu-Fe bimetallic catalyst. 23rd North American Catalysis Society Meeting. Louisville, KY. June 2-7. Poster.

4. Yan, Q., and F. Yu. 2013. Catalytic Conversion Wood Syngas to 'Wide Cut' Diesel over A Multifunctional Catalyst. 23rd North American Catalysis Society Meeting. Louisville, KY. June 2-7. Poster.

5. Lu, Y., Yu, F., Hu, J., Zhou, P. Syngas to Higher Alcohols via Three-dimentionally Ordered Macroporous Cu-Fe Bimetallic Catalyst. A Poster Presentation presented for the 2013 SEC Symposium. Atlanta, GA, February 10-12, 2013.

6. Street, J., Yu, F., Columbus, E., Wooten, J., and Yan, Q. Scale up of Gasoline-Range Hydrocarbon Production from Gasified Woody Biomass using a Bi-Functional Catalyst. A Poster Presentation presented for the 2013 SEC Symposium. Atlanta, GA, February 10-12, 2013.

7. Hu, J., Yu, F., Lu, Y., Street, J., Wooten, J., Columbus, E. 2012. Transportation Fuels Production from Biomass through Biomass Gasification, Gas Cleaning and Fischer-Tropsch Synthesis: A Technical and Economic Analysis, Paper: 121337425, An ASABE Meeting Presentation written for the 2012 ASABE Conference, Dallas, TX, July 29-August 1, 2012.

8. Lu,Y., Hu,J., Zhou, P., Street, J., Wooten, J, Columbus, E., Yu, F. 2012. Catalytic conversion of syngas to mixed alcohols via three-dimentionally ordered macroporous Cu-Fe based catalyst. Paper:121337229, An ASABE Meeting Presentation written for the 2012 ASABE Conference, Dallas, TX, July 29-August 1, 2012.

9. Street, J., Yu, F., Columbus, E., Wooten, J. 2012. Scale-Up of Liquid Hydrocarbon Production using Gasified Biomass. Paper: 121337524, An ASABE Meeting Presentation written for the 2012 ASABE Conference, Dallas, TX, July 29-August 1, 2012.

10. Lu, Y., Yu, F., Hu, J., Zhou, P. Mixed alcohols Synthesis from Syngas via Zn-Mn promoted Cu-Fe based catalyst. 2012. A Poster Presentation

presented for the 2012 Southeast Biofuels Conference. Jackson, MS, August 8-9, 2012.

11. Street, J., Wooten, J., Columbus, E., and Yu, F. 2012. Scale-up of Gasoline-Range Hydrocarbon Production from Gasified Woody Biomass using Bi-functional Catalysts. A Poster Presentation presented for the 2012 Southeast Biofuels Conference. Mississippi State, MS, August 8-9, 2012.

12. Lu, Y., Yu, F., Hu, J., Zhou, P. 2012. Syngas to mixed alcohols via 3D ordered macroporous Cu-Fe based catalyst. Paper number: 172, An oral presentation presented for 244th American Chemical Society National Meeting & Exposition. Philadelphia, PA, August 19-23, 2012.

13. Yan, Q., Yu, F., Liu, J. 2012. Carbon encapsulated iron nanoparticles for catalytic conversion biosyngas to liquid hydrocarbons. 244th ACS National Meeting, Philadelphia, PA, August 19-25, 2012.

14. Yu, F. 2011. Higher Alcohol Synthesis from Syngas over Copper-Iron Based Catalyst. Strategic Environmental Research and Development Program (SERDP) and Environmental Security Technology Certification Program (ESTCP) annual Technical Symposium & Workshop. Washington, D.C. November 29 – December 1, 2011.

15. Yu, F. 2011. Liquid Hydrocarbon Production over MO/HZSM-5 Using Gasified Biomass. Strategic Environmental Research and Development Program (SERDP) and Environmental Security Technology Certification Program (ESTCP) annual Technical Symposium & Workshop. Washington, D.C. November 29 – December 1, 2011

16. Yu, F. Yan, Q., Columbus, E., and Wooten. J. 2011. Catalytic Conversion of Biomass Derived Synthesis Gas to Liquid Hydrocarbons. 107$^{th}$ Gulf Coast Conference. Galveston, TX. October 11-12, 2011.

*Poste*rs:

1. Lu, Y., F. Yu, J. Hu, and P. Zhou. 2013. Catalytic conversion of syngas to higher alcohols via Zn-Mn promoted Cu-Fe based catalysts. 246$^{th}$ American Chemical Society National Meeting. Indianapolis, IN. September 8-12. Poster presentation.

2. Street, J., Yu, F., Columbus, E., and Wooten, J. 2013. Process Design and Economic Analysis of a Gas-to-Liquid Plant with Aspen Plus using a Woody

Biomass Feedstock. Mississippi Biomass and Renewable Energy Council Conference. Tunica, MS. September 17-18. Poster presentation.

3. Yan, Q., Street, J., Wooten, J., Columbus J., and Yu. F. 2011. Biomass to liquid (BTL) fuels via gasification and catalytic conversion. A Poster Presentation presented
4. for the Mississippi State 2011 Biofuels Conference. Mississippi State, MS, October 5-7, 2011.

**5.** Lu, Y., Yan, Q., Hu, J., Street, J., Wooten, J., Columbus, E., Yu, F. 2011. Higher Alcohols Synthesis from Syngas over Copper-Iron Based Catalyst. A Poster Presentation presented for the Mississippi State 2011 Biofuels Conference. Mississippi State, MS, October 5-7, 2011.

6. Hu, J., Yu, F., Lu, Y., Yan, Y., Wooten, J., Columbus. E. 2011. Green Flight: Renewable Jet Fuel Production Through Integrated Biomass Gasification, Gas Cleaning and Catalytic Conversion System. A Poster Presentation presented for the Mississippi State 2011 Biofuels Conference. Mississippi State, MS, October 5-7, 2011.

7. Street, J., Columbus, E., Wooten, J., White, M., and Yu, F. Scale-up of Gasoline-Range Hydrocarbon Production from Biomass Synthesis Gas over Mo/HZSM-5 and other Bi-functional Catalysts. A Poster Presentation presented for the Mississippi State 2011 Biofuels Conference. Mississippi State, MS, October 5-7, 2011.

8. Yu, F. 2011. Liquid Hydrocarbons Production via Biomass Gasification and Catalytic Conversion. 4th Annual Waste-to-Fuels Conference & Trade Show. San Diego, CA. September 25-27, 2011.

9. Lu, Y., Yan, Q., Hu, J., Street, J., Wooten, J., Columbus, E., Yu, F. 2011. Development of copper-iron based catalyst for mixed alcohol synthesis from syngas. Microscopy & Microanalysis annual meeting. Nashville TN, August 7-11, 2011.

10. Hu, J., Yu, F., Lu, Y., Yan, Q., Wooten, J., Columbus, E., Lin, W. 2011. Catalytic Conversion of Biomass-derived Syngas to Gasoline Range Hydrocarbons. Paper: 1110878, An ASABE Meeting Presentation written for the 2011 ASABE Conference, Louisville, KY, August 7-10, 2011.

11. Lu, Y., Yan, Q., Hu, J., Street, J., Wooten, J., Columbus, E., Yu, F. 2011. Mixed Alcohols Synthesis from Syngas Over Copper-Iron Based Catalyst.

Paper: 1110834, An ASABE Meeting Presentation written for the 2011 ASABE Conference, Louisville, KY, August 7-10, 2011.

12. Street, J., Columbus, E., Warnock, J., Wooten, J., White, M., Yu, F. 2011. Liquid Hydrocarbon Production over Mo/HZSM-5 Using Gasified Biomass. Paper: 1110541, An ASABE Meeting Presentation written for the 2011 ASABE Conference, Louisville, KY, August 7-10, 2011.

13. Zhang, Y., J. Wooten, E. Columbus, and F. Yu. 2011. The otential for Improvements of A Pilot-Plant Scale Downdraft Gasifier Through Material Balance and Energy Balance Analysis. S1041 (The Science and Engineering for a Biobased Industry and Economy) Symposium. Stillwater, OK, August 2, 2011.

14. Street, J., J. Wooten, E. Columbus, J. Warnock, M. White, and F. Yu. 2011. Liquid Hydrocarbon Production over Mo/HZSM-5 Using Gasified Biomass. S1041 (The Science and Engineering for a Biobased Industry and Economy) Symposium. Stillwater, OK, August 2, 2011.

15. Lu, Y. and F. Yu. 2011. Higher Alcohol Synthesis from Syngas over Copper-Iron Based Catalyst. S1041 (The Science and Engineering for a Biobased Industry and Economy) Symposium. Stillwater, OK, August 2, 2011.

16. Livingston, D., F. Yu, Q. Li, and P. Steele, 2011. Ethanolic Fermentation of Bio-oil Hydrolysate. S1041 (The Science and Engineering for a Biobased Industry and Economy) Symposium. Stillwater, OK, August 2, 2011.

17. Chen, J., L. Sun, A. Hao, W. Jiang, and F. Yu. 2011. Bioconversion of Fiber Crops into High-Value Fiber, Film, Composite, and Hydrocarbon. S1041 (The Science and Engineering for a Biobased Industry and Economy) Symposium. Stillwater, OK, August 2, 2011.

18. Yu, F., P. Steele, E. Columbus, and G. Steele. 2011. Thermochemical Conversion of Biomass to Biofuel, Sustainable Energy Research Center. S1041 (The Science and Engineering for a Biobased Industry and Economy) Symposium. Stillwater, OK, August 2, 2011.

19. Street, J., Wooten, J., Columbus, E., Warnock, J., White, M., Yu, F. Hindrances to Liquid Hydrocarbon Production over Mo/HZSM-5 using Biomass Syngas. An IBE Meeting Presentation presented for IBE 2011 Conference. Atlanta, GA, March 3-5, 2011.

20. Hu, J., Yu, F., Lu, Y., Yan, Q., Wooten, J., Columbus, E., Batchelor, W. Gasoline Range Hydrocarbons Synthesis From Biomass-derived Syngas over Mo/HZSM-5 Catalyst. An IBE Meeting Presentation presented for IBE 2011 Conference. Atlanta, GA, March 3-5, 2011.

## Task 4.9. - Develop a grain drying model that includes parameters for CHP technologies

**Description:**
The Recipient shall develop and integrate a grain drying model with a CHP technology. In order to develop the model, a complete literature search for existing grain drying models will be performed. In addition, a testing commodity storage bin will be developed. This subtask also includes the model validation and verification.

**Percentage of completion**: 100%

**Accomplishments:**
*Develop a grain drying energy model that is compatible with existing CHP technology models.*

Combined heat and power (CHP) systems are a specific suite of cogeneration technologies designed to allow the distributed generation of energy while efficiently utilizing waste heat for downstream processes (USDOE, 2012). Typical applications for large CHP systems include manufacturing or processing facilities, hotels, or office buildings. CHP units can be up to 80% efficient in converting fuel energy into usable energy (Mago et al., 2009). The increased efficiency is directly related to the reuse of waste heat created by electrical power generation. CHP systems can be optimized to follow primarily electrical or thermal demand depending on their application and the availability of grid-based electricity and can reduce greenhouse gas emissions (Mago and Chamra, 2009). In addition to the large scale applications of CHP technology, there are a number of small scale applications that can utilize the same efficient approach to distributed energy and heat generation.

Agricultural processes, specifically the post-harvest drying of grain crops, can leverage these same technologies and increased efficiencies. Producers utilize post-harvest drying to have an earlier harvest, a larger harvest window, and to reduce the risk of losses to standing crops. Post-harvest management of grain crops can require large energy inputs from both electricity and heat. Bern (1998) estimated that drying 1.3 billion bushels of corn in Iowa consumed 11 900 TJ of fuel energy and 139 GWh of electricity. Bennett et al. (2007) estimated that $300 million was spent to dry Iowa's 2004 corn crop and proposed the use of corn stover combustion combined with CHP technology. The authors found that a modified dryer was a technologically and economically viable option. Harchegani et al. (2012) utilized a test scale heat pump system to condition rough rice and found 10% reduction in power consumption and an improvement in stored rice quality. Interest in alternative forms of post-harvest management is increasing.

Operational costs associated with drying and management of stored grain come as a result of aeration and preconditioning air. There are a number of approaches to drying and storing grain, but the most common in Mississippi is to allow corn crops to field dry to approximately 18% - 20% wet-basis moisture content (MCwb) prior to harvest. Corn is marketed at 15.5% MCwb, therefore the remaining moisture must be removed or the producer will pay a penalty when selling the crop. Similarly, this moisture content is considered the maximum level for safe storage of the crop to prevent quality loss during short-term holding. When wet grain enters the bin, aeration must begin immediately and cannot stop until the drying front is pushed upwards through the entire vertical grain column. Depending on the depth of grain, flow rate of the fan, and a number of other factors, this process can take up to a week. After initial drying, further aeration is required to reduce stored grain temperature as ambient conditions allow. Preheating the air is used not to increase grain temperature, but to increase the water holding capacity of air entering the bin. Increasing the drying gradient between grain and air allows the drying process to proceed faster and can reduce initial aeration time. The use of refrigeration systems to dehumidify air prior to drying have not been readily adopted.

Constructing a CHP system for use with grain drying or modifying a grain dryer to utilize CHP technologies can increase efficiency and decrease energy consumption. Both are valid approaches and further effort is needed to bring them to the marketplace. Additionally, there may be ways to utilize off-the-shelf technologies to for distributed electricity generation and waste heat recovery in the post-harvest environment. In addition to the energy savings, there are locations without access to three-phase power or in which single-phase motor size is limited based on capacity of the rural electrical infrastructure. Therefore, the objectives of this study were to assess the utility of CHP approaches to grain drying and to propose a basic system to implement these technologies.

*Methods*

To assess the application of CHP systems to post-harvest management in Mississippi, a test case was developed based on an existing grain bin owned and operated by a cooperating producer near Columbus, Miss. The grain bin is constructed with corrugated metal sheet and has a diameter of 27 ft and an eave height of 21.5 ft. At level full, the grain bin has a capacity of 10,000 bushels of shelled corn. The producer utilizes a corn-soybean rotation and stores either commodity based on excess production or marketing strategy. Corn was being stored while this study was in progress. Common in aerated grain storage, there is a plenum floor constructed of perforated metal with 40% open area. Aeration is accomplished with a 10 hp 20 in. vane axial fan (Nebraska Engineering Company, Omaha, Neb.). This fan is 230 V single phase and draws 47 A at full load. In addition to the fan, other electrical loads are two 2 hp augers used for loading and unloading the grain bin. There is no system to preheat air entering the grain bin.

The grain bin was instrumented to measure plenum static pressure(673-1, Dwyer Instruments, Michigan City, In.), plenum temperature (Type T Thermocouple, Omega Engineering, Stamford, Conn.) and energy consumption (H0851, Veris Industries, Tualatin, Or.) of the fan. The grain bin was outfitted with internal temperature cables to record grain temperature in the vertical column. A weather station was placed adjacent to the grain bin to record ambient environmental conditions (Hobo U30, Onset, Bourne, Mass.). Prior to harvest, the producer stated that the instrumented bin would be for long-term storage. During harvest, however, market conditions created a premium for early delivery grain. As a result, the measured dataset was limited but sections of the data were complete enough to allow conservative validation and analysis. Data were collected beginning 16 August 2012 at 12:00 AM and continued until 6 December 2012 at 11:00 PM. This resulted in 2712 hours of data.

A thin-layer model was developed to simulate drying conditions within the cooperating producer's grain bin. Aeration fan flow rate is determined by the static pressure exerted on the fan by the column of grain. A system characteristic curve was developed based on grain type, depth, bin diameter, plenum floor characteristics, and superficial velocity of air flow developed by the fan. The fan characteristic curve was developed from manufacturer's specifications. The intersection of these two curves determined the aeration fan operating point for volumetric flow. Volumetric flow was converted into mass air flow using the specific volume of the air at external ambient conditions.

The thin-layer model simulates mass and energy balance in a 0.1 m depth of grain. The first layer is in direct contact with the plenum floor. Subsequent layers are stacked vertically to simulate the entire vertical grain column. Assumptions of the model are that the grain bin is adiabatic, the only direction of air flow is normal to the thin-layers, and that convective currents are not occurring within the grain mass. The primary focus of the model is to test the effects of using waste heat generated from distributed energy generation in forced aeration, therefore, the effects of ambient environment and solar radiation on the grain column and the grain bin environment were ignored. Air enters the grain column through the plenum and passes into the first layer of grain. Heat and moisture are transferred between the air and the grain in the layer. The second layer receives as an input what was output from the first layer. The calculations iterate through the grain column and then the next set of hourly ambient conditions enter the first layer. One important aspect of the model is preventing the calculation of unrealistic conditions in which air in the bin is oversaturated with moisture. Saturated air will develop during the drying process, which is why the drying front must be pushed through the entire column or an area of high moisture grain will develop, which can rapidly deteriorate

A traditional CHP solution to this application would include a power generation unit driven by a steam boiler, a heat recovery unit, and an absorption chiller. The limitation to this solution is the availability of a steam turbine generator designed to generate less than 100 kW. The model design case is a single grain bin, however, grain

storage facilities typically utilize more than one bin, and therefore a larger-scale CHP solution may be applicable. A 20 kW generator can meet the entire electrical demand for the single grain bin at half load and provide overhead for start-up loads of the electric motors. A towable generator could have many applications on the farmstead and would not be a single-use purchase. On-farm grain bins in the Mid-south are typically used for 4-6 month short term storage and power is not needed at the facility year-round. A diesel generator is a low-barrier, off-the-shelf solution with which many producers would have experience in maintenance and operation. Diesel fuel is readily available on the farm and is typically purchased in bulk. Therefore, a 20 kW diesel generator with a heat recovery system was used to provide electricity and process heat to the grain bin. A liquid propane generator powered generator could be used in a similar application. Heat from the engine coolant system is delivered to the airstream entering the grain bin through an external radiator. Theoretical heat source capacity was estimated from the coolant volume, coolant flow rate, heat delivery to the coolant system, and the minimum thermostat operating temperature as specified by the manufacturer's data sheet (A25KBS, Armstrong Power Systems, Miami, Fl.).

Design conditions for estimating performance of the heat delivery system was based on model climactic conditions as defined the Typical Meteorological Year 3 (TMY3) dataset (Wilcox and Marion, 2008)

*Results*

*Grain Drying Model*

The developed grain drying model, while basic it its approach, met the need of assessing the design parameters associated with testing this application of CHP systems. The system airflow operating point determined by resistance of the grain column and fan performance was 7300 CFM (Figure 1). The fan was undersized for the volume of grain typically stored in the design case grain bin at 0.8 CFM/bu. For natural air drying in the South, 1.0 CFM/bu or greater is preferred.

The mass and energy balance carried out the model performed within expectations. Figure 2 shows the mean grain moisture content decreasing over time and reaching a minimum after 20 hours of drying. The equilibrium moisture content (EMC) of ambient air was less than the moisture content of the grain, leading to drying. The rise is moisture content after the minimum was driven by continued aeration under ambient conditions that introduced moisture back into the stored grain. This kind of response is common and was expected for the ambient conditions that were input into the model. This result further supports the need for artificial heat to be added to the process so that rewetting will not occur which leads to long-term grain storage grain quality degradation.

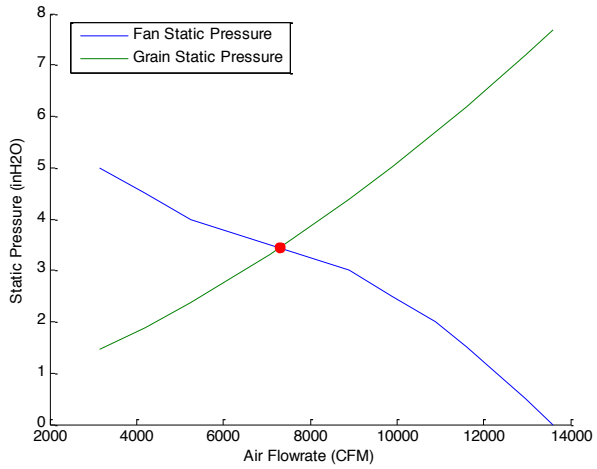


Figure 1. Grain Bin System Performance Curve

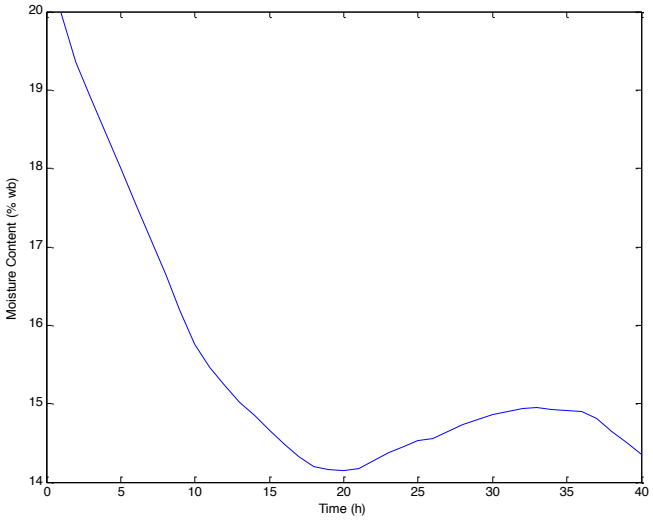


Figure 2. Mean Stored Grain Moisture Content

*Grain Bin Model Validation*

Static pressure created by the grain column during aeration is of high importance because it directly relates to the mass flow of air entering the grain bin which is a primary input into both the heat and mass balance. Calculated static pressure was approximately 3.5 inH2O. The pressure readings recorded from the instrumented grain bin reflected similar static plenum pressure. The only difference was that as the crop dried while in storage, the static pressure decreased to approximately 3 inH2O due to the changing physical and airflow characteristics of the stored grain. The model operated only at the initially calculated set point.

A commercially available grain bin management system (Bullseye, Agridry, LLC, Edon, Oh.) was installed in partnership with the grower. Management systems monitor external ambient conditions and only operate the fans when external conditions are

appropriate for drying or aeration. Generally, in the Midsouth, this means that fans are only operated in the mid-afternoon when temperature and relative humidity are conducive to drying. This system uploads daily grain temperature readings taken at midnight to the company's servers. The grower allowed access to the recorded data. Measured grain temperature was approximately 4°C warmer than model predicted grain temperature. This difference was expected as the model did not take into account solar radiation on the grain bin. The trends in grain temperature were similar between predicted and measured. This difference could be calibrated out of the model or the model could be improved to include radiative effects.

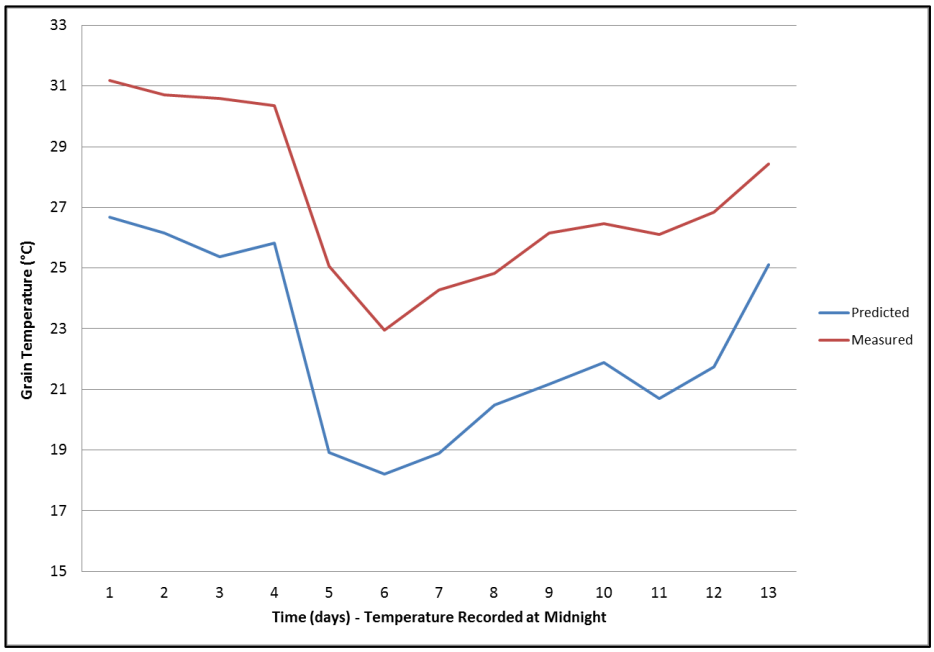


Figure 3. Measured and Predicted Stored Grain Temperature (°C)

A final measure of the grain bin model validity was to test for the effects of evaporative cooling on grain temperature. The model resulted in the grain temperature being lower than ambient while the grain mass was actively drying, as expected (Figure 4). Based on the measures discussed, the model was accepted as valid to generally estimate drying performance.

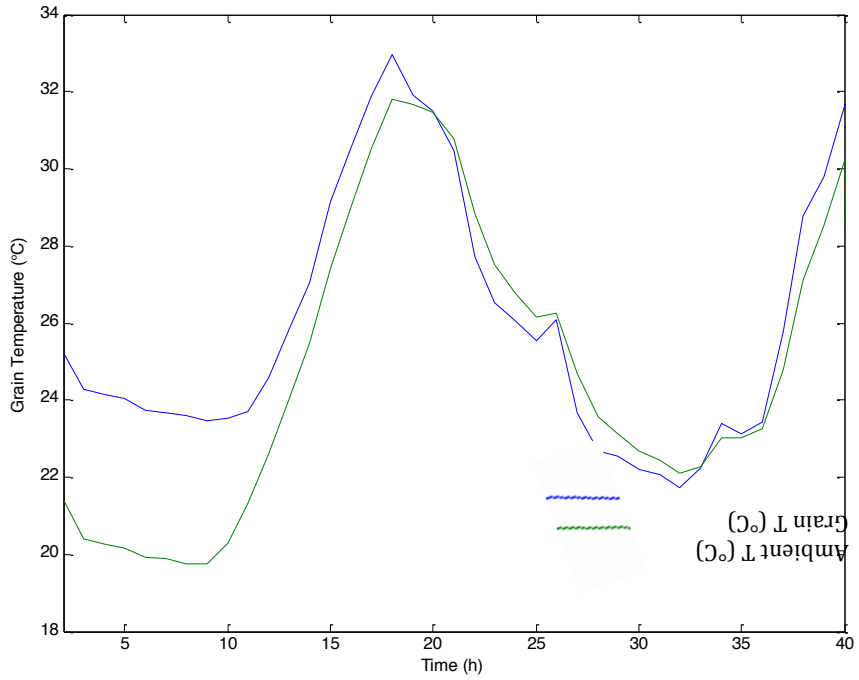


Figure 4. Grain and Ambient Temperature During Drying

*Grain Bin Electrical Energy Consumption*

The aeration fan was operating for 1200 hours out of 2712 hours during which data recorded. This resulted in a 44% mean duty cycle during periods of grain drying and aeration. This result can be misleading because during initial drying phases, the fan was operated at near 100% duty cycle. While the fan was running, it consumed a total of 9366 kWh of electricity or approximately 7.8 kW. This equates to 2521 kWh/month where the average residential Mississippi consumer uses 1193 kWh/month (US Energy Information Administration, 2014). During the limited the three to four months that aeration is needed, a grain bin can use over double the amount of a typical home.

*Waste Heat Recovery and Utilization*

Using the fuel consumption rate from the generator data sheet, at half load the generator consumes 42.5 kW of energy and will produce 10 kW, for a 24% efficiency. The remaining 32.5 kW are lost to friction and heat in the internal combustion engine. The data sheet also describes heat rejection to the engine coolant system of 19 kW. In order to maintain the minimum engine operating temperature of 71°C, up to 20% of the heat delivered to the coolant system is required. Depending on the ambient temperature of the air, some of this waste heat can be delivered to the incoming grain bin air stream through an external radiator to increase drying performance. There will be efficiency losses associated with capturing and delivering this waste heat to the grain bin inlet. An

80% capture efficiency and a 70% delivery efficiency were assumed. In general, the heat recovery system can increase drying temperature by 4°C. This temperature change had a direct effect on air relative humidity and will increased drying efficiency.

A design condition of 27°C and 75% relative humidity was calculated from TMY3 climactic data as mean daytime ambient conditions during early harvest season. This time can be challenging for producers since harvested grain has the highest moisture content and is more likely to spoil while ambient conditions are least effective for drying. Using the heat recovery system described above these the ambient conditions were treated with waste heat as they enter the grain bin, the resulting grain drying conditions were 31°C and 60% relative humidity. Simulating the grain drying conditions as a full bin of shelled corn, the design condition and the treated air treated as static inputs into the grain drying model (Figure 5). The added heat does not add moisture to the airstream which occurs from direct combustion heating. While the time to dry may not be measurably decreased, the final moisture content is much safer for grain storage with no additional fossil fuels consumed. Liquid propane is typically used for heating incoming air; a dryer using this system gets the benefits of extra heat without added energy consumption. The added heat was equivalent to 0.6 gallons of liquid propane per hour of runtime.

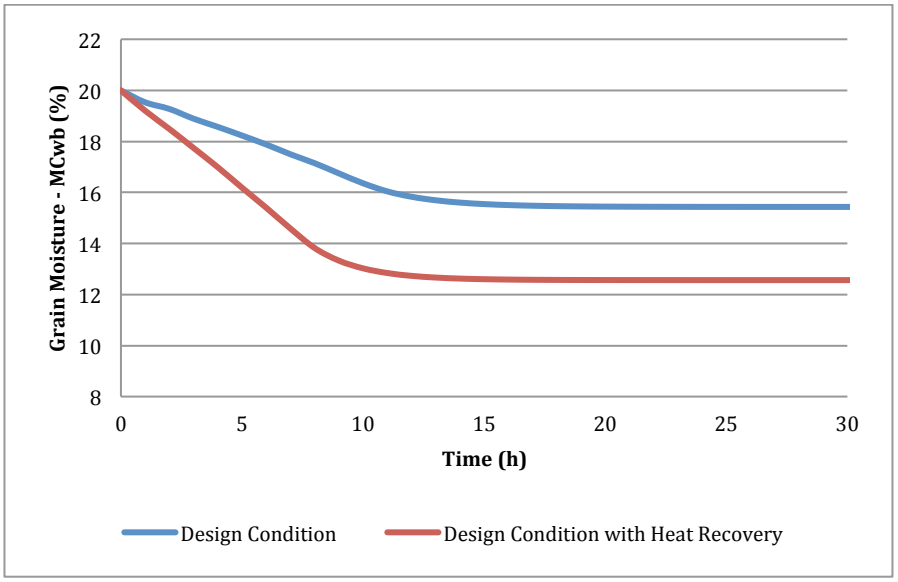


Figure 5. Grain Drying Response to Recovered Heat.

*Conclusions*

Utilizing a generator with waste heat recovery may not be a traditional CHP application, but this analysis has shown that grain drying and storage can be improved by applying CHP concepts to off-the-shelf components. For larger bins or grain storage facilities consisting of multiple bins, CHP is a viable option. Utilizing waste heat recovery was shown to dry to improved moisture content with no additional energy

input as compared to using only natural air dying conditions. The short time period of use and serious consequences for failure to dry stored grain, makes distributed power and heat generation an attractive tool for grain managers. Further development to create an applied suite of CHP or waste heat recovery systems for agricultural systems is needed to bring these final concepts to market.

*References*


Bennett, A. S., C. J. Bern, T. L. Richard, and R. P. Anex. 2007. Corn Grain Drying Using Corn Stover Combustion and CHP Systems. *Transactions of the ASABE* 50(6):2161-2170.

Bern, C. J. 1998. Preserving the Iowa Corn Crop: Energy Use and $CO_2$ Release. *Applied Engineering in Agriculture* 14(3):293-299.

Harchegani, M. T., M. Sadeghi, M. D. Emami, and A. Mohed. 2012. Investigating energy consumption and quality of rough rice drying process using a grain heat pump dryer. *Australian Jounal of Crop Science* 6(4):592-597.

Mago, P. J., and L. M. Chamra. 2009. Analysis and optimization of CCHP systems based on energy, economical, and environmental considerations. *Energy and Buildings* 41(10):1099-1106.

Mago, P. J., N. Fumo, and L. M. Chamra. 2009. Performance analysis of CCHP and CHP systems operating following the thermal and electric load. *International Journal of Energy Research* 33(9):852-864.

US Department of Energy. 2012. US Department of Energy Southeast Clean Application Center. Available at: http://www.southeastcleanenergy.org. Accessed on 27 Sept. 2012.

Wilcox, S., and W. Marion. 2008. Users Manual for TMY3 Data Sets. National Renewable Energy Laboratory. Golden, Co.

## Task 4.10 Analysis of Syngas Production Systems for CHP Applications

**Description:**
The Recipient shall analyze syngas production systems for CHP applications. This shall include the following activities:

- Optimization of Biomass Unit Operations for Syngas Production
- Economic Modeling of Syngas Production at Micro-scale
- Standardized Energy Audit Methodology for Renewable Energy Provider Systems of CHP
- Utilization of char and waste heat from syngas production
- Biomass feedstocks drying

**Percentage of Completion:** 100%

**Accomplishments:**
Characterized biomass and biochar from syngas production by elemental analysis and TGA. Preliminary GIS analysis was conducted to determine the distribution of available biomass feedstock near existing CHP plants in Scott and Washington counties. The amount of biomass feedstock was determined at the county level using data from National Agricultural Statistics Service and Mississippi Forest Inventory. It was assumed that the biomass in each county was evenly distributed. The proximity analysis tool in ArcGIS was used to create buffers around the CHP plant and provide information on the available feedstock that can support a CHP plant. The shortest path between the locations of biomass supply and CHP plants were determined using ArcGIS network analysis tool.

Preliminary sensitivity analysis of the economic model input parameters with production capacities ranging from 60 to1,800 $Nm^{-3}h^{-1}$ showed that larger bio-gasification capacity will have lower syngas production unit cost. Further analysis is needed to identify ranking of the sensitive parameters. We are analyzing economics of potential feedstock source yields from the Mississippi watershed using a regional scale model. We are also updating our economic models for the evaluation of bio-gasification system.

- Measured the elemental compositions of wood chips and biochar by elemental analysis and ICP.
- Measured the thermal stability and ash content of wood chips and biochars by TGA.

Biochar is one major byproduct for bio-syngas production. Its applications depend on their physical and chemical properties. Some properties of biochar were characterized in this quarter. Below are the details.

*Elemental compositions of wood chips and biochar from syngas production*

The elemental composition (C, H, N) of wood chips and biochars was analyzed with a CE-40 Elemental Analyzer (EAI Exeter Analytical, Inc.). Mineral analysis was conducted on an ICP spectrophotometer (Optima, model: 4300 DV, PerkinElmer Instruments). The coarse char was collected from the bottom of the gasifier and the fine char was collected from the filters.

Table 1 shows the C, H, N composition of biochars. Table 2 shows the mineral composition (Si, Al, N, P, K, Ca, Mg, S, Fe, Mn, Zn, Cu, B) of biochars. The coarse char from the gasifier has much higher carbon content than fine char. Both coarse char and fine char have a much lower H content compared with biomass (wood chips), because most of the biomass H has been converted to $H_2$ and water during gasification. Biochars also have much higher mineral content (K, Ca, Mg, S, Fe, Mn, Zn, Cu, B) than biomass (Table 2). These minerals are good plant nutrients.

Table 1. Elemental analysis results of wood chips and biochars (wt %).

| Sample | carbon (%) | hydrogen (%) | nitrogen (%) | remaining (%) |
|---|---|---|---|---|
| Wood chips | 44.67± 0.40 | 5.93±0.06 | 0.43±0.10 | 48.96 |
| Coarse char from gasifier | 47.2±2.4 | 0.9±0.1 | 0.4±0.03 | 51.5 |
| Fine char from filter | 32.4±0.6 | 0.9±0.02 | 0.3±0.00 | 66.4 |

Table 2. Mineral analysis results of wood chips and biochars (wt %) by ICP method.

| | %Si | %Al | %N | %P | %K | %Ca | %Mg | %S | Fe, ppm | Mn,ppm | Zn, ppm | Cu, ppm | B, ppm |
|---|---|---|---|---|---|---|---|---|---|---|---|---|---|
| Wood chips | 3.45 | 0.81 | 0.28 | 0.01 | 0.01 | 0.49 | 0.03 | 0.02 | 1 | 149 | 4 | 3 | 10 |
| Coarse char | 6.29 | 1.43 | 0.24 | 0.15 | 4.88 | 8.79 | 0.98 | 0.1 | 465 | 2280 | 34 | 51 | 94 |
| Fine char | 4.63 | 1.59 | 0.6 | 0.03 | 4.1 | 10.7 | 1.33 | 0.99 | 1030 | 2530 | 286 | 96 | 126 |
| Activated carbon | 2.88 | 2.16 | 0.55 | 0.01 | 0.01 | 0.13 | 0.02 | 0.05 | 443 | 1 | 1 | 252 | 9 |

*Note: The measurements were conducted by Soil Testing Laboratory (N, P, K, Ca, Mg, S, Fe, Mn, Zn, Cu, B) and State Chemical Lab (Si, Al) at Mississippi State University.*

The composition of wood chips and coarse char changed dramatically after TGA measurements (see Table 1). These results show that activated carbon and Fine Char have much higher stability, which is the consistent with the results of Figure 2.

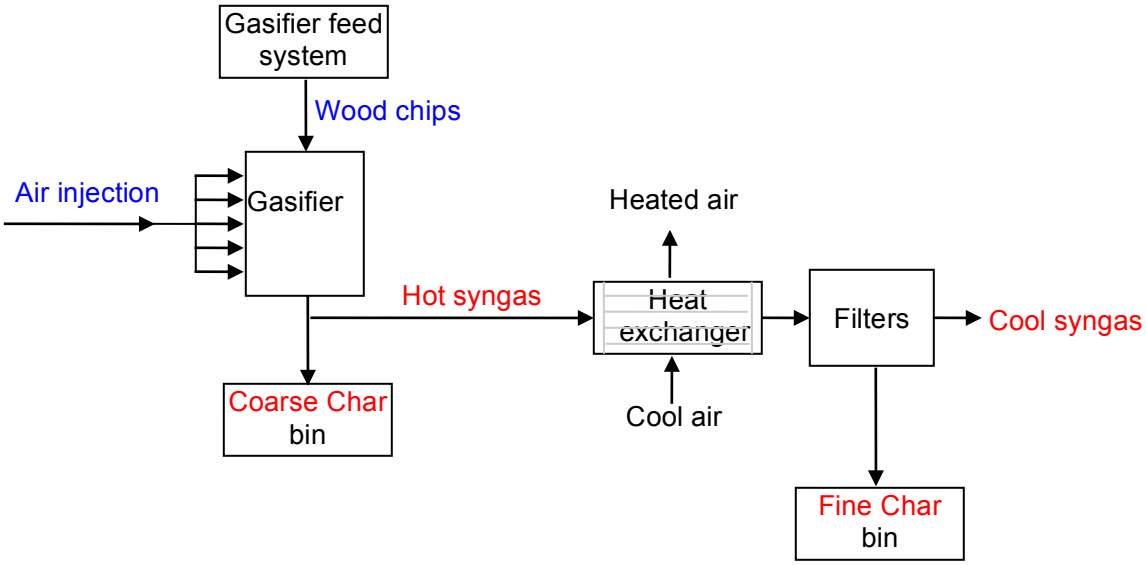


Figure 1. BioMax 25 gasification system

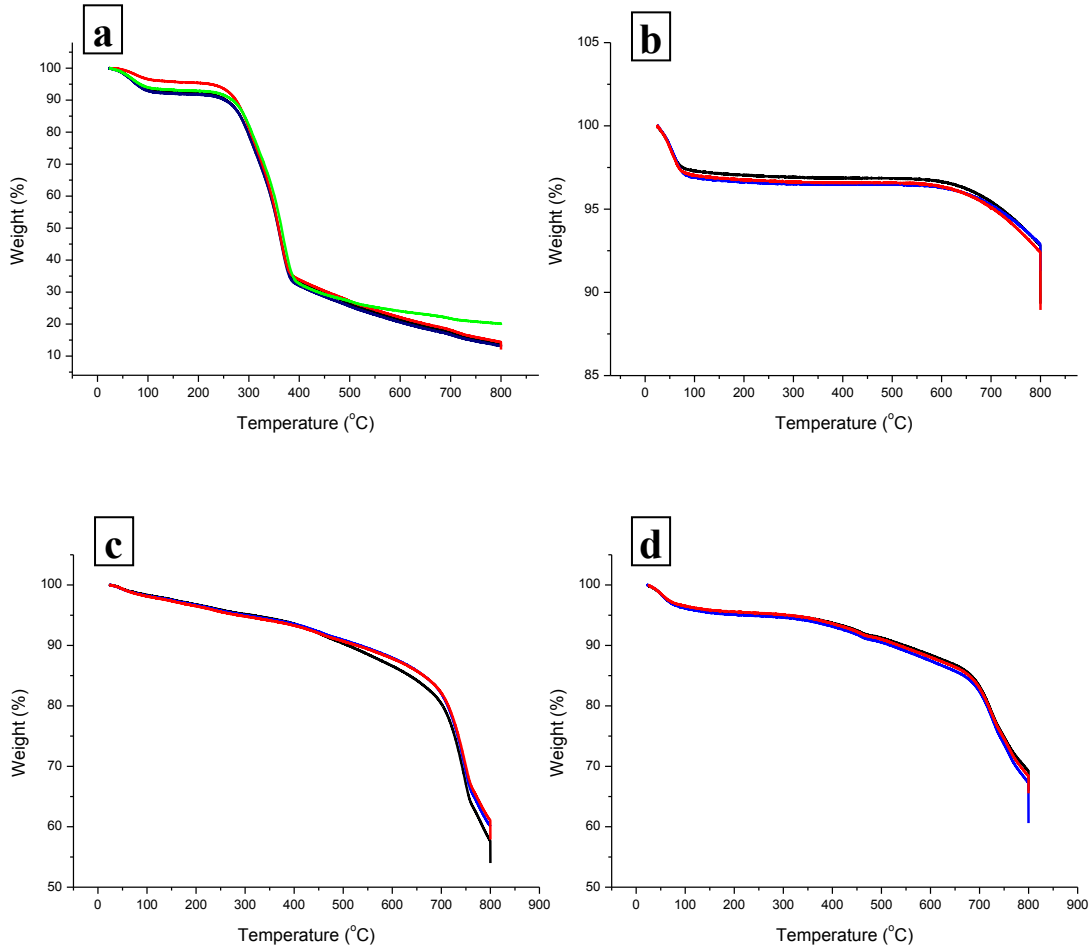


Figure 2. TGA graphs of: a, wood chips; b, activated carbon Filtersorb 200; c, coarse char from gasification; d, fine char from gasification. At least hree TGA tests were conducted for every sample, under $N_2$ flow of 30 ml/min and with a heating rate of 10 °C/min.

*SEM microscopic studies*

Figure 3 shows the pictures of original ungrinded biochars. Figure 4 shows the SEM micrographs of biochars. SEM was performed on a JEOL JSM-6500F 5.0 kV scanning electron microscope. The sample surfaces to be observed were coated with a thin layer of platinum (~15 nm) before testing. Coarse Char has a larger average particle size than Fine Char (Figures 3 and 4). Both Coarse Char and Fine Char are mixtures of big char particles and fine ashes (Figure 4). From SEM graph, large pieces of chars with original cell wall structures can be found in Coarse Chars (Figure 4b). The major carbonized structures in Fine Chars are small fragments (Figure 4d) due to incomplete combustion and gasification. The elemental analysis results also showed that the major component of biochars was carbon. The appearance of fine ashes in biochar samples looks like they were solidified from their melted state. It is possible because the gasification temperature was usually kept between 800-900 °C and the local gasifier temperature could reach 1100 °C, which is above the melting points of many inorganic alkalis and salts. Hard glass-like blocks and deposits can be found at the bottom of the gasifier and on the walls of heat exchanger after a long running time. Probably the carbon fragments in the biochars helped prevent them being melted into big blocks.

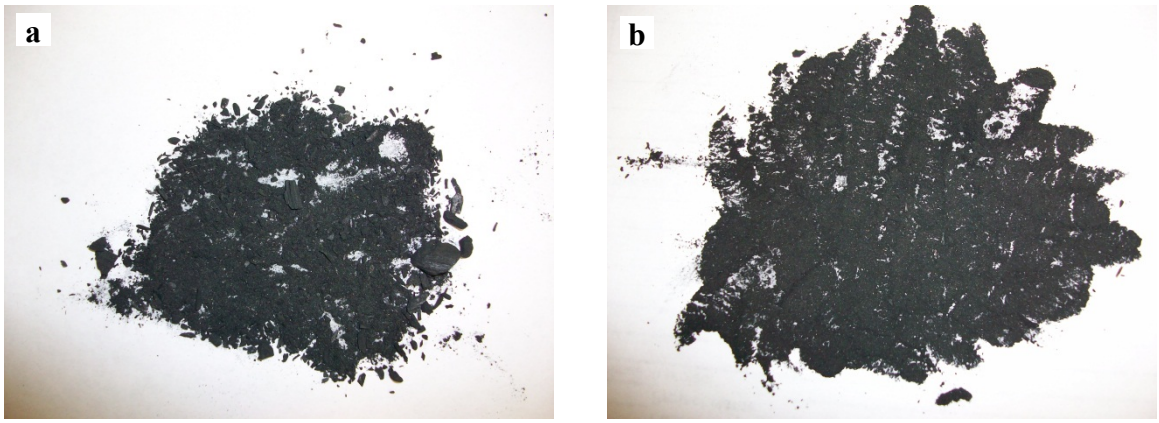


Figure 3. Pictures of biochars: a, Coarse Char; b, Fine Char.

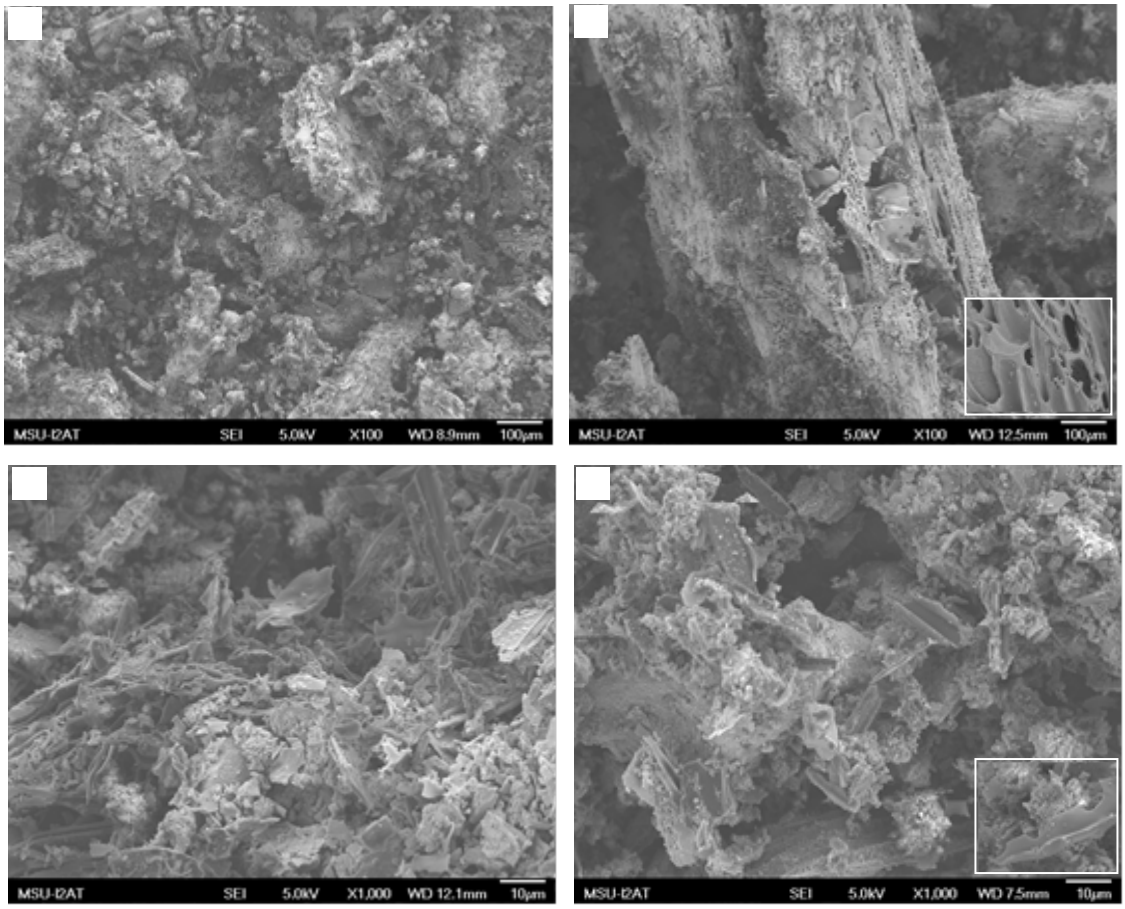


Figure 4. SEM micrographs of biochars

*Heating values of biochars*

Table 3 shows the higher heating values of biochars. Higher heating value (HHV) was measured with an oxygen bomb calorimeter (Parr Instrument Company, Moline, IL) according to Parr Sheet No. 240M, 205M, and 207M. The biochars still showed considerable of HHV compared to wood chips. Coarse Char showed a much higher HHV than Fine Char because Coarse Char has higher carbon content than Fine Char. The results show that biochars still can be used as an energy resource.

Table 3. HHV of wood chips and biochars

| Sample | HHV (MJ/kg) | Carbon content (%) |
|---|---|---|
| Wood chips | 17.7± 0.1 | 44.7± 0.4 |
| Coarse Char | 14.5± 0.3 | 47.2±2.4 |
| Fine Char | 10.0± 0.1 | 32.4±0.6 |
| Activated carbon (Filtersorb 200) | 30.7± 0.2 | 88.1±0.6 |

The biochars collected from the bottom of the gasifier (Coarse Char) and from the filters (Fine Char) showed different properties. Both biochars were composed of bigger particles and fine ashes. Coarse Char has a larger average size than Fine Char. Original cell structures were found in Coarse Char particles. Coarse Char has higher carbon content (47.2%) than Fine Char (32.4%). Both biochars showed much lower carbon content than commercial activated carbon (Filtersorb 200, 88.1%). Thus, biochars had higher mineral content than Filtersorb 200. Both Coarse Char and Fine Char kept considerable HHV (14.5 and 10.0 MJ/kg respectively), but their HHV were lower than that of wood chips (17.7 MJ/kg) and much lower than that of activated carbon (30.7 MJ/kg). Activated carbon, Filtersorb 200, was thermally stable under nitrogen environment when the temperature was below 660 oC. Fine Char showed higher thermal stability than Coarse Char. Both Coarse Char and Fine Char were more thermally stable than wood chips, but less stable than activated carbon.

*Properties of syngas:*

The syngas composition was measured by GC. Figure 5 showed a typical syngas GC graph. The produced syngas was composed of ~48% $N_2$, ~21% CO, ~ 18% $H_2$ and ~10% $CO_2$ (See Table 4). The composition of the producer gas was stable during gasification.

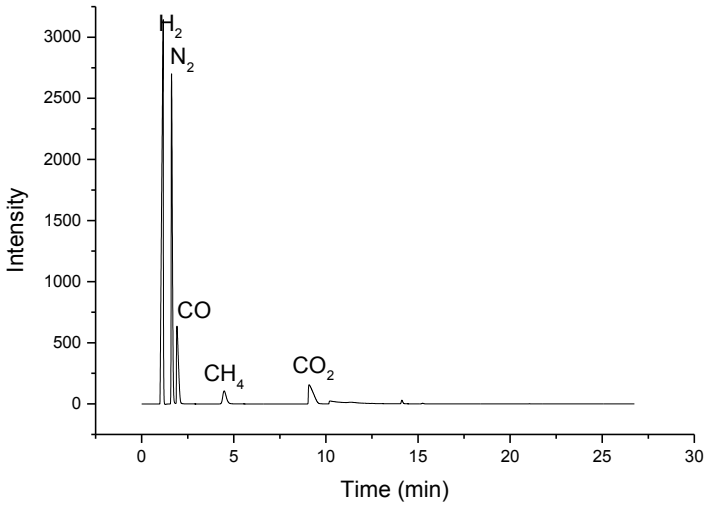


Figure 5. A typical GC graph of syngas.

Table 4 Syngas volume composition of 12-6-2010 batch

| | 12:10 | 13:10 | Average |
|---|---|---|---|
| $H_2$ | 17.5 | 17.3 | 17.4 |
| $N_2$ | 47.6 | 48.3 | 48.0 |
| CO | 20.8 | 20.8 | 20.8 |
| $CO_2$ | 10.3 | 10.2 | 10.3 |
| $CH_4$ | 1.7 | 1.7 | 1.7 |
| Other | 2.1 | 1.7 | 1.9 |
| Total | 100 | 100 | 100 |

The LHV (low heating value) of syngas was calculated by equation1. The calculated LHV of the resulting syngas was 5.1-5.3 MJ/ $Nm^3$. The LHV of our wood chips was 19.59 MJ/ $Nm^3$.

$$LHV = 12.622\ P_{CO} + 10.788 P_{H_2} + 35.814 P_{CH_4} \quad (1)$$

$P_{CO}$, $P_{H_2}$ and $P_{CH_4}$ are the volume percentage of CO, $H_2$ and $CH_4$ in syn-gas respectively.

***Economic analysis***

We analyzed cost parameters associated with increasing the energy capacity of two existing CHP plants in Mississippi. The proximity analysis tool was used to spatially analyze the feedstock residue available within the haul zones, and the network analyst tool was used to find the shortest distance in each haul zone or radial zone from the biomass source to the CHP plant. The effect of plant capacity on the cost of energy production was examined by determining the costs involved, namely, capital cost,

biomass cost and operating cost. Different cost components including feedstock farm gate cost, transportation cost, CHP plant capital cost, and operating cost were used to calculate the total unit cost (TUC) for each CHP plant. Higher plant capacity has the advantage of economy of scale because the capital cost on a per capacity basis decreases as plant capacity increases. However, the disadvantage with higher capacity is that the increased cost of biomass makes the transportation costs higher.

Transporting feedstock within a smaller source area (10-mile radius) had lower transportation costs but higher total unit cost than the two other source buffer scenarios. However, capital costs associated with higher plant capacities were significantly higher and plant expansion may not be economically advantageous. TUC decreased as the CHP capacity increased regardless of the type of feedstock used for energy production. The results show that for low capacity plants, renting a truck to transport feedstock would be a better option than owning a truck. For higher capacity CHP plants, the option of owning a truck was cheaper than renting a truck. In Washington County, the lowest TUC was $0.018/kWh. In Scott County, the lowest TUC was $0.015/kWh. A modest increase in CHP capacity, which is from 1 MW to 2 MW in Scott county and 5 MW to 10 MW in Washington county, might be a feasible approach by drawing feedstock from a smaller area and at lower utilization rates (33% for CS and 30% for FLR), while keeping transportation costs low. A summary of economic analysis for a pilot plant based on our biomass gasification, syngas cleaning and catalytic conversion system was given below. In order to enhance the working efficiency, we set the working mode to three working shifts to maximize the operating hours. The basic cost information and the hydrocarbon yield information was presented in Table 5 and Table 6. The summaries of annual production capital costs and operating costs are presented in Table 7 and Table 8. The cost summary of unit price of bio-syngas and biofuels are presented in Table 9.

Table 5. Basic cost information based on our biomass gasification, syngas cleaning and catalytic conversion system in three working shifts mode.

| Basic Cost Information | Unit | Value |
|---|---|---|
| Biomass Gasifier Capacity | $Nm^3/h$ | 65.00 |
| Annual Working Hours | h | 6,240.00 |
| Gasifier Actually Operating Hours | h | 6,188.00 |
| Annual Syngas Yield | $Nm^3$ | 402,220.00 |
| Annual Biomass Consumption | Kg | 167,591.67 |
| Daily Biomass Consumption | ton | 0.64 |
| $CO+H_2$ | $Nm^3$ | 160,888.00 |
| Total Syngas Weight | Kg | 107,737.50 |
| CO Conversion Rate | None | 0.80 |
| Total CO Moles | Mole | 3591,250.00 |
| Char | Kg | 3,351.83 |
| Mass Balance Error | % | -3.47 |

Table 6. Biofuels information in three working shifts mode.

| Production | Selectivity | Mass(Kg) | Mass With Recycle(Kg) | Volume | Unit |
|---|---|---|---|---|---|
| $CO_2$ | 0.08 | 10,112.96 | 12,641.20 | | |
| Liquid Hydrocarbons | 0.42 | 16,893.24 | 21,116.55 | 7,791.07 | Gallon |
| Oxygenates | 0.30 | 18,961.80 | 23,702.25 | 7,935.98 | Gallon |
| Light Hydrocarbons | 0.20 | 8,044.40 | 10,055.50 | 498.15 | MMBTU |
| $H_2O$ | None | 28,442.70 | 35,553.38 | | |
| Unreacted Syngas | None | 21,547.50 | | | |
| Total Weight | None | 104,002.60 | | | |

Table 7. Annual production capital cost information based on our biomass gasification, syngas cleaning and catalytic conversion system in three working shifts mode.

| Capital Cost | Unit | Value |
|---|---|---|
| Total Purchased Equipment Base Cost | $ | 385,000.00 |
| Total Purchased Equipment Cost | $ | 266,501.71 |
| Total Installed Cost | $ | 658,259.22 |
| Total Indirect Cost | $ | 256,721.09 |
| Total Project Investment | $ | 914,980.31 |
| Annual Total Project Investment | $ | 45,749.02 |
| Annual Loan Interest Cost | $ | 23,697.33 |
| Annual Capital Cost | $ | 69,446.35 |

Table 8. Annual production operating cost information based on our biomass gasification, syngas cleaning and catalytic conversion system in three working shifts mode.

| Operating Cost | Unit | Value |
|---|---|---|
| Annual Feedstock Cost | $ | 5,865.71 |
| Annual Electricity Cost | $ | 1,197.11 |
| Annual Waste Water Treatment Cost | $ | 25.99 |
| Annual Catalyst Cost | $ | 1,004.75 |
| Annual Variable Operating Cost | $ | 8,093.56 |
| Annual Labor Cost | $ | 199,680.00 |
| Annual Maintenance Cost | $ | 914.98 |
| Annual General Expense | $ | 189,696.00 |
| Annual Insurance & Taxes | $ | 914.98 |
| Annual Fixed Operating Cost | $ | 391,205.96 |
| Annual Operating Cost | $ | 399,299.52 |

Table 9. Cost summary based on our biomass gasification, syngas cleaning and catalytic conversion system in three working shifts mode.

| Cost Summary | Unit | Value | Market Price | Unit |
|---|---|---|---|---|
| Annual Total Capital Cost | $ | 69,446.35 | | |
| Annual Total Operating Cost | $ | 399,299.52 | | |
| Annual Total Production Cost | $ | 468,745.87 | | |

| | | | | |
|---|---|---|---|---|
| Annual Heat Recovery | $ | 4,424.42 | | |
| Annual Total Production Cost* | $ | 464,321.45 | | |
| Liquid Hydrocarbons Volume Unit Cost | $/Gallon | 30.89 | 3.00 | $/Gallon |
| Oxygenates Volume Unit Cost | $/Gallon | 25.74 | 2.50 | $/Gallon |
| Light Hydrocarbons Volume Unit Cost | $/MMBTU | 38.92 | 3.78 | $/MMBTU |
| Syngas Volume Unit Cost | $/Nm3 | 1.15 | | |

The cost analysis results show that the total annual production cost of biofuels was $ 46,8745.87 with the annual total capital cost of $ 69,446.35 and the annual total operating cost of $ 399,299.52, thereby giving a syngas unit cost of $1.15 /Nm3 in three operating mode. This unit cost is equivalent to $0.01 /MJ of energy cost. The term of energy cost is defined as the cost per unit low heating value (MJ) of the syngas. Therefore the annual total production cost with heat recovery was $ 464,321.45. The biofuels unit cost of gas (Light Hydrocarbons) was $38.92 /MMBTU. The biofuels unit cost of oil (Liquid Hydrocarbons) was $30.89 /Gallon. The biofuels unit cost of aqueous (Oxygenates) was $25.74 /Gallon. The market price was also listed to help compare and calculate the biofuels unit costs.

A graduate student completed her MS degree in Engineering Technology. Part of her MS research involved the analysis of cost parameters associated with increasing the energy capacity of two existing CHP plants in Mississippi. The proximity analysis tool in ArcGIS was used to spatially analyze the feedstock residue available within the haul zones, and the network analyst tool was used to find the shortest distance in each haul zone or radial zone from the biomass source to the CHP plant. The effect of plant capacity on the cost of energy production was examined by determining the costs involved, namely, capital cost, biomass cost and operating cost. Different cost components including feedstock farm gate cost, transportation cost, CHP plant capital cost, and operating cost were used to calculate the total unit cost (TUC) for each CHP plant. Higher plant capacity has the advantage of economy of scale because capital cost on a per capacity basis decreases as plant capacity increases. However, the disadvantage with higher capacity is that the increased cost of biomass makes the transportation costs higher.

The changes in cost for bio-gasification facilities operating at different operating modes and capacities were analyzed by using the formula used in the economic model or the cost calculator (Fig. 10). The results showed that the unit cost of syngas production continually decreased as the production capacity of bio-gasification increased and the operating mode changed from one shift to two and three shifts. The unit production cost of syngas was close to the price of natural gas ($0.378 $Nm^{-3}$) when the bio-gasification capacity was increased to 290 $Nm^3$ $h^{-1}$ in one shift, 160 $Nm^3$ $h^{-1}$ in two shifts, and 120 $Nm^3$ $h^{-1}$ in three shifts.

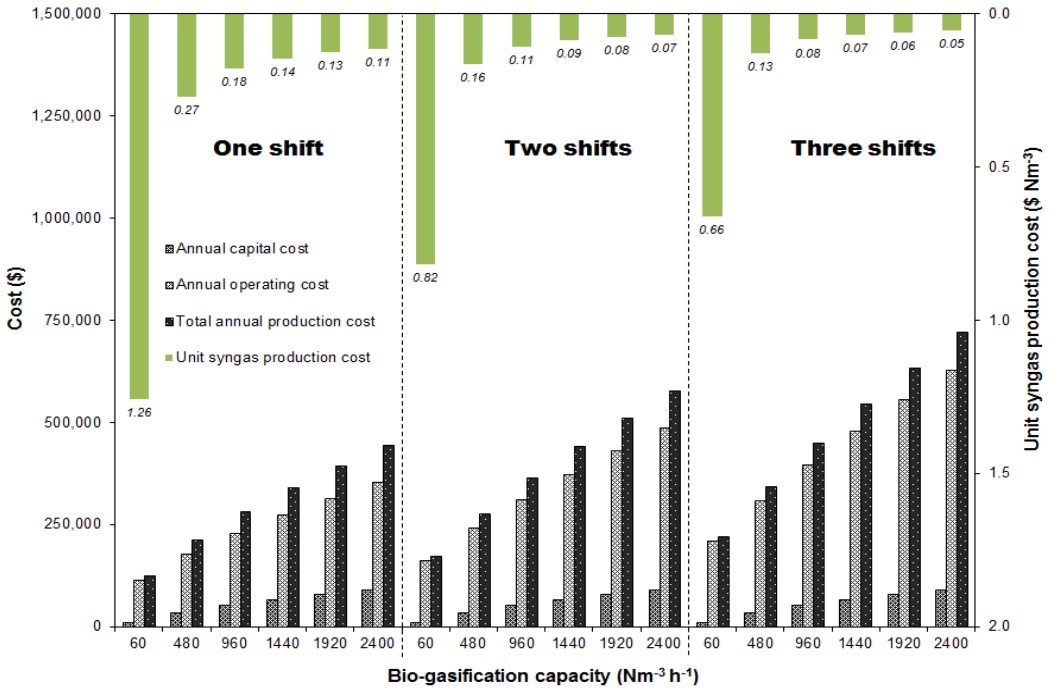


Figure 10. Syngas production unit cost and annual capital, operating, and production costs in different operating modes and bio-gasification capacities.

In the present work we chose feedstock preparation as the start point of economic analysis and the bio-product output, including oil, gas, and aqueous, as the end point. A pilot-scale power facility with equivalent syngas production capacity of 65 $Nm^3/h$, corresponding to wood consumption of 0.64 ton per day, was designed and evaluated for various costs.

Based on the previous quarterly reports, the total annual production cost of biofuels from the above pilot-scale facility was $ 46,8745.87 with the annual total capital cost of $ 69,446.35 and the annual total operating cost of $ 399,299.52, thereby giving a syngas unit cost of $1.15 /$Nm^3$ in three operating mode. The total annual production cost compositions significantly changed when the gasification facilities were operated at different capacities. As shown in Fig. 11, the percentages of operating costs decreased as production capacity increased from micro-scale around to 18,00 $Nm^3/h$ and then started to increase. At production capacity of 1,800 $Nm^3/h$, the percentage of capital costs was up to about one third of total annual cost. When the production capacity further increased to 10,000 $Nm^3/h$, labor was required up to 12 employees and the feedstock consumption was also significantly increased to satisfy larger production capacity, both of which mainly contributed to increased percentage of operating costs at larger production capacity.

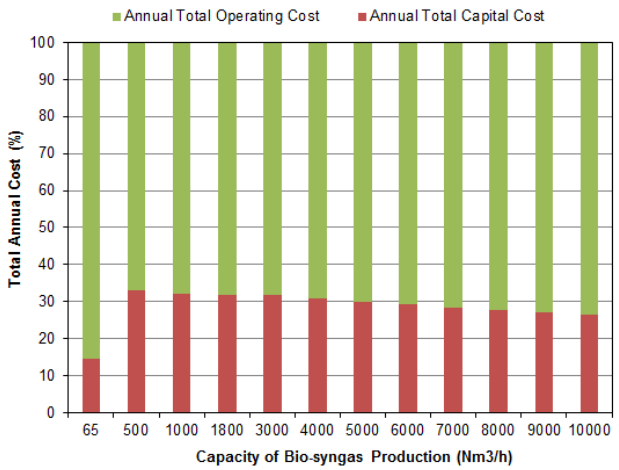


Figure 11. Percentages of capital and operating cost at different production capacities.

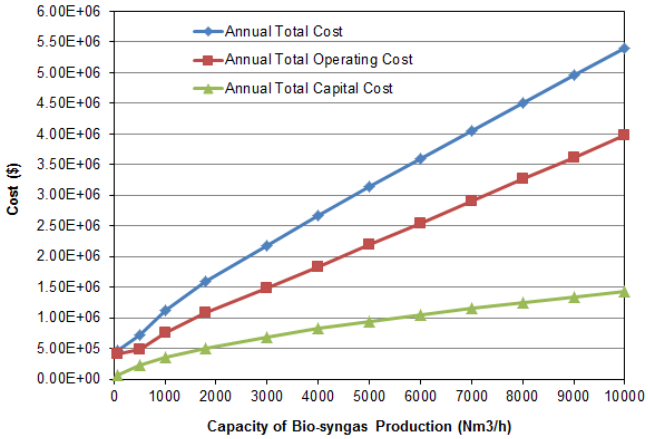


Figure 12. Annual production cost of a gasification facility operating at different capacities.

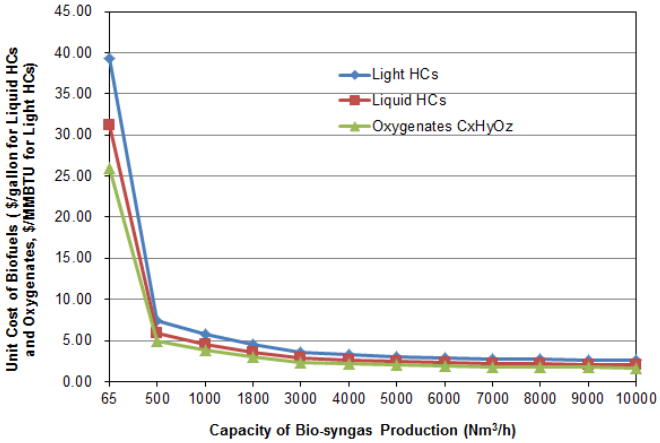


Figure 13. Product unit costs of gasification facility operating at different capacities.

The effects of gasification facility production capacity on total annual costs and product unit cost are shown in Figs. 12 and 13, respectively. Although total annual cost continually increased with scaling-up production capacities (Fig.12), product unit

cost still significantly decreased with an increase of the production capacity from the pilot-scale (65 $Nm^3/h$) to 1,800 $Nm^3/h$ and then tended to level off with further increase in production capacity (Fig.13). For example, when the production capacity increased from 65 to 1,800 $Nm^3/h$, the unit cost of gas (light hydrocarbons), oil (liquid hydrocarbons), and aqueous (oxygenates) products drastically decreased from $39.31 /MMBTU, $31.20 /Gallon, and $26.00/Gallon to $4.46/MMBTU, $3.54/Gallon, and $2.95/Gallon, respectively. Further increase to gasification capacity of 10,000 $Nm^3/h$ slowly brought down corresponding product unit cost to $3.05/MMBTU, $2.42/Gallon, and $2.01/Gallon, respectively. As a result, unit costs of the hydrocarbon products were economically competitive with the market prices ($3.78/BBTU for light hydrocarbons, $3.00/ gallon for liquid hydrocarbons, and $2.50/gallon for oxygenates). These results indicate that increasing gasification facility production capacity could be an effective way to reduce product unit cost and improve the economic feasibility of Biomass-To-Liquid technology.

*Publications / Presentations:*

*Journals:*


1. Radhakrishnan, S., J.O. Paz, F. Yu, S. Eksioglu, and D.L. Grebner. 2013. Assessment of potential capacity increases at combined heat and power facilities based on available corn stover and forest logging residue. Energies (6): 4418-4428. doi:10.3390/en6094418

2. Kim H., and Parajuli Prem B. 2012. Economic Analysis Using SWAT-simulated Potential Switchgrass and Miscanthus Yields in the Yazoo River Basin. Transactions of the Agricultural and Biological Engineers, 55(6): 2123-2134.

3. Street, J. and F. Yu. *2011.* Production of high-value products including gasoline hydrocarbons from thermochemical conversion of syngas. *Biofuels* 2(6):677-691.

4. Yan, Q., H. Toghiani, F. Yu, Z. Cai, J. Zhang. 2011. Effects of Pyrolysis Conditions on Yield of Bio-chars from Pine Chips. *Forest Prod. J.* 61(5):367-371.


*Conferences:*


1. Kim H., and Parajuli Prem B. 2012. Assessment of the Impacts of Land Use and Future Climate Changes on Optimal Selection and Placement of Best

Management Practices. Cincinnati, OH, ASA-CSSA-SSSA. Available at: http://scisoc.confex.com/scisoc/2012am/webprogram/Paper75066.html

2. Paz, J.O., S. Radhakrishnan, F. Yu, S. Eksioglu and D.L. Grebner. 2012. Assessment of potential capacity increases at combined heat and power facilities in Mississippi based on available corn stover and forest logging residue. Sun Grant Initiative 2012 National Conference: Science for Biomass Feedstock Production and Utilization. October 2-5, 2012. New Orleans, LA.

3. Street, J., F. Yu, J. Wooten, E. Columbus, M. White, and J. Warnock. *2012.* Gasoline-range hydrocarbon production using biomass derived synthesis gas over Mo/H+ZSM-5. *Fuel.*

4. Yu, F. 2011. Higher Alcohol Synthesis from Syngas over Copper-Iron Based Catalyst. Strategic Environmental Research and Development Program (SERDP) and Environmental Security Technology Certification Program (ESTCP) annual Technical Symposium & Workshop. Washington, D.C. November 29 – December 1, 2011.

5. Yu, F. 2011. Liquid Hydrocarbon Production over MO/HZSM-5 Using Gasified Biomass. Strategic Environmental Research and Development Program (SERDP) and Environmental Security Technology Certification Program (ESTCP) annual Technical Symposium & Workshop. Washington, D.C. November 29 – December 1, 2011

6. Hakkwan Kim, and Parajuli P. B. 2011. Assessment of the Potential Crop Yield for Bio-Energy Production Using the SWAT Model. ASA/CSSA/SSSA, International annual meeting, October 16-19, San Antonio, TX.

7. Yu, F. Yan, Q., Columbus, E., and Wooten. J. 2011. Catalytic Conversion of Biomass Derived Synthesis Gas to Liquid Hydrocarbons. 107$^{th}$ Gulf Coast Conference. Galveston, TX. October 11-12, 2011.

*Posters:*

1. Yan, Q., Street, J., Wooten, J., Columbus J., and Yu. F. 2011. Biomass to liquid (BTL) fuels via gasification and catalytic conversion. A Poster Presentation presented for the Mississippi State 2011 Biofuels Conference. Mississippi State, MS, October 5-7, 2011.

2. Lu, Y., Yan, Q., Hu, J., Street, J., Wooten, J., Columbus, E., Yu, F. 2011. Higher Alcohols Synthesis from Syngas over Copper-Iron Based Catalyst. A Poster Presentation presented for the Mississippi State 2011 Biofuels Conference. Mississippi State, MS, October 5-7, 2011.

3. Hu, J., Yu, F., Lu, Y., Yan, Y., Wooten, J., Columbus. E. 2011. Green Flight: Renewable Jet Fuel Production Through Integrated Biomass Gasification, Gas Cleaning and Catalytic Conversion System. A Poster Presentation presented for the Mississippi State 2011 Biofuels Conference. Mississippi State, MS, October 5-7, 2011.

4. Street, J., Columbus, E., Wooten, J., White, M., and Yu, F. Scale-up of Gasoline-Range Hydrocarbon Production from Biomass Synthesis Gas over Mo/HZSM-5 and other Bi-functional Catalysts. A Poster Presentation presented for the Mississippi State 2011 Biofuels Conference. Mississippi State, MS, October 5-7, 2011.

5. Yangyang Deng and Parajuli P. B. 2011. Economic Analysis and Optimization of Syngas Production: Model Development and Application. Poster Presentation at the Biofuels conference, October 5-7, Mississippi State University.

## Students Involved in Task 4.0

*Ph.D. Students*

1. Aditya Samala PhD, Graduated, Xylo-oligosaccharides production from corn fiber and *in-vitro* evaluation for prebiotic effect.
2. Tejas Pandya PhD, Graduated, Fiber separation from milled corn and sorghum using the Elusieve process for value addition to feed and biofuel production.
3. John Lowe PhD, TBD.
4. Brian Luck PhD, Graduated, Spatial analysis of air velocity distribution as affected by house size and design in commercial broiler production facilities.

*M.S. Students*

1. Chris Ryals MS, Graduated, Simulation of Emergency Power Productions from Disaster Debris in a Combined Heat & Power (CHP) System Using Geographic Information Systems.
2. Ajay Shah MS, Graduated, Syngas from Biomass as Fuel for Generator.
3. Darrell Livingston MS, Graduated, Ethanolic Fermentation of Bio-oil Hydrolysate.
4. John Lowe MS, Graduated, Investigation of in-field cubing as a method of densification of grass-based biomass.
5. Jonathan Olsen MS, Graduated, Improving commercial broiler attic inlet ventilation through data acquisition coupled with CFD analysis.
6. Rui Li MS, Graduated, Syngas production from biomass pellets in a downdraft gasifier and the removal of oxygen from syngas.
7. William Massey MS, Graduated, Non-thesis.
8. Yangyang Deng MS, Graduated, Economic evaluation of biofuel production through bio-gasification power facility using modeling method.
9. Selvarani Radhakrishnan MS, Graduated, Assessing the potential for increased capacity of combined heat and power facilities based on available corn stover and forest logging residue in Mississippi.

## Publications – Task 4.0

*Journal Papers:*


1. Radhakrishnan, S., J.O. Paz, F. Yu, S. Eksioglu, and D.L. Grebner. 2013. Assessment of potential capacity increases at combined heat and power facilities based on available corn stover and forest logging residue. Energies (6): 4418-4428. doi:10.3390/en6094418

2. Wan, C., F. Yu, Y. Zhang, Q. Li, and J. Wooten. *2013.* Material Balance and Energy Balance Analysis for Syngas Generation by a Pilot-plant Scale Downdraft Gasifier. *Journal of Biobased Materials and Bioenergy.* 7: 690-695.

3. Yan, Q., C. Wan, J. Street, D. Yan, J. Han, and F. Yu. *2013.* Catalytic Removal of Oxygen from Biomass-derived Syngas. *Bioresource Technology.* 147:117–123.

4. Zhang, Y., C., Wan, Q. Li, P.H. Steele, and F. Yu. *2013.* Studies of Biochars Generated from Pilot-scale Downdraft Gasification. *Transactions of the ASABE. 56(3): 995-1001.*

5. Yan, Q., C. Wan, J. Liu, J. Gao, F. Yu, J. Zhang, and Z. Cai. *2013.* Iron Nanoparticles in situ Encapsulated in Biochar-based Carbon as an Effective Catalyst for Conversion of Biomass-derived Syngas to Liquid Hydrocarbons * *Green Chemistry.* 15:1631-1640.

6. Yan, Q., F. Yu, Z. Cai, and J. Zhang. 2012. Catalytic upgrading nitrogen-riched wood syngas to liquid hydrocarbon mixture over a Fe–Pd/ZSM-5 catalyst. Biomass and Bioenergy. 47: 469-473.

7. Kim H., and Parajuli Prem B. 2012. Economic Analysis Using SWAT-simulated Potential Switchgrass and Miscanthus Yields in the Yazoo River Basin. Transactions of the Agricultural and Biological Engineers, 55(6): 2123-2134.

8. Yan, Q., F. Yu, J. Liu, J. Street, J. Gao, Z. Cai, and J. Zhang. 2012. Catalytic Conversion Wood Syngas to Synthetic Aviation Turbine Fuels over A Multifunctional Catalyst. Bioresource Technology.127:281-290.

9. Wang, H., D. Livingston, R. Srinivasan, Q. Li, P. Steele, and F. Yu. 2012. Detoxification and fermentation of pyrolytic sugar for ethanol production. Applied Biochemistry and Biotechnology. 168:1568–1583.

10. Street, J. and F. Yu. *2011.* Production of high-value products including gasoline hydrocarbons from thermochemical conversion of syngas. *Biofuels* 2(6):677-691.

11. Yan, Q., H. Toghiani, F. Yu, Z. Cai, J. Zhang. 2011. Effects of Pyrolysis Conditions on Yield of Bio-chars from Pine Chips. *Forest Prod. J.* 61(5):367-371.

12. Igathinathane, C., J.D. Davis, J.L. Purswell, and E.P. Columbus. 2010. Application of 3D scanned imaging methodology for volume, surface area, and envelope density evaluation of densified biomass. *Bioresource Technology.* 101(11): 4220-4227.

13. Yang, P., E.P. Columbus, J. Wooten, W.D. Batchelor, P. R. Buchireddy, X. Ye and L. Wei. 2009. Evaluation of syngas storage under different pressures and temperatures. *Applied Engineering in Agriculture* 25(1):121-128.

14. L. Wei, L. O. Pordesimo, S. D. Filip To, C. W. Herndon, W. D. Batchelor. (2009). Evaluation of Micro-Scale SYNGAS Production Costs Through Modeling. *Trans ASAE* Vol. 52(5): 1649-1659.

15. Shah, A., Srinivasan, R., To, F.D., and Columbus, E.P. 2010. Performance and emissions of a spark-ignited engine driven generator on biomass based syngas. *Bioresource Technol.* 101:4656-4661.

*Conference Papers:*

1. Yu, F. 2013. Wide-cut diesel production from an integrated gasification, syngas cleaning, and catalytic conversion process. 2013 Mid-South Area Engineering and Sciences Conference. October 28-29. Oral presentation.

2. Lu, Y., F. Yu, J. Hu, and P. Zhou. 2013. CO hydrogenation to higher alcohols over three-dimensionally ordered macroporous Cu-Fe catalysts. 246$^{th}$ American Chemical Society National Meeting. Indianapolis, IN. September 8-12. Oral presentation.

3. Olsen, J.W.W., J.L. Purswell, J.D. Davis, B.D. Luck and E.J. Koury. 2012. Improving commercial broiler attic inlet ventilation through CFD analysis. Procs. Of the 9th International Symposium: Livestock Env. IX. Jul 8-12. Valencia, Spain.

4. Kim H., and Parajuli Prem B. 2012. Assessment of the Impacts of Land Use and Future Climate Changes on Optimal Selection and Placement of Best Management Practices. Cincinnati, OH, ASA-CSSA-SSSA. Available at: http://scisoc.confex.com/scisoc/2012am/webprogram/Paper75066.html

5. Paz, J.O., S. Radhakrishnan, F. Yu, S. Eksioglu and D.L. Grebner. 2012. Assessment of potential capacity increases at combined heat and power facilities in Mississippi based on available corn stover and forest logging residue. Sun Grant Initiative 2012 National Conference: Science for Biomass Feedstock Production and Utilization. October 2-5, 2012. New Orleans, LA.

6. Hu, J., Yu, F., Lu, Y., Street, J., Wooten, J., Columbus, E. 2012. Transportation Fuels Production from Biomass through Biomass Gasification, Gas Cleaning and Fischer-Tropsch Synthesis: A Technical and Economic Analysis, Paper: 121337425, An ASABE Meeting Presentation written for the 2012 ASABE Conference, Dallas, TX, July 29-August 1, 2012.

7. Lu,Y., Hu,J., Zhou, P., Street, J., Wooten, J, Columbus, E., Yu, F. 2012. Catalytic conversion of syngas to mixed alcohols via three-dimentionally ordered macroporous Cu-Fe based catalyst. Paper:121337229, An ASABE Meeting Presentation written for the 2012 ASABE Conference, Dallas, TX, July 29-August 1, 2012.

8. Street, J., Yu, F., Columbus, E., Wooten, J. 2012. Scale-Up of Liquid Hydrocarbon Production using Gasified Biomass. Paper: 121337524, An ASABE Meeting Presentation written for the 2012 ASABE Conference, Dallas, TX, July 29-August 1, 2012.

9. Lu, Y., Yu, F., Hu, J., Zhou, P. Mixed alcohols Synthesis from Syngas via Zn-Mn promoted Cu-Fe based catalyst. 2012. A Poster Presentation presented for the 2012 Southeast Biofuels Conference. Jackson, MS, August 8-9, 2012.

10. Street, J., Wooten, J., Columbus, E., and Yu, F. 2012. Scale-up of Gasoline-Range Hydrocarbon Production from Gasified Woody Biomass using Bi-functional Catalysts. A Poster Presentation presented for the 2012 Southeast Biofuels Conference. Mississippi State, MS, August 8-9, 2012.

11. Lu, Y., Yu, F., Hu, J., Zhou, P. 2012. Syngas to mixed alcohols via 3D ordered macroporous Cu-Fe based catalyst. Paper number: 172, An oral presentation presented for 244th American Chemical Society National Meeting & Exposition. Philadelphia, PA, August 19-23, 2012.

12. Street, J., F. Yu, J. Wooten, E. Columbus, M. White, and J. Warnock. *2012.* Gasoline-range hydrocarbon production using biomass derived synthesis gas over Mo/H+ZSM-5. *Fuel.*

13. Yan, Q., Yu, F., Liu, J. 2012. Carbon encapsulated iron nanoparticles for catalytic conversion biosyngas to liquid hydrocarbons. 244th ACS National Meeting, Philadelphia, PA, August 19-25, 2012.

14. Yu, F. 2011. Higher Alcohol Synthesis from Syngas over Copper-Iron Based Catalyst. Strategic Environmental Research and Development Program (SERDP) and Environmental Security Technology Certification Program (ESTCP) annual Technical Symposium & Workshop. Washington, D.C. November 29 – December 1, 2011.

15. Yu, F. 2011. Liquid Hydrocarbon Production over MO/HZSM-5 Using Gasified Biomass. Strategic Environmental Research and Development Program (SERDP) and Environmental Security Technology Certification Program (ESTCP) annual Technical Symposium & Workshop. Washington, D.C. November 29 – December 1, 2011

16. Yu, F. Yan, Q., Columbus, E., and Wooten. J. 2011. Catalytic Conversion of Biomass Derived Synthesis Gas to Liquid Hydrocarbons. 107$^{th}$ Gulf Coast Conference. Galveston, TX. October 11-12, 2011.

17. Yu, F. 2011. Higher Alcohol Synthesis from Syngas over Copper-Iron Based Catalyst. Strategic Environmental Research and Development Program (SERDP) and Environmental Security Technology Certification Program (ESTCP) annual Technical Symposium & Workshop. Washington, D.C. November 29 – December 1, 2011.

18. Yu, F. 2011. Liquid Hydrocarbon Production over MO/HZSM-5 Using Gasified Biomass. Strategic Environmental Research and Development Program (SERDP) and Environmental Security Technology Certification Program (ESTCP) annual Technical Symposium & Workshop. Washington, D.C. November 29 – December 1, 2011

19. Hakkwan Kim, and Parajuli P. B. 2011. Assessment of the Potential Crop Yield for Bio-Energy Production Using the SWAT Model. ASA/CSSA/SSSA, International annual meeting, October 16-19, San Antonio, TX.

20. Yu, F. Yan, Q., Columbus, E., and Wooten. J. 2011. Catalytic Conversion of Biomass Derived Synthesis Gas to Liquid Hydrocarbons. 107th Gulf Coast Conference. Galveston, TX. October 11-12, 2011.

21. Olsen, J.W.W., J.D. Davis, J.L. Purswell. 2011. 2D simulation of air flow in commercial broiler house attics. Presentation for the 2011 ASABE International Meeting, Aug 7-10. Louisville, KY.

22. Yangyang Deng, and Parajuli P. B. 2011. Economic Evaluation of Electricity Generation from a Small-Scale Bio-Gasification Facility using an Optimization Model. IBE Annual Conference, Loews Atlanta, March 3-5, 2011, Atlanta, GA.

23. HakKwan Kim, Parajuli P. B., Fei Yu, Joel O. Paz, and Eugene Columbus. 2011. Economic Model for Evaluating Syngas Production Cost of Bio-gasification Facility. IBE Annual Conference, Loews Atlanta, March 3-5, 2011, Atlanta, GA.

24. Hakkwan Kim, Parajuli P. B., Yu F., and Columbus E. P. 2011. Economic Analysis and Assessment of Syngas Production using a Modeling Approach. ASABE Publication No. 1110814, ASABE, St. Joseph, MI. Available at: http://asae.frymulti.com/azdez.asp?search=1&JID=5&AID=37322&CID=loui2011&v=&i=&T=2.

25. Yangyang Deng, and Parajuli P. B. 2011. Evaluation of Syngas Production Unit Cost of Bio-Gasification Facility using Regression Analysis Techniques. ASABE Publication No. 1110711, ASABE, St. Joseph, MI. Available at: http://asae.frymulti.com/azdez.asp?search=1&JID=5&AID=37284&CID=loui2011&v=&i=&T=2.

26. Parajuli P. B. 2011. Bio-energy Feedstock Yields and their Water Quality Benefits in Mississippi. ASABE Publication No. 1111416, ASABE, St. Joseph, MI. Available at: http://asae.frymulti.com/azdez.asp?search=1&JID=5&AID=38511&CID=loui2011&v=&i=&T=2.

27. Hakkwan Kim, and Parajuli P. B. 2011. Assessment of the Potential Crop Yield for Bio-Energy Production Using the SWAT Model. ASA/CSSA/SSSA, International annual meeting, October 16-19, San Antonio, TX.

28. Ryals, C.S., J.D. Davis, S. Samson, and D. Evans. 2011 Prediction of woody debris from a hurricane event using geographic information systems. Presentation for the 2011 ASABE International Meeting, Aug 7-10. Louisville, KY.

29. Production of Syngas from Downdraft Fixed-bed Biomass Gasification Systems, Lin Wei, Filip To, Eugene Columbus, Fei Yu, James Wooten, William D. Batchelor, Presentation, International Conference on Bioenergy Technology (ICBT), Beijing China, August 22, 2010.

30. Yu, F., Q. Yan, J. Hu, Y. Lu, L. Wei, J. Wooten, E. Columbus and W. Batchelor. 2010. Mixed Hydrocarbons from Biomass Gasification Syngas over Mo/HZSM-5 Catalyst. 9th International Conference on Sustainable Energy Technologies (SET). Shanghai, China. August 24-27.

31. Yu, F., Q. Yan, J. Hu, L. Wei, E. Columbus and J. Wooten. 2010. Mixed Hydrocarbon Production from Biomass-derived Syngas over A Bi-functional Catalyst. International Symposium on Renewable Feedstock for Biofuel and Bio-based Products. Austin, TX, August 11-13.

32. Hu, J., Yu, F., Wei, L., Columbus, E., and Batchelor, W. Preliminary Study of the Conversion of Biomass Gasification Syngas to Gasoline-range Hydrocarbons over Mo/HZSM-5. Paper 1008573, ASABE 2010 Annual International Meeting, Pittsburgh, Pennsylvania, June 20-23, 2010.

33. Biomass-based Syngas from Downdraft Fixed-bed Gasifier, Lin Wei, Filip To, Eugene Columbus, Fei Yu, James Wooten, William D. Batchelor, Poster, International Sustainable Energy Technology (ISET), Shanghai, China, August 25, 2010.

34. Effects of Feedstock Properties on the Performance of A Downdraft Gasifier. Lin Wei, Lester O. Pordesimo, S. D. Filip To, James R. Wooten, Agus Haryanto, and Eugene P. Columbus. Paper no. 096873, presented at the 2009 ASABE Annual International Meeting ASABE, Reno, Nevada, June 21 – June 24, 2009.

35. Crude Glycerol Co-gasification with Hardwood Chips in a Pilot-Scale Downdraft gasifier. Agus Haryanto, Lester R. Pordesimo, Sandun D. Fernando, James R. Wooten, Eugene P. Colombus, and Lin Wei. Paper no. 09742, presented at the 2009 ASABE Annual International Meeting ASABE, Reno, Nevada, June 21 – June 24, 2009.

36. Massey, W.A., C. Igathinathane, J.D. Davis, J.L. Purswell, and E.P. Columbus. 2009. Densified biomass mass properties determination using 3D laser scanning and image analysis. Abstract for the MSU Biofuels Conference. August 6-7. Jackson, MS.

37. Massey, W.A., C. Igathinathane, J.D. Davis, J.L. Purswell, and E.P. Columbus. 2009. Densified biomass mass properties determination using 3D laser scanning and image analysis. Abstract for the MSU 8th Annual Graduate Research Symposium. Nov. 6th. Starkville, MS.

*Posters*

1. Lu, Y., Yu, F., Hu, J., Zhou, P. Syngas to Higher Alcohols via Three-dimentionally Ordered Macroporous Cu-Fe Bimetallic Catalyst. A Poster Presentation presented for the 2013 SEC Symposium. Atlanta, GA, February 10-12, 2013.

2. Street, J., Yu, F., Columbus, E., Wooten, J., and Yan, Q. Scale up of Gasoline-Range Hydrocarbon Production from Gasified Woody Biomass using a Bi-Functional Catalyst. A Poster Presentation presented for the 2013 SEC Symposium. Atlanta, GA, February 10-12, 2013.

3. Lu, Y., F. Yu, J. Hu, and P. Zhou. 2013. Higher alcohols synthesis from syngas over three-dimensionally ordered macroporous Cu-Fe bimetallic catalyst. 23rd North American Catalysis Society Meeting. Louisville, KY. June 2-7. Poster.

4. Yan, Q., and F. Yu. 2013. Catalytic Conversion Wood Syngas to 'Wide Cut' Diesel over A Multifunctional Catalyst. 23rd North American Catalysis Society Meeting. Louisville, KY. June 2-7. Poster.

5. Lu, Y., F. Yu, J. Hu, and P. Zhou. 2013. Catalytic conversion of syngas to higher alcohols via Zn-Mn promoted Cu-Fe based catalysts. 246$^{th}$ American Chemical Society National Meeting. Indianapolis, IN. September 8-12. Poster presentation.

6. Street, J., Yu, F., Columbus, E., and Wooten, J. 2013. Process Design and Economic Analysis of a Gas-to-Liquid Plant with Aspen Plus using a Woody Biomass Feedstock. Mississippi Biomass and Renewable Energy Council Conference. Tunica, MS. September 17-18. Poster presentation.

7. Yan, Q., Street, J., Wooten, J., Columbus J., and Yu. F. 2011. Biomass to liquid (BTL) fuels via gasification and catalytic conversion. A Poster Presentation presented

8. Lu, Y., Yan, Q., Hu, J., Street, J., Wooten, J., Columbus, E., Yu, F. 2011. Higher Alcohols Synthesis from Syngas over Copper-Iron Based Catalyst. A Poster Presentation presented for the Mississippi State 2011 Biofuels Conference. Mississippi State, MS, October 5-7, 2011.

9. Hu, J., Yu, F., Lu, Y., Yan, Y., Wooten, J., Columbus. E. 2011. Green Flight: Renewable Jet Fuel Production Through Integrated Biomass Gasification, Gas Cleaning and Catalytic Conversion System. A Poster Presentation presented for the Mississippi State 2011 Biofuels Conference. Mississippi State, MS, October 5-7, 2011.

10. Street, J., Columbus, E., Wooten, J., White, M., and Yu, F. Scale-up of Gasoline-Range Hydrocarbon Production from Biomass Synthesis Gas over Mo/HZSM-5 and other Bi-functional Catalysts. A Poster Presentation presented for the Mississippi State 2011 Biofuels Conference. Mississippi State, MS, October 5-7, 2011.

11. Yu, F. 2011. Liquid Hydrocarbons Production via Biomass Gasification and Catalytic Conversion. 4th Annual Waste-to-Fuels Conference & Trade Show. San Diego, CA. September 25-27, 2011.

12. Lu, Y., Yan, Q., Hu, J., Street, J., Wooten, J., Columbus, E., Yu, F. 2011. Development of copper-iron based catalyst for mixed alcohol synthesis from syngas. Microscopy & Microanalysis annual meeting. Nashville TN, August 7-11, 2011.

13. Hu, J., Yu, F., Lu, Y., Yan, Q., Wooten, J., Columbus, E., Lin, W. 2011. Catalytic Conversion of Biomass-derived Syngas to Gasoline Range Hydrocarbons. Paper: 1110878, An ASABE Meeting Presentation written for the 2011 ASABE Conference, Louisville, KY, August 7-10, 2011.

14. Lu, Y., Yan, Q., Hu, J., Street, J., Wooten, J., Columbus, E., Yu, F. 2011. Mixed Alcohols Synthesis from Syngas Over Copper-Iron Based Catalyst. Paper: 1110834, An ASABE Meeting Presentation written for the 2011 ASABE Conference, Louisville, KY, August 7-10, 2011.

15. Street, J., Columbus, E., Warnock, J., Wooten, J., White, M., Yu, F. 2011. Liquid Hydrocarbon Production over Mo/HZSM-5 Using Gasified Biomass.

Paper: 1110541, An ASABE Meeting Presentation written for the 2011 ASABE Conference, Louisville, KY, August 7-10, 2011.

16. Zhang, Y., J. Wooten, E. Columbus, and F. Yu. 2011. The otential for Improvements of A Pilot-Plant Scale Downdraft Gasifier Through Material Balance and Energy Balance Analysis. S1041 (The Science and Engineering for a Biobased Industry and Economy) Symposium. Stillwater, OK, August 2, 2011.

17. Street, J., J. Wooten, E. Columbus, J. Warnock, M. White, and F. Yu. 2011. Liquid Hydrocarbon Production over Mo/HZSM-5 Using Gasified Biomass. S1041 (The Science and Engineering for a Biobased Industry and Economy) Symposium. Stillwater, OK, August 2, 2011.

18. Lu, Y. and F. Yu. 2011. Higher Alcohol Synthesis from Syngas over Copper-Iron Based Catalyst. S1041 (The Science and Engineering for a Biobased Industry and Economy) Symposium. Stillwater, OK, August 2, 2011.

19. Livingston, D., F. Yu, Q. Li, and P. Steele, 2011. Ethanolic Fermentation of Bio-oil Hydrolysate. S1041 (The Science and Engineering for a Biobased Industry and Economy) Symposium. Stillwater, OK, August 2, 2011.

20. Chen, J., L. Sun, A. Hao, W. Jiang, and F. Yu. 2011. Bioconversion of Fiber Crops into High-Value Fiber, Film, Composite, and Hydrocarbon. S1041 (The Science and Engineering for a Biobased Industry and Economy) Symposium. Stillwater, OK, August 2, 2011.

21. Yu, F., P. Steele, E. Columbus, and G. Steele. 2011. Thermochemical Conversion of Biomass to Biofuel, Sustainable Energy Research Center. S1041 (The Science and Engineering for a Biobased Industry and Economy) Symposium. Stillwater, OK, August 2, 2011.

22. Street, J., Wooten, J., Columbus, E., Warnock, J., White, M., Yu, F. Hindrances to Liquid Hydrocarbon Production over Mo/HZSM-5 using Biomass Syngas. An IBE Meeting Presentation presented for IBE 2011 Conference. Atlanta, GA, March 3-5, 2011.

23. Hu, J., Yu, F., Lu, Y., Yan, Q., Wooten, J., Columbus, E., Batchelor, W. Gasoline Range Hydrocarbons Synthesis From Biomass-derived Syngas over Mo/HZSM-5 Catalyst. An IBE Meeting Presentation presented for IBE 2011 Conference. Atlanta, GA, March 3-5, 2011.

24. Yan, Q., Street, J., Wooten, J., Columbus J., and Yu. F. 2011. Biomass to liquid (BTL) fuels via gasification and catalytic conversion. A Poster Presentation presented for the Mississippi State 2011 Biofuels Conference. Mississippi State, MS, October 5-7, 2011.

25. Lu, Y., Yan, Q., Hu, J., Street, J., Wooten, J., Columbus, E., Yu, F. 2011. Higher Alcohols Synthesis from Syngas over Copper-Iron Based Catalyst. A Poster Presentation presented for the Mississippi State 2011 Biofuels Conference. Mississippi State, MS, October 5-7, 2011.

26. Hu, J., Yu, F., Lu, Y., Yan, Y., Wooten, J., Columbus. E. 2011. Green Flight: Renewable Jet Fuel Production Through Integrated Biomass Gasification, Gas Cleaning and Catalytic Conversion System. A Poster Presentation presented for the Mississippi State 2011 Biofuels Conference. Mississippi State, MS, October 5-7, 2011.

27. Street, J., Columbus, E., Wooten, J., White, M., and Yu, F. Scale-up of Gasoline-Range Hydrocarbon Production from Biomass Synthesis Gas over Mo/HZSM-5 and other Bi-functional Catalysts. A Poster Presentation presented for the Mississippi State 2011 Biofuels Conference. Mississippi State, MS, October 5-7, 2011.

28. Yangyang Deng and Parajuli P. B. 2011. Economic Analysis and Optimization of Syngas Production: Model Development and Application. Poster Presentation at the Biofuels conference, October 5-7, Mississippi State University.

29. Street, J., Columbus, E., Warnock, J., Wooten, J., White, M. Scale-Up of Gasoline-range Hydrocarbons over Mo/H-Y and Mo/HZSM-5 Catalysts. An IBE Poster Presentation presented for IBE 2010 Conference. Cambridge, MA, March 4-6, 2010.

30. Street, J., Columbus, E., Warnock, J., Wooten, J., White, M., Yu, F. Scale-Up of Gasoline-Range Hydrocarbon Production over Mo/HZSM-5 using Synthesis Gas. A Poster Presentation presented for the Mississippi State 2010 Biofuels Conference. Jackson, MS, August 12-13, 2010.

# Summary of Project Activities

## Task 5. CHP System Optimization

## Task 5.1. Diesel Engine/Generator

**Description:**

Task 5.1.1 – Engine modifications - The Recipient shall make necessary modifications to a diesel/generator system (genset) to allow for heat recovery and CHP operation. Heat recovery methods similar to those already employed on the natural gas engine/generator will be utilized.

Task 5.1.2 –Waste Heat Recovery - The Recipient shall install an exhaust gas heat exchanger as well as an engine coolant heat exchanger on the genset in order to recover heat from the diesel exhaust and coolant. This recovered heat will be used to supply hot water to either the hydronic heating system or absorption chiller, depending on the climate conditions.

Task 5.1.3 – Alternative fuel operation – The Recipient shall operate the genset operating on diesel and alternative fuels, including biodiesel, bio-oil, and other suitable fuels.

**Percentage of completion**: 100%

**Accomplishments:**

- A multicylinder engine was modified to operate on several alternative fuels such as natural gas, propane and biodiesel.

- The potential for waste heat recovery from alternative fuelled engines was analyzed and disseminated in the publication titled, "K. K. Srinivasan, P. J. Mago, S. R. Krishnan (2010) "Analysis of Exhaust Waste Heat Recovery from a Dual Fuel Low Temperature Combustion Engine using an Organic Rankine Cycle," Energy, Vol. 35, pp. 2387-2399, doi:10.1016/j.energy.2010.02.018." In addition, an M.S. thesis titled," "Analysis of exhaust waste heat recovery techniques from stationary power generation engines using organic rankine cycles," Sham, D. K., M.S. Thesis, December 2008," discussing the best practices to recover waste heat from alternative fueled engines was published.

- The range of operation possible with alternative to diesel fueling was identified for several fuels such as propane, natural gas and syngas. For example, the paper titled," N. Shoemaker[1], C.M. Gibson[1], A. Polk[1], K.K. Srinivasan, and S.R. Krishnan, 2011, "Performance and Emissions Characteristics of Bio-Diesel Ignited Methane and Propane Combustion in a Four Cylinder Turbocharged Compression Ignition Engine," Paper No. GTP-11-1347, accepted for publication in *Trans. ASME: Journal of Engineering for Gas Turbines and Power," discusses the limits of operation possible with biodiesel as a pilot fuel in dual fuel engines.*

- The potential for waste heat recovery from exhaust gases using organic Rankine cycles (ORC) was identified and analyzed from a fundamental thermodynamics basis. For example, the paper titled, "K. K. Srinivasan, P. J. Mago, G. J. Zdaniuk, L. M. Chamra, K. C. Midkiff (2008) "Improving the Efficiency of the Advanced Injection Low Pilot Ignited Natural Gas Engine Using Organic Rankine Cycles," Journal of Energy Resources Technology, Trans. ASME, Vol.130, pp. 022201-1 – 022201-7, DOI 10.1115/1.2906123," discusses the improvement in efficiency in advanced dual fuel combustion engines operating on natural gas as the primary fuel. The essential finding of this paper was that about 10% improvement in net thermal efficiency of the system can be expected from waste heat recovery using ORCs.

- Waste heat recovery using ORCs was identified to be dependent on the type of organic fluid selected. The paper titled, P. J. Mago, L. M. Chamra, K. Srinivasan, and C. Somayaji (2008) "An Examination of Regenerative Rankine Cycles Using Dry Fluids." Applied Thermal Engineering, Vol. 28, No. 8-9, pp. 998-1007," discussed the general rules in selecting ORCs to obtain optimal benefits from waste heat recovery.

**Publications / Presentations:**

*Journal Articles:*

1. K. K. Srinivasan, P. J. Mago, S. R. Krishnan (2010) "Analysis of Exhaust Waste Heat Recovery from a Dual Fuel Low Temperature Combustion Engine using an Organic Rankine Cycle," Energy, Vol. 35, pp. 2387-2399, doi:10.1016/j.energy.2010.02.018

2. H. Cho[1], S. R. Krishnan, R. Luck, and K. K. Srinivasan (2009) "Comprehensive uncertainty analysis of a Wiebe function-based combustion model for pilot-ignited natural gas engines," Proceedings of the Institution of Mechanical Engineers, Part D: Journal of Automobile Engineering, 223, Number 11 / 2009, pp. 1481-1498, DOI: 10.1243/09544070JAUTO1103

3. K. K. Srinivasan, P. J. Mago, G. J. Zdaniuk, L. M. Chamra, K. C. Midkiff (2008) "Improving the Efficiency of the Advanced Injection Low Pilot Ignited Natural Gas Engine Using Organic Rankine Cycles," Journal of Energy Resources Technology, Trans. ASME, Vol.130, pp. 022201-1 – 022201-7, DOI 10.1115/1.2906123

*Conference Papers:*

1. S.K. Jha[1], S.R. Krishnan, K.K. Srinivasan, 2010, "Quasi-Two-Zone Modeling of Diesel Ignition Delay in Pilot-Ignited Partially Premixed Low Temperature Natural Gas Combustion," Paper No. ICEF2010-35127, Proceedings of the ASME

IC Engines Division 2010 Fall Technical Conference (ICEF2010), September 12-15, San Antonio, TX; Presenter – S. K. Jha

2. G. A. Adebiyi, K. K. Srinivasan, C. M. Gibson[1], "Thermodynamic Performance Optimization of Reciprocating Internal Combustion (IC) Engines," Proceedings of the IMECE 2008, Paper No. IMECE 2008-66026, 2008 ASME International Mechanical Engineering Congress and Exposition November 2-6, 2008, Boston, Massachusetts, USA; Presenter – C. M. Gibson

*Posters:*

1. S.K. Jha, K.K. Srinivasan, S. R. Krishnan, "Simulation of Autoignition Phenomena of Hydrocarbon Fuels in Engine-Like Conditions" at the recently concluded MSU Biofuels Conference at Jackson, MS August 6-7 2009 (The poster won 2nd place at the MSU Biofuels Conference at Jackson, MS August 6-7 2009)

2. S. K. Jha, K. K. Srinivasan, S. R. Krishnan, R. Luck, "Simulation of Autoignition Phenomena of Hydrocarbon Fuels in Engine-Like Conditions," poster presented at the 2nd Energy Workshop, April 15, 2009, Mississippi State University

3. M. M. Tripathi, S. R. Krishnan, K. K. Srinivasan, F-, Y. Yueh, J. P. Singh, "Study of Emissions Spectra of Syngas-Methane-Air Premixed Flames for Simultaneous Measurement of Flame Temperature and Equivalence Ratio," poster presented at the 2nd Energy Workshop, April 15, 2009, Mississippi State University

## Task 5.2. Performance and emissions studies of a stationary IC engine optimized for syngas and other biomass-derived alternative fuels

**Description:** The Recipient shall determine the performance, efficiency, and emissions benefits of a stationary compression ignition engine operating on syngas (CO + $H_2$) and other biomass-derived fuels. Specific emphasis will be placed on quantifying the pollutant emissions (CO, UHC, NOx, and smoke) as well as greenhouse gas emissions ($CO_2$). A high compression ratio engine will be used to investigate potential efficiency improvements and dual fueling strategies will be employed to reduce pollutant emissions. The potential of other biomass-derived fuels (besides syngas) for stationary power generation will be explored.

**Percentage of completion**: 100%

**Accomplishments:**

- Dual fuel experiments with biodiesel-propane and methane and diesel –E85 have been investigated.
- Parametric studies of effect of injection timing, intake pressure and temperature have been performed and these experiments will be continued.
- Investigations reveal that biodiesel ignited combustion of propane and methane yield higher nitrogen oxide emissions and lower engine-out smoke compared to diesel-ignited propane and methane operation.
- Investigations with diesel-ignited E-85 revealed that the combustion characteristics are extremely different from their gaseous counterparts owing to increased evaporation of injected E85 fuel.
- Biodiesel – ignited propane and methane experiments have been performed and in addition, diesel-ignited syn gas experiments were performed on a four cylinder turbocharged engine

  Syn gas obtained from gasification of cellulosic biomass was not a good candidate for an engine fuel since its calorific value was very low (of the order of 5 MJ/m3). Also, because of this low calorific value, the engine could only be operated for about 20 minutes before the fuel was totally consumed.
- Measure emissions including, CO, CO2, O2, NOx, smoke and THC for all of the aforementioned experiments and compare with biodiesel baseline
- Measure combustion pressure data along with engine performance and emissions

**Publications / Presentations:**

*Journal Articles:*

1. N. Shoemaker[1], C.M. Gibson[1], A. Polk[1], K.K. Srinivasan, and S.R. Krishnan, 2011, "Performance and Emissions Characteristics of Bio-Diesel Ignited Methane and Propane Combustion in a Four Cylinder Turbocharged Compression Ignition Engine," Paper No. GTP-11-1347, accepted for publication in *Trans. ASME: Journal of Engineering for Gas Turbines and Power.*

*Conference Papers:*

1. S. R. Krishnan, K. K. Srinivasan, K. C. Midkiff, "Ignition In Pilot-Ignited Natural Gas Low Temperature Combustion: Multi-Zone Modeling and Experimental Results," 2009, Proceedings of the ASME Internal Combustion Engines Division, Spring 2009 meeting, Milwaukee, WI, May 2009; Presenter – S. R. Krishnan

## Task 5.3. Commission an alternative-fueled Stirling engine generator for CHP applications

**Description:** The Recipient shall commission a Stirling engine generator capable of operating on alternative fuels, and install it in the micro-CHP center. This Stirling engine generator will serve as a unique engine platform for simultaneous investigation of CHP performance as well as the potential for selling power back to electric utility companies.

## Task 5.4. Investigate the feasibility of CHP with a Stirling engine generator in the CHP facility at MSU

**Description:** The Recipient shall integrate the Stirling engine generator with the CHP facility and explore strategies to utilize excess electrical power produced by the Stirling engine generator. The Stirling engine generator will be enabled to work on natural gas fueling to study the feasibility of performing CHP experiments with the Stirling engine generator.

Percentage of completion: 100%

*Note: This task were modified and embedded into other tasks as per discussion with Aaron Yocum (former DoE Technical Project Manager)*

## Students Involved in Task 5.0

*Masters Students:*

1. Marvel, B. T. (2008). "Uncertainty analysis of net heat release rate predictions in a single cylinder pilot compression ignited natural gas engine."
2. Sham, D. K. (2009). "Analysis of exhaust waste heat recovery techniques from stationary power generation engines using organic rankine cycles."

## Publications - Task 5.0

*Journal Articles:*

1. N. Shoemaker[1], C.M. Gibson[1], A. Polk[1], K.K. Srinivasan, and S.R. Krishnan, 2011, "Performance and Emissions Characteristics of Bio-Diesel Ignited Methane and Propane Combustion in a Four Cylinder Turbocharged Compression Ignition Engine," Paper No. GTP-11-1347, accepted for publication in *Trans. ASME: Journal of Engineering for Gas Turbines and Power,*

2. K. K. Srinivasan, P. J. Mago, S. R. Krishnan (2010) "Analysis of Exhaust Waste Heat Recovery from a Dual Fuel Low Temperature Combustion Engine using an Organic Rankine Cycle," Energy, Vol. 35, pp. 2387-2399, doi:10.1016/j.energy.2010.02.018

3. H. Cho[1], S. R. Krishnan, R. Luck, and K. K. Srinivasan (2009) "Comprehensive uncertainty analysis of a Wiebe function-based combustion model for pilot-ignited natural gas engines," Proceedings of the Institution of Mechanical Engineers, Part D: Journal of Automobile Engineering, 223, Number 11 / 2009, pp. 1481-1498, DOI: 10.1243/09544070JAUTO1103

4. K. K. Srinivasan, P. J. Mago, G. J. Zdaniuk, L. M. Chamra, K. C. Midkiff (2008) "Improving the Efficiency of the Advanced Injection Low Pilot Ignited Natural Gas Engine Using Organic Rankine Cycles," Journal of Energy Resources Technology, Trans. ASME, Vol.130, pp. 022201-1 – 022201-7, DOI 10.1115/1.2906123

*Conference Papers:*

1. S.K. Jha[1], S.R. Krishnan, K.K. Srinivasan, 2010, "Quasi-Two-Zone Modeling of Diesel Ignition Delay in Pilot-Ignited Partially Premixed Low Temperature Natural Gas Combustion," Paper No. ICEF2010-35127, Proceedings of the ASME IC Engines Division 2010 Fall Technical Conference (ICEF2010), September 12-15, San Antonio, TX; Presenter – S. K. Jha.

2. S. R. Krishnan, K. K. Srinivasan, K. C. Midkiff, "Ignition In Pilot-Ignited Natural Gas Low Temperature Combustion: Multi-Zone Modeling and Experimental Results," 2009, Proceedings of the ASME Internal Combustion Engines Division, Spring 2009 meeting, Milwaukee, WI, May 2009; Presenter – S. R. Krishnan

3. G. A. Adebiyi, K. K. Srinivasan, C. M. Gibson[1], "Thermodynamic Performance Optimization of Reciprocating Internal Combustion (IC) Engines," Proceedings of the IMECE 2008, Paper No. IMECE 2008-66026, 2008 ASME International Mechanical Engineering Congress and Exposition November 2-6, 2008, Boston, Massachusetts, USA; Presenter – C. M. Gibson

*Posters:*

1. S.K. Jha, K.K. Srinivasan, S. R. Krishnan, "Simulation of Autoignition Phenomena of Hydrocarbon Fuels in Engine-Like Conditions" at the recently concluded MSU Biofuels Conference at Jackson, MS August 6-7 2009 (The poster won 2nd place at the MSU Biofuels Conference at Jackson, MS August 6-7 2009)

2. S. K. Jha, K. K. Srinivasan, S. R. Krishnan, R. Luck, "Simulation of Autoignition Phenomena of Hydrocarbon Fuels in Engine-Like Conditions," poster presented at the 2nd Energy Workshop, April 15, 2009, Mississippi State University

3. M. M. Tripathi, S. R. Krishnan, K. K. Srinivasan, F-, Y. Yueh, J. P. Singh, "Study of Emissions Spectra of Syngas-Methane-Air Premixed Flames for Simultaneous Measurement of Flame Temperature and Equivalence Ratio," poster presented at the 2nd Energy Workshop, April 15, 2009, Mississippi State University

# Summary of Project Activities

## Task 6. Distributed Generation and Grid Interconnection

## Task 6.1. Development of CHP system to utility grid interconnection

**Description:** The Recipient shall develop micro-CHP to utility grid interconnection archetypes. CHP to utility interconnection converter topologies and controls will be investigated, and appropriate systems will be identified that meet the requirements of micro-CHP systems. This will require an additional level of complexity as compared to renewable sources that directly feed the utility grid, since in addition to maximum energy extraction from the renewable sources the percentage that is supplied to the utility versus that used by the CHP leads must be determined, and controls for efficient switching between stand-alone and grid connected mode are to be determined.

**Percentage of completion**: 100%

**Accomplishments:**

Penetration of distributed generation (DG) has significantly increased over the last few decades. Several states in USA have set their own target to meet significant percentage of DG penetration over the years. These requirements will have impacts on grid reliability and operational requirements given inherent intermittency for some of the DG. Energy storage integrated with DG has been proposed as a solution by several researchers to provide greater levels of flexibility and reliability. Energy storage will have impact on electric grid in several other ways including stability. This work addresses the impact of DG with storage on transient stability of the electric grid system. DG based on wind energy and biomass has been modeled based on synchronous and induction generators. Wind based DG has been modeled as both the fixed and variable speed wind energy farms. Battery and ultra-capacitor have been modeled as storage with suitable power electronics interface. MATLAB/ Simulink and PSS/E have been used as a tool for this study. Transient stability of the test systems has been assessed for different types and locations of faults as well as for different penetration levels of the DGs, with and without the energy storage devices. Transient stability have been analyzed in terms of generator rotor speed deviation, rotor angle and terminal voltage of the DGs. Results indicate that the presence of DGs and storage devices enhances the transient stability of the system in most of the cases. This work also identifies the lack of dynamic model for storage in most of the commercial available tools.

The integration of distributed generations (DGs) to power system will increase percentage of electricity produced from renewable energy sources (RES) to increase sustainability of electricity and ideally will also provide reliable, secure, flexible, affordable, and sustainable electricity. Renewable energy is naturally intermittent and has several other challenges. For instances, there are possibilities of fully cloudy or non-breezing day which relates to no energy produced from photovoltaic (PV) arrays or wind turbines. In addition, higher penetration of renewable energy sources to a local power system may cause a stability problem.

In order to utilize renewable energy optimally without having problems related to variability and intermittency of energy and also instability of electric grid system, a well designed storage system must be integrated with big penetration of RES.

Owing to the facts that different RES have different characteristics and the likeliness of hybrid energy sources in future power systems, the design of versatile energy storage systems having capability to operate in wide ranges of power and energy density is required. Since no single energy-storage technology has this capability, system will incorporate combinations of viable storage technologies such as super capacitors, batteries, superconducting magnetic energy storage (SMES), and flywheels. These energy storages provide valuable added benefits to improve stability, power quality, and reliability of supply.

Modeling and simulation of power system with integration of different type of DG and storage is required for scenarios analysis and discussion to characterize the impact of higher penetration of DG and storage. This project addresses the impact of DG with storage on transient stability of power system. This work examines the impact of increasing levels of wind and biomass power generation with energy storage on the grid. Specifically, impacts to the transient stability of the electric grid due to disturbances will be examined. Modeling and simulation of energy storage indicate lack of dynamic model in most of the commercial available tools.

***DG Modeling***

Models of the wind and biomass generation system have been developed in MATLAB Simulink and PSS/E.

The PSS/E CIMTR1 model is used to represent the fixed speed squirrel cage induction generator (SCIG) wind power generator. According to PSS/E's literature, the wind generator in the power flow case has a positive electrical power output. Also, since there are no sub-transient time constants associated with a single cage machine, T" is set equal to zero and ZSORCE (generator dynamic impedance) is set equal to X' in the power flow. The general model for a SCIG is shown in Figure 6.1.1.

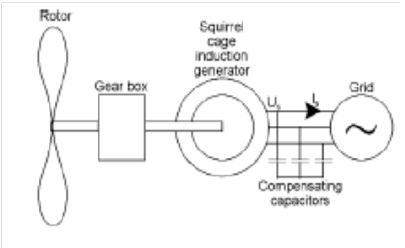


Figure 6.1.1: SCIG Model

The PSS/E WT3 model is used to represent the variable speed doubly fed induction generator (DFIG) wind power generator. This is a generic user model developed by PTI for use in variable speed wind turbine simulations. The general model for a DFIG is shown in Figure 6.1.2.

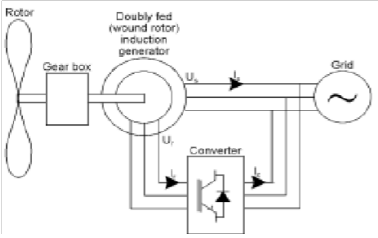


Figure 6.1.2: DFIG Model

The biomass DG's are represented by synchronous generators and induction generator available in Simulink library.

***Storage Modeling***

Ideally, energy storages must be able to rapidly damp oscillations, respond to sudden load, continue load supply during transmission or distribution interruptions, correct load voltage profiles with rapid reactive power control, and allow generators-loads balancing at normal generator speed.

Two fundamental parameters for energy storage devices are energy density and power density. The energy density defines the amount of energy that can be stored in the device, while the power density defines the rate at which energy can be transferred into or out of the storage device, which depends mainly on the peak power rating of the power conversion unit and is also affected by the response rate of the storage device itself. The ideal storage device should have both high energy and power densities.

There are many studies on energy storage modeling. However, the current available model is not completely accurate, especially to simulate dynamic characteristics of energy storage devices due to dynamic operations of power systems. Among all available energy storage technologies, battery is the most widely used and has the most advanced model. An accurate battery model must include all parameters that affect the battery characteristics. These parameters are specifically state of charge (SOC), rate of charge/discharge, storage capacity, temperature, and age. The available battery models include electrochemical models, equivalent-circuit models, electrical-circuit models, temperature model, stochastic models, and analytical models. Moreover, commercial softwares provide very basic built-in energy storage models that cannot simulate the dynamic characteristics completely.

Battery and ultracapacitor retaining required characteristic have been developed in Simulink and PSS/E have been used for the study. The battery energy storage model that is used for this

project is the CBEST (EPRI Battery Energy Storage). This model has the ability to simulate the dynamic characteristics of a battery and can be used to improve first-swing transient stability, provide damping, and/or limit frequency excursions. The Block Diagrams for this model are shown in Figures 6.1.3.

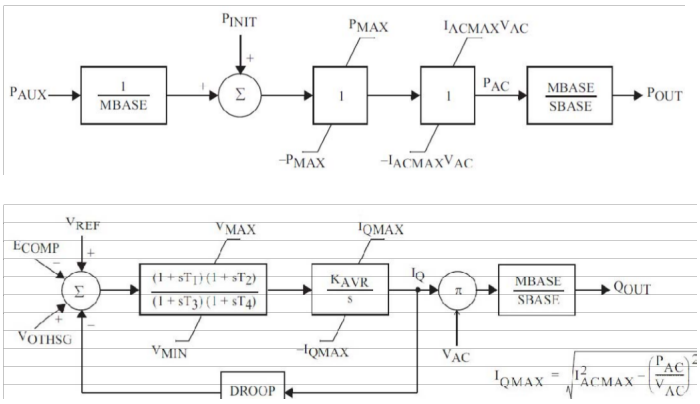


Figure 6.1.3: CBEST Model Block Diagrams

This model was developed by Siemens PTI under EPRI sponsorship. PSS/E models this device in the load flow as a generator with a large ZSOURCE impedance. A voltage source converter is included within the CBEST model for dc to ac conversion.

Since there are no models of energy storage devices in the Simulink library, models of the battery and ultracapacitor have been developed in Simulink. Linear model of the battery is used. The equivalent circuit of the linear battery is as shown in Figure 6.1.4.

Using the first order linear circuit, the model of the ultra capacitor is developed similar to that of the battery in Simulink. The model that has been selected represents only the electrical properties of the cell and neglects most of the chemical properties. Figure 6.1.5 shows the equivalent circuit of the ultra capacitor.

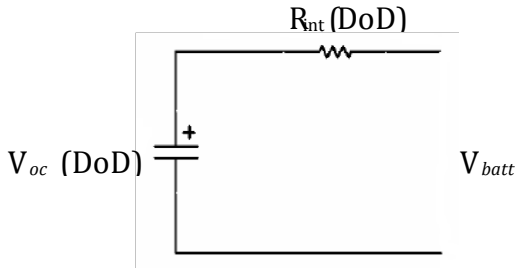


Figure 6.1.4. Equivalent circuit model of a battery

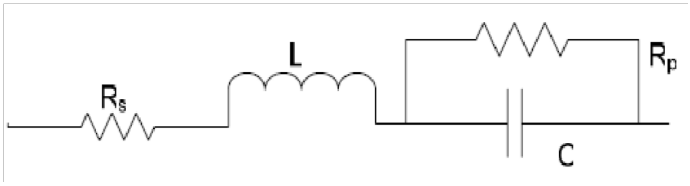

Figure 6.1.5. Equivalent circuit of the ultra capacitor

**Results:**

This research work focuses on analyzing the transient stability of a system with both energy storage devices and distributed generators. The transient stability of the test system was analyzed with biomass, wind, battery and ultra capacitors. The responses of the transient stability indicators to different simulation scenarios were observed. The different scenarios include different types and locations of faults and different penetration levels of the distributed generators. The result analysis suggests that energy storage devices in the system along with distributed generators can improve the transient stability of the system. The impact on transient stability is system specific and depends on the location and type of disturbances.

***Impact of Wind and Battery on Stability***

The power system used is an IEEE test system developed for power system transient stability study testing purposes. The system contains seventeen (17) generators and one hundred sixty-two (162) buses with voltages from 69 to 345 kV. The software used was PSS/E version 30.3., the most commonly used power flow tool in the electric power transmission planning industry. It is also used for dynamic simulation.

The test plan involved replacing existing synchronous generators with SCIG and DFIG generators while adding battery energy storage.

It was seen that when the fixed speed turbine (SCIG) is introduced, there are certain fault conditions that produce instability. There are also instances where the system becomes unstable as penetration of fixed speed turbine generation is increased. All of these instances of instability have a characteristic of a superimposed high frequency oscillation that occurs a number of seconds after application of the fault.

When the variable speed turbines (DFIG) were introduced into the system, all instances of transient disturbance produced a stable response. Additional tests were then performed to attempt more instability, without success, by removing generation, as well as entire buses from the system. The conclusion is made that the test system is very strong network that requires a very severe disturbance to produce instability for the DFIG.

It was decided that the investigation should conclude with a study of the impact of the loss of generation and the loss of a bus with generation and transmission lines with integration of

storage. A generator was replaced with a SCIG and then with a DFIG. The addition of battery energy storage was then applied to determine the effects.

The research shows that the addition of the battery provides voltage support when added to synchronous generators as well as SCIG generators; however, very little support is provided for the DFIG. The minimal DFIG support is due to its intrinsic ability to control voltage and power output, meaning little support is required.

Figure 6.1.6 shows a typical voltage response for a synchronous generator and a SCIG wind turbine with battery energy installed at the generator bus.

Figure 6.1.6 shows that the voltage response continues to fall throughout the duration of the fault and regains its pre-fault value a number of seconds later. In contrast, the inclusion of the battery provides support at the instant of fault initiation and gains its pre-fault value immediately after clearing. Table 6.1.1 summarizes the voltage response for the Synchronous and SCIG generators for all fault types along with the improvements due to the addition of the battery energy storage.

It was seen that the technical benefits of adding storage are a function of system strength, wind farm location, fault type, and fault location. Care should be exercised in determining the wind farms that require battery storage since not all wind farms require it. Therefore much study is required to determine the best location. Therefore, energy storage installation costs will be considered sunk cost if it is not required where it is installed. It is also concluded that should the system topology change, a re-evaluation of the battery's impact will be required. Costs verses benefit must be also be weighed for any given location.

***Impact of Biomass And Storage on Stability***

With biomass generation modeling and storage modeling for 8bus test case, in all the test cases, it was observed that the stability of the system changes with the addition of the energy storage devices. In this study, we have considered two different types of energy storage devices namely battery and ultracapacitor as mentioned in section III. Figure 6.1.7 shows the comparison of the maximum deviation in rotor speed due to a three phase fault at bus 4, without any storage device, with a battery and with an ultracapacitor.

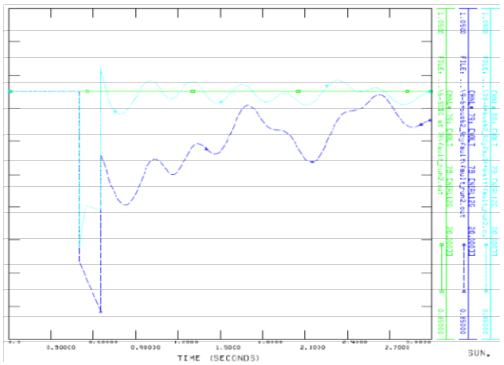


Figure 6.1.6: Voltage Response with Battery

Table 6.1.1: Voltage response improvements with battery

| Fault Type | Configuration | | PreFault Voltage (p.u.) | Volt- age at Fault Iniation (p.u.) | Voltage at Fault Concl -usion (p.u.) | Voltage at Fault Clear- ing (p.u.) |
|---|---|---|---|---|---|---|
| Fault and no topology change | 1 | Synch Gen | 1.0 | .904 | .901 | .988 |
| | 2 | Synch Gen with Battery | 1.0 | .904 | .938 | 1.015 |
| | 3 | SCIG | 1.0 | .897 | .866 | .958 |
| | 4 | SCIG with Battery | 1.0 | .905 | .928 | 1.014 |
| Fault and Loss of Gen | 5 | Synch Gen | 1.0 | .906 | .901 | .987 |
| | 6 | Synch Gen with Battery | 1.0 | .906 | .927 | 1.013 |
| | 7 | SCIG | 1.0 | .895 | .867 | .961 |
| | 8 | SCIG with Battery | 1.0 | .906 | .928 | 1.013 |
| Fault and Loss of Bus | 9 | Synch Gen | 1.0 | .906 | .902 | .984 |
| | 10 | Synch Gen with Battery | 1.0 | .906 | .928 | 1.01 |
| | 11 | SCIG | 1.0 | .896 | .869 | .958 |
| | 12 | SCIG with Battery | 1.0 | .906 | .927 | 1.01 |

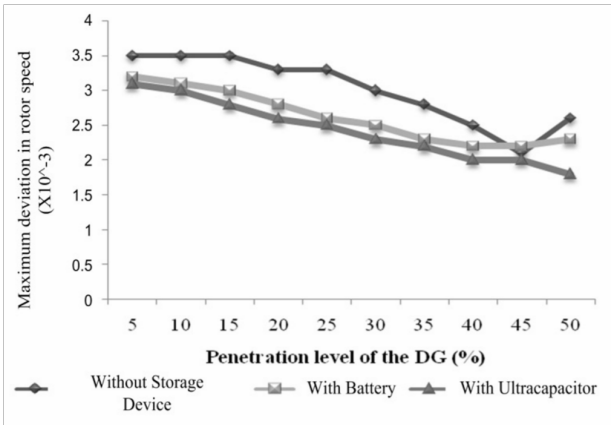


Figure 6.1.7. Comparison of impacts of storage devices on rotor speed deviation

It can be clearly seen that with the addition of an energy storage device, the maximum deviation in rotor speed deviation decreases which implies that the transient stability improves. For the two energy storage devices, adding an ultra capacitor to the system seemed to improve the stability more than the addition of a battery. But on the contrary, Figure 6.1.8 shows that addition of the battery has better stability than the addition of the ultra capacitor in terms of oscillation duration. Stability of the system is a very nonlinear phenomenon and depends on available energy, rate of energy and inertia of the component. Due to these characteristics, a battery and ultra capacitor may have different impacts on the system stability parameters. In general the analysis showed that the addition of a storage device to the system increases its transient stability.

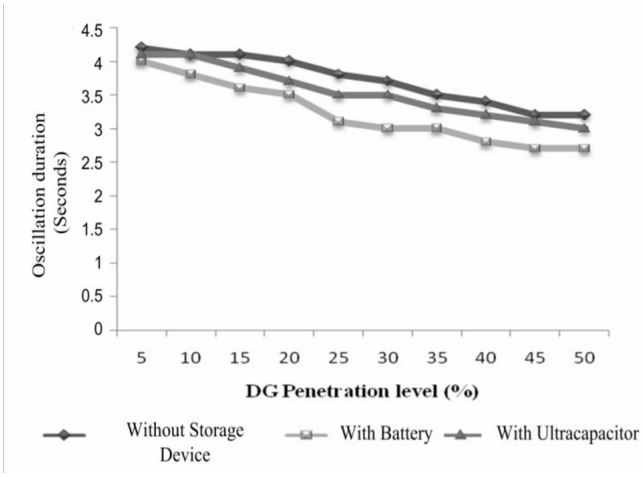


Figure 6.1.8. Comparison of impacts of storage devices on oscillation duration

It was also seen that in a majority of the cases the stability of the system increases as the penetration level of the DG increases, but after a certain percentage it starts decreasing. This level is considered as the ideal penetration level of the DG and it depends upon the size and type of system and various other factors. DG power help in stability by providing needed energy

to keep up with required energy for disturbances. But if the power provided by DG is more than some threshold then it may cause problems. From the analysis, based on Figure 6.1.7 and 6.1.8 and additional analysis, 45% – 50% was observed to be the ideal penetration level of the DG for the 8bus test system.

**Publications / Presentations:**

*Conference Papers:*

1. Shravana Musunuri, Herbert L. Ginn, "Comprehensive Review of Wind Energy Maximum Power Extraction Algorithms", Power Electronics Drives and Systems, Taiwan, November 2009.

2. Shravana Musunuri, Herbert L. Ginn, "Comprehensive Review of Wind Energy Maximum Power Extraction Algorithms", Energy Conversion and Congress Exposition, Atlanta, GA, Sep 2010.

3. Shravana Musunuri, Herbert L. Ginn, " A modified maximum power extraction algorithm for Wind energy systems", IEEE Workshop on Control and Modeling for Power Electronic, Boulder, CO, June 2010.

*Posters:*

1. Shravana Musunuri, Herbert L. Ginn, "Power electronic Interface of Multiple Energy Sources to Utility Grid", Poster Presentation, Electric Ship Technology Symposium, Starkville, May 2009.

## Task 6.2. Modeling and analysis of reconfigurable Micro-grid controller with uncertainty

**Description:** The Recipient shall model, simulate and analyze reconfigurable micro-grid controller with uncertainty using multi-agent approach. A model will be developed incorporating uncertainty analysis to provide for flexible, controllable and efficient power management for the CHP micro-grid.

**Percentage of completion**: 100%

**Accomplishments:**

With the advancements in the variable speed direct drive design and control of wind energy systems, the efficiency and energy capture of these systems is also increasing. As such, many maximum power point tracking (MPPT) methods have been developed and implemented. These MPPT algorithms can be broadly categorized into three types: Tip-Speed control, PowerSignal feedback, and Hill climb search based. However, it is required to develop advanced controls that require minimum sensors and independent of turbine characteristics to extract maximum power from them. As such many hill climb search based algorithms have been proposed over the years but they are suitable for systems whose inertia is negligible. This project proposes a modified algorithm that takes into account the system inertia and extracts maximum power faster than the earlier methods while requiring no knowledge of the system parameters. The project presents the proposed maximum power point tracking algorithm along with simulation results.

In recent years wind power has become a rapidly growing technology for renewable power generation owing to its environmental, social and economic benefits. The advancements in the machine drive technologies and grid interconnection controls have increased the feasibility of more wind power penetration into the system. Studies have shown that the installed wind power generation capacity in the world has been increasing at more than 30% per year over the past decade and it could supply 12% of world's electrical demand by 2020. The installed wind capacity in United States grew about 19 GW from 2003 to 2008. Although the wind energy systems have lower installation and maintenance costs when compared to other renewable energy technologies, the overall system cost and hence the cost/ kW ratio can be further reduced by using high-efficiency power converters. Further, compared to constant speed operation, variable speed wind turbines provide 10–15% higher energy output, and have lower mechanical stress and less power fluctuation. Traditionally, a gearbox is used to couple a low speed wind turbine rotor with a high-speed generator. The cost, weight and maintenance needs of a gear box place a serious limitation on its usage. Hence recently, much effort has been placed on the use of a low speed direct-drive variable speed generator to eliminate the gearbox. However, in order to fully obtain the benefits of variable speed wind generation systems without gearboxes, it is important to develop advanced control methods to extract maximum power output from wind turbines. As such, many maximum power point tracking (MPPT) algorithms have been developed over the years. The developed methods vary in technique used, complexity,

sensors required, convergence speed, memory requirement, range of effectiveness etc. Of these various methods, the hill climb search based maximum power algorithm has been the most proposed algorithm. While the algorithms based on this method work well for systems without inertia, for complex electromechanical systems like wind energy systems which have a significant amount of inertia, the algorithm does not work well. As such a modification of the algorithm that takes into account the inertia of the system is required for truly driving the wind system to operate at maximum power point. This project proposes a modified algorithm that takes into account the system inertia and extracts maximum power faster than the earlier methods while requiring no knowledge of the system parameters. The proposed algorithms along with simulation results are presented.

***Issues with Maximum Power Tracking***

The mechanical output power of a wind turbine at a given wind speed depends on the turbine's tip speed ratio (TSR), which is defined as the ratio of turbine rotor tip speed to the wind speed. The maximum turbine energy conversion efficiency occurs at a particular TSR for a particular wind speed and blade pitch angle. Hence, as wind speed changes, the turbine's rotor speed needs to be changed accordingly in order to extract maximum power. Equation (6.2.1) gives the relation between power extracted from the wind turbine and the turbine variables.

$$P_{turbine}=\frac{1}{2}\rho A v^3 C_p \tag{6.2.1}$$

where: $\varrho$ is the air density, $A$ is the turbine area of cross section, $v$ is the wind speed, $C_p$ is the power coefficient given by:

$$C_p = C_1 \left(\frac{C_2}{\Lambda} - C_3\ \beta - C_4\ \beta^x - C_5\ \right) e^{\frac{-C_6}{\Lambda}} \tag{6.2.2}$$

where: $C_1$ – $C_6$, x are turbine specific coefficients, $\beta$ is the pitch angle in degrees. Finally, the parameter $\Lambda$ is given by:

$$\frac{1}{\Lambda} = \frac{1}{\lambda+0.08\beta} - \frac{0.035}{1+\beta^3} \tag{6.2.3}$$

where: $\lambda$ is the tip speed ratio.

Fig. 6.2.1 shows the turbine power variation for various wind speeds as a function of rotor speed. It can be seen that for each wind speed there exists a particular rotor speed at which the power available is maximum. The problem considered by the various MPPT methods is to determine the optimum rotor speed corresponding to the wind speed at which maximum energy capture could be achieved. As such many maximum power extraction algorithms have been proposed over the years, and they can be broadly categorized into three types: Tip-Speed Ratio method, Power-Signal feedback (PSF), and Hill climb search (HCS) based. TSR method controls the turbine rotor speed so as to maintain an optimal TSR. However, the implementation of this requires the knowledge of the wind turbine characteristics which changes from manufacturer to manufacturer, and the wind speed and turbine speed need to be measured

for TSR calculation. The wind speed measurement adds to system cost and has difficulties in practical implementations.

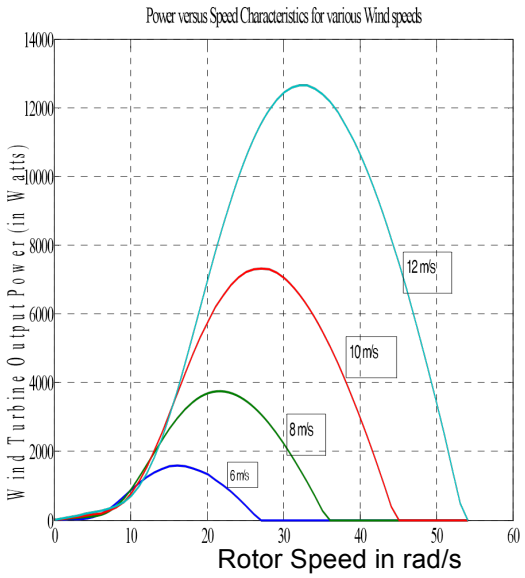

Figure 6.2.1. Wind turbine power-speed characteristics

The PSF method requires the knowledge of the wind turbine's maximum power curve, and tracking of this curve through its control mechanisms. The maximum power curve for this method is typically obtained through simulations or tests for individual wind turbines, which makes PSF control difficult and expensive to implement in practice. To overcome the aforementioned drawbacks, HCS based algorithms have been proposed which have the advantage of not requiring the knowledge of turbine characteristics, or wind speed measurement. As such many algorithms have been proposed over the years as mentioned in the next section.

***Hill Climb Search Algorithm***

The process of the general hill climb search for maximum power extraction is explained using Figure 6.2.2. Assume that a wind turbine generator is initially operating to the left of point A. The generator speed is increased and the corresponding generator output power is calculated. If the output power increases when compared to the earlier step, the search is in the correct direction and the generator speed is increased again. This process is continued until the powers slope becomes zero, signaling that the top of the hill (or the maximum power point) is reached, which in the Figure 6.2.2 corresponds to the point at the right of point A. If however the output power decreases when compared to the earlier step, then the generator speed is decreased and the search is continued in the opposite direction.

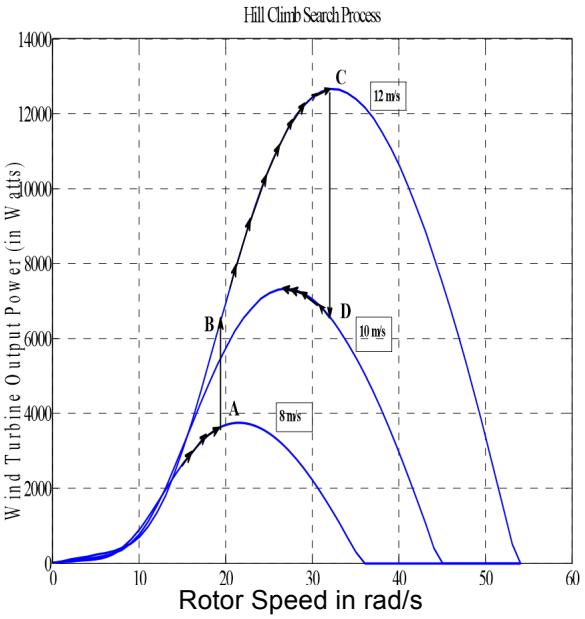

Figure 6.2.2. Hill climb search process

In case of a sudden change in the wind speed, as in the point A, where the wind speed is suddenly increased and the corresponding operating point is now B, the power-speed slope is technically very large resembling a change in wind speed and depending on the slope sign the direction of search is continued. In Figure 6.2.2, the search is continued until point C is reached at which the maximum power point corresponding to the wind speed is attained. Now if there is a decrease in wind speed, and the operating point shifts from point C to D, the power-speed slope is negative and the generator speed is decreased and the slope is observed until it becomes zero. While the algorithm implementation is simple and is independent of turbine characteristics, many issues exist like the selection of step size, inability to effectively track the true maximum power point when the system inertia is considered, oscillations around the maximum power point etc. The inertia of the system causes a time lag in response or inability to track the maximum point. Reducing the perturbation step size can minimize the oscillations around MPP. However, a smaller perturbation size slows down the MPPT process. A solution to this conflicting situation is to have a variable perturbation size that gets smaller towards the MPPT.

It is clear that the traditional hill climb search algorithm is not very efficient for small scale wind systems whose inertia is not negligible and at the same time is not as high as in the case of MW systems. When the system inertia is neglected, the turbine-generator system responds immediately to a change in wind speed or tracking process without any delay. However, when the system inertia is considered, a sudden increase in the wind speed is not reflected in the generator speed as the inertia acts as an interlace. When the wind speed is suddenly increased, the rotational speed cannot change abruptly because of the inertia of the system. Therefore, the generator speed keeps operating at the same point, whereas the aerodynamic torque increases

immediately. As a consequence of this positive torque unbalance, the rotor slowly accelerates reaching a steady state speed after a certain time lag. This causes a time lag in response and the generator speed takes time to reach steady state. This decreases the algorithms' ability to reach the maximum power at a faster rate.

Due to this time lag in response, the traditional hill climb search algorithm could not be used directly for wind energy systems when the inertia of the system is considered. Hence, a modification of the hill climb search algorithm is required for systems like the one under consideration with inertia.

***Proposed Algorithm***

In order to be able to use the hill climb search effectively for systems with inertia, certain modifications have to be made. For the purpose of explanation of the proposed algorithm, a variable speed wind turbine connected to a permanent magnet synchronous generator (PMSG) is considered. The electrical output power from the PMSG is given by:

$$P_g = P_m - J\omega d\omega/dt \tag{6.2.4}$$

where: Pg is the generator output power, Pm is the mechanical power input to generator, Jωdω/dt is the power stored in the inertia of the machine. Now, if the rate of change of generator speed dω/dt in the above equation is kept constant equal to A, the above equation can be rewritten as:

$$P_g = P_m - J\omega A \tag{6.2.5}$$

The rate of change of generator output power is then given by:

$$\frac{dP_g}{dt} = \frac{dP_m}{dt} - JA^2 \tag{6.2.6}$$

Assuming the rate of change of mechanical power $dP_m/d\omega$ is also given by constant B, the above equation can be written as:

$$\frac{dP_g}{dt} = BA - JA^2 \tag{6.2.7}$$

It can be seen from Figure 6.2.3 that for each slope B, there exists a particular rate of generator speed increase dω/dt at which the rate of generator output power increase is maximum. If the rotor speed increase rate dω/dt is more than this optimal value, more energy is stored as a kinetic energy than that extracted from the system. If a lesser value is chosen, more time is taken for the algorithm to reach the maximum power point. It can be seen from the wind turbine Power – Speed characteristics in Figure 6.2.1 that the slope of the curve could be assumed to be varying linearly over a certain range i.e., the curve to the left of the maximum power point can be assumed to be composed of a set of lines, each with a different slope. By determining and fixing the slope value B until it changes to a predetermined value with respect to previous slope, say for example until it becomes 0.75B or so, the optimal rate of change of generator speed increase dω/dt could be determined for that slope B, and be kept constant. Once when the slope B decreases to the predetermined level when compared to the earlier value, the equation (6.2.7) is evaluated once again and the new optimal A i.e., the rate of generator

speed increase is determined. This way, the inertia of the machine is taken into consideration when determining the optimal step length of the hill climb algorithm and hence the maximum power point is reached at a faster rate when compared to the traditional algorithm. When the wind speed changes, since the generator speed cannot change instantaneously due to inertia of the system, the generator torque (and hence the current) changes suddenly. This sudden change in the current is recognized by the algorithm as a change in wind speed, and the prior optimal generator speed increase rate A is used for the next iteration. The equation (6.2.7) is then solved again, and the new optimal A is determined.

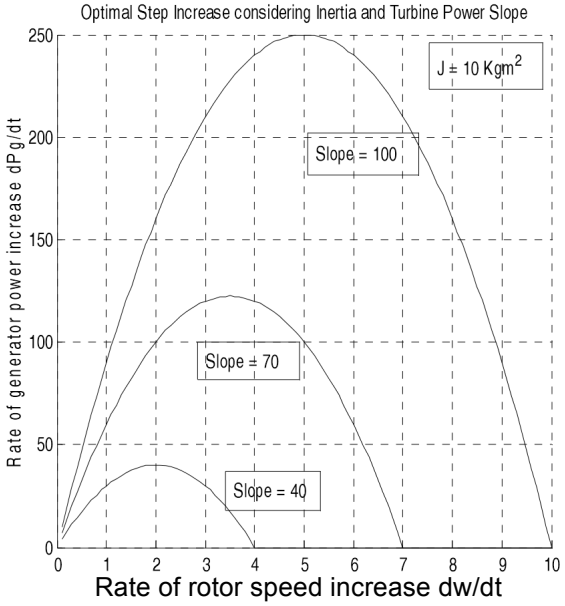

Figure 6.2.3. Rate of change of generator speed

Figure 6.2.4 shows the flow chart representation of the modified hill climb search algorithm. An optimum step length change C is determined based on the wind turbine power – speed slope, and the generator speed is changed in accordance to that. It should be noted that the rectified dc voltage of the generator is controlled rather than the actual generator speed in the above flowchart as is explained further in the next section. When the power-speed slope of the wind turbine is reduced to 70% of the initial value, the new optimum step length change is determined again and the process continues.

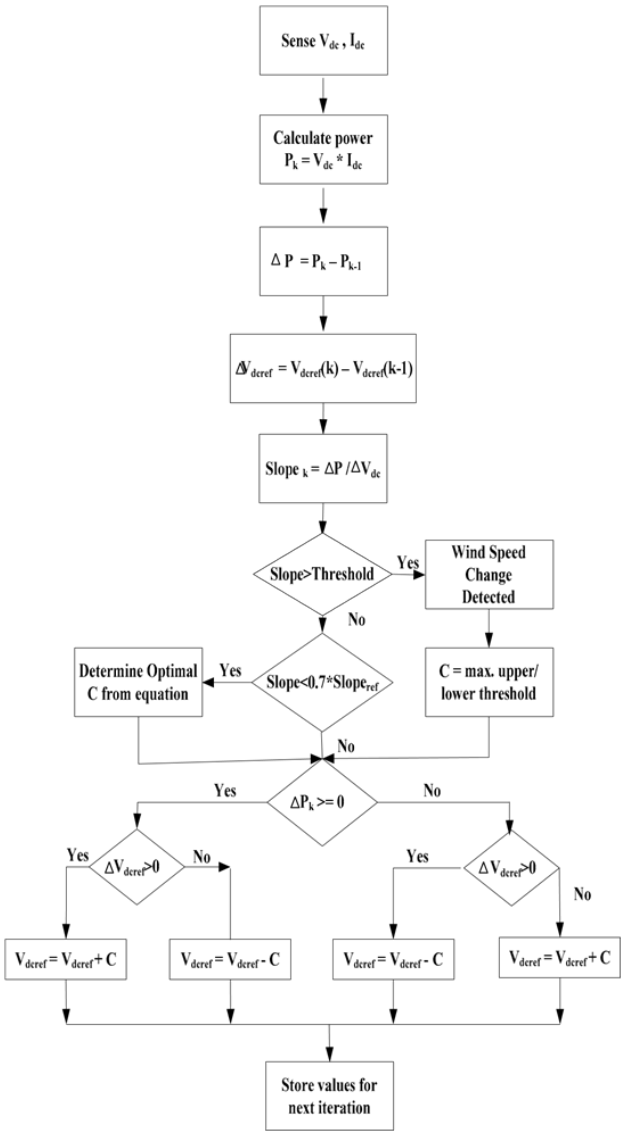

Figure 6.2.4. Flow chart of the proposed methodology

**Results:**

The increasing demand for electricity and clean energy necessitates the advancements in the variable speed direct drive design and control of wind energy systems, and hence the need for extracting maximum power from the wind energy systems. As such, many maximum power point tracking methods have been developed and implemented. While some methods require measuring the wind speed or knowledge of turbine characteristics, hill climb search based algorithms have been proposed which do not have any such constraints. However, the traditional hill climb search algorithms' performance is not efficient when inertia of the system is considered. Hence, a modified hill climb search algorithm that takes into account the system inertia and extracts maximum power faster than the earlier methods while requiring no knowledge of the system parameters is proposed in the work. The results show the comparison of the proposed algorithm with the traditional hill climb algorithm. It could be seen that the

proposed algorithm extracts maximum power at a faster rate when compared to the traditional hill climb search algorithm.

***Wind Energy System***

The system under study consists of a variable speed wind generation system with the wind turbine connected to a permanent magnet synchronous generator. For lower and medium power levels up to a 1 MW range, permanent magnet synchronous generator (PMSG) are being used more and are quickly becoming the next-generation variable speed ac motor drives due to the availability of high-energy permanent magnet materials. The PMSG has widely found its application as a high performance machine drive because of the ripple free torque characteristics and simple control strategies. Compared to induction machine drives, PMSG has less rotor losses hence, it is more efficient. In addition, the PMSM can achieve higher torque densities than its wound rotor counterpart.

The generator speed is controlled by controlling the duty ratio of the DC-DC converter which connected through a diode bridge rectifier to the generator. Since the generator output voltage is analogous to the rotor speed, the voltage at the output terminals of the diode bridge rectifier is controlled for the implementation of hill climb search algorithm, thus resulting in the minimum number of sensors. Figure 6.2.5 shows the wind energy system architecture under study with the turbine and generator parameters given in Table 6.2.1 and 6.2.2 respectively. The maximum power tracker controller commands a voltage reference that is compared to the actual value of Vdc and it is fed into a PI controller. The output of the PI controller is compared to a triangular waveform to determine the boost converter switching. As it was previously stated, wind turbines have an optimal speed that will yield maximum power for each wind speed. Therefore controlling the dc voltage (Vdc) allows the control of the current flow through the generator, which controls the speed of the turbine, to reach maximum power point.

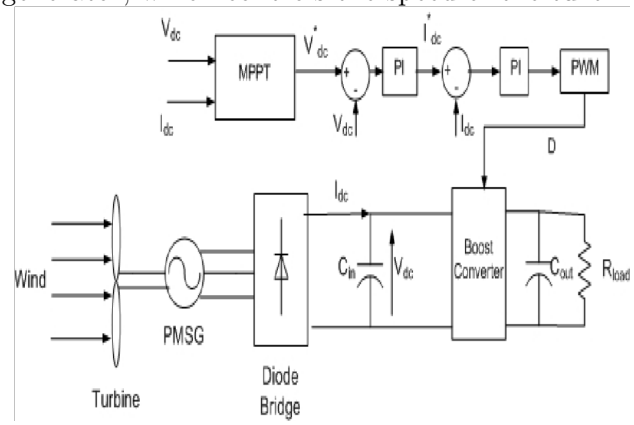


Figure 6.2.5. Wind system for MPPT algorithm test

Table 6.2.1. Wind turbine parameters

| Parameter | Value |
|---|---|
| Nominal power | 12.5 kW |
| Cut-in wind speed | 5 m/s |
| Maximum wind speed | 12 m/s |
| Rotor radius | 2.5 m |
| Pitch angle | 0 deg |

Table 6.2.2. Generator parameters

| Parameter | Value |
|---|---|
| Nominal power | 14 kW |
| Poles | 8 |
| Stator resistance | 0.5 ohms |
| Stator inductances ($L_d$, $L_q$) | 0.5 mH |
| Moment of Inertia | 10 kg.m$^2$ |
| Rated mechanical speed | 314 rad/s |

***Simulation Results***

Figures 6.2.6-6.2.9 show the simulation results of the proposed maximum power extraction algorithm for the system under study. For comparison, the traditional hill climb search algorithm results are also shown. In the Figure 6.2.6, the wind speed is changed at different time instants (time t = 7, 10.5, 13, 16 seconds). It could be seen that the proposed algorithm extracts maximum power at a faster rate when compared to the traditional hill climb search algorithm, which is also evident from the higher performance coefficient for the proposed algorithm when compared to the traditional algorithm. The figure also shows the variable step change of the proposed algorithm when compared to the fixed step size.

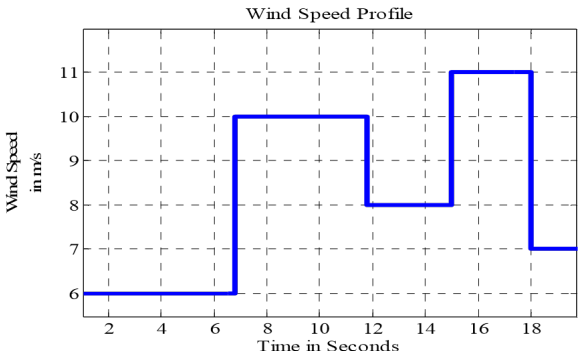


Figure 6.2.6. Wind speed profile

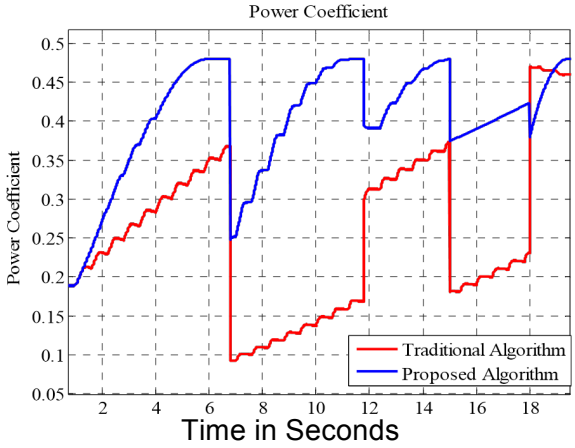


Figure 6.2.7. Power coefficient

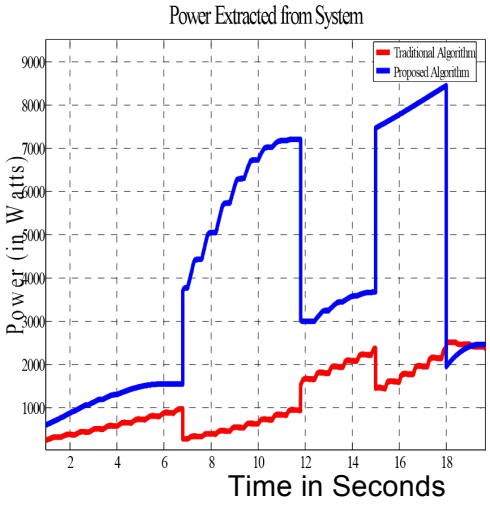


Figure 6.2.8. Electrical power output of wind energy system

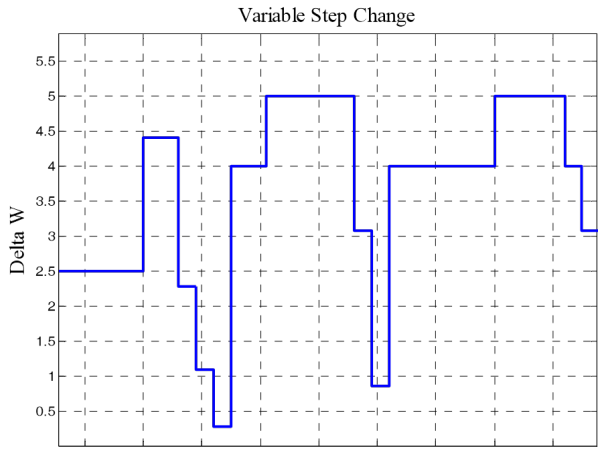


Figure 6.2.9 Variable step change

**Publications / Presentations:**

*Journal Articles:*

1. Ramon Zamora and Anurag K. Srivastava, "Controls for Microgrids with Storage: Review, Challenges, and Research Needs", Journal of Renewable and Sustainable Energy Reviews vol. 14, issue 7, pp. 2009-2018, September 2010.

2. Anurag K Srivastava, Aarthi Asok Kumar and Noel N Schulz, "Impact of Distributed Generations with Energy Storage Devices on the Electric Grid", in press, IEEE Systems Journal.

*Conference Papers:*

1. Anurag Srivastava, Ramon Zamora, Doug Bowman, "Impact of Distributed Generation with Storage on Electric Grid Stability", IEEE PES General Meeting, July 26 - July 29, 2011, Detroit, MI (Invited Panel)

2. R. Zamora, A. K. Srivastava and Syukriyadin, "Microgrids for Reliable, Clean, and Efficient Power Delivery," presented at the 4th Annual International Workshop & Expo on Sumatra Tsunami Disaster & Recovery 2009, Nov. 23-25, Banda Aceh, Indonesia.

3. Aarthi Asok Kumar, Anurag K Srivastava and Noel N. Schulz, "Impact of Biomass Based Distributed generation with Energy Storage on Transient

Stability of Grid", Proceedings of Power System Conference (PSC), March 11-14, 2008, Clemson, SC.

4. Abhilash R Masannagari, Anurag K Srivastava and Noel N. Schulz, "Optimizing Siting and Sizing of DG to maximize Grid Stability", Proceedings of Power System Conference (PSC), March 11-14, 2008, Clemson, SC.

5. Aarthi Asok Kumar, Abhilash R Masannagari, Anurag K Srivastava and Noel N Schulz, "Impact of Biomass Based Distributed generation on Electric Grid", Clean technology and Sustainable Industries Conference and Trade Show, Boston, MA, June 1-5, 2008.

6. Shireesha Methuku, Anurag K Srivastava and Noel N Schulz, "Comprehensive Modeling and Stability Analysis of Biomass Generation", North American Power Symposium, October 2-4, Mississippi State, MS, 2009.

*Posters:*

1. Ramon Zamora, and *Anurag K. Srivastava,* "Modeling and Control of Microgrid", IEEE T&D conference, New Orleans, LA, April, 2010.

2. Shireesha Methuku, *Anurag K. Srivastava* and Noel N Schulz, "Comprehensive Modeling and Technical-Economical Impacts of Biomass Generation", IEEE T&D conference, New Orleans, LA, April, 2010.

## Task 6.3. Co-optimize the Operation and Maintenance of CHP Systems under the Utility Grid Interconnection

**Description:** The Recipient shall develop a co-optimization tool to economically schedule operation and maintenance for all components in CHP systems under the utility grid interconnection. The reliable and efficient operation of complex CHP systems will not solely depend on the high-reliability and high-efficiency design of cooling, heating power components. The fact that CHP systems lack optimal and coordinated operation and maintenance schedules is decreasing the reliability and efficiency of the CHP system operation. The developed tool will be able to consider uncertainties including changes in thermal and power loads, unplanned outages of equipments, and fuel price fluctuations. The research result will provide proper operation and maintenance schedules which ensure that the CHP system can be operated as continuously as possible to improve energy supply reliability and efficiency, and ensure that the CHP system can be repaired on time to reduce equipment down time and maintenance cost.

Percentage of completion: 100%

**Accomplishments:**

- Developed mixed integer programming model for four types of loads: interruptible and deferrable, non-interruptible and deferrable, and non-interruptible and non-deferrable framework
- Developed mixed integer programming model for CHP systems
- Developed multiple-stage stochastic model for optimally operate the energy-efficiency building with CHP systems

**Publications / Presentations:**

*Journal Articles:*

[J1] P. Liu and Y. Fu, "Multiple-stage Stochastic Optimal Operation for the Energy-Efficiency Building with CHP System", IEEE Transactions on Smart Grid, 2012 (under preparation).

*Conference Papers:*

[C1] S. Albatran, Y. Fu and A. Albanna, "A Hybrid 2D-3D Space Vector Modulation Control Algorithm for Three Phase Voltage Source Inverters," 2012 IEEE Symposium on Power Electronics and Machines in Wind Applications (PEMWA 2012), Denver, July 2012 (under review)

**Completion date:** Tasks 6.3 will be done by January 2013

## Task 6.4. Technical and Economic Integration of CHP Systems with Utility Grid

**Description:** The Recipient shall study the impact of CHP systems on power losses, voltage profiles and stability. CHP systems are usually interconnected to the electric utility grid in order to maintain a high-reliability and high-efficiency operation. The CHP system can obtain electricity from the utility when the CHP system fails to supply its electrical load due to component failures, and can feed excessive electricity to the utility for supplying the peak electrical demand on the grid. In order to successfully connect CHP systems with the utility distribution grid, existing technical and economic barriers to this interconnection should be studied and removed. This research results will improve their reliability and quality through the interconnection between CHP systems and the utility grid; therefore, assure a successful utility grid interconnection of CHP systems.

Percentage of completion: 100%

**Accomplishments:**

Combined heat and power (CHP) systems have proven to be beneficial for energy performance of buildings in many industrial situations through increasing the total thermal efficiency, reducing the overall power demand, and providing higher quality as well as more reliable power supply. Applying CHP technology to the utility grid is an attractive option in that it enhances the advantages of conventional power generation and novel distributed technologies by the simultaneous production of electricity and heat. In recent years, CHP has been widely developed around the world. Oak Ridge National Laboratory reported that 20% of generating capacity from CHP by the year 2030 will save 5.3 GW of energy, which is half of all residential energy usage in the United States right now; and also reduce the projected CO2 emission by over 60%. Energy performance of buildings is also crucial to achieve the EU climate & energy objectives, namely the reduction of a 20% of the Greenhouse gases (GHG) emissions and a 20% energy savings by 2020. Being the second-largest GHG emitter in the world, China began to use CHP as thermal sources in urban commercial buildings, like Beijing and Shanghai, while Japan had applied CHP in buildings for over one thousand cases. As a result, CHP is essential to efficiently reduce global energy use in buildings and improve the local environmental sustainability.

Note that certain uncontrollable factors will impose significant influences on the operation of energy-efficiency building systems, which include energy price and energy demand changes. Furthermore, the integration of dispersed generation into building systems introduces more challenges, one of which comes from the volatile characteristic of solar power output. Therefore, the optimal energy supply and consumption for buildings within the specified time horizon is inherently a stochastic decision-making problem.

Due to the integration of renewable energy and imprecise energy consumption, uncertainties are a big concern for the operation of utility grid with CHP system. In order to minimize energy import/export expenses under uncertainty, it's necessary to determine the power production for utility grid from various energy sources including electric grid, battery, CHP with boiler.

The project developed both stochastic and robust models to simulate the energy consumption of CHP system when interconnected with utility grid under the impact of uncertainties. The models incorporated the uncertain characteristics of solar energy as well as electric and thermal demand to predict CHP systems operation and performance.

Firstly, a multistage mixed integer stochastic programming model had been proposed for the optimal operation of utility grid with CHP system considering controllable electric and thermal load. By taking into account the randomness of future uncontrollable electric and thermal load as well as solar power production through multistage scenario tree, the operation of utility grid with CHP system became more robust against changes in uncertainties. With information of uncertainties updated hourly, the rolling scheduling method was introduced to decide operation status and power output of electric grid, charging and discharging power from battery, power output of CHP with boiler. The simulation results can offer a set of robust decision solutions within the scheduling horizon, which could be extended to demand-responsive energy management systems.

Secondly, the robust optimization model had been established based on the deterministic method in the operation problem of utility grid with CHP system. The robustness of the model can be adjusted against the level of conservatism of the solution which can be obtained by solving a mixed integer linear programming.

The utility grid system is shown in Fig. 6.4.1, where various power sources such as electric grid, solar panel, battery, and CHP with boiler systems are considered to supply electric and thermal load for the building. The optimal energy distribution for buildings within the time horizon of one day is inherently a stochastic decision problem since the forecasts on electric and thermal load are not precise in nature. Moreover, the output of solar panel for any future time horizon cannot be accurate. Hence, the daily least-cost production of power grid, battery, and CHP with boiler in utility grid is modeled as a multistage mixed integer stochastic programming model.

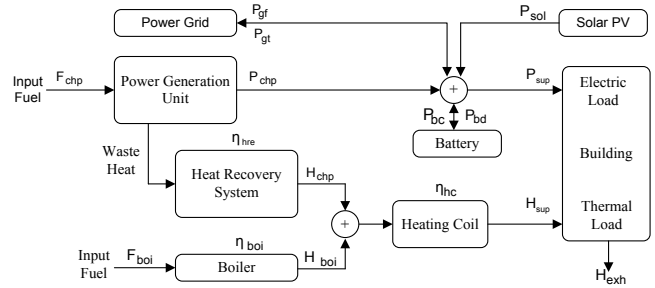

Fig. 6.4.1 Utility grid integrated with various power sources and household load

*Multistage stochastic model*

Parameters at time t, jth scenario:

| | |
|---|---|
| $J_t$ | Number of scenarios |
| $\rho_t^j$ | Scenario probability |
| $c_{gf,t}$ | Electric energy supply price |
| $c_{gt,t}$ | Electric energy price fed into electric grid |
| $c_{gas,t}$ | Natural gas price |
| $\eta_{hre}$ | Thermal recovery efficiency of CHP |
| $\eta_{hc}$ | Thermal coil efficiency |
| $\eta_{boiler}$ | Efficiency of boiler |
| $\eta_{bc}, \eta_{bd}$ | Energy efficiency for charging and discharging |
| $\alpha$ | marginal fuel consumption for electricity production |
| $\beta$ | minimum fuel consumption |
| $T_{ele,ON}, T_{heat,ON}$ | Minimum continuous operating period for controllable electric and thermal load |
| $p_{solar,t}^j$ | Solar power production |
| $M_{gf}$, $M_{gt}$ | Big-M constant for maximum power supplied from or to electric grid |
| $s_{bat}^{max}, s_{bat}^{min}$ | Bounds of state of charge (SOC) for battery |
| $\hat{s}_{bat}$ | Predefined value for initial and final SOC |
| $c_{bat}^{max}, c_{bat}^{min}$ | Limits of battery capacity |
| $p_{bc}^{max}, p_{bc}^{min}$ | Power limits for charging battery |
| $p_{bd}^{max}, p_{bd}^{min}$ | Power limits for discharging battery |
| $p_{chp}^{max}, p_{chp}^{min}$ | Electrical capacity bounds of CHP |
| $E_j^{max}, E_j^{min}$ | Upper and lower controllable energy |
| $H_{boiler}^{max}, H_{boiler}^{min}$ | Thermal capacity limits of boiler |
| $p_{CNTR,t}^j, p_{NC,t}^j$ | Controllable and uncontrollable electric load |
| $H_{CNTR,t}^j, H_{NC,t}^j$ | Controllable and uncontrollable thermal load |
| $H_{load}^{max}, H_{load}^{min}$ | Upper and lower hourly thermal load |

Variables at time t, jth scenario:

| | |
|---|---|
| $p_{gf,t}^j$ | power supplied from grid to household load |
| $p_{gt,t}^j$ | power supplied to electric grid |
| $p_{bc,t}^j, p_{bd,t}^j$ | Battery power for charging and discharging |
| $p_{chp,t}^j$ | Electric power production from CHP |
| $H_{chp,t}^j$ | Thermal power supplied by CHP and boiler |
| $H_{boiler,t}^j$ | Thermal power supplied by boiler |
| $H_{dump,t}^j$ | Wasted heat from CHP |
| $s_{bat,t}^j$ | State of charge (SOC) of battery |
| $F_{chp,t}^j$ | Fuel power consumed by CHP |

$F^j_{boiler,t}$ Fuel power consumed by boiler

$x^j_{gf,t}$ Integer variable for power supplied from the grid

$x^j_{gt,t}$ Integer variable for power supplied to the grid

$x^j_{bc,t}, x^j_{bd,t}$ Charging and discharging status of battery

$x^j_{chp,t}$ Integer variable for CHP

$x^j_{boiler,t}$ Integer variable for boiler

$x^j_{ele,t}$ Integer variable for controllable electric load

$x^j_{heat,t}$ Integer variable for controllable thermal load

### *Objective function*

The optimal scheduling decisions for all power units minimize the expected production costs subject to the operational requirements of the utility grid with CHP system. The general objective function is given by the total daily cost for purchasing energy from electric grid and CHP with boiler or selling energy to the electric grid over the whole time horizon. The cost for CHP is taken as linear to the fuel input.

Min

$$\sum_{t=1}^{T}\sum_{j=1}^{J_t}\rho_t^j[C_{gf,t}\cdot P^j_{gf,t}+C_{gt,t}\cdot P^j_{gt,t}+C_{gas,t}\cdot(F^j_{chp,t}+F^j_{boiler,t})] \tag{6.4.1}$$

$$\sum_{j=1}^{J_t}\rho_t^j=1 \tag{6.4.2}$$

When the actual household loads $(P_{NC}, H_{NC})$ and the solar power generation $(P_{solar})$ are already known at the 1st stage, the power $(P_{gf}, P_{gt}, P_{chp}, P_{bc}, P_{bd})$ and thermal $(F_{chp}, F_{boiler})$ outputs represent "here-and-now" decisions. In contrast, when implementing every one of the subsequent decisions at the following stages, either the household loads or solar power output is unknown. As the future operation status and power outputs of the electric grid, battery, CHP with boiler unit will depend on the household loads and solar power generations, they can only be decided after the uncovering of uncertainties. Therefore, those decisions belong to "wait-and-see" variables.

Further operating constraints are capacity limits for electricity from and to electric grid, charging and discharging capacity of battery, power generation limits of CHP units with boiler.

### *Constraints for electric grid*

The scheduling decisions for power grid are: how much of the electricity fed from or back into the electric grid in each period, and the status of electricity flowing to or from the electric grid. The electric power supplied from or fed into the electric grid is supposed to be unlimited. Therefore, they are set to be a big value.

$$0\le p^j_{gf,t}\le M_{gf}\cdot x^j_{gf,t} \tag{6.4.3}$$

$$0\le p^j_{gt,t}\le M_{gt}\cdot x^j_{gt,t} \tag{6.4.4}$$

$$x^j_{gf,t}+x^j_{gt,t}\le 1 \tag{6.4.5}$$

*Constraints for battery*

The system is supposed to be supplied with certain amounts of energy at certain times. It's clear that there is shortage or surplus due to the uncertain solar PV output or household demand. With the battery storage device, it's more likely to meet the household demand. The decision variables for battery are status of charge and charging/discharging rates.

The dynamics of the charging level of the battery, which is measured in charging and discharging energy, is modeled by (6.4.6), which creates a link between the charge rate of battery in a given time period and its future state. The availability of battery energy depends on the amount of electricity charged and discharged in the battery, which will be influenced by the uncertain household demand. By defining as a Boundary Value Problem, both the initial and the final SOC for battery are specified as the same predefined value, so that the battery can meet the requirement during the next day. Due to the energy loss in the storage device, the energy efficiency for battery is considered in the storage transition constraint.

$$s_{bat,t+1}^{j} = s_{bat,t}^{j} + (\eta_{bc} \cdot p_{bc,t+1}^{j} - p_{bd,t+1}^{j} / \eta_{bd}) \cdot T_d / c_{bat}^{\max} \quad (6.4.6)$$

$$s_{bat}^{\min} = c_{bat}^{\min} / c_{bat}^{\max} \quad (6.4.7)$$

$$s_{bat}^{0} = s_{bat}^{T} = \hat{s}_{bat} \quad (6.4.8)$$

The upper and lower limits for the charging level are imposed to allow the battery to provide enough power to the system when necessary.

$$s_{bat}^{\min} \le s_{bat,t}^{j} \le s_{bat}^{\max} \quad (6.4.9)$$

$$p_{bd}^{\min} \cdot x_{bd,t}^{j} \le p_{bd,t}^{j} \le p_{bd}^{\max} \cdot x_{bd,t}^{j} \quad (6.4.10)$$

$$p_{bc}^{\min} \cdot x_{bc,t}^{j} \le p_{bc,t}^{j} \le p_{bc}^{\max} \cdot x_{bc,t}^{j} \quad (6.4.11)$$

$$0 \le x_{bc,t}^{j}, x_{bd,t}^{j} \le 1 \quad (6.4.12)$$

*Constraints for CHP with boiler unit*

In this project, the conventional power plants and boilers are considered. For the CHP with boiler unit, the control variables are operation status and power output. CHP unit is considered to coordinate the household supply for electric and thermal load, from which the lower and upper bounds for power supply are limited within [5, 55] kW.

$$F_{chp,t}^{j} = \alpha \cdot p_{chp,t}^{j} + \beta \cdot x_{chp,t}^{j} \quad (6.4.13)$$

$$H_{chp,t}^{j} = \eta_{hre}(F_{chp,t}^{j} - p_{chp,t}^{j}) \quad (6.4.14)$$

$$p_{chp}^{\min} \cdot x_{chp,t}^{j} \le p_{chp,t}^{j} \le p_{chp}^{\max} \cdot x_{chp,t}^{j} \quad (6.4.15)$$

Boiler is coordinated with CHP to provide thermal load for the system. Therefore, the upper thermal supply from the boiler is bounded to the maximum hourly thermal load. The parameter α,β is set to 2.67, and 17.4, respectively.

$$H_{boiler,t}^{j} = \eta_{boiler} \cdot F_{boiler,t}^{j}$$

(6.4.16)

$$H_{boiler}^{\max} = H_{load}^{\max} / \eta_{hc}$$

(6.4.17)

$$H_{boiler}^{\min} \cdot x_{boiler,t}^{j} \le H_{boiler,t}^{j} \le H_{boiler}^{\max} \cdot x_{boiler,t}^{j}$$

(6.4.18)

*Constraints of controllable load*

Response characteristics of controllable load will be modeled as interruptible and non-interruptible types. For interruptible electric load, it includes PEV; dishwasher, cloth dryer and washing machine belong to the type of non-interruptible electric load; electrical water heater is either non-interruptible or interruptible thermal load. In addition, operating characteristics of controllable load including energy consumption pattern and preferences will be incorporated into the proposed model. For controllable electric and thermal load, the major constraints include that 1) the load must run for $T_{ON}$ hours for each scenario during the whole time horizon; 2) the total energy consumption requirement.

1) Interruptible load

For interruptible load, the minimum continuous operation period is 1 hour. The constraints for interruptible load are the minimum and maximum power consumption requirements, as shown in (6.4.19) for electric load and in (6.4.20) for thermal load.

$$E_{p}^{\min} \le \sum_{t=1}^{T} p_{CNTR,t} \cdot x_{ele,t}^{j} \le E_{p}^{\max}$$

(6.4.19)

$$E_{H}^{\min} \le \sum_{t=1}^{T} H_{CNTR,t} \cdot x_{Heat,t}^{j} \le E_{H}^{\max}$$

(6.4.20)

2) Non-interruptible load

For non-interruptible electric and thermal load, the minimum continuous operation requirements are formulated as in (6.4.21)-(6.4.22). Because of the non-interruptible nature of the load, the minimum and maximum energy consumptions are therefore the same.

$$\sum_{t=k}^{k+T_{ele,ON}-1} x_{ele,t}^{j} \ge T_{ele,ON} \cdot (x_{ele,k}^{j} - x_{ele,k-1}^{j}), k = 1,\ldots,(T - T_{ele,ON} + 1)$$

(6.4.21)

$$\sum_{t=k}^{k+T_{heat,ON}-1} x_{heat,t}^{j} \ge T_{heat,ON} \cdot (x_{heat,k}^{j} - x_{heat,k-1}^{j}), k = 1,\ldots,(T - T_{heat,ON} + 1)$$

(6.4.22)

*Constraints for energy balance*

1) Power balance

The basic system requirement is to meet electric and thermal load. Electric load is fulfilled by grid power, battery power, solar PV power and CHP power at the same time as shown in (6.4.23).

$$p^j_{gf,t} - p^j_{gt,t} + p^j_{chp,t} + p^j_{bd,t} - p^j_{bc,t} + p^j_{solar} = p^j_{NC,t} + p_{CNTR,t} \cdot x^j_{ele,t}$$

(6.4.23)

2) Thermal balance

Thermal power is fully supplied by CHP and boiler unit, which should satisfy the demand of uncontrollable and controllable thermal load. It's much more economic to provide thermal power from boiler than CHP due to the higher heat conversion efficiency of boiler. Meanwhile, because the energy price for natural gas from CHP is much cheaper than that for electricity from power grid, so CHP would certainly contribute to the electric power supply, hence fulfilling part of thermal load at the same time.

$$\eta_{hc}(H^j_{chp,t} + H^j_{boiler,t}) = H^j_{NC,t} + H_{CNTR,t} \cdot x^j_{heat,t} + H^j_{dump,t} \quad (6.4.24)$$

*Multistage Scenario Tree Generation*

1) Multivariate ARMA time series model

The evolution of electric load is determined by several factors, including the level of people's activities, energy savings in general and the electricity producers' rate policy. The randomness of thermal load is influenced by the weather; the power output of solar panel can be impacted by the radiation of the sun and the ambient weather. Therefore, they're assumed to be independent from each other. The profiles for these three uncertainties are got from historical data. The stochastic processes for the forecast error of these three uncertainties are generated by multivariate ARMA time series model. For the ARMA (n, m) model, it's defined as

$$v^j_t = (p^j_{solar,t}, p^j_{NC,t}, H^j_{NC,t})^T$$

(6.4.25)

$$v^j_0 = 0, z^j_0 = 0$$

(6.4.26)

$$v^j_t = \alpha_1 v^j_{t-1} + \alpha_2 v^j_{t-2} + \ldots + \alpha_n v^j_{t-n}$$
$$+ z^j_t + \beta_1 z^j_{t-1} + \beta_2 z^j_{t-2} + \ldots + \beta_m z^j_{t-m}$$

(6.4.27)

Where $v^j_t$ is the forecast error in any forecast hour; $z^j_t$ is the normal white noise process with standard deviation $\sigma_z$; $\alpha_i$ for i=1,2,...,n is auto-regressive parameter; $\beta_i$ for i=1, 2, ...,m is moving average parameter.

The assumed uncertainty forecasts for each hour can then be calculated as the sum of the measured time series and the forecast error. In this project, $\sigma_z$is 0.2, 0.3, 0.5 for non-controllable

electric and thermal load, solar power output respectively. In the ARMA (1,1) model, both n and m are 1, $\alpha_1 = 0.95, \beta_1 = 0.02$. For each uncertainty, 12 groups of scenarios will be obtained for each uncertainty through the ARMA (1,1) model, the combination of which will be used as the input of the scenario tree generation.

2) Multivariate stochastic scenario tree generation

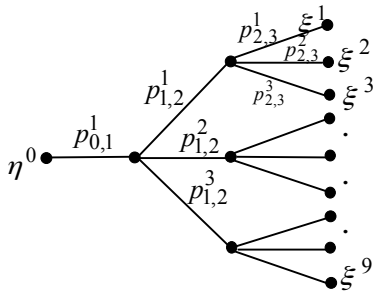


Fig. 6.4.2 Multistage scenario tree with probability

The incorporation of uncertainties with solar power production, uncontrollable electric and thermal load in the optimization model is considered by using a multistage scenario tree, which represents forecasts corresponding to each hour in the optimization period. For a given forecast horizon, the scenarios of forecasts in the scenario tree are represented as a number of outcomes with associated probabilities. At this point, the multiple input scenarios with a probability tree were captured as illustrated in Fig. 6.4.2. The scheduling horizon of one day is hourly discretized into 3 stages, branching at hour 1 and 6. Accordingly, the stochastic data is approximated by a discrete-time stochastic process in the form of a scenario tree. Because the data forecast may be reliable till hour 1, so the process for the first stage is deterministic. The resulting problem to be solved is a mixed-integer linear program by CPLEX.

The scenario $\xi_s^j$ is defined as a sequence of nodes $\eta_t^j$.

$$\xi_s^j = (\eta_0, \eta_1^j, \ldots, \eta_{T_s}^j), j = 1, \ldots, J_s$$

(6.4.28)

Where $\eta^0$ is the root of all scenarios, $J_s$ is the number of scenarios at stage s, $T_s$ is the terminal time at stage s. Therefore, each node $\eta_t^j$ has a vector parameter $v_t^j$ at different stages. $J_s = 1, T_s = 1$ when $s = 1$; $J_s = 3, T_s = 6$ when $s = 2$; $J_s = 9, T_s = 24$ when $s = 3$. Each of these scenarios at stage s has a single ancestor scenario at stage s-1 and 3 descendant scenarios in stage s+1.

The multistage scenario tree generation consists of 2 major procedures. Firstly, during the process of one-stage scenario tree generation, the pure number of scenarios is reduced; while for multistage scenario tree generation, both inner nodes will be deleted and branching will be created within the scenario tree. The process of one-stage scenario tree generation will be briefly described here.

Step 1: Determine the scenario to be deleted.

The scenario reduction for multiple variables can be reached by calculating the distance between different scenarios.

$$d(\xi_s^j, \xi_s^k) = (\sum_{t=0}^{T_s} (\left\| V_t^j - V_t^k \right\|)^2)^{1/2}$$

(6.4.29)

If the probability for scenario $\xi_s^j$ is given by $p_s^j$, $p_{s,s+1}^j$is the transition probability from the ancestor of scenario $\xi_{s+1}^j$ to $\xi_{s+1}^j$.

$$p_s^j = \prod_{m=0}^{T_s-1} p_{m,m+1}^j$$

(6.4.30)

The scenario $\xi_s^{q^*}$ $(q^* = 1, \ldots, J_s)$ to be deleted can then be determined if satisfying

$$p_s^{q^*} \cdot \min_{\substack{q=1,\ldots,J_s, \\ q \neq q^*}} d_s(\xi_s^q, \xi_s^{q^*}) = \min_{j=1,\ldots,J_s} (p_s^j \cdot \min_{\substack{k=1,\ldots,J_s, \\ k \neq j}} d_s(\xi_s^j, \xi_s^k))$$

(6.4.31)

Step 2: Renew the probability of the scenario $\xi_s^{\bar{q}}$ nearest to the deleted one.

$$d_s(\xi_s^{\bar{q}}, \xi_s^{q^*}) = \min_{q=1,\ldots,J_s, q \neq q^*} d_s(\xi_s^q, \xi_s^{q^*})$$

(6.4.32)

$$p_{0,1}^{\bar{q}} = p_{0,1}^{\bar{q}} + p_{0,1}^{q^*}$$

(6.4.33)

Step 3: Change the number of scenarios.

$$J_s := J_s - 1$$

(6.4.34)

For the 2nd procedure, steps for creation of a multi-stage scenario tree include

1) Set s to be the actual stage with the terminal time $T_s$ ;

2) Determine the series of admissible nodes $q^*$ whose inner nodes have to be deleted;

$$\{\prod_{k=0}^{s-1} p_{k,k+1}^{q^*}\} \min_{q=1,\ldots,J_{s-1}, q \neq q^*} d_{s-1}(\xi_{s-1}^q, \xi_{s-1}^{q^*})$$

$$= \min_{j=1,\ldots,J_{s-1}} \{\{\prod_{k=0}^{s-1} p_{k,k+1}^j\} \min_{k=1,\ldots,J_{s-1}, k \neq j} d_{s-1}(\xi_{s-1}^j, \xi_{s-1}^k)\}$$

(6.4.35)

3) Delete the inner nodes from the set of nodes on each stage of the tree;

4) Determine the new predecessors $\bar{q}$ of the last node.

$$d_{s-1}(\xi_{s-1}^{\bar{q}}, \xi_{s-1}^{q^*}) = \min_{q=1,\ldots,J_{s-1}, q \neq q^*} \{d_{s-1}(\xi_{s-1}^q, \xi_{s-1}^{q^*}) : s(\eta_{s-1}^q) < 2\}$$

(6.4.36)

5) The deleted nodes $q^*$ on the stages 1, 2, 3 are then changed to equal the corresponding nodes $\bar{q}$ in the predecessor;

6) Change the probabilities.

$$p_{s-1,s}^{\bar{q}} := p_{0,1}^{\bar{q}} \Big/ (p_{0,1}^{\bar{q}} + p_{0,1}^{q^*})$$

(6.4.37)

$$p^{q^*}_{s-1,s} := p^{q^*}_{0,1} \Big/ (p^{\bar{q}}_{0,1} + p^{q^*}_{0,1})$$

(6.4.38)

7) set s:=s-1 and return to 2) until more inner nodes have to be deleted at the actual stage.

*Rolling scheduling*

From the viewpoint of the stochastic programming model, policies should be made when less information of uncertainties is available under stochastic situation. However, basing the scenarios on forecasts of uncertainties will not give a valuation that is consistent with the true value of those three uncertainties. Scenarios must be adjusted in order to give consistent valuation; they need to be adjusted so that the values of derivatives calculated in the scenario tree are the same as can be observed in the reality for futures. All of the elements together imply that it is more realistic to optimize the operation of the system in the rolling view. In general, new information arrives on a continuous basis and provides updated information about solar power production, uncontrollable electric and thermal load, the operational status of electric grid, battery, CHP with boiler. Thus, an hourly basis for updating information would be most adequate.

In the current version of the model, a three stage model is implemented. The model steps forward in time using rolling scheduling with a 1 hour step. For each time step, new forecasts for solar power production, uncontrollable electric and thermal load that consider the changes in forecast horizons are used. The decision structure is illustrated in Fig. 6.4.3 (a) showing the scenario tree for several scheduling periods. For each scheduling period, a three-stage, stochastic programming problem is solved having a deterministic first stage covering 1 hour, a stochastic second stage with 3 scenarios covering 5 hours, and a stochastic third stage with 9 scenarios covering 18 hours. Fig. 6.4.3 (b) shows the flow chart for rolling scheduling purpose, where the multi-stage stochastic programming will be iterated until the max rolling horizon is met.

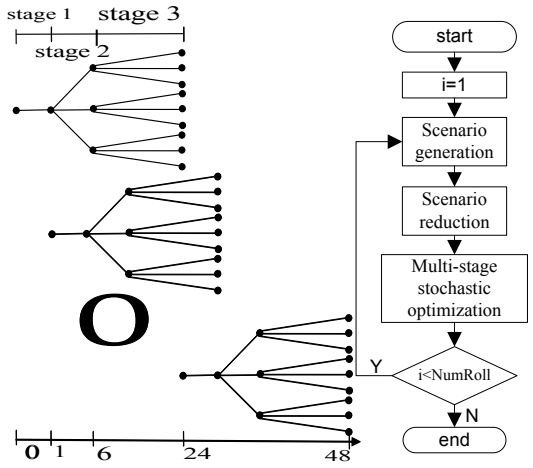


(a) Decision structure (b) Flow chart

Fig. 6.4.3 Diagram of rolling scheduling

*Robust Model*

The optimal scheduling decision for all electric power and thermal units in the utility grid with CHP system minimizes the total operating costs subject to the operational requirements. The objective function (6.4.39) is defined by the total cost for purchasing/selling energy from/into electric grid and running CHP with boiler over the entire time horizon.

$$Min \sum_{t=1}^{T} [c_{gf}^t \cdot p_{gf}^t - c_{gt}^t \cdot p_{gt}^t + c_{gas}^t \cdot (F_{chp}^t + F_{boiler}^t)] \cdot T_d$$

(6.4.39)

where the superscript $t$ is time index; $T_d$ is the time interval (one hour in this project); $c_{gf}^t, c_{gt}^t$ are the energy prices supplied from or fed into the electric grid (\$/kWh); $c_{gas}^t$ is the natural gas price (\$/kWh); $F_{chp}^t, F_{boiler}^t$ are the fuel power consumed by both CHP and boiler (kW); $p_{gf}^t, p_{gt}^t$ are the electric power supplied from or fed into electric grid (kW), respectively.

In the deterministic model, both electric and thermal loads should be balanced by energy sources as follows,

$$p_{gf}^t - p_{gt}^t + p_{chp}^t - p_{bc}^t + p_{bd}^t + p_{solar}^t = p_{load}^t \quad (6.4.40)$$

$$\eta_{hc}(H_{chp}^t + H_{boiler}^t) = H_{load}^t + H_{exh}^t \quad (6.4.41)$$

$$H_{chp}^t = \eta_{hre}(F_{chp}^t - p_{chp}^t) \quad (6.4.42)$$

$$H_{boiler}^t = \eta_{boiler} \cdot F_{boiler}^t \quad (6.4.43)$$

where $p_{bc}^t, p_{bd}^t$ are the battery charging and discharging power; $p_{chp}^t$ is the electric power production from CHP; $p_{solar}^t$ is the solar power production; $p_{load}^t$ is the electric load; $H_{chp}^t$, $H_{boiler}^t$ are the thermal power supplied by CHP and boiler, respectively; $H_{load}^t$ is thermal load;$H_{exh}^t$ represents the excess thermal power from CHP when balancing the electric load; $\eta_{hre}$ is the heat recovery efficiency of CHP; $\eta_{hc}$ is the thermal coil efficiency; $\eta_{boiler}$ is the efficiency of boiler.

Further operating constraints include the grid interface capacity limits for the electric power fed and supplied by the electric load in the system (6.4.44)-(6.4.46).

$$0 \le p_{GF}^t \le p_{GF}^{\max} \cdot x_{GF}^t$$

(6.4.44)

$$0 \le p_{GT}^t \le p_{GT}^{\max} \cdot x_{GT}^t$$

(6.4.45)

$$x_{GF}^t + x_{GT}^t \le 1$$

(6.4.46)

where $p_{gf}^{max}$ , $p_{gt}^{max}$ is the maximum power supplied from or fed to the electric grid; the binary variable $x_{gf}^t = 1$ indicates that the grid power is supplying household electric loads, otherwise, $x_{gf}^t = 0$ ; the binary variable $x_{gt}^t = 1$ indicates that the excess power is fed into the electric grid, otherwise, $x_{gt}^t = 0$.

The system is supposed to be supplied with certain amounts of energy at certain times. It's clear that with the battery storage device, it's more likely to meet the load requirement economically. Charging and discharging capacity limits of battery are formulated in (6.4.47)-(6.4.49), and the state of charge (SOC) of battery, $s_{bat}^{t}$ , is constrained as (6.4.50)-( 6.4.52).

$$p_{bd}^{\min} \cdot x_{bd}^{t} \le p_{bd}^{t} \le p_{bd}^{\max} \cdot x_{bd}^{t}$$

(6.4.47)

$$p_{bc}^{\min} \cdot x_{bc}^{t} \le p_{bc}^{t} \le p_{bc}^{\max} \cdot x_{bc}^{t}$$

(6.4.48)

$$0 \le x_{bd}^{t}, x_{bc}^{t} \le 1$$

(6.4.49)

$$s_{bat}^{t+1} = s_{bat}^{t} + (p_{bc}^{t+1} - p_{bd}^{t+1}) \cdot T_d \big/ c_{bat}^{\max}$$

(6.4.50)

$$s_{bat}^{\min} \le s_{bat}^{t} \le s_{bat}^{\max}$$

(6.4.51)

$$s_{bat}^{\min} = c_{bat}^{\min} \big/ c_{bat}^{\max}$$

(6.4.52)

where $p_{bc}^{max}, p_{bc}^{min}, p_{bd}^{max}, p_{bd}^{min}$ are the charging/discharging power limits of battery; $s_{bat}^{max}, s_{bat}^{min}$ are the upper and lower bounds of SOC of battery; $c_{bat}^{max}, c_{bat}^{min}$ are the capacity limits of battery; $x_{bc}^{t}, x_{bd}^{t}$ indicate charging or discharging status of battery, respectively.

For the CHP with boiler system, the control variables are operating status and power output. Power generation limits of CHP units with boiler are shown in (6.4.53)-(6.4.55).

$$p_{chp}^{\min} \cdot x_{chp}^{t} \le p_{chp}^{t} \le p_{chp}^{\max} \cdot x_{chp}^{t}$$

(6.4.53)

$$H_{boiler}^{\min} \cdot x_{boiler}^{t} \le H_{boiler}^{t} \le H_{boiler}^{\max} \cdot x_{boiler}^{t}$$

(6.4.54)

$$H_{boiler}^{\max} = H_{load}^{\max} \big/ \eta_{hc}$$

(6.4.55)

where $p_{chp}^{max}, p_{chp}^{min}$ are the electric power capacity limits of CHP; $H_{boiler}^{max}, H_{boiler}^{min}$ are the thermal capacity limits of boiler; $x_{chp}^{t}, x_{boiler}^{t}$ are the operating status of CHP and boiler, respectively.

Assume all the decision variables should be made before the reveal of uncertainties, such as solar power generation, electric and thermal loads, which are included in both electric and thermal power balances. Uncertainties $p_{solar}^{t}, p_{load}^{t}, H_{load}^{t}$ are modeled as unsymmetrical and bounded variables $\tilde{p}_{solar}^{t}, \tilde{p}_{load}^{t}, \tilde{H}_{load}^{t}$ ,which respectively take values in $\tilde{p}_{solar}^{t} = p_{solar}^{t} + \Delta p_{solar}^{t}$ ($\hat{p}_{solar}^{lt} \le \Delta p_{solar}^{t} \le \hat{p}_{solar}^{ut}$) , $\tilde{p}_{load}^{t} = p_{load}^{t} + \Delta p_{load}^{t}$($\hat{p}_{load}^{lt} \le \Delta p_{load}^{t} \le \hat{p}_{load}^{ut}$, $\tilde{H}_{load}^{t} = H_{load}^{t} + \Delta H_{load}^{t}$ ($\widehat{H}_{load}^{lt} \le \Delta H_{load}^{t} \le \widehat{H}_{load}^{ut}$). In the robust model, the electric and thermal power balances in the system should be met when the worst case of uncertainties occurs. For the electric load balance, the worst case would occur at the maximum increase in electric load and the maximum decrease in solar power generations. For the thermal load balance, the worst case would occur when the thermal load reaches its possible maximum value.

$$Min \sum_{t=1}^{T} [c_{gf}^t \cdot p_{gf}^t - c_{gt}^t \cdot p_{gt}^t + c_{gas}^t \cdot (F_{chp}^t + F_{boiler}^t)] \cdot T_d$$

(6.4.56)

s.t.

$$p_{gf}^t - p_{gt}^t + p_{chp}^t - p_{bc}^t + p_{bd}^t + p_{solar}^t = p_{load}^t + Max\left\{\hat{p}_{load}^{ut}\eta_p^{ut} + \hat{p}_{load}^{lt}\eta_p^{lt} - \hat{p}_{solar}^{ut}\eta_{solar}^{ut} - \hat{p}_{solar}^{lt}\eta_{solar}^{lt}\right\} \quad (6.4.57)$$

$$\eta_p^{ut} + \eta_p^{lt} + \eta_{solar}^{ut} + \eta_{solar}^{lt} \le \Gamma_1^t$$

(6.4.58)

$$0 \le \eta_p^{ut}, \eta_p^{lt}, \eta_{solar}^{ut}, \eta_{solar}^{lt} \le 1$$

(6.4.59)

$$\eta_{hc}(H_{chp}^t + H_{boiler}^t) = H_{load}^t + H_{exh}^t + Max\left\{\hat{H}_{load}^{ut}\eta_H^{ut} + \hat{H}_{load}^{lt}\eta_H^{lt}\right\} \quad (6.4.60)$$

$$\eta_H^{ut} + \eta_H^{lt} \le \Gamma_2^t$$

(6.4.61)

$$0 \le \eta_H^{ut}, \eta_H^{lt} \le 1$$

(6.4.62)

and constraints (6.4.42)-(6.4.55). where $\eta_p^{ut}, \eta_p^{lt}, \eta_{solar}^{ut}, \eta_{solar}^{lt}$ are the scaled deviations for random electric load and solar power generation; $\Gamma_1^t$ is the robust measurement used to adjust the robustness of the problem against the level of conservation of the solution. Similarly, $\eta_H^{ut}, \eta_H^{lt}$ are the scaled deviations for random thermal loads; $\Gamma_2^t$ is the robust measurement.

In order to make the above problem tractable, the following two sub-problems need be converted into their corresponding dual problems by introducing dual variables $\lambda_1^t, \pi_{11}^{t+}, \pi_{11}^{t-}, \pi_{12}^{t+}, \pi_{12}^{t-}$ for constraints (6.4.64)-(6.4.65), and dual variables $\lambda_2^t, \pi_{21}^{t+}, \pi_{21}^{t-}$ for constraints (6.4.67)-(6.4.68), respectively.

$$Max\ \hat{p}_{load}^{ut}\eta_p^{ut} + \hat{p}_{load}^{lt}\eta_p^{lt} - \hat{p}_{solar}^{ut}\eta_{solar}^{ut} - \hat{p}_{solar}^{lt}\eta_{solar}^{lt}$$

(6.4.63)

s.t. $\eta_p^{ut} + \eta_p^{lt} + \eta_{solar}^{ut} + \eta_{solar}^{lt} \le \Gamma_1^t$

(6.4.64)

$$0 \le \eta_p^{ut}, \eta_p^{lt}, \eta_{solar}^{ut}, \eta_{solar}^{lt} \le 1$$

(6.4.65)

$$Max\ \hat{H}_{load}^{ut}\eta_H^{ut} + \hat{H}_{load}^{lt}\eta_H^{lt}$$

(6.4.66)

s.t. $\eta_H^{ut} + \eta_H^{lt} \le \Gamma_2^t$

(6.4.67)

$$0 \le \eta_H^{ut}, \eta_H^{lt} \le 1$$

(6.4.68)

$$Min\ \lambda_1^t\Gamma_1^t + \pi_{11}^{t+} + \pi_{11}^{t-} + \pi_{12}^{t+} + \pi_{12}^{t-}$$

(6.4.69)

s.t. $\lambda_1^t + \pi_{11}^{t+} \ge \hat{p}_{load}^{ut}, \lambda_1^t + \pi_{11}^{t-} \ge \hat{p}_{load}^{lt}$

(6.4.70)

$$\lambda_1^t + \pi_{12}^{t+} \geq -\hat{p}_{solar}^{ut}, \lambda_1^t + \pi_{12}^{t-} \geq -\hat{p}_{solar}^{lt}$$

(6.4.71)

$$\lambda_1^t, \pi_{11}^{t\pm}, \pi_{12}^{t\pm} \geq 0$$

(6.4.72)

$$Min\ \lambda_2^t \Gamma_2^t + \pi_{21}^{t+} + \pi_{21}^{t-}$$

(6.4.73)

s.t. $\lambda_2^t + \pi_{21}^{t+} \geq \hat{H}_{load}^{ut}, \lambda_2^t + \pi_{21}^{t-} \geq \hat{H}_{load}^{lt}$

(6.4.74)

$$\lambda_2^t\ , \pi_{21}^{t\pm} \geq 0$$

(6.4.75)

Finally, a tractable robust model can be formulated as follows,

$$Min \sum_{t=1}^{T} [c_{gf}^t \cdot p_{gf}^t - c_{gt}^t \cdot p_{gt}^t + c_{gas}^t \cdot (F_{chp}^t + F_{boiler}^t)] \cdot T_d$$

(6.4.76)

s.t. $p_{gf}^t + p_{gt}^t + p_{chp}^t - p_{bc}^t + p_{bd}^t = p_{load}^t - p_{solar}^t + \lambda_1^t \Gamma_1^t + \pi_{11}^{t+} + \pi_{11}^{t-} + \pi_{12}^{t+} + \pi_{12}^{t-}$

(6.4.77)

$$\eta_{hc}(H_{chp}^t + H_{boiler}^t) = H_{load}^t + H_{exhausted}^t + \lambda_2^t \Gamma_2^t + \pi_{21}^{t\pm} \quad (6.4.78)$$

and constraints (6.4.42)-(6.4.55), (6.4.70)-(6.4.72), and (6.4.74)-(6.4.75).

**Results:**

In order to decide the operation status and power output of electric grid, battery, CHP with boiler, the optimal operation problem of utility grid integrated with CHP system will be solved in the way of both multistage stochastic programming and robust optimization with considerations of uncertainties. The main contributions in this project are

(1) By categorizing the load into uncontrollable load, non-interruptible load and interruptible load, the impact of load with different characteristics on the operation of CHP has been investigated.

(2) Rolling scheduling method had been introduced in the stochastic operation of utility grid with CHP system, to utilize the hourly updated information of uncertainties so that the real-time scheduling decisions will be provided.

(3) Conduct stochastic analysis to investigate: a) Impact of CHP on load supply; b) Impact of battery on operation of CHP; c) Impact of controllable load on operation of CHP; d) Comparison of Rolling stochastic analysis and deterministic analysis;

(4) Conduct robust case studies to investigate a) Influence of uncertain electric load and solar power; b) Effect of battery; c) Effect of CHP; d) Influence of budget of robustness on the energy supply.

*Stochastic Case Studies*

First, we obtain the expected data for all of the uncertainties from historic data; Then by applying the multivariate ARMA time series model, 12 scenarios are generated for each of the uncertainties; with the assumption that these three uncertainties are independent from each other, there will be 1728 combinations; Finally, we generate a multistage scenario tree with hourly discretized data within one day by conducting the scenario reduction algorithm, which are used as the input for stochastic analysis.

In the real-time market, the prices to supply electricity from the electric grid vary according to the time period. Table 6.4.1 shows the daily energy supply price from electric grid and nature gas. Thermal recovery efficiency of CHP unit is set to 0.72; efficiencies for both thermal coil and boiler are 0.9; the bound for battery capacity is [5, 50] kW. The limit of battery charging and discharging power output is [8, 15] kW. The initial and final value of SOC is defined as 0.15. Table 6.4.2 shows the controllable load data for case study purpose. The following analysis for stochastic cases is based on the randomly chosen one among 9 scenarios.

Table 6.4.1 Energy Price ($/KWH)

| Energy | Hours 1-8 | Hours 9-14 | Hours 15-18 | Hours 19-22 | Hours 23-24 |
|---|---|---|---|---|---|
| Electricity from Grid | 0.051 | 0.119 | 0.071 | 0.119 | 0.051 |
| Electricity to Grid | 0.067 | 0.067 | 0.067 | 0.067 | 0.067 |
| Natural Gas | 0.031 | 0.031 | 0.031 | 0.031 | 0.031 |

Table 6.4.2 Controllable Load Data

| Controllable Load | | Ini. State | Min. ON Hours | Power Demand per Hour (kW) | Energy Demand Range (kWh) | Total Operating Hours |
|---|---|---|---|---|---|---|
| Electric Load | Interruptible | OFF | 1 | 18 | [50,56] | 3 |
| | Non-interruptible | OFF | 4 | 29 | [116,116] | 4 |
| thermal Load | Interruptible | OFF | 1 | 30 | [80,100] | 3 |
| | Non-interruptible | OFF | 5 | 47 | [235,235] | 5 |

*Impact of CHP on load supply*

As mentioned in the CHP model, it's desirable to involve CHP unit in the system. Therefore, we are going to discuss the operation decision with and without the commitment of CHP. In this case, only uncontrollable load is considered. Compared to the daily cost of $211.1 without the operation of CHP, it would be decreased to $173.8 when CHP is involved in the system.

1) Power supply

Without CHP as shown in Fig.6.4.4 (a), most of the power will be supplied from electric grid. Battery takes the role of storage, it charges when there is extra power from electric grid and solar panel; and discharges when the power is not enough. Solar power has a big contribution during noon time.

For hours 1-4, 6, 21-24 in Fig. 6.4.4 (b), the electric load is totally supplied by CHP, and the extra power will be fed back to the electric grid or charging the battery; For hour 5, CHP and the grid are working together to supply the electric load. During hours 7-18, there is no power fed back to the electric grid, it is supplying power to the load; battery is charging at hours 7, 8, 17, 18, and discharging at hour 10,11,13,14.

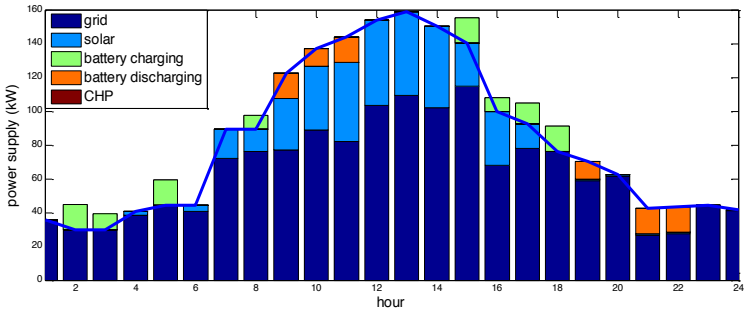


(a) Without CHP

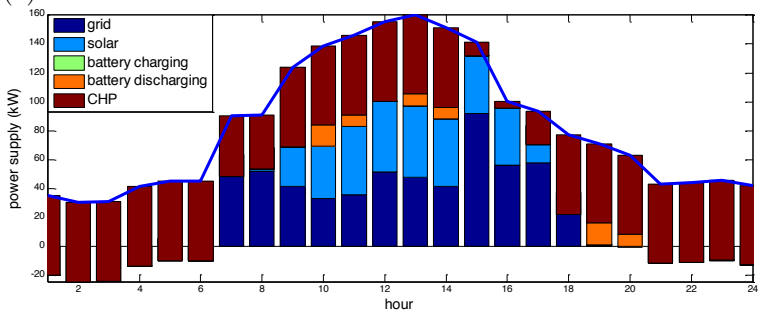


(b) With CHP

Fig. 6.4.4 comparison of power supply

2) Thermal supply

From Fig. 6.4.5 (a), when CHP has no commitment, boiler will take the responsibility for providing the thermal load. However, when CHP is involved in the utility grid system, then most of the thermal load will be supplied by CHP as can be seen in Fig. 6.4.5 (b). When the electricity price from the electric grid is too high during hours 9-14 &19-22, there is constant maximum thermal output from CHP; it only fluctuates during hours 7-8 &15-17. Moreover, during hours 9-13, there will be extra thermal supply from CHP which decreases the daily operation cost by 17.6%.

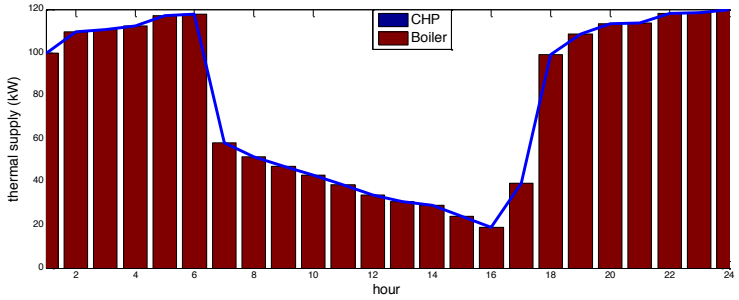


(a)Without CHP

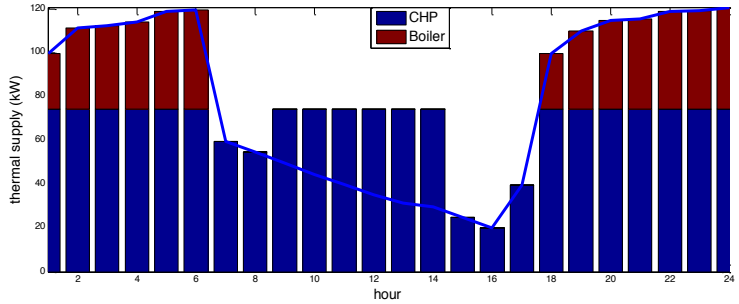


(b) With CHP

Fig. 6.4.5 Comparison of thermal supply

*Impact of battery on operation of CHP*

This case is designed in order to investigate the impact of battery on the operation of CHP, where controllable load is not considered either. Fig. 6.4.6 shows the power supply from various energy sources. From Fig. 6.4.7, it's seen that there is no change on power output from CHP unit because it's decided by the thermal demand. The change in grid power is due to the charging and discharging effect of the battery. The operation of battery can decrease the daily cost from \$176.5 to \$173.8.

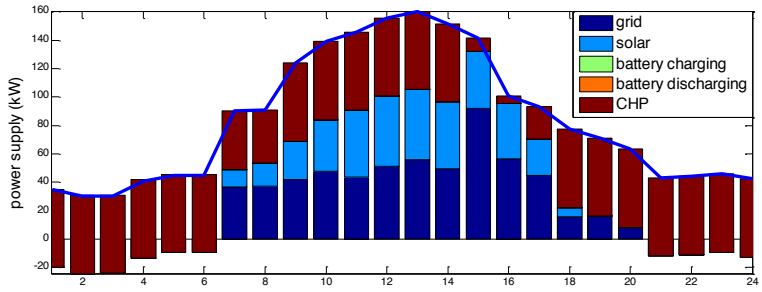


Fig. 6.4.6 Power supply without battery

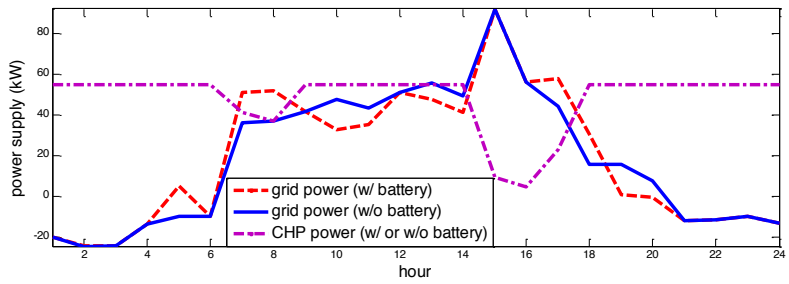


Fig. 6.4.7 Impact of battery on Power supply

*Impact of Controllable load on operation of CHP*

1) Controllable electric load

From Fig. 6.4.8 (a), interruptible electric load is operated at hours 1, 7, 8; non-interruptible electric load is in operation from hour 1-4 due to the low energy price. Fig. 6.4.8 (b) shows the power supply with the consideration of controllable electric load, which increases the daily operation cost from $173.8 to $183.6.

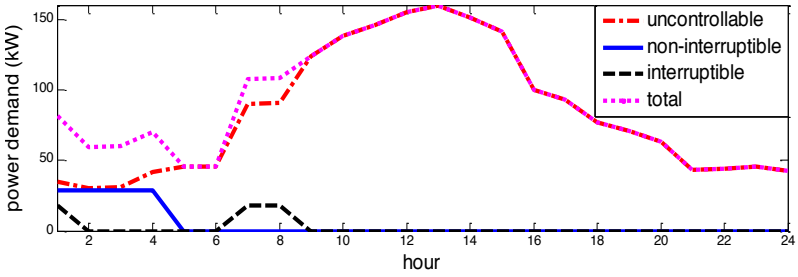


(a)Power demand

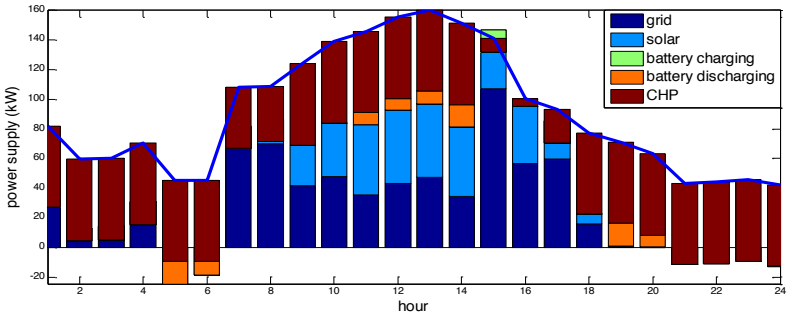


(b) Power supply

Fig. 6.4.8 Impact of Controllable electric load

Fig. 6.4.9 shows the comparison of power supply from the electric grid and battery due to the controllable electric load. There is no change in power output from CHP which is the same as shown in Fig. 6.4.7. During hours 1-4, electric grid will supply more power than before to fulfill the extra demand from interruptible electric load; while battery will charge more energy so as to discharge at high energy price period (hour 11-14).

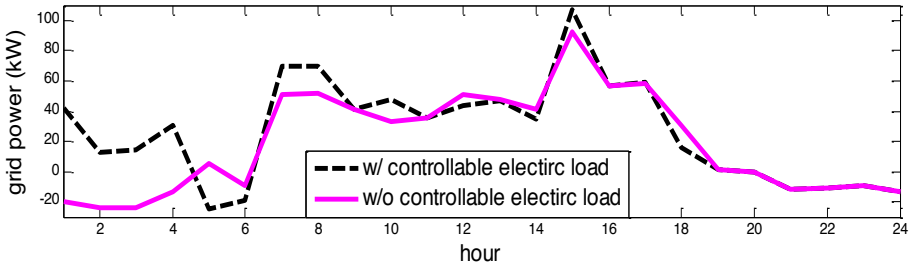


(a) Power supply from electric grid

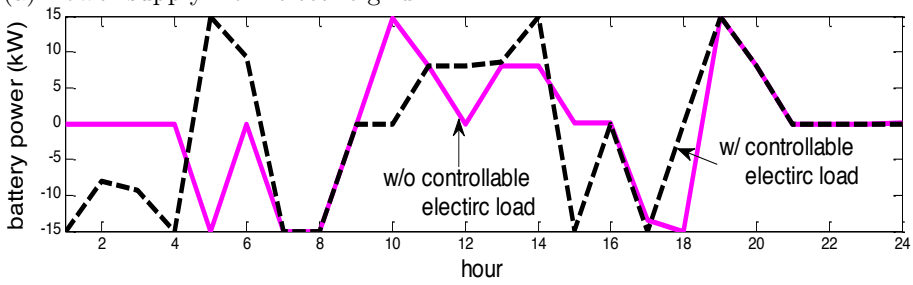


(b) Power supply from battery

Fig. 6.4.9 Comparison of power supply

2) Controllable thermal load

For interruptible thermal load in Fig. 6.4.10 (a), it's operated at hours 1, 11, 13; while for non-interruptible thermal load, it works from hours 1-5. The power and thermal output from CHP unit will be slightly impacted by the operation of controllable thermal load. From hours 7-17 in Fig. 6.4.10 (b)-(c) and Fig. 6.4.11 (a), CHP is contributing due to the interruptible thermal load and the high energy price from electric grid. The maximum thermal output from CHP will be decreased from 74.1kW to 70.8kW in Fig. 6.4.10 (a); while boiler has more output for hours 1-6 and 18-24 in Fig. 6.4.10 (b). The interruptible thermal load will be taken over by CHP at hour 11, 13 when boiler has no any output; the extra controllable thermal load will be covered by boiler at hours 1-5. Therefore the daily operation cost will be increased from \$173.8 to \$179.3.

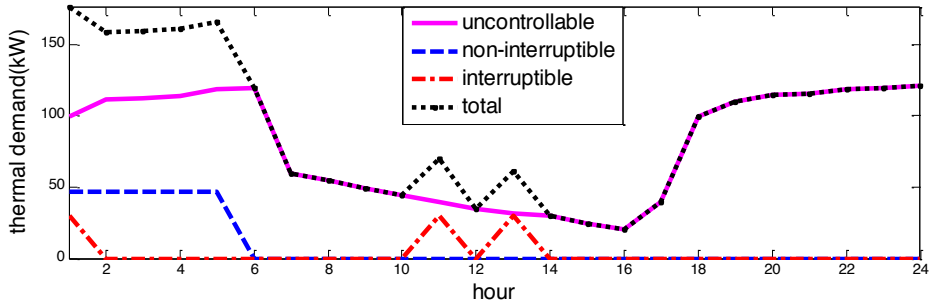


(a)Thermal demand

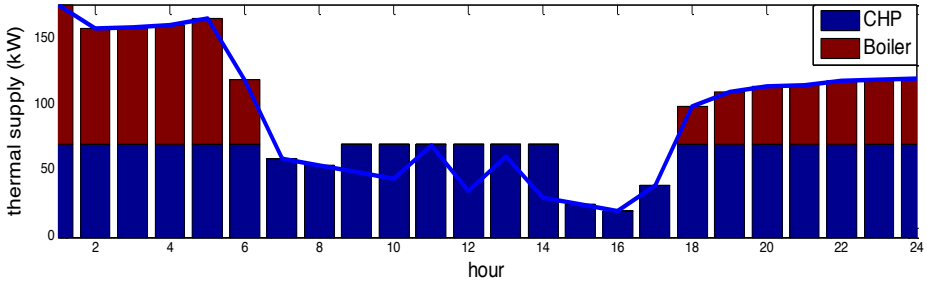


(b)Thermal supply

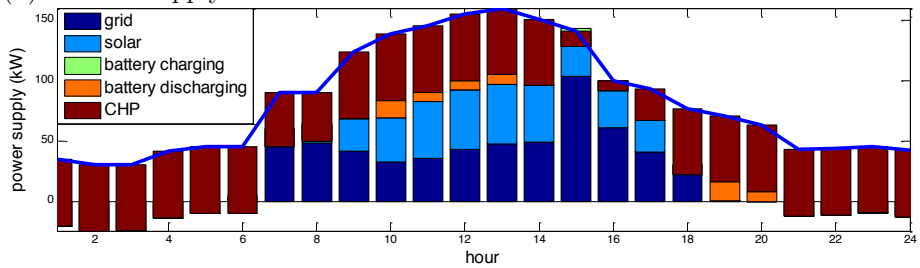


(c)Power supply

Fig. 6.4.10 Impact of Controllable thermal load

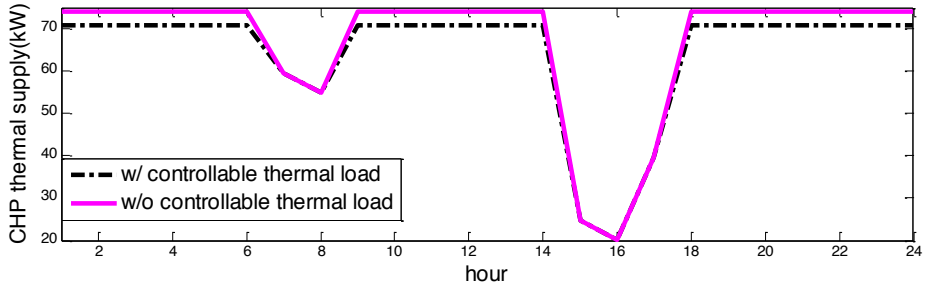


(a) Thermal supply from CHP

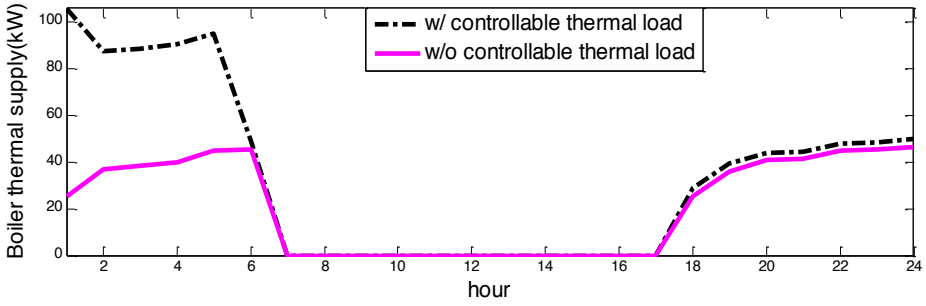


(b) Thermal supply from boiler

Fig. 6.4.11 Comparison of thermal supply

*Rolling stochastic analysis*

Compared with the deterministic case where the daily cost will be \$173.6, rolling scheduling is conducted with the daily cost of \$186.2 due to the updated information of uncertainties. Fig. 6.4.12 shows the power and thermal supply for the rolling case, there is no surplus heat from CHP in Fig. 6.4.12 (b) because the rolling decisions are taken from hour 1 for every iteration. Comparison of power supply is shown in Fig. 6.4.13 (a)-(c). With rolling scheme applied, CHP decreases its power output in Fig. 6.4.13(c) and thermal output in Fig. 6.4.14 (a). Battery in Fig.

6.4.13 (b) is coordinating with the electric grid in Fig. 6.4.13 (a) to supply the actual electric load. As shown in Fig. 6.4.14 (b), there is more thermal supply from boiler than the deterministic case.

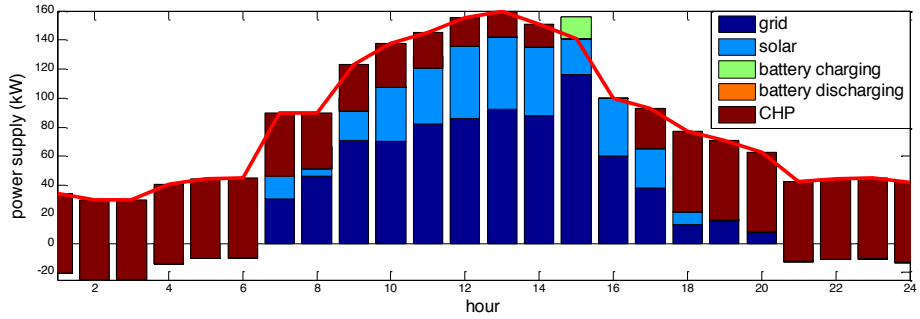


(a)Power supply

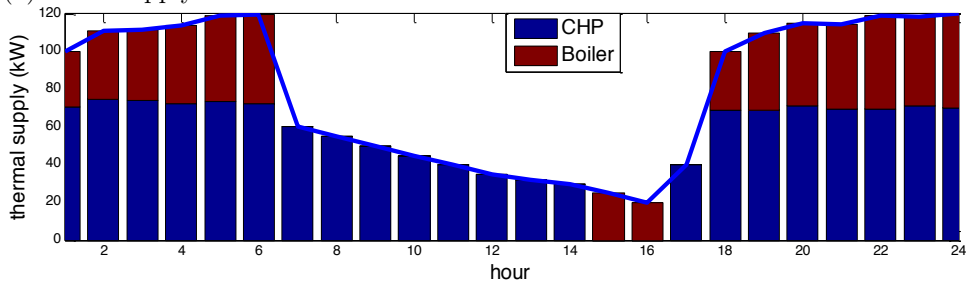


(b)Thermal supply

Fig. 6.4.12 Rolling scheduling

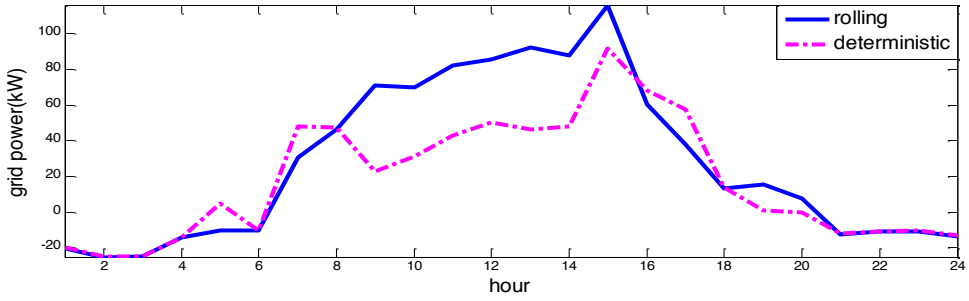


(a)Grid power

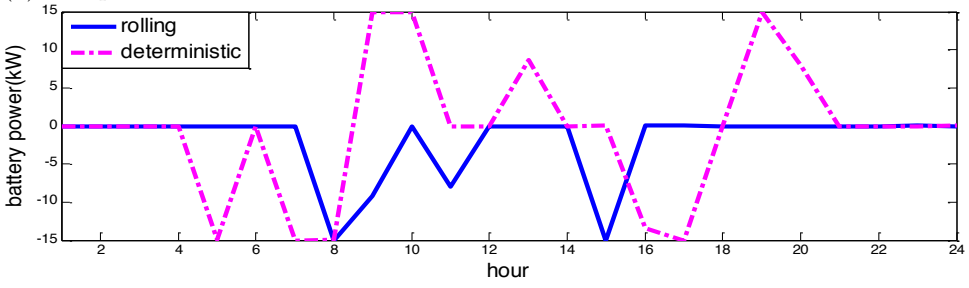


(b) Battery power

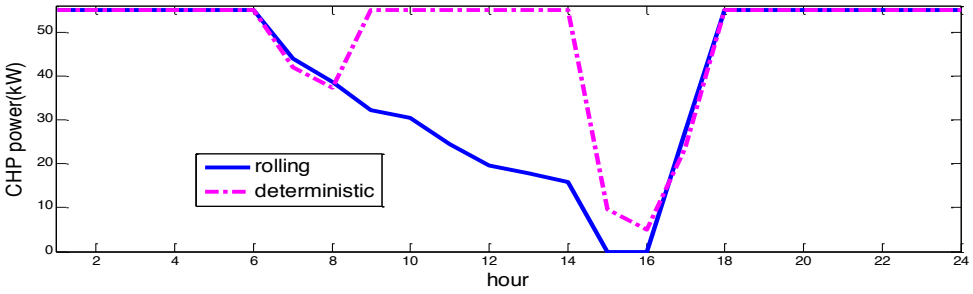


(c)CHP power

Fig. 6.4.13 Comparison of power supply

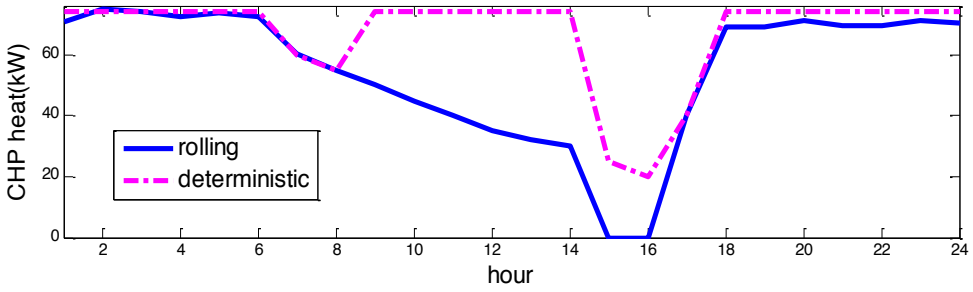


(a)CHP heat

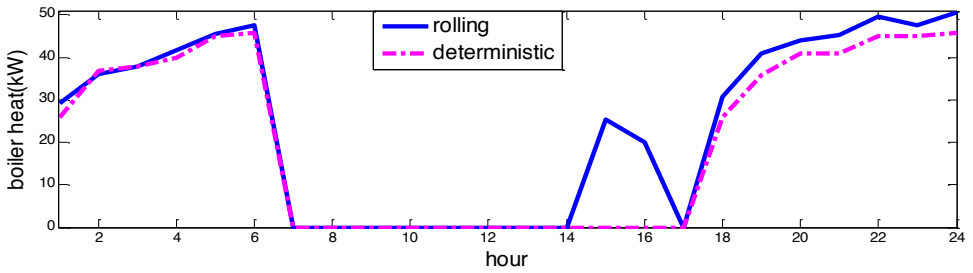


(b)Boiler heat

Fig. 6.4.14 Comparison of thermal supply

*Robust Case Studies*

In this section, the operation of utility grid with CHP system is studied. As shown in Table 6.4.3, both deterministic and robust analysis are conducted to investigate 1) the influence of uncertain electric load and solar power generations; 2) the effect of battery; 3) the effect of CHP; 4) the influence of budget of robustness in the robust model. $\Delta p_{load}^{t}$ is set to be within the range of [-4%, 5%] of the nominal electric load; $\Delta H_{load}^{t}$ lies in the range of [-9%, 10%] of the nominal thermal load; $\Delta p_{solar}^{t}$ is within [-20%, 19%] of the nominal solar power generation.

TABLE 6.4.3 Cases for Deterministic and Robust Models

| Cases | | 1 | 2 | 3 | 4 | 5 |
|---|---|---|---|---|---|---|
| Power Generation | Electric Grid | × | × | × | × | × |
| | Solar | | × | × | × | × |
| | Battery | | | × | × | × |
| | CHP | | | | | × |
| | Boiler | | | | × | × |
| Household Load | Electric Load | × | × | × | × | × |
| | Thermal Load | | | | × | × |

The heat recovery efficiency of CHP system is set to 72%. The efficiencies for both heat coil and boiler are 90%. The battery capacity is [5, 50] kW. The charging/discharging power limit of battery is [8, 15] kW. The initial SOC is defined as 15%. Table 6.4.4 listed hourly prices for electricity from/to the grid and natural gas.

TABLE 6.4.4 Energy Price ($/kwh)

| Energy | Hours 1-8 | Hours 9-14 | Hours 15-18 | Hours 19-22 | Hours 23-24 |
|---|---|---|---|---|---|
| Electricity from Grid | 0.051 | 0.119 | 0.071 | 0.119 | 0.051 |
| Electricity to Grid | 0.067 | 0.067 | 0.067 | 0.067 | 0.067 |
| Natural Gas | 0.031 | 0.031 | 0.031 | 0.031 | 0.031 |

Table 6.4.5 summarizes the comparison of costs between different cases.

TABLE 6.4.5 Operating Cost in Cases 1-5 ($)

| Case | 1 | 2 | 3 | 4 | 5 |
|---|---|---|---|---|---|
| Deterministic | 184.7 | 143.5 | 138.2 | 211.1 | 172.3 |
| Robust | 193.9 | 160.9 | 155.7 | 235.9 | 195.6 |
| Increase (%) | 4.98 | 12.13 | 12.66 | 11.75 | 13.52 |

*Influence of uncertain electric load and solar power*

As shown in Fig. 6.4.15, compared with the deterministic Case 1, the uncertainties in electric load lead to a higher grid power supply in the robust Case 1 which has a cost increase by 4.98%. In Case 2, the integration of solar energy contributes to provide a portion of electric load, which can be observed from the reduction in grid power supply for both deterministic and robust cases, while the robust Case 2 has a lower reduction as the solar generation is reduced due to uncertainty. Compared with deterministic Case 2, the combined influence of uncertain electric load and solar generation results in the increase in operating cost by by 12.13%.

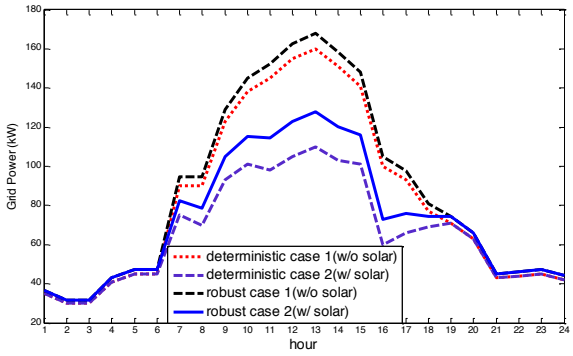


Fig. 6.4.15 Grid power for Cases 1 and 2

*Effect of battery*

In Fig. 6.4.16 (a), the commitment of battery causes the difference in grid power supply between Cases 2 and 3. When the grid power in Case 3 is lower than the corresponding one in Case 2, the battery is discharging. For example, discharging hours 6, 9, 10, 12, 14, 19, 21, 22, 24 in the deterministic Case 3, and discharging hours 2, 4, 10, 11, 13, 14, 19, 21, 22, 24 in the robust Case

3. When the grid power in Case 3 is higher than the corresponding one in Case 2, the battery is charging. For example, charging hours 1, 2, 7, 8, 13, 15-18, 23 in the deterministic Case 3, and charging hours 1, 3, 5-8, 12, 15, 17, 18, 23 in the robust Case 3. There is no change in SOC at remaining hours 3-5, 11, 20 in the deterministic Case 3 and at remaining hours 9, 16, 20 in the robust Case 3. Compared with Case 2, the total operating cost is reduced by 3.69% and 3.23% for deterministic and robust Case 3, respectively, due to the battery charging and discharging effect.

Without the battery, the robust Case 2 always needs a higher grid power supply than the deterministic Case 2 due to the combined influence of uncertain electric load and solar generation. However, with the battery, it is possible that the grid power supply in the robust Case 3 is lower than that in the deterministic Case 3 due to the response of battery to uncertainties, which is leading the increase in the operating cost by 12.66%.
By comparing the robust Case 3 with the deterministic Case 2, we explore the effect of battery on the uncertainties. When the SOC is increasing (the battery is charging) or keeps constant at hours 1, 3, 5-9, 12, 15-18, 20, 23 as shown in Fig. 6.4.16 (b), the additional power demand caused by uncertain load and solar generation is only supplied by the grid. When the SOC is decreasing (battery is discharging) but the grid provides a lower power supply at hours 2, 4, 10, 11, 13, 14, 19, 21, 22, 24, the battery not only supplies the additional power demand, but also cover a potion of normal power.

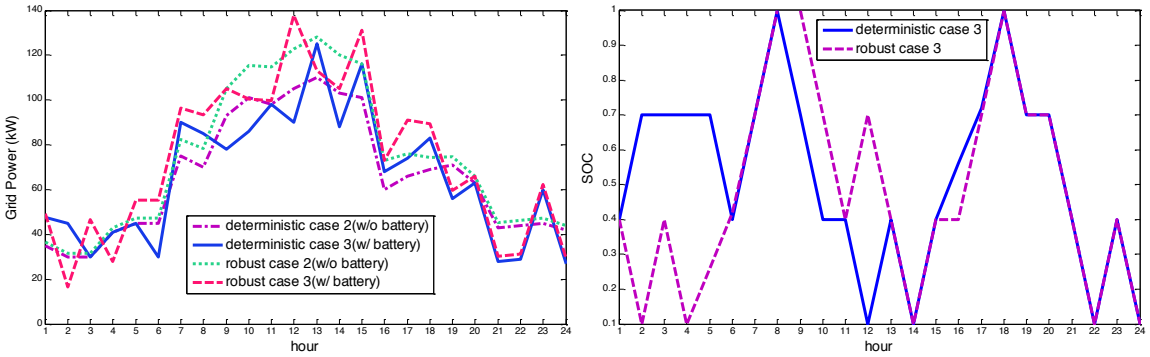


(a) Grid Power for Cases 2 and 3 (b) SOC of battery for Case 3

Fig. 6.4.16 Effect of battery on grid power supply

*Effect of CHP*

In Fig. 6.4.17 (a), the introduction of CHP which is linking electic and thermal energy supply, results in the reduction in the power supply from both grid and battery in Case 5. Without the CHP, the power and thermal energy supplies in the system are decoupled. The power supply from both grid and battery in the robust Case 4 is always higher than that in the deterministic Case 4 because of the uncertain electric load and solar generation, which results in an increase in the operating cost by 11.75%. With the CHP, the difference between deterministic and robust Cases 5 is introduced due to the response of CHP to both uncertain electric and thermal energy requests, which consequently increases the cost by 13.52%.

Compared with the deterministic Case 4, the CHP supplies the additional power demand at hours 1-14,17-24 when the robust Case 5 has a lower power supply from both grid and battery. However, all of the grid, battery and CHP contribute to the additional power demand together during hours 15 and 16 when the robust Case 5 has a higher power supply from both grid and battery.

In Fig. 6.4.17 (b), the robust Case 4 has a higher thermal power demand than the deterministic Case 4 due to the uncertainty in the thermal load. In the robust Case 5, the thermal power supplied by the CHP is higher than the actual thermal demand during hours 9-14, which means that there is an excess thermal power supply which can be exhausted.

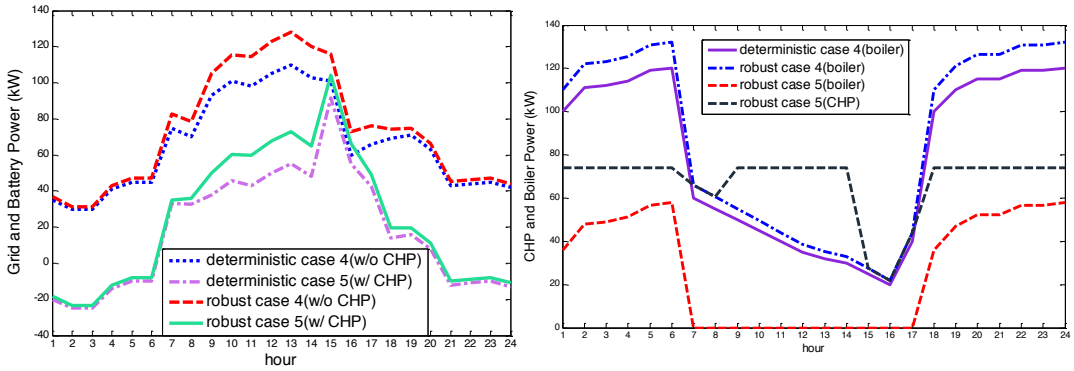


(a) Electric power supply (b) Thermal power supply

Fig. 6.4.17 Effect of CHP on the energy supply

*Influence of budget of robustness on the energy supply*

Fig. 6.4.18 shows the effect of budget of robustness in controlling the uncertain range of electric and thermal loads, and solar generation. In Fig. 6.4.18 (a), $\Gamma_2$ is fixed at 1 and $\Gamma_1$ is adjusted from 0 to 2. Here, $\Gamma_1$=0 means that no protection against uncertainties in electric load and solar generation will be taken; $\Gamma_1$=2 means that uncertainties in electric load and solar generation are fully ensured. Table 6.4.6 summaries the operating cost change as the increase of budget of robustness $\Gamma_1$.

TABLE 6.4.6 Operating Cost with Various $\Gamma_1$ ($\Gamma_2$=1)

| GAMMA1 | COST ($) | INCREASE (%) |
|---|---|---|
| 0.0 | 172.3 | 0 |
| 0.5 | 183.5 | 6.5 |
| 0.8 | 186.6 | 8.3 |
| 1.0 | 188.7 | 9.52 |
| 1.3 | 190.8 | 10.74 |
| 1.6 | 192.8 | 11.90 |
| 1.8 | 194.2 | 12.71 |
| 2.0 | 195.6 | 13.52 |

In Fig. 6.4.18 (b), $\Gamma_1$ is fixed at 2 and the uncertainty set of thermal load is enlarged by increasing the robustness $\Gamma_2$ from 0 to 1. From Fig. 6.4.18 (b), the additional thermal load will be supplied by boiler during hours 1-6, 18-24 and by the CHP in hours 7 and 8. However, no

change in power outputs from either CHP or boiler during hours 9-14 means that the surplus thermal power supply during this period is enough to cover uncertainties in the thermal load. The resulted excess thermal power is exhausted.

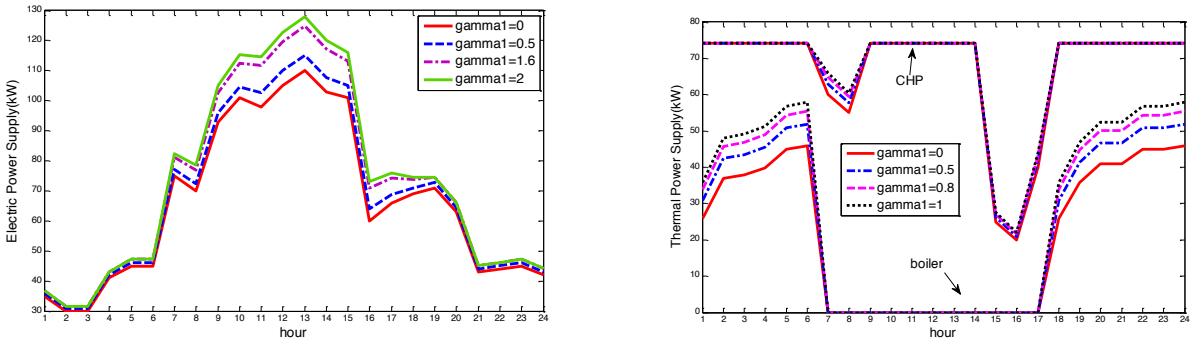


(a) Electric power supply from grid, battery and CHP ($\Gamma_2$=1) (b) Thermal power supply ($\Gamma_1$=2)
Fig. 6.4.18 Effect of budget of robustness

**Publications / Presentations:**

*Journal Articles:*

1. Ping Liu, Yong Fu, Multistage Stochastic Optimal Operation of Energy-Efficiency Building with CHP System (in preparation for submission to IEEE transactions on smart grid)

2. Ping Liu, Yong Fu, Robust Stochastic Optimization of Energy-Efficiency Building with Multiband Uncertainty (in preparation for submission to IEEE transactions on smart grid).

*Conference Papers:*

1. Ping Liu, Yong Fu, Optimal Operation of Energy-Efficiency Building: A Robust Optimization Approach, IEEE PES general meeting, 2013 (Accepted)

*Posters:*

1. Ping Liu, Yong Fu, Multistage Stochastic Optimal Operation of Energy-Efficiency Building with CHP System, IEEE PES general meeting, San Diego, July, 2012.

## Students Involved in Task 6.0

*Ph.D. Students*

1. Shravana Musunuri, "Power Electronic Interface and Control Issues in the Hybrid Renewable Energy Interconnection to the Grid", May 2011.
2. Derrick Cherry, "Technical Evaluation and Optimal Placement of Distributed Gene ration on the Distribution Power System Using Artificial Intelligence, December 2010.
3. Saher Albatran, "Integration of CHP Systems with Power Grid", May 2014.
4. Ping Liu, "CHP Building Energy Management", May 2014..

*Masters Students:*

1. Shireesha Methuku, "Modeling of the Biomass Power Generation and Techno-Economic Analysis", December 2009.
2. Abhilash Reddy Masannagari, "Optimizing the Size and Location of Distributed Generators to Maximize the Grid Stability", December 2008.

## Publications - Task 6

*Journal Articles:*

1. Ramon Zamora and Anurag K. Srivastava, “Controls for Microgrids with Storage: Review, Challenges, and Research Needs”, Journal of Renewable and Sustainable Energy Reviews vol. 14, issue 7, pp. 2009-2018, September 2010.

2. Anurag K Srivastava, Aarthi Asok Kumar and Noel N Schulz, “Impact of Distributed Generations with Energy Storage Devices on the Electric Grid”, in press, IEEE Systems Journal.

*Conference Papers:*

1. Shravana Musunuri, Herbert L. Ginn, "Comprehensive Review of Wind Energy Maximum Power Extraction Algorithms", Accepted for Presentation at Power Electronics Drives and Systems, Taiwan, November 2009.

2. Shravana Musunuri, Herbert L. Ginn, "Comprehensive Review of Wind Energy Maximum Power Extraction Algorithms", Submitted for Presentation at Energy Conversion and Congress Exposition, Atlanta, GA, Sep 2010.

3. Shravana Musunuri, Herbert L. Ginn, " A modified maximum power extraction algorithm for Wind energy systems”, to be submitted at IEEE Workshop on Control and Modeling for Power Electronic, Boulder, CO, June 2010.

4. Anurag Srivastava, Ramon Zamora, Doug Bowman, “Impact of Distributed Generation with Storage on Electric Grid Stability”, IEEE PES General Meeting, July 26 - July 29, 2011, Detroit, MI (Invited Panel)

5. R. Zamora, A. K. Srivastava and Syukriyadin, “Microgrids for Reliable, Clean, and Efficient Power Delivery,” presented at the 4th Annual International Workshop & Expo on Sumatra Tsunami Disaster & Recovery 2009, Nov. 23-25, Banda Aceh, Indonesia.

6. Aarthi Asok Kumar, Anurag K Srivastava and Noel N. Schulz, “Impact of Biomass Based Distributed generation with Energy Storage on Transient Stability of Grid”, Proceedings of Power System Conference (PSC), March 11-14, 2008, Clemson, SC.

7. Abhilash R Masannagari, Anurag K Srivastava and Noel N. Schulz, “Optimizing Siting and Sizing of DG to maximize Grid Stability”, Proceedings of Power System Conference (PSC), March 11-14, 2008, Clemson, SC.

8. Aarthi Asok Kumar, Abhilash R Masannagari, Anurag K Srivastava and Noel N Schulz, “Impact of Biomass Based Distributed generation on Electric Grid”, Clean technology and Sustainable Industries Conference and Trade Show, Boston, MA, June 1-5, 2008.

9. Shireesha Methuku, Anurag K Srivastava and Noel N Schulz, “Comprehensive Modeling and Stability Analysis of Biomass Generation”, North American Power Symposium, October 2-4, Mississippi State, MS, 2009.

*Posters:*

1. Shravana Musunuri, Herbert L. Ginn, "Power electronic Interface of Multiple Energy Sources to Utility Grid", Poster Presentation, Electric Ship Technology Symposium, Starkville, May 2009.

2. Ramon Zamora, and *Anurag K. Srivastava,* “Modeling and Control of Microgrid”, IEEE T&D conference, New Orleans, LA, April, 2010.

3. Shireesha Methuku, *Anurag K. Srivastava* and Noel N Schulz, “Comprehensive Modeling and Technical-Economical Impacts of Biomass Generation”, IEEE T&D conference, New Orleans, LA, April, 2010.

## Products Developed

### Journal Papers

1. Knizley, A., Mago, P.J., Smith, A.D. (2014). Evaluation of the performance of combined cooling, heating, and power systems with dual power generation units, Energy Policy, Volume 66, pages 654-665.
2. Carpenter, J., Mago, P.J., Luck, R., and Cho, H. (2014). Passive Energy Management Through Increased Thermal Capacitance, *Energy and Buildings*, 75, 465-471.
3. Carpenter, J, Mago, P.J., Luck, R., & Cho, H. Parametric Analysis of Passive Energy Management Through Increased Thermal Capacitance, *Energy and Buildings. Under Review.*
4. Mago, P. J., & Luck, R. (2013). Energetic And Exergetic Analysis Of Waste Heat Recovery From A Micro-Turbine Using Organic Rankine Cycles. *International Journal of Energy Research*, 37 (8), 888–898.
5. Mago, P. J., & Luck, R. (2013). Evaluation of the Potential Use of a Combined Micro-Turbine Organic Rankine Cycle for Different Geographic Locations. *Applied Energy,* 102, 1324-1333
6. Mago, P. J., Luck, R. and Knizley, A. (2013), Combined heat and power systems with dual power generation units and thermal storage. *International Journal of Energy Research*. doi: 10.1002/er.3089.
7. Mago, P. J., and Luck, R. (Jan 2012). Prime Mover Sizing for Based-Loaded Combined Heating and Power Systems. *IMechE Journal of Power and Energy*, *226*(1), 17-27.
8. Mago, P. J., & Smith, A. (Jul 2012). Evaluation of the Potential Emissions Reductions from the Use of CHP Systems in Different Commercial Buildings. *Building and Environment, 53, 74–82*
9. Yun, K., Luck, R., Mago, P. J., & Smith, A. (Jan 2012). Analytic Solutions for Optimal Power Generation Unit Operation in Combined Heating and Power Systems. *ASME Journal of Energy Resources Technology*, *134*(1), 011301(8 pages).
10. Wheeley, C., Mago, P. J., & Luck, R. (Jan 2012). Methodology to Perform a Combined Heating and Power System Feasibility Study for Industrial Manufacturing Facilities. *Distributed Generation and Alternative Energy Journal*, *27*(1), 8-32.
11. Mago, P. J., Luck, R., & Smith, A. (Nov 2011). Environmental Evaluation of Base-Loaded CHP Systems for Different Climate Conditions in the US. *International Journal of Ambient Energy*, *32*(4), 203-214.
12. Yun, K.4, Luck, R., Mago, P. J., & Cho, H. (2012). Building Hourly Thermal Load

Prediction using an Indexed ARX model. Energy and Buildings, 54, 225-233.

13. Fumo, N., Mago, P. J., & Smith, A. (Dec 2011). Analysis of Combined Cooling, Heating, and Power Systems Operating Following the Electric Load and Following the Thermal Load Strategies with No Electricity Exporting. *Journal of Power and Energy*, *225*(8), 1016-1025.
14. Mago, P. J., & Luck, R. (2013). Evaluation of a Base-Loaded Combined Heating and Power System with Thermal Storage for Different Small Buildings Applications. *International Journal of Energy Research*, 37(2), 179-188.
15. Smith, A., Luck, R., & Mago, P.J. (2012). Integrated Parameter Estimation of Multicomponent Thermal Systems with Demonstration on a Combined Heat and Power System. *ISA Transactions,* 51(4):507-13.
16. Yun, K.4, Cho, H., Luck, R., & Mago, P. J. (2011). Real Time Combined Heat and Power (CHP) Operational Strategy Using a Hierarchical Optimization Algorithm. *Journal of Power and Energy*, 225, 403-412.
17. Wheeley, C., Mago, P. J., & Luck, R. (Dec 2011). A Comparative Study of the Economic Feasibility of Employing CHP Systems in Different Industrial Manufacturing Applications. *Energy and Power Engineering*, *3*, 630-640.
18. Hueffed, A., & Mago, P. J. (Feb 2011). Energy, Economic, and Environmental Analysis of Combined Heating and Power-organic Rankine Cycle and Combined Cooling, Heating, and Power-organic Rankine Cycle Systems. *IMechE Journal of Power and Energy*, *225*(1), 24-32
19. Yun, K., Cho, H., Luck, R., & Mago, P. J. (Jun 2011). Real Time Combined Heat and Power (CHP) Operational Strategy Using a Hierarchical Optimization Algorithm. *Journal of Power and Energy*, *225*, 403-412.
20. Fumo, N., Mago, P. J., & Jacobs, K. (Jan 2011). Design Considerations for Combined Cooling, Heating, and Power Systems at Altitude. *Energy Conversion and Management*, *52*(2), 1459-1469.
21. Smith, A., Fumo, N., & Mago, P. J. (Feb 2011). Spark Spread - A Screening Parameter for Combined Heating and Power Systems. *Applied Energy*, *88*, 1494-1499.
22. Smith, J. A., Fumo, N., Luck, R., & Mago, P. J. (Jun 2011). Robustness of a Methodology for Estimating Hourly Energy Consumption of Buildings Using Monthly Electrical Bills. *Energy and Buildings*, *43*, 779-786.
23. Mago, P. J., & Hueffed, A. (Jun 2010). Evaluation of a Turbine Driven CCHP System for Large Office Buildings under Different Operating Strategies, Energy, and Buildings. *Journal of Power and Energy*, *42*(10), 1628-1636.
24. Mago, P. J., Chamra, L., & Ramsay, J. (Mar 2010). Micro-combined Cooling, Heating and Power Systems Hybrid Electric-thermal Load Following Operation. *Applied Thermal Engineering*, *30*(8-9), 800-806.
25. Weathers, J.B., Luck, R., Weathers, J.W. "A Modular Approach to Uncertainty Analysis", *ISA Transactions*, 49, pp. 19-26, 2010

26. Mago, P. J., Hueffed, A., & Chamra, L. (Sep 2010). Analysis and Optimization of the Use of CHP-ORC Systems for Small Commercial Buildings. *Energy & Buildings*, *42*(9), 1491-1498.
27. Fumo, N., Mago, P. J., & Luck, R. (Oct 2010). Methodology to Estimate Building Energy Consumption Using EnergyPlus Benchmark Models. *Energy and Buildings*, *42*, 2331-2337.
28. Hueffed, A., & Mago, P. J. (Jun 2010). Influence of Prime Mover Size and Operational Strategy on the Performance of CCHP Systems under Different Cost Structures. *IMechE Journal of Power and Energy*, *224*(5), 591-605.
29. Smith, A., Luck, R., & Mago, P. J. (Sep 2010). Analysis of a CCHP System Model Under Different Operating Strategies with Input and Model Data Uncertainty. *Energy and Buildings*, *42*, 2231-2240.
30. Mago, P. J., & Chamra, L. (May 2009). Analysis and Optimization of CCHP Systems Based on Energy, Economical and Environmental Considerations. *Energy and Buildings*, *41*, 1099-1106.
31. Mago, P. J., Chamra, L., & Hueffed, A. (May 2009). A Review on Energy, Economical, and Environmental Benefits of the Use of CHP Systems for Small Commercial Buildings for the North American Climate. *International Journal of Energy Research*, *33*, 1252-1265.
32. Cho, H., Luck, R., S.D. Eksiouglu, Chamra, L. M., "Cost-optimized real -time operation of CHP systems," Energy and Buildings, Vol. 41, No. 4, April, pp. 445-451, 2009.
33. Fumo, N., Mago, P. J., & Chamra, L. (Jun 2009). Analysis of Cooling, Heating, and Power Systems Based on Site Energy Consumption. *Applied Energy*, *86*(6), 928-932.
34. Mago, P. J., Fumo, N., & Chamra, L. (Jun 2009). Performance Analysis of CCHP and CHP Systems Operating Following the Thermal and Electric Load. *International Journal of Energy Research*, *33*, 852-864.
35. Fumo, N., Mago, P. J., & Chamra, L. (Sep 2009). Energy and Economic Evaluation of Cooling, Heating, and Power Systems Based on Primary Energy. *Applied Thermal Engineering*, *29*(13), 2665-2671.
*36.* Weathers, J.B., Luck, R., Weathers, J.W., "An Exercise in Model Validation: Comparing Univariate Statistics and Monte-Carlo based Multivariate Statistics", *Reliability Engineering and System Safety*, Volume 94, Issue 11, November 2009, Pages 1695-1702.
37. Cho, H., Mago, P. J., Luck, R., & Chamra, L. (Oct 2009). Evaluation of CCHP Systems Performance Based on Operational Cost, Primary Energy Consumption, and Carbon Dioxide Emission by Utilizing an Optimal Operation Scheme. *Applied Energy*, *86*, 2540-2549.
*38.* Cho, H., Krishnan, S.R., Luck, R. and Srinivasan, K.K. Comprehensive uncertainty analysis of a Wiebe function-based combustion model for pilot-ignited natural gas

engines. *Proc. IMechE, Part D: J. Automobile Engineering,* Vol. 223, No. 11, 2009

39. Fumo, N., Mago, P. J., & Chamra, L. (Nov 2009). Emission Operational Strategy for Combined, Cooling, and Power Systems. *Applied Energy Journal*, *86*(11), 2344-2350.
40. Hueffed, A., Chamra, L., & Mago, P. J. (May 2009). A Simplified Model of Heat and Mass Transfer Between Air and Falling-Film Desiccant in Parallel-Plate Humidifier. *ASME Journal of Heat Transfer*, *131*, 0520011-0520017.
41. Fumo, N., Mago, P. J., & Chamra, L. (Jul 2009). Hybrid-cooling Combined Cooling, Heating, and Power Systems. *IMechE Journal of Power and Energy*, *223*(5), 761-770.
42. Harrod, J., & Mago, P. J. (Jan 2011). Performance Analysis of a CCHP System Driven by a Waste Biomass Fired Stirling Engine. *Journal of Mechanical Engineering Science*, 225(2), 420-428
43. Harrod, J., Mago, P. J., & Luck, R. (Jan 2012). Sizing Analysis of a Combined Cooling, Heating, and Power System for a Smal Office Building Using a Wood Waste Biomass-Fired Stirling Engine. *International Journal of Energy Research*, *36*(1), 64-74.
44. Smith, A., Fumo, N., & Mago, P. J. (Feb 2011). Spark Spread - A Screening Parameter for Combined Heating and Power Systems. *Applied Energy, 88,* 1494-1499.
45. Smith, A., Mago, P. J., & Fumo, N. (May 2011). Emissions Spark Spread and Primary Energy Spark Spread - Environmental and Energy Screening Parameters for Combined.
46. M.M. Tripathi, S.R. Krishnan, K.K. Srinivasan, F.-Y. Yueh, J.P. Singh (2011). "Chemiluminescence-based multivariate sensing of local equivalence ratios in premixed atmospheric methane-air flames," Fuel, doi:10.1016/j.fuel.2011.08.038
47. C.M. Gibson[1], A. Polk[1], N. Shoemaker[1], K.K. Srinivasan, and S.R. Krishnan (2011). Comparison of propane and methane performance and emissions in a turbocharged direct injection dual fuel engine. Trans. ASME: Journal of Engineering for Gas Turbines and Power, 133(9), Article GTP-092806, (DOI: 10.1115/1.4002895)
48. S. R. Krishnan and K. K. Srinivasan (2010). Multi-Zone Modeling of Partially Premixed Low Temperature Combustion in Pilot-Ignited Natural Gas Engines. Proc. Instn. Mech. Engrs.: Part D: Journal of Automobile Engineering, 224, pp. 1597-1622 (DOI 10.1243/09544070JAUTO1472) (This paper won the 2010 SAGE Best Paper Award by the Editor and Editorial Board of Proceedings of the Institution of Mechanical Engineers, Part D: Journal of Automobile Engineering)
49. K. K. Srinivasan, P. J. Mago, S. R. Krishnan (2010) "Analysis of Exhaust Waste Heat Recovery from a Dual Fuel Low Temperature Combustion Engine using an Organic Rankine Cycle," Energy, Vol. 35, pp. 2387-2399, doi:10.1016/j.energy.2010.02.018

50. Radhakrishnan, S., J.O. Paz, F. Yu, S. Eksioglu, and D.L. Grebner. 2013. Assessment of potential capacity increases at combined heat and power facilities based on available corn stover and forest logging residue. Energies (6): 4418-4428. doi:10.3390/en6094418
51. Wan, C., F. Yu, Y. Zhang, Q. Li, and J. Wooten. *2013*. Material Balance and Energy Balance Analysis for Syngas Generation by a Pilot-plant Scale Downdraft Gasifier. *Journal of Biobased Materials and Bioenergy*. 7: 690-695.
*52.* Yan, Q., C. Wan, J. Street, D. Yan, J. Han, and F. Yu. *2013.* Catalytic Removal of Oxygen from Biomass-derived Syngas. *Bioresource Technology.* 147:117–123.
*53.* Zhang, Y., C., Wan, Q. Li, P.H. Steele, and F. Yu. *2013.* Studies of Biochars Generated from Pilot-scale Downdraft Gasification. *Transactions of the ASABE. 56(3): 995-1001.*
54. Yan, Q., C. Wan, J. Liu, J. Gao, F. Yu, J. Zhang, and Z. Cai. *2013.* Iron Nanoparticles in situ Encapsulated in Biochar-based Carbon as an Effective Catalyst for Conversion of Biomass-derived Syngas to Liquid Hydrocarbons * *Green Chemistry.* 15:1631-1640.
55. Yan, Q., F. Yu, Z. Cai, and J. Zhang. 2012. Catalytic upgrading nitrogen-riched wood syngas to liquid hydrocarbon mixture over a Fe–Pd/ZSM-5 catalyst. Biomass and Bioenergy. 47: 469-473.
56. Kim H., and Parajuli Prem B. 2012. Economic Analysis Using SWAT-simulated Potential Switchgrass and Miscanthus Yields in the Yazoo River Basin. Transactions of the Agricultural and Biological Engineers, 55(6): 2123-2134.
57. Yan, Q., F. Yu, J. Liu, J. Street, J. Gao, Z. Cai, and J. Zhang. 2012. Catalytic Conversion Wood Syngas to Synthetic Aviation Turbine Fuels over A Multifunctional Catalyst. Bioresource Technology.127:281-290.
58. Wang, H., D. Livingston, R. Srinivasan, Q. Li, P. Steele, and F. Yu. 2012. Detoxification and fermentation of pyrolytic sugar for ethanol production. Applied Biochemistry and Biotechnology. 168:1568–1583.
59. Street, J. and F. Yu. *2011.* Production of high-value products including gasoline hydrocarbons from thermochemical conversion of syngas. *Biofuels* 2(6):677-691.
60. Yan, Q., H. Toghiani, F. Yu, Z. Cai, J. Zhang. 2011. Effects of Pyrolysis Conditions on Yield of Bio-chars from Pine Chips. *Forest Prod. J.* 61(5):367-371.
61. Igathinathane, C., J.D. Davis, J.L. Purswell, and E.P. Columbus. 2010. Application of 3D scanned imaging methodology for volume, surface area, and envelope density evaluation of densified biomass. *Bioresource Technology.* 101(11): 4220-4227.
62. Yang, P., E.P. Columbus, J. Wooten, W.D. Batchelor, P. R. Buchireddy, X. Ye and L. Wei. 2009. Evaluation of syngas storage under different pressures and temperatures. *Applied Engineering in Agriculture* 25(1):121-128.
63. L. Wei, L. O. Pordesimo, S. D. Filip To, C. W. Herndon, W. D. Batchelor. (2009). Evaluation of Micro-Scale SYNGAS Production Costs Through Modeling. *Trans ASAE* Vol. 52(5): 1649-1659.

64. Shah, A., Srinivasan, R., To, F.D., and Columbus, E.P. 2010. Performance and emissions of a spark-ignited engine driven generator on biomass based syngas. *Bioresource Technol.* 101:4656-4661.
65. N. Shoemaker[1], C.M. Gibson[1], A. Polk[1], K.K. Srinivasan, and S.R. Krishnan, 2011, "Performance and Emissions Characteristics of Bio-Diesel Ignited Methane and Propane Combustion in a Four Cylinder Turbocharged Compression Ignition Engine," Paper No. GTP-11-1347, accepted for publication in *Trans. ASME: Journal of Engineering for Gas Turbines and Power,*
66. K. K. Srinivasan, P. J. Mago, S. R. Krishnan (2010) "Analysis of Exhaust Waste Heat Recovery from a Dual Fuel Low Temperature Combustion Engine using an Organic Rankine Cycle," Energy, Vol. 35, pp. 2387-2399, doi:10.1016/j.energy.2010.02.018
67. H. Cho[1], S. R. Krishnan, R. Luck, and K. K. Srinivasan (2009) "Comprehensive uncertainty analysis of a Wiebe function-based combustion model for pilot-ignited natural gas engines," Proceedings of the Institution of Mechanical Engineers, Part D: Journal of Automobile Engineering, 223, Number 11 / 2009, pp. 1481-1498, DOI: 10.1243/09544070JAUTO1103
68. K. K. Srinivasan, P. J. Mago, G. J. Zdaniuk, L. M. Chamra, K. C. Midkiff (2008) "Improving the Efficiency of the Advanced Injection Low Pilot Ignited Natural Gas Engine Using Organic Rankine Cycles," Journal of Energy Resources Technology, Trans. ASME, Vol.130, pp. 022201-1 – 022201-7, DOI 10.1115/1.2906123
69. Ramon Zamora and Anurag K. Srivastava, "Controls for Microgrids with Storage: Review, Challenges, and Research Needs", Journal of Renewable and Sustainable Energy Reviews vol. 14, issue 7, pp. 2009-2018, September 2010.
70. Anurag K Srivastava, Aarthi Asok Kumar and Noel N Schulz, "Impact of Distributed Generations with Energy Storage Devices on the Electric Grid", in press, IEEE Systems Journal.

## Books

1. Chamra, L.M. and Mago, P.J. Micro-CHP Power Generation for Residential and Small Commercial Buildings. Nova Science Publishers, Inc., New York, 2008. ISBN: 1-60456-867-7

## Book Chapters

1. Fumo, N., Mago, P. J., & Chamra, L. (Sep 2009). Energy and Economic Evaluation of Cooling, Heating, and Power Systems Based on Primary Energy. *Applied Thermal Engineering, 29(13),* 2665-2671.

2. Mago, P. J., & Hueffed, A. (May 2011). Energy, Economic, And Environmental Analysis of CHP and CCHP Systems. Morena J. Acosta (Eds.), *Advances in Energy Research - Volume 7*, New York: Nova Science Publishers, Inc., 229-271. ISBN: 978-1-61122-956-1. (Invited).
3. Mago, P. J., Luck, R., & Smith. (2013). Evaluation of the Potential Carbon Dioxide Emissions Reductions from the Use of CHP Systems in Commercial Buildings. Mitchell Carpenter and Everett J. Shelton (Eds.), Carbon Dioxide Emissions: New Research, New York: Nova Science Publishers, Inc. 61-76. ISBN: 978-1-62257-436-0. (Invited).

## Conference Papers

1. Cho, H., Luck, R., Eksioglu, S.D., Chamra, L. M., "Operation of a CCHP System using an Optimal Energy Dispatch Algorithm." *ASME Proceedings of Energy Sustainability* 2008, August 10-13, Jacksonville, FL.
2. Robert Thomas, Rogelio Luck, and Pedro J. Mago, "Optimal Power Generation Unit Sizing and Cost Savings Methodology Using Monthly vs. Hourly Time-steps Applied to Base-Loaded Combined Heat and Power Systems", *ASME International Mechanical Engineering Congress and Exposition (IMECE2012)*, Houston, TX
3. Fumo, N., & Mago, P. J. (May 2010). Tools for Small Office Buildings Energy Consumption Estimation. *ASME Energy Sustainability 2010 - Paper No. ES2010-90135*, Phoenix, Arizona.
4. Cho, H., Luck, R., Mago, P. J., & Chamra, L. (Jul 2009). Assessment of CHP System Performance with Commercial Building Benchmark Models in Different U.S. Climate Zones. *ASME Proceedings of Energy Sustainability 2009*, San Francisco, CA.
5. Fumo, N., Mago, P. J., & Chamra, L.M., (July 2008). Effect of the Power Generation Unit Size on the Energy Performance of Cooling, Heating, and Power Systems. *ASME Power Conference, Paper No. PWR2008-60057*, Orlando, FL, 635-640.
6. Smith, A. & Mago, P. J. (July 2012). Impact of Thermal Storage Option for CHP Systems on the Optimal Prime Mover Size and the Need for Additional Heat Production. *ASME 2012 6th International Conference on Energy Sustainability & 10th Fuel Cell Science, Engineering and Technology Conference*, San Diego, CA.
7. Fumo, N., Mago, P. J., & Spence, J. D. (July 2012). Screening Tool for the Evaluation of Combined, Heating, and Power Systems in existing Office Buildings. *ASME 2012 6th International Conference on Energy Sustainability & 10th Fuel Cell Science, Engineering and Technology Conference*, San Diego, CA.
8. Hueffed, A., Mago, P. J., & Chamra, L. (Nov 2009). Effect of the Power Generation Unit Operation on the Energy, Economical, and Environmental Performance of CCHP Systems for Small Commercial Building. *ASME International Mechanical*

*Engineering Congress and Exposition (IMECE2009),* Orlando, FL.

9. Knizley, A. & Mago, P. J. (July 2012). Evaluation of Combined Heat and Power (CHP) Systems Performacne with Dual Power Generation Units. *ASME 2012 6th International Conference on Energy Sustainability & 10th Fuel Cell Science, Engineering and Technology Conference*, San Diego, CA.
10. Harrod, J., & Mago, P. J. (Nov 2010). Sensitivity Analysis of CHP Stirling Engine Systems. In Paper No. IMECE2010-37316 (Eds.), *ASME International Mechanical Engineering Congress and Exposition (IMECE2010)*, Vancouver.
11. Smith, A., Mago, P. J., & Fumo, N. (Nov 2011). Impact of CHP System Component Efficiencies on The Economic Benefits of CHP Systems Using Spark Spread Analysis. *ASME International Mechanical Engineering Congress and Exposition (IMECE2011),* Denver, CO.
12. N. Shoemaker[1], C.M. Gibson[1], A. Polk[1], K.K. Srinivasan, and S.R. Krishnan, 2011, "Performance and Emissions Characteristics of Bio-Diesel Ignited Methane and Propane Combustion in a Four Cylinder Turbocharged Compression Ignition Engine," Paper No. ICEF2011-60081, (accepted) Proceedings of the ASME IC Engines Division 2011 Fall Technical Conference (ICEF2011), October 2-5, Morgantown, West Virginia, USA, *Presenter – C. M. Gibson*
13. A. Polk[1], C.M. Gibson[1], N. Shoemaker[1], S.R. Krishnan, and K.K. Srinivasan, 2011, "Analysis of Ignition Delay Behavior in a Dual Fuel Turbocharged Direct Injection Engine Using Propane and Methane as Primary Fuels," Paper No. ICEF2011-60080, (accepted) Proceedings of the ASME IC Engines Division 2011 Fall Technical Conference (ICEF2011), October 2-5, Morgantown, West Virginia, USA, *Presenter – A C Polk*
14. C.M. Gibson[1], A. Polk[1], N. Shoemaker[1], K.K. Srinivasan, and S.R. Krishnan, 2010, "Comparison of Propane and Natural Gas Performance and Emissions in a Turbocharged Direct Injection Dual Fuel Engine," Paper No. ICEF2010-35128, Proceedings of the ASME IC Engines Division 2010 Fall Technical Conference (ICEF2010), September 12-15, San Antonio, TX; *Presenter – C. M. Gibson.*
15. Yu, F. 2013. Wide-cut diesel production from an integrated gasification, syngas cleaning, and catalytic conversion process. 2013 Mid-South Area Engineering and Sciences Conference. October 28-29. Oral presentation.
16. Lu, Y., F. Yu, J. Hu, and P. Zhou. 2013. CO hydrogenation to higher alcohols over three-dimensionally ordered macroporous Cu-Fe catalysts. 246th American Chemical Society National Meeting. Indianapolis, IN. September 8-12. Oral presentation.
17. Olsen, J.W.W., J.L. Purswell, J.D. Davis, B.D. Luck and E.J. Koury. 2012. Improving commercial broiler attic inlet ventilation through CFD analysis. Procs. Of the 9th International Symposium: Livestock Env. IX. Jul 8-12. Valencia, Spain.
18. Kim H., and Parajuli Prem B. 2012. Assessment of the Impacts of Land Use and Future Climate Changes on Optimal Selection and Placement of Best Management

Practices. Cincinnati, OH, ASA-CSSA-SSSA. Available at: http://scisoc.confex.com/scisoc/2012am/webprogram/Paper75066.html

19. Paz, J.O., S. Radhakrishnan, F. Yu, S. Eksioglu and D.L. Grebner. 2012. Assessment of potential capacity increases at combined heat and power facilities in Mississippi based on available corn stover and forest logging residue. Sun Grant Initiative 2012 National Conference: Science for Biomass Feedstock Production and Utilization. October 2-5, 2012. New Orleans, LA.
20. Hu, J., Yu, F., Lu, Y., Street, J., Wooten, J., Columbus, E. 2012. Transportation Fuels Production from Biomass through Biomass Gasification, Gas Cleaning and Fischer-Tropsch Synthesis: A Technical and Economic Analysis, Paper: 121337425, An ASABE Meeting Presentation written for the 2012 ASABE Conference, Dallas, TX, July 29-August 1, 2012.
21. Lu,Y., Hu,J., Zhou, P., Street, J., Wooten, J, Columbus, E., Yu, F. 2012. Catalytic conversion of syngas to mixed alcohols via three-dimentionally ordered macroporous Cu-Fe based catalyst. Paper:121337229, An ASABE Meeting Presentation written for the 2012 ASABE Conference, Dallas, TX, July 29-August 1, 2012.
22. Street, J., Yu, F., Columbus, E., Wooten, J. 2012. Scale-Up of Liquid Hydrocarbon Production using Gasified Biomass. Paper: 121337524, An ASABE Meeting Presentation written for the 2012 ASABE Conference, Dallas, TX, July 29-August 1, 2012
23. Lu, Y., Yu, F., Hu, J., Zhou, P. Mixed alcohols Synthesis from Syngas via Zn-Mn promoted Cu-Fe based catalyst. 2012. A Poster Presentation presented for the 2012 Southeast Biofuels Conference. Jackson, MS, August 8-9, 2012.
24. Street, J., Wooten, J., Columbus, E., and Yu, F. 2012. Scale-up of Gasoline-Range Hydrocarbon Production from Gasified Woody Biomass using Bi-functional Catalysts. A Poster Presentation presented for the 2012 Southeast Biofuels Conference. Mississippi State, MS, August 8-9, 2012.
25. Lu, Y., Yu, F., Hu, J., Zhou, P. 2012. Syngas to mixed alcohols via 3D ordered macroporous Cu-Fe based catalyst. Paper number: 172, An oral presentation presented for 244th American Chemical Society National Meeting & Exposition. Philadelphia, PA, August 19-23, 2012.
26. Street, J., F. Yu, J. Wooten, E. Columbus, M. White, and J. Warnock. *2012.* Gasoline-range hydrocarbon production using biomass derived synthesis gas over Mo/H+ZSM-5. *Fuel.*
27. Yan, Q., Yu, F., Liu, J. 2012. Carbon encapsulated iron nanoparticles for catalytic conversion biosyngas to liquid hydrocarbons. 244th ACS National Meeting, Philadelphia, PA, August 19-25, 2012.
28. Yu, F. 2011. Higher Alcohol Synthesis from Syngas over Copper-Iron Based Catalyst. Strategic Environmental Research and Development Program (SERDP) and Environmental Security Technology Certification Program (ESTCP) annual

Technical Symposium & Workshop. Washington, D.C. November 29 – December 1, 2011.

29. Yu, F. 2011. Liquid Hydrocarbon Production over MO/HZSM-5 Using Gasified Biomass. Strategic Environmental Research and Development Program (SERDP) and Environmental Security Technology Certification Program (ESTCP) annual Technical Symposium & Workshop. Washington, D.C. November 29 – December 1, 2011
30. Yu, F. Yan, Q., Columbus, E., and Wooten. J. 2011. Catalytic Conversion of Biomass Derived Synthesis Gas to Liquid Hydrocarbons. 107th Gulf Coast Conference. Galveston, TX. October 11-12, 2011.
31. Yu, F. 2011. Higher Alcohol Synthesis from Syngas over Copper-Iron Based Catalyst. Strategic Environmental Research and Development Program (SERDP) and Environmental Security Technology Certification Program (ESTCP) annual Technical Symposium & Workshop. Washington, D.C. November 29 – December 1, 2011.
32. Yu, F. 2011. Liquid Hydrocarbon Production over MO/HZSM-5 Using Gasified Biomass. Strategic Environmental Research and Development Program (SERDP) and Environmental Security Technology Certification Program (ESTCP) annual Technical Symposium & Workshop. Washington, D.C. November 29 – December 1, 2011
33. Hakkwan Kim, and Parajuli P. B. 2011. Assessment of the Potential Crop Yield for Bio-Energy Production Using the SWAT Model. ASA/CSSA/SSSA, International annual meeting, October 16-19, San Antonio, TX.
34. Yu, F. Yan, Q., Columbus, E., and Wooten. J. 2011. Catalytic Conversion of Biomass Derived Synthesis Gas to Liquid Hydrocarbons. 107th Gulf Coast Conference. Galveston, TX. October 11-12, 2011.
35. Olsen, J.W.W., J.D. Davis, J.L. Purswell. 2011. 2D simulation of air flow in commercial broiler house attics. Presentation for the 2011 ASABE International Meeting, Aug 7-10. Louisville, KY.
36. Yangyang Deng, and Parajuli P. B. 2011. Economic Evaluation of Electricity Generation from a Small-Scale Bio-Gasification Facility using an Optimization Model. IBE Annual Conference, Loews Atlanta, March 3-5, 2011, Atlanta, GA.
37. HakKwan Kim, Parajuli P. B., Fei Yu, Joel O. Paz, and Eugene Columbus. 2011. Economic Model for Evaluating Syngas Production Cost of Bio-gasification Facility. IBE Annual Conference, Loews Atlanta, March 3-5, 2011, Atlanta, GA.
38. Hakkwan Kim, Parajuli P. B., Yu F., and Columbus E. P. 2011. Economic Analysis and Assessment of Syngas Production using a Modeling Approach. ASABE Publication No. 1110814, ASABE, St. Joseph, MI. Available at: http://asae.frymulti.com/azdez.asp?search=1&JID=5&AID=37322&CID=loui2011&v=&i=&T=2.
39. Yangyang Deng, and Parajuli P. B. 2011. Evaluation of Syngas Production Unit Cost of Bio-Gasification Facility using Regression Analysis Techniques. ASABE

Publication No. 1110711, ASABE, St. Joseph, MI. Available at: http://asae.frymulti.com/azdez.asp?search=1&JID=5&AID=37284&CID=loui2011&v=&i=&T=2.

40. Parajuli P. B. 2011. Bio-energy Feedstock Yields and their Water Quality Benefits in Mississippi. ASABE Publication No. 1111416, ASABE, St. Joseph, MI. Available at: http://asae.frymulti.com/azdez.asp?search=1&JID=5&AID=38511&CID=loui2011&v=&i=&T=2.
41. Hakkwan Kim, and Parajuli P. B. 2011. Assessment of the Potential Crop Yield for Bio-Energy Production Using the SWAT Model. ASA/CSSA/SSSA, International annual meeting, October 16-19, San Antonio, TX.
42. Ryals, C.S., J.D. Davis, S. Samson, and D. Evans. 2011 Prediction of woody debris from a hurricane event using geographic information systems. Presentation for the 2011 ASABE International Meeting, Aug 7-10. Louisville, KY.
43. Production of Syngas from Downdraft Fixed-bed Biomass Gasification Systems, Lin Wei, Filip To, Eugene Columbus, Fei Yu, James Wooten, William D. Batchelor, Presentation, International Conference on Bioenergy Technology (ICBT), Beijing China, August 22, 2010.
44. Yu, F., Q. Yan, J. Hu, Y. Lu, L. Wei, J. Wooten, E. Columbus and W. Batchelor. 2010. Mixed Hydrocarbons from Biomass Gasification Syngas over Mo/HZSM-5 Catalyst. 9th International Conference on Sustainable Energy Technologies (SET). Shanghai, China. August 24-27.
45. Yu, F., Q. Yan, J. Hu, L. Wei, E. Columbus and J. Wooten. 2010. Mixed Hydrocarbon Production from Biomass-derived Syngas over A Bi-functional Catalyst. International Symposium on Renewable Feedstock for Biofuel and Bio-based Products. Austin, TX, August 11-13.
46. Hu, J., Yu, F., Wei, L., Columbus, E., and Batchelor, W. Preliminary Study of the Conversion of Biomass Gasification Syngas to Gasoline-range Hydrocarbons over Mo/HZSM-5. Paper 1008573, ASABE 2010 Annual International Meeting, Pittsburgh, Pennsylvania, June 20-23, 2010.
47. Biomass-based Syngas from Downdraft Fixed-bed Gasifier, Lin Wei, Filip To, Eugene Columbus, Fei Yu, James Wooten, William D. Batchelor, Poster, International Sustainable Energy Technology (ISET), Shanghai, China, August 25, 2010.
48. Effects of Feedstock Properties on the Performance of A Downdraft Gasifier. Lin Wei, Lester O. Pordesimo, S. D. Filip To, James R. Wooten, Agus Haryanto, and Eugene P. Columbus. Paper no. 096873, presented at the 2009 ASABE Annual International Meeting ASABE, Reno, Nevada, June 21 – June 24, 2009.
49. Crude Glycerol Co-gasification with Hardwood Chips in a Pilot-Scale Downdraft gasifier. Agus Haryanto, Lester R. Pordesimo, Sandun D. Fernando, James R. Wooten, Eugene P. Colombus, and Lin Wei. Paper no. 09742, presented at the 2009

ASABE Annual International Meeting ASABE, Reno, Nevada, June 21 – June 24, 2009.

50. Massey, W.A., C. Igathinathane, J.D. Davis, J.L. Purswell, and E.P. Columbus. 2009. Densified biomass mass properties determination using 3D laser scanning and image analysis. Abstract for the MSU Biofuels Conference. August 6-7. Jackson, MS.
51. Massey, W.A., C. Igathinathane, J.D. Davis, J.L. Purswell, and E.P. Columbus. 2009. Densified biomass mass properties determination using 3D laser scanning and image analysis. Abstract for the MSU 8th Annual Graduate Research Symposium. Nov. 6th. Starkville, MS.
52. S.K. Jha[1], S.R. Krishnan, K.K. Srinivasan, 2010, "Quasi-Two-Zone Modeling of Diesel Ignition Delay in Pilot-Ignited Partially Premixed Low Temperature Natural Gas Combustion," Paper No. ICEF2010-35127, Proceedings of the ASME IC Engines Division 2010 Fall Technical Conference (ICEF2010), September 12-15, San Antonio, TX; Presenter – S. K. Jha.
53. S. R. Krishnan, K. K. Srinivasan, K. C. Midkiff, "Ignition In Pilot-Ignited Natural Gas Low Temperature Combustion: Multi-Zone Modeling and Experimental Results," 2009, Proceedings of the ASME Internal Combustion Engines Division, Spring 2009 meeting, Milwaukee, WI, May 2009; Presenter – S. R. Krishnan
54. G. A. Adebiyi, K. K. Srinivasan, C. M. Gibson[1], "Thermodynamic Performance Optimization of Reciprocating Internal Combustion (IC) Engines," Proceedings of the IMECE 2008, Paper No. IMECE 2008-66026, 2008 ASME International Mechanical Engineering Congress and Exposition November 2-6, 2008, Boston, Massachusetts, USA; Presenter – C. M. Gibson
55. Shravana Musunuri, Herbert L. Ginn, "Comprehensive Review of Wind Energy Maximum Power Extraction Algorithms", Accepted for Presentation at Power Electronics Drives and Systems, Taiwan, November 2009.
56. Shravana Musunuri, Herbert L. Ginn, "Comprehensive Review of Wind Energy Maximum Power Extraction Algorithms", Submitted for Presentation at Energy Conversion and Congress Exposition, Atlanta, GA, Sep 2010.
57. Shravana Musunuri, Herbert L. Ginn, " A modified maximum power extraction algorithm for Wind energy systems", to be submitted at IEEE Workshop on Control and Modeling for Power Electronic, Boulder, CO, June 2010.
58. Anurag Srivastava, Ramon Zamora, Doug Bowman, "Impact of Distributed Generation with Storage on Electric Grid Stability", IEEE PES General Meeting, July 26 - July 29, 2011, Detroit, MI (Invited Panel)
59. R. Zamora, A. K. Srivastava and Syukriyadin, "Microgrids for Reliable, Clean, and Efficient Power Delivery," presented at the 4th Annual International Workshop & Expo on Sumatra Tsunami Disaster & Recovery 2009, Nov. 23-25, Banda Aceh, Indonesia.

60. Aarthi Asok Kumar, Anurag K Srivastava and Noel N. Schulz, “Impact of Biomass Based Distributed generation with Energy Storage on Transient Stability of Grid”, Proceedings of Power System Conference (PSC), March 11-14, 2008, Clemson, SC.
61. Abhilash R Masannagari, Anurag K Srivastava and Noel N. Schulz, “Optimizing Siting and Sizing of DG to maximize Grid Stability”, Proceedings of Power System Conference (PSC), March 11-14, 2008, Clemson, SC.
62. Aarthi Asok Kumar, Abhilash R Masannagari, Anurag K Srivastava and Noel N Schulz, “Impact of Biomass Based Distributed generation on Electric Grid”, Clean technology and Sustainable Industries Conference and Trade Show, Boston, MA, June 1-5, 2008.
63. Shireesha Methuku, Anurag K Srivastava and Noel N Schulz, “Comprehensive Modeling and Stability Analysis of Biomass Generation”, North American Power Symposium, October 2-4, Mississippi State, MS, 2009.

## Dissertations

1. Fumo, N. (Summer 2008). “Cooling, Heating, and Power Systems Energy Performance and Non-Conventional Evaluation Based On Energy Use.”
2. Weathers, J. (2008). “Verification and Validation of Micro-CHP Simulation at multiple levels.”
3. Cho, H. (2009). “Dynamic Simulation and Optimal Real-Time Operation of CHP Systems for Buildings.”
4. Hueffed, A. (Spring 2010). “Analysis and Optimization of CHP, CCHP, CHP-ORC, and CCHP-ORC Systems.”
5. Giffin, P. (Spring 2010). “Energy Analysis of a Micro-CHP Demonstration Facility.”
6. Wheeley, C. (Fall 2011). “Experimental Study and Feasibility of an Stirling Engine-CHP System.”
7. Smith, A. (Fall 2012). “Combined Heat and Power Systems for Commercial Buildings: Investigating Cost, Emissions, and Primary Energy Reduction Based on System Components.”
8. Yun, K. (Spring 2012). “Optimal PGU Operation Strategy in CHP Systems.”
9. Smith, A. (Fall 2012). “Methodologies for Addressing Errors and Uncertainty in CHP System Modeling.”
10. Knizley, A. (Summer 2013). “Evaluation of Dual Power CHP System Operation in Different Types of Commercial Buildings.”
11. Long, W. (Fall 2015). “Using Modular Uncertainty Analysis to Evaluate the Performance of Energy Systems.”
12. Ledbury, E. (Fall 2015). “Evaluation of a Solar Powered Organic Rankine Cycle.”
13. Harrod, J. (Fall 2010). “The Stirling Engine: Thermodynamics and Applications in Combined Cooling, Heating, and Power Systems.”
14. Jha, S. K. (Spring 2012) “ A phenomenological investigation of ignition and

combustion in alternative-fueled engines,"

15. Tripathi, M. M. "Optical and Laser Spectroscopic Diagnostics for Energy Applications,", Ph.D. dissertation, May 2012.
16. Aditya Samala PhD, Graduated, Xylo-oligosaccharides production from corn fiber and *in-vitro* evaluation for prebiotic effect.
17. Tejas Pandya PhD, Graduated, Fiber separation from milled corn and sorghum using the Elusieve process for value addition to feed and biofuel production.
18. John Lowe PhD, TBD.
19. Brian Luck PhD, Graduated, Spatial analysis of air velocity distribution as affected by house size and design in commercial broiler production facilities.
20. Shravana Musunuri, "Power Electronic Interface and Control Issues in the Hybrid Renewable Energy Interconnection to the Grid", May 2011.
21. Derrick Cherry, "Technical Evaluation and Optimal Placement of Distributed Gene ration on the Distribution Power System Using Artificial Intelligence, December 2010.
22. Saher Albatran, "Integration of CHP Systems with Power Grid", May 2014.
23. Ping Liu, "CHP Building Energy Management", May 2014.

## Posters

3. Fumo, N., Mago, P. J., and Chamra, L. M. (Apr 2009). Hybrid-Cooling, Combined Cooling, Heating, and Power Systems. *2nd Energy-Synergy Workshop,* Mississippi State University.
4. Cho, H., Luck, R., Chamra, L.M., "Supervisory Feed-Forward Control of Building CHP Systems Using Short-Term Weather Forecasting", Poster presentation in International Building Performance Simulation Association (IBPSA) – USA meeting, January 24, 2009, Chicago, IL, USA.
5. Harrod, J., Mago, P. J., Srinivasan, K. K., & Chamra, L. M. (Apr 2009). First and Second Law Analysis of a Stirling Engine with Imperfect Regeneration and Dead Volume and its Application in CHP Systems. *2nd Energy-Synergy Workshop*, Mississippi State University.
6. Wang, Z., Srinivasan, K. K., Krishnan, S. R., Som, S. "A computational investigation of diesel and biodiesel combustion and NOx formation in a light-duty compression ignition engine," To be presented at the Central States Meeting of the Combustion Institute, Hosted by the University of Dayton, Dayton, OH, April 22-24, 2012.
7. M.M. Tripathi, S.R. Krishnan, K.K. Srinivasan, F.-Y. Yueh, J.P. Singh, "Development of a Robust Sensor for Monitoring Equivalence Ratio in Premixed Flames Using Chemiluminescence and Multivariate Data Analysis," presented at the 7th US National Technical Meeting of the Combustion Institute, Hosted by the

Georgia Institute of Technology, Atlanta, GA, March 20-23, 2011.

8. A.A. Knizley, K.K. Srinivasan, S.R. Krishnan, "Fuel and Diluent Effects on Entropy Generation in a Constant Internal Energy-Volume (UV) Combustion Process," presented at the 7th US National Technical Meeting of the Combustion Institute, Hosted by the Georgia Institute of Technology, Atlanta, GA, March 20-23, 2011.
9. Lu, Y., Yu, F., Hu, J., Zhou, P. Syngas to Higher Alcohols via Three-dimentionally Ordered Macroporous Cu-Fe Bimetallic Catalyst. A Poster Presentation presented for the 2013 SEC Symposium. Atlanta, GA, February 10-12, 2013.
10. Street, J., Yu, F., Columbus, E., Wooten, J., and Yan, Q. Scale up of Gasoline-Range Hydrocarbon Production from Gasified Woody Biomass using a Bi-Functional Catalyst. A Poster Presentation presented for the 2013 SEC Symposium. Atlanta, GA, February 10-12, 2013.
11. Lu, Y., F. Yu, J. Hu, and P. Zhou. 2013. Higher alcohols synthesis from syngas over three-dimensionally ordered macroporous Cu-Fe bimetallic catalyst. 23rd North American Catalysis Society Meeting. Louisville, KY. June 2-7. Poster.
12. Yan, Q., and F. Yu. 2013. Catalytic Conversion Wood Syngas to 'Wide Cut' Diesel over A Multifunctional Catalyst. 23rd North American Catalysis Society Meeting. Louisville, KY. June 2-7. Poster.
13. Lu, Y., F. Yu, J. Hu, and P. Zhou. 2013. Catalytic conversion of syngas to higher alcohols via Zn-Mn promoted Cu-Fe based catalysts. 246$^{th}$ American Chemical Society National Meeting. Indianapolis, IN. September 8-12. Poster presentation.
14. Street, J., Yu, F., Columbus, E., and Wooten, J. 2013. Process Design and Economic Analysis of a Gas-to-Liquid Plant with Aspen Plus using a Woody Biomass Feedstock. Mississippi Biomass and Renewable Energy Council Conference. Tunica, MS. September 17-18. Poster presentation.
15. Yan, Q., Street, J., Wooten, J., Columbus J., and Yu. F. 2011. Biomass to liquid (BTL) fuels via gasification and catalytic conversion. A Poster Presentation presented
16. Lu, Y., Yan, Q., Hu, J., Street, J., Wooten, J., Columbus, E., Yu, F. 2011. Higher Alcohols Synthesis from Syngas over Copper-Iron Based Catalyst. A Poster Presentation presented for the Mississippi State 2011 Biofuels Conference. Mississippi State, MS, October 5-7, 2011.
17. Hu, J., Yu, F., Lu, Y., Yan, Y., Wooten, J., Columbus. E. 2011. Green Flight: Renewable Jet Fuel Production Through Integrated Biomass Gasification, Gas Cleaning and Catalytic Conversion System. A Poster Presentation presented for the Mississippi State 2011 Biofuels Conference. Mississippi State, MS, October 5-7, 2011.
18. Street, J., Columbus, E., Wooten, J., White, M., and Yu, F. Scale-up of Gasoline-Range Hydrocarbon Production from Biomass Synthesis Gas over Mo/HZSM-5 and other Bi-functional Catalysts. A Poster Presentation presented for the

Mississippi State 2011 Biofuels Conference. Mississippi State, MS, October 5-7, 2011.

19. Yu, F. 2011. Liquid Hydrocarbons Production via Biomass Gasification and Catalytic Conversion. 4th Annual Waste-to-Fuels Conference & Trade Show. San Diego, CA. September 25-27, 2011.
20. Lu, Y., Yan, Q., Hu, J., Street, J., Wooten, J., Columbus, E., Yu, F. 2011. Development of copper-iron based catalyst for mixed alcohol synthesis from syngas. Microscopy & Microanalysis annual meeting. Nashville TN, August 7-11, 2011.
21. Hu, J., Yu, F., Lu, Y., Yan, Q., Wooten, J., Columbus, E., Lin, W. 2011. Catalytic Conversion of Biomass-derived Syngas to Gasoline Range Hydrocarbons. Paper: 1110878, An ASABE Meeting Presentation written for the 2011 ASABE Conference, Louisville, KY, August 7-10, 2011.
22. Lu, Y., Yan, Q., Hu, J., Street, J., Wooten, J., Columbus, E., Yu, F. 2011. Mixed Alcohols Synthesis from Syngas Over Copper-Iron Based Catalyst. Paper: 1110834, An ASABE Meeting Presentation written for the 2011 ASABE Conference, Louisville, KY, August 7-10, 2011.
23. Street, J., Columbus, E., Warnock, J., Wooten, J., White, M., Yu, F. 2011. Liquid Hydrocarbon Production over Mo/HZSM-5 Using Gasified Biomass. Paper: 1110541, An ASABE Meeting Presentation written for the 2011 ASABE Conference, Louisville, KY, August 7-10, 2011.
24. Zhang, Y., J. Wooten, E. Columbus, and F. Yu. 2011. The otential for Improvements of A Pilot-Plant Scale Downdraft Gasifier Through Material Balance and Energy Balance Analysis. S1041 (The Science and Engineering for a Biobased Industry and Economy) Symposium. Stillwater, OK, August 2, 2011.
25. Street, J., J. Wooten, E. Columbus, J. Warnock, M. White, and F. Yu. 2011. Liquid Hydrocarbon Production over Mo/HZSM-5 Using Gasified Biomass. S1041 (The Science and Engineering for a Biobased Industry and Economy) Symposium. Stillwater, OK, August 2, 2011.
26. Lu, Y. and F. Yu. 2011. Higher Alcohol Synthesis from Syngas over Copper-Iron Based Catalyst. S1041 (The Science and Engineering for a Biobased Industry and Economy) Symposium. Stillwater, OK, August 2, 2011.
27. Livingston, D., F. Yu, Q. Li, and P. Steele, 2011. Ethanolic Fermentation of Bio-oil Hydrolysate. S1041 (The Science and Engineering for a Biobased Industry and Economy) Symposium. Stillwater, OK, August 2, 2011.
28. Chen, J., L. Sun, A. Hao, W. Jiang, and F. Yu. 2011. Bioconversion of Fiber Crops into High-Value Fiber, Film, Composite, and Hydrocarbon. S1041 (The Science and Engineering for a Biobased Industry and Economy) Symposium. Stillwater, OK, August 2, 2011.
29. Yu, F., P. Steele, E. Columbus, and G. Steele. 2011. Thermochemical Conversion of Biomass to Biofuel, Sustainable Energy Research Center. S1041 (The Science and Engineering for a Biobased Industry and Economy) Symposium. Stillwater, OK, August 2, 2011.

30. Street, J., Wooten, J., Columbus, E., Warnock, J., White, M., Yu, F. Hindrances to Liquid Hydrocarbon Production over Mo/HZSM-5 using Biomass Syngas. An IBE Meeting Presentation presented for IBE 2011 Conference. Atlanta, GA, March 3-5, 2011.
31. Hu, J., Yu, F., Lu, Y., Yan, Q., Wooten, J., Columbus, E., Batchelor, W. Gasoline Range Hydrocarbons Synthesis From Biomass-derived Syngas over Mo/HZSM-5 Catalyst. An IBE Meeting Presentation presented for IBE 2011 Conference. Atlanta, GA, March 3-5, 2011.
32. Yan, Q., Street, J., Wooten, J., Columbus J., and Yu. F. 2011. Biomass to liquid (BTL) fuels via gasification and catalytic conversion. A Poster Presentation presented for the Mississippi State 2011 Biofuels Conference. Mississippi State, MS, October 5-7, 2011.
33. Lu, Y., Yan, Q., Hu, J., Street, J., Wooten, J., Columbus, E., Yu, F. 2011. Higher Alcohols Synthesis from Syngas over Copper-Iron Based Catalyst. A Poster Presentation presented for the Mississippi State 2011 Biofuels Conference. Mississippi State, MS, October 5-7, 2011.
34. Hu, J., Yu, F., Lu, Y., Yan, Y., Wooten, J., Columbus. E. 2011. Green Flight: Renewable Jet Fuel Production Through Integrated Biomass Gasification, Gas Cleaning and Catalytic Conversion System. A Poster Presentation presented for the Mississippi State 2011 Biofuels Conference. Mississippi State, MS, October 5-7, 2011.
35. Street, J., Columbus, E., Wooten, J., White, M., and Yu, F. Scale-up of Gasoline-Range Hydrocarbon Production from Biomass Synthesis Gas over Mo/HZSM-5 and other Bi-functional Catalysts. A Poster Presentation presented for the Mississippi State 2011 Biofuels Conference. Mississippi State, MS, October 5-7, 2011.
36. Yangyang Deng and Parajuli P. B. 2011. Economic Analysis and Optimization of Syngas Production: Model Development and Application. Poster Presentation at the Biofuels conference, October 5-7, Mississippi State University.
37. Street, J., Columbus, E., Warnock, J., Wooten, J., White, M. Scale-Up of Gasoline-range Hydrocarbons over Mo/H-Y and Mo/HZSM-5 Catalysts. An IBE Poster Presentation presented for IBE 2010 Conference. Cambridge, MA, March 4-6, 2010.
38. Street, J., Columbus, E., Warnock, J., Wooten, J., White, M., Yu, F. Scale-Up of Gasoline-Range Hydrocarbon Production over Mo/HZSM-5 using Synthesis Gas. A Poster Presentation presented for the Mississippi State 2010 Biofuels Conference. Jackson, MS, August 12-13, 2010.
39. Shravana Musunuri, Herbert L. Ginn, "Power electronic Interface of Multiple Energy Sources to Utility Grid", Poster Presentation, Electric Ship Technology Symposium, Starkville, May 2009.
40. Ramon Zamora, and *Anurag K. Srivastava,* "Modeling and Control of Microgrid", IEEE T&D conference, New Orleans, LA, April, 2010.

41. Shireesha Methuku, *Anurag K. Srivastava* and Noel N Schulz, “Comprehensive Modeling and Technical-Economical Impacts of Biomass Generation”, IEEE T&D conference, New Orleans, LA, April, 2010
42. S.K. Jha, K.K. Srinivasan, S. R. Krishnan, "Simulation of Autoignition Phenomena of Hydrocarbon Fuels in Engine-Like Conditions" at the recently concluded MSU Biofuels Conference at Jackson, MS August 6-7 2009 (The poster won 2nd place at the MSU Biofuels Conference at Jackson, MS August 6-7 2009)
43. S. K. Jha, K. K. Srinivasan, S. R. Krishnan, R. Luck, “Simulation of Autoignition Phenomena of Hydrocarbon Fuels in Engine-Like Conditions,” poster presented at the 2nd Energy Workshop, April 15, 2009, Mississippi State University
44. M. M. Tripathi, S. R. Krishnan, K. K. Srinivasan, F-, Y. Yueh, J. P. Singh, “Study of Emissions Spectra of Syngas-Methane-Air Premixed Flames for Simultaneous Measurement of Flame Temperature and Equivalence Ratio,” poster presented at the 2nd Energy Workshop, April 15, 2009, Mississippi State University.